PROGRESS IN METAL PHYSICS 3

OL.
3

Editor
BRUCE CHALMERS, D.Sc., Ph.D.

NEW YORK
INTERSCIENCE PUBLISHERS INC
LONDON
PERGAMON PRESS LTD
1952

VOL
3

Published in Great Britain by Pergamon Press, Ltd., 2, 3 & 5 *Studio Place, London, S.W.*1,
and in U.S.A. by Interscience Publishers Inc., 250 *Fifth Avenue, New York* 1, *N.Y.*
Printed in Great Britain by The Pitman Press, Bath, Somerset

CONTENTS

PAGE

FOREWORD TO VOLUME 1 ..

ACKNOWLEDGMENTS

1 CRYSTALLOGRAPHY OF TRANSFORMATIONS 1
J. S. Bowles and C. S. Barrett

2 PROPERTIES OF METALS AT LOW TEMPERATURES 42
D. K. C. MacDonald

3 RECENT ADVANCES IN THE ELECTRON THEORY OF METALS 76
N. F. Mott

4 TWINNING 115
R. Clark and G. B. Craig

5 FERROMAGNETISM 140
Ursula M. Martius

6 QUANTITATIVE X-RAY DIFFRACTION OBSERVATIONS ON STRAINED METAL AGGREGATES 176
G. B. Greenough

7 RECRYSTALLIZATION AND GRAIN GROWTH 220
J. E. Burke and D. Turnbull

8 STRUCTURE OF CRYSTAL BOUNDARIES 293
B. Chalmers

NAME INDEX 321

SUBJECT INDEX 328

VOL.
3

AUTHOR INDEX

Akulov, N. S. 172, 175
Alexander, B. H. 278, 291
Amstel, J. J. A. 138
Anand, V. B. 53, 73
Anderson, W. A. 229, 235, 237, 240, 241, 243, 244, 248, 250, 252, 253, 259, 290
Andrade, E. N. da C. 137, 138
Andrew, E. A. 69, 74
Andrews, D. H. 68, 74
Ansel, O. 129, 139
Appleyard, E. T. S. 74
Archer, R. S. 292
Arkel, A. E. van 200, 218
Aubertin, F. 179, 198, 217
Aust, K. T. 31, 41, 139, 291
Averbach, B. L. 207, 214, 215, 216, 219
Avrami, M. 224, 225, 226, 227, 229, 290

Baber, W. G. 65, 74
Backer, R. F. 105, 114
Bailey, G. L. J. 291
Bain, E. C. 5, 8, 13, 40
Bakalar, I. D. 291
Bakarian, P. W. 122, 123, 138
Balicki, M. 227, 290
Barbers, J. 181, 184, 217
Bardeen, J. 84, 113
Bardwell, E. S. 137
Barkhausen, H. 162, 174
Barrett, C. S. 16, 18, 31, 32, 39, 40, 41, 118, 119, 120, 121, 123, 124, 125, 126, 127, 128, 129, 131, 132, 134, 136, 137, 138, 139, 177, 210, 217, 219, 279, 282, 284, 291, 292
Barrett, Marjorie A. 40
Bates, L. F. 157, 159, 174
Beck, P. A. 41, 234, 238, 253, 262, 264, 272, 273, 274, 278, 279, 280, 291, 292
Becker, J. 281, 282, 292
Becker, R. 141, 144, 147, 148, 149, 158, 159, 160, 165, 171, 172, 173, 174
Benedicks, C. 123, 138, 277, 292
Berg, W. F. 139
Berg, G. J. van den 60, 66, 73, 74
Bethe, H. 143, 174
Betteridge, W. 40
Birch, A. J. 74
Bitter, F. 157, 174
Blackman, M. 48, 49, 52, 53, 63, 72, 75
Blank, A. I. 287, 292
Bloch, F. 58, 64, 73, 77, 80, 83, 113, 141, 151, 153, 166, 174
Boas, W. 92, 93, 114, 124, 125, 127, 138, 183, 213, 217, 219, 220, 254, 279, 290, 291
Boer, J. de 60, 66, 73
Bohm, D. 85, 113
Bollenrath, F. 189, 191, 192, 193, 217, 218
Bolton, M. J. 41, 139
Bolton, M. S. 291
Boorse, J. A. 74
Born, M. 45, 46, 48, 52, 53, 68, 72, 73, 74
Bousu, A. E. 291
Bowles, J. S. 8, 11, 13, 14, 15, 16, 18, 25, 39, 40, 254, 279, 291
Bozorth, R. M. 147, 152, 155, 157, 158, 174
Bradley, A. J. 35, 41
Bragg, W. L. 193, 196, 204, 205, 209, 210, 218, 219, 227, 267, 290, 292
Brick, R. M. 120, 121, 137
Bridgman, P. W. 55
Brill, R. 213, 219
Brillouin, L. 46, 56, 61, 65, 67, 71, 72
Brindley, G. W. 202, 212, 213, 218
Brooks, H. 174
Brown, W. F. 175
Brown, W. G. 122, 137
Bruggeman, D. A. G. 183, 217
Buerger, M. J. 115, 117, 137
Burgers, W. G. 9, 10, 11, 19, 40, 122, 138, 220, 234, 289, 290, 291, 292
Burke, J. E. 121, 122, 137, 138, 220, 233, 251, 254, 272, 273, 275, 277, 283, 287, 290, 291, 292
Burton, K. V. 112
Butler, C. C. 199, 218

Cahn, R. W. 207, 219, 262, 263, 290, 291
Campbell, W. E. 175
Carapella, L. A. 127, 138
Carlile, S. J. 40
Carpenter, H. C. H. 115, 122, 137, 266, 283, 292
Carrington, W. E. 32, 41
Cartaud, G. 128, 138
Cauchois, Y. 108, 114
Cech, R. 22
Chalmers, B. 31, 41, 118, 134, 135, 137, 139, 157, 170, 174, 199, 256, 265, 268, 291

Chambers, R. G. 69, 70, 74
Chandler, W. 273, 292
Chang, L. C. 3, 26, 27, 39
Cheng, K. C. 68, 74
Chodorow, M. I. 86, 113
Chou, A. 35, 41
Christian, J. W. 40
Clark, C. W. 30, 72, 113
Clark, R. 118, 134, 137, 139
Clusius, K. 50, 72
Clifton, D. F. 25, 40
Cohen, M. 22, 23, 24, 27, 39, 40, 291
Collins, J. A. 228, 243, 290
Cook, D. B. 74
Cook, M. 227, 231, 232, 241, 254, 290, 291
Cornish, F. H. 57, 75
Coster, D. 106, 114
Cottrell, A. H. 76, 112
Cox, H. L. 117, 125, 127, 133, 137, 138, 139
Craig, G. B. 118, 134, 137, 139
Cramer, H. 122, 137
Cristescu, S. 52, 73
Crussard, C. 179, 198, 217
Czochralski, J. 138, 220, 267, 290, 292

Daniel, V. 35, 36, 41
Daniels, F. W. 41, 139, 291
Darwin, Ch. 210
Daunt, J. G. 74, 86, 113
Davidenkov, N. N. 193, 218
Davidson, N.N . 125, 127, 138
Davis, W. G. 114
Dawson, I. M. 112
Dayal, B. 53, 73
Debye, P. 45, 46, 47, 48, 49, 51, 52, 53, 58, 59, 60, 63, 72, 73, 83
Decker, B. F. 231, 232, 241, 252, 262, 282, 291
Dehlinger, U. 204, 209, 218, 219
Demer, L. J. 272, 273, 291
Derge, G. 40
Desirant, M. C. 74, 113
Devonshire, A. F. 114
Dewinap, N. 196, 218
Dietrich, R. L. 125, 127, 138
Dijkstra, L. J. 163, 167, 174
Dingle, R. B. 69, 74
Döring, W. 144, 147, 148, 158, 159, 160, 164, 165, 171, 172, 173, 174, 175
Dorn, J. E. 127, 138
Drigo, A. 169, 175
Dulong, P.-L. 43, 44
Dunn, C. G. 31, 41, 234, 256, 268, 291
Dunn, G. D. 139
Duyckaerts, G. 51, 72, 113

Eastwood, L. W. 241, 291
Eckstein, H. 211, 219
Eddy, C. T. 291
Edmunds, G. H. 128, 138
Edwards, O. S. 39
Einstein, A. 43, 44, 49, 53, 57, 72, 83
Elam, C. F. 120, 124, 132, 137, 138, 139, 266, 292
Elmore, W. C. 155, 157, 174
Elson, R. G. 51, 72, 113
Endo, H. 114
Eucken, A. 46, 72
Evans, E. Ll. 114
Evans, J. W. 115, 137
Ewald, P. P. 211, 219
Ewen, D. E. 137
Ewing, F. J. 113
Ewing, J. A. 138, 267, 292
Eyring, H. 291

Farineau, J. 114
Fedorov, K. V. 126, 127, 138
Finch, L. G. 179, 189, 190, 191, 194, 195, 217, 218
Fine, P. C. 63, 74
Fink, W. L. 41
Fisher, A. 139
Fisher, J. C. 21, 22, 23, 24, 39, 41, 255, 256, 271, 285, 291, 292
Focke, A. B. 133, 139
Foex, M. 54, 73
Förster, F. 5, 40
Forsythe, W. R. 55, 73
Fournet, G. 219
Fowler, R. H. 46, 72
Frank, F. C. 76, 112
Fricke, R. 218
Friedel, J. 98, 103, 105, 107, 114
Fröhlich, H. 66, 74, 84, 113
Fuchs, K. 74, 87, 92, 93, 114
Fullman, R. 283, 285, 288, 289, 292

Galt, J. K. 175
Gans, R. 172, 175
Garrod, R. I. 189, 191, 194, 195, 218
Gawranek, V. 40
Gayler, M. L. V. 32, 41
Geisler, A. H. 32, 36, 37, 38, 41
Germer, L. H. 158, 174
Gerritsen, A. N. 66, 75
Giauque, W. F. 55, 73
Glasstone, S. 291
Glocker, R. 181, 189, 192, 217, 218
Goens, E. 185, 217
Göler, F. von 224, 230, 290
Gorter, C. J. 66, 74
Goudsmit, S. 105, 114
Gough, H. J. 117, 125, 127, 133, 137, 138, 139, 209, 210, 219

Gow, K. V. 157, 170, 174
Grayson-Smith, H. 113
Greenough, A. P. 199, 218
Greenough, G. B. 189, 191, 194, 195, 196, 214, 218, 219
Greninger, A. B. 2, 10, 11, 12, 14, 15, 16, 18, 39, 40, 117, 118, 137
Griffin, L. J. 112
Grüneisen, E. 58, 61, 64, 73
Guggenheim, E. A. 46, 72
Guinier, A. 33, 41, 177, 211, 214, 216, 217, 219
Gurney, R. W. 104, 105, 106, 114
Guthrie 76
Guttman, L. 16, 18, 39, 40

Haas, W. J. de 60, 66, 73, 74
Haayman, P. W. 112
Hadfield, R. A. 139
Hall, G. G. 112
Hall, W. H. 205, 207, 211, 214, 216, 217, 218, 219
Haller, C. T. 123, 124, 125, 137
Hanstock, R. F. 186, 217
Hardy, H. K. 41
Hargreaves, M. E. 36, 41
Harker, D. 36, 41, 231, 232, 241, 252, 262, 266, 267, 269, 277, 282, 291, 292
Hasenmaier, H. 189, 192, 218
Hauk, V. 181, 184, 185, 189, 191, 217, 218
Heidenreich, R. D. 282, 284, 292
Heisenberg, W. 74, 77, 78, 83, 84, 85, 113, 140, 141, 174
Heitler, W. H. 78, 79, 80, 82, 83
Hengstenberg, J. 212, 213, 214, 219
Herring, C. 83, 84, 88, 90, 113
Hess, J. B. 121, 125, 127, 138
Heusler, O. 143
Heyn, E. 194
Hibbard, W. R. 121, 138, 281, 282, 292
Hill, A. G. 90, 114
Hill, J. K. 32, 41
Hirsch, P. B. 207, 219
Hoffman, R. E. 112, 114, 292
Hollomon, J. H. 21, 22, 23, 24, 41
Holstein, T. 172, 175
Holzworth, M. L. 264, 272, 273, 274, 278, 291, 292
Honda, K. 158
Honeycombe, R. W. K. 124, 138
Horne, van 120, 137
Horn, K. R. van 220, 290
Hsun, Hu 291, 292
Houston, W. V. 57, 58, 65, 73, 74
Howe, H. M. 138
Hu V. 234, 280
Huang, K. 112
Hume-Rothery, W. 42, 72, 87, 94, 98, 102, 114
Huntingdon, H. B. 112, 114
Hutchings, P. 138
Huttner, R. A. 112, 114

Irving, H. M. 114
Isaichev, I. 39
Isartschew, I. 40
Isenberg, I. 98, 114
Iwata, T. 157

Jackson, L. C. 74
Jaswon, M. A. 4, 8, 12, 13, 14, 40
Jeffries 274, 292
Jetter, L. K. 38, 41
John, M. E. 114
Johnson, F. J. 139
Johnson, W. A. 224, 225, 226, 227, 228, 229, 230, 290, 291
Johnston, J. E. 107, 114
Jones, F. W. 200, 218
Jones, H. 46, 51, 56, 72, 73, 86, 87, 88, 90, 91, 94, 95, 98, 106, 108, 112, 113, 114
Joule, P. 174

Kaiser, H. F. 32, 41
Kalisher, R. 220, 290
Kamerlingh Onnes, H. 62, 67, 74
Kaminsky, E. 40
Kamio, K. 139
Karman, Th. von 45, 46, 48, 72
Karnop, R. 228, 230, 234, 235, 250, 253, 290
Kaya, S. 158
Keeping, E. S. 114
Keesom, W. H. 50, 51, 72, 73, 86, 113
Kellar, J. N. 207, 219
Kellerman, E. W. 49, 72
Kelley, K. K. 55, 73
Kelvin, Lord 46
Kersten, M. 166, 167, 174
Kiestra, S. 106, 114
Kirchner, F. 122, 137
King, R. 139, 199, 218
Kittel, C. 83, 84, 113, 144, 145, 148, 149, 153, 156, 163, 165, 169, 173, 174, 175
Kochanovska, A. 181, 217
Kochendörfer, A. 204, 215, 216, 218, 219
Kohler, M. 58, 73
Kohn, W. 88, 113
Kok, J. A. 51, 73, 113
Kolesnikov, A. F. 125, 127, 138
Komar, A. 72, 74
Kondorski, E. 166, 174
Koppe, H. 84, 113

KORNFELD, M. 228, 233, 234, 236, 240, 241, 242, 243, 250, 253, 254, 290, 291
KRAMERS, H. A. 81, 113
KREMER, J. C. 272, 273, 291
KRONBERG, M. L. 138, 278, 279, 280, 292
KRONIG, R. DE L. 106, 114
KUBASCHEWSKI, O. 101, 114
KRUPKOWSKI, A. 227, 290
KUHN, T. S. 88, 113
KULIN, S. A. 22, 40
KURDJUMOW, G. V. 6, 8, 9, 11, 12, 13, 14, 15, 22, 39, 40, 41
KURRELMEYER, B. 51, 72, 86, 113
KÜRTI, N. 74

LACOMBE, P. 138
LAEN, P. H. VAN DER 113
LAER, P. H. VAN 51, 72
LAIDLER, K. J. 291
LANDAU, L. 141, 154, 157, 174
LANDAUER, R. 112, 114
LANDSBERG, P. T. 85, 103, 110, 113
LANGEVIN, P. 140
LAUE, M. VON 177
LAWTON, H. 158, 174
LEE-WHITING, G. E. 85, 104, 110, 113
LEIGH, R. S. 94, 96, 97, 114
LEIGHTON, R. B. 63, 74
LENNARD-JONES, J. E. 77, 78, 80, 112, 114
LIFSCHITZ, E. 141, 154, 155, 157, 174
LIHL, F. 193, 218
LILLEY, B. A. 154, 174
LINDE, J. O. 66, 75
LINDEMANN, F. A. 44, 49, 53, 54, 63, 72
LINK, Z. 128, 129, 138
LIONETTI, F. 41
LIPSON, H. 35, 36, 39, 40, 41, 201, 203, 218
LITTLETON, M. J. 112, 114
LIU, Y. C. 121, 138, 292
LIU, Y. H. 198, 199, 218
LLOYD, E. H. 186, 217
LONDON, H. 70, 74, 77, 78, 79, 80, 82, 83
LOS, J. 208, 219
LOUERWERSE, P. C. 291
LOVELL, A. C. B. 74
LYMAN, T. 4, 40

MACDONALD, D. K. C. 52, 37, 60, 62, 63, 66, 69, 70, 73, 74, 75
MACHLIN, E. S. 16, 22, 23, 24, 27, 40
MACKENZIE, J. K. 111,114
MACKENZIE, J.R. 92, 93, 114
MADDIGAN, S. E. 287, 292
MADDIN, R. H. 121, 138, 281, 282, 292
MAKSIMOVA, O. V. 22, 41
MANLEY, W. O. 292
MANNING, M. F. 86, 113
MARK, H. 212, 213, 214, 219
MARTIN, G. 181, 217
MARTIUS, U. M. 157, 170, 171, 174, 175
MASING, G. 194
MASON, W. P. 120, 138
MATHEWSON, C. H. 119, 120, 121, 122, 123, 124, 127, 128, 137, 138, 228, 243, 281, 282, 284, 280. 290, 292
MATTHIESSEN, A. 56, 73
MAY, W. 234, 291
MCGUIRE, F. T. 39
MCKEEHAN, L. W. 115, 129, 137, 139
MCMINN, J. 128, 138
MCREYNOLDS, A. W. 3, 23, 25, 26, 39
MCSKIMIN, H. J. 120, 138
MEADS, P. F. 55, 73
MEADS, W. P. 55, 73
MEE, C. D. 158, 174
MEGAW, H. D. 203, 218
MEHL, R. F. 29, 30, 32, 38, 40, 41, 129, 139, 220, 224, 225, 226, 227, 228, 229, 230, 232, 235, 237, 240, 241, 243, 244, 248, 250, 252, 253, 259, 290
MEISSNER, W. 58, 60, 62, 63, 73, 74
MELVIN, M. A. 224, 290
MENDELSSOHN, K. 52, 60, 62, 63, 66, 68, 73
MENDOZA, E. W. 66, 75
MILLER, O. O. 272, 273, 292
MILLER, R. F. 123, 127, 138
MILTON, R. M. 74
MOLLER, H. 181, 184, 193, 217
MOORADIAN, V. G. 40
MORRIS, D. P. 198, 199, 218
MOTT, N. F. 31, 33, 37, 41, 42, 46, 51, 56, 65, 72, 73, 74, 86, 87, 88, 90, 91, 95, 98, 104, 105, 106, 108, 112, 113, 114, 244, 248, 291
MÜGGE, O. 129, 133, 139
MÜLLER, H. G. 229, 232, 233, 238, 239, 240, 243, 252, 253, 259, 263

NABARRO, F. R. N. 31, 33, 37, 41
NAYAR 53
NEALE, F. E. 157, 159, 174
NÉEL, L. 141, 155, 158, 159, 166, 167, 172, 173, 174, 175
NEERFELD, H. 179, 181, 184, 185, 190, 193, 217
NERNST, W. 43, 44, 49, 53, 54, 72
NEWKIRK, J. B. 36, 37, 41
NEWTON, I. 46, 72
NICHOLSON, M. M. 199, 218
NIEHRS, H. 114

Niemann, F. 210, 211, 219
Nishiyama, Z. 6, 8, 9, 11, 12, 13, 14, 40
Nix, F. C. 55, 73, 291
Nordheim, L. 56, 73
Norris, R. 53, 73

Ochsenfeld, R. 74
Ogg, R. A. 68, 69, 74
O'Neil, H. 128, 138
Orowan, E. 193, 208, 219
Osborn, J. A. 150, 174
Osmond, F. 128, 138
Osswald, E. 189, 191, 217, 218
Owen, E. A. 95, 96, 114, 198, 199, 218

Paranjpe, V. G. 22, 23, 24, 27, 40
Parker, A. M. B. 40
Parker, E. A. 266, 267, 269, 277, 292
Parkinson, D. H. 54, 73
Parratt, L. J. 104, 114
Pascoe, K. J. 201, 203, 218
Paterson, M. S. 208, 219
Pauling, L. 89, 90, 113
Pavlov, W. 228, 234, 236, 240, 241, 242, 250, 253, 290
Peierls, R. 64, 65, 74
Petch, N. J. 40
Petit, A. T. 43, 44
Pfarr, B. 186, 189, 218
Pfeil, L. B. 139
Phillips, A. J. 119, 121, 123, 127, 137, 138, 139
Pickard, G. L. 51, 52, 73, 113
Pickup, L. 95, 96, 114
Pippard, A. B. 70, 74
Pizzo, M. 169, 175
Ploos van Amstel, 138
Polanyi, M. 238, 291
Pontius, R. B. 74
Près, F. K. du 112, 114
Preston, G. D. 33, 115, 136, 137
Primakoff, H. 172, 175

Quinney, H. 223, 245, 290

Rachinger, W. A. 179, 205, 209, 217, 218
Rado, G. T. 173, 175
Raimes, S. 90, 114
Raman, C. V. 52, 53, 73
Raynor, G. V. 94, 96, 114
Read, T. A. 3, 26, 27, 31, 39
Read, W. T. 41
Reiter, S. F. 121, 138, 292
Reuss, A. 183, 184, 217
Reuter, G. E. H. 70, 74
Rhodes, P. 58, 73
Richards, T. L. 227, 231, 232, 241, 254, 290, 291, 292
Rittner, E. S. 112, 114
Robin 139
Robinson, C. S. jr. 273, 292
Rogers, B.A. 35, 41
Romeyn, F. C. 112
Romig, O. E. 138
Rosenhain, W. 128, 137, 138, 267, 292
Rosi, F. D. 278, 291
Rybalko, F. 233, 254, 291
Rymer, T. B. 199, 218

Sachs, G. 6, 8, 9, 11, 12, 13, 14, 15, 40, 220, 224, 228, 230, 234, 235, 250, 253, 290
Sadebeck, M. 128, 138
Salli, I. 39
Samans, C. H. 120, 137
Sarginson, K. 69, 70, 74
Sauveur, A. 35, 41
Sawizki, F. 228, 290
Schaaber, O. 181, 217
Schachinger, L. 50, 72
Schamarin, A. 243, 291
Scheil, E. 3, 5, 25, 26, 39, 40
Scherrer, P. 202, 204, 218
Schiebold, E. 138
Schmid, E. 125, 127, 138, 183, 217, 220, 290
Schottky, W. 47, 48, 54, 61, 72
Schrödinger, E. 46, 72, 77
Sears, G. W. 223, 290
Seitz, F. 87, 112, 114, 194, 218
Seymour, W. E. 231, 291
Shaw, W. E. 127, 138
Shiau, Y. G. 287, 292
Shockley, W. 31, 41, 55, 73, 120, 138, 155, 158, 159, 163, 174, 282, 284, 291, 292
Shoenberg, D. 74
Shull, C. G. 219
Shuttleworth, R. 139
Sidorov, S. 74
Siebel, G. 138
Silverman, A. A. 88, 113
Silvidi, A. A. 113
Simon, F. E. 47, 48, 51, 52, 54, 61, 72, 73, 74, 113
Sixtus, K. J. 163, 174
Skinner, H. W. B. 65, 74, 90, 106, 107, 109, 114
Slater, J. C. 65, 74, 80, 86, 113, 143, 174
Smart, J. S. 239, 291
Smekal, A. 291
Smith, A. A. 239, 291
Smith, C. S. 41, 139, 203, 218, 267, 275, 292
Smith, D. W. 20, 31, 38, 40, 41

Smith, G. C. 41
Smith, G. V. 29, 40
Smith, H. G. 51, 72
Smith, H. J. 49, 72
Smith, S. L. 181, 185, 188, 189, 191, 193, 194, 211, 216, 217, 218
Smoluchowski, R. 31, 41
Snoek, J. L. 163, 174
Sommerfeld, A. 50, 51, 52, 72, 143, 174
Sondheimer, E. H. 58, 70, 74, 111, 114
Sorbo, de W. 74
Spedding, F. H. 54, 73
Spencer, J. E. 114
Sperry, P. R. 41, 234, 264, 274, 278, 291
Spillett, E. E. 197, 218
Sproull, W. T. 139
Stamm, K. O. 35, 41
Stanley, J. K. 229, 230, 241, 243, 290
Steigman, J. 291
Stephenson, S. T. 210, 211
Sternheimer, R. 73, 88, 113
Stewart, K. H. 158, 163, 174
Stewart, M. 137
Stickley, E. E. 203, 218
Stokes, A. R. 200, 201, 203, 218, 219
Stoner, E. C. 50, 72, 82, 83, 113, 144, 147, 163, 169, 171, 173, 175
Sucksmith, W. 173, 175
Supek, I. 58, 73
Sutoki, T. 266, 292
Swain, R. C. 73

Tamura, S. 115, 122, 137, 283, 292
Tanaka, K. 139
Taylor 118
Taylor, A. 35, 41, 217, 218
Taylor, G. I. 120, 137, 138, 195, 218, 223, 245, 252, 290
Templeton, I. M. 66, 75
Tennevin, J. 217
Terminassov, J. C. 210, 216, 217, 219
Thomas, J. G. 66, 75
Thomas, R. 137
Thomsen, E. 127, 138
Thomson, J. J. 69, 74
Thorp, J. S. 207, 219
Thorpe, P. L. 198, 209, 218
Tiedema, T. S. 234, 291
Timofeeva, M. N. 193, 218
Tokich, J. L. 40
Tonks, L. 163, 174
Towers, J. (jr.) 292
Trautz, O. R. 40
Treaftis, H. 235, 252, 291
Troiano, A. R. 2, 10, 11, 12, 14, 15, 16, 18, 39, 40
Trombe, F. 54, 73, 81, 113
Tschermak, S. B. 128, 138
Turkalo, A. M. 233, 254, 278, 291, 292
Turnbull, D. 21, 23, 24, 41, 112, 114, 235, 252, 255, 278, 291, 292

Vand, V. 112
Venkateswaran, C. S. 53, 73
Verwey, E. J. W. 112
Vlack, L. H. van 291
Vleck, J. H. van 81, 88, 113, 144, 174
Vogel, R. 127, 138, 267, 292
Vogt, G. 73
Voigt, B. 60, 62, 63, 73
Voigt, W. 183, 217

Waals, J. D. van der 90, 111
Wagner, G. 215, 219
Walker, H. L. 241, 273, 291
Walker, J. G. 157, 174
Ward, R. 230, 235, 248, 252, 278, 291
Warren, B. E. 202, 207, 214, 215, 216, 218, 219
Wassermann, G. 40, 138
Watkins, H. C. 291
Webster, W. L. 158
Weerts, J. 185, 217
Weil, L. 175
Weiss, P. 83, 140, 162, 174
Weiss, P. R. 174
Went, J. J. 82, 113
Wert, C. 167, 174
West, J. 210, 219
Wever, F. 186, 189, 218
Wheeler, J. A. 4, 8, 12, 13, 14, 40
Wigner, E. 84, 113
Wilhelm, J. O. 51, 72, 113
Williams, E. J. 227, 290
Williams, H. J. 141, 155, 157, 158, 159, 163, 166, 174
Williams, R. J. P. 114
Williamson, G. K. 214, 219
Williamson, M. A. 120, 121, 137
Wilson, A. H. 56, 73, 78, 112
Wilson, A. J. C. 200, 201, 211, 218, 219
Wilson, F. H. 138, 278, 279, 280, 292
Winegard, W. 137
Wohlfarth, E. P. 83, 84, 86, 88, 113, 169, 175
Woltjer, H. R. 62, 74
Wood, W. A. 181, 185, 188, 189, 190, 191, 193, 194, 196, 197, 198, 200, 203, 204, 205, 208, 209, 210, 211, 216, 217, 218, 219
Wooster, W. A. 183, 217
Worrell, F. T. 40

Wyllie, G. 112

Yakovleva, E. S. 127, 138
Yakutovich, M. V. 127, 138
Yamamoto, M. 157
Yoshidu, S. 114
Young, J. 23, 29, 30, 41

Zachariasen, W. H. 211, 218
Zapffe, C. A. 133, 139
Zay 292
Zemansky, M. W. 74
Zener, C. 4, 23, 25, 26, 27, 40, 78, 83, 86, 89, 91, 93, 94, 98, 103, 112, 113, 114, 191, 218, 275

VOL. 3

SUBJECT INDEX

Activation energy 5, 22
Alkali metals
— — cohesive energy 87, 88, 91
— — elastic constants 93
— — electrical conductivity 52, 56, 61, 63, 69
— — frequency of absorption edges, calculation 105 *et seq*
— — specific heat, anomalies 52, 55
— — x-ray emission bands 108
Alkaline earth metals, electrical conductivity 56, 64, 66
Aluminium, elastic constants 94, 96, 97
— energy of twin boundaries 288, 313
— grain growth 233, 236, 272, 273
— — — activation energy 249
— — — dependence on strain 238
— — — free energy 249
— lattice spacing changes, size of particles 199
— lattice strain 181, 194
— nucleation 240–242
— orientation after recrystallisation 234
— plastic extension 214, 215
— recovery anneals 243
— recrystallisation 197, 223, 228, 230, 237, 249, 252, 258, 279
— twinning 289
— twins, crystallography 120, 121
— x-ray emission bands 109
— — line broadening impurities 216
Aluminium-copper
— — Guinier Preston zones 33
— — martensitic phases 3
— — martensitic transformation 4, 19
— — precipitation 37
— — strain transformation 25
— — superlattice 33
Aluminium-iron-nickel, precipitation 31, 35
Aluminium-magnesium, grain growth 273
Aluminium-silver
— — orientation 30
— — precipitation 37
— — superlattice 33
Aluminium-zinc, precipitation 37
Anisotropy constants 145 *et seq*
— — cubic metals 147
— — hexagonal metals 147
Anti-ferromagnetic materials 80, 81
Anti-ferromagnetism 80, 81
Antimony, grain growth 266
— twins, crystallography 133
Antimony-silver
— — martensitic transformation 3
— — martensitic transformation, faults 28
Arsenic, twins, crystallography 133
Athermal transformations (*see* Martensitic transformations)
Atomic heats (*see* Specific heats)
Austenite, crystal structure 4, 5, 8
Bainite, orientation 29
Barkhausen discontinuity 162, 163
Beryllium
— cohesive energy 90
— elastic constants 95
— specific heat, anomalies 52
— twins, crystallography 121, 122
— x-ray emission bands 109
Beryllium-copper, Guinier-Preston zones 33
Bismuth, twins, crystallography 133
Bloch's theorem 77
Bloch walls 151 *et seq*
— — anisotropy constants 153
— —energy and width 153 *et seq*
— — exchange energy 153
— — movement 159 *et seq*
— — movement, effect of inclusions 166, 167
Boltzmann's constant 43
Boundaries between different phases 314 *et seq*
— dihedral angles 314, 315
— movement 314, 315
Boundary energy (*see* Energy of interfaces)
Bragg's law 178
Brass, cold-worked, x-ray intensities 215
— grain growth 237 *et seq*, 272 *et seq*
— grain growth, activation energy 251
— limiting grain size 276
— nucleation 242
— paramagnetism 103
— recrystallisation 241
— secondary recrystallisation 279
— strain transformation 25
— twins 118 *et seq*, 132
Brillouin zones 61, 65, 66, 80, 94, 95
— — cubic metals 97
— — hexagonal metals 95
Bulk modulus 90–94

Cadmium, recrystallisation 228
— superconductivity 67
— twins 121 *et seq*, 135
Cadmium-gold
— — martensitic transformations 19, 26, 27
— — strain transformation 25
Cadmium-indium, martensitic transformation 18
Cesium, electrical resistance 55
— electronic transition 55
— volume transition 55
— low temp. anomalous behaviour 61, 63
Chromium-manganese, martensitic transformation 18
Cobalt, anisotropy constants 147
— coercive forces, maximum of particles 169
— direction of magnetization of domains 154

Cobalt (*contd.*)
— ferromagnetic domains structure 155, 157
— martensitic transformation 3, 10, 28, 30
— saturation magnetization 144
— specific heat 51
— transition state 34
Cobalt-copper, precipitation 31
Cobalt-copper-nickel, precipitation 31, 36, 37
Cobalt-iron, anisotropy energy 147
Cobalt-nickel, anisotropy energy 147
— — ferromagnetic domains pattern 157
Coercive force 88, 165 *et seq*
— — effect of inclusions 167
Coercive forces, maximum of particles, iron, cobalt, nickel 169
— — polycrystalline material 170
— — size of particle 168, 169
Coercive force theories 165 *et seq*
Cohesive energy, metals 87 *et seq*
— — alkali metals 87, 88, 91
— — beryllium 90
— — copper, silver, gold 87, 88
— — nickel, palladium, platinum 88
— — transition metals 88, 89
Collective electron approximation 80, 82, 83, 87
— — treatment 77, 78
Conduction, metallic 76, 77
— nickel oxide 79, 80
Congenital twins (*see* Growth twins)
Copper
Copper, cohesive energy 87
— alloys, electrical conductivity 71
— — electron distribution in alloys 98
— — magneto-resistance effect 71
— — x-ray emission from alloys 108
— elastic constants 93, 94
— energy of the bottom of the Fermi distribution 102
— energy of interfaces 223, 256
— energy of twin interfaces 288, 312
— grain growth 254, 273
— — — energies 249
— lattice distortions in filed metals 213
— — spacings after working 197
— — strain, 181, 194
— magnetic properties 81
— nucleation 240, 265
— recrystallisation 231, 237, 249
— recrystallisation, activation energy 252
— secondary recrystallisation 230 *et seq*, 252, 279
— specific heat 51
— strain/stress ratio 185
— surface tension 308, 309
— twin faults 284
— twins 120, 121, 122, 289
— vacant lattice site energy 112
— x-ray intensities after deformation 214
Copper-gold, precipitation 36
Copper-lead, surface tension 309
Copper-magnesium, paramagnetic substances 103
Copper-manganese, martensitic transformation 18
Copper-nickel, specific heats 84
Copper-nickel-iron, precipitation 31
Copper-silicon, martensitic transformation 3
— — martensitic transformation, faults 27, 28
— — strain induced precipitation 38
Copper-silver
— — precipitation 31
— — strain energy 32
Copper-tin, martensitic phases 3
Copper-zinc (*see* Brass)
Cubic metals, anisotropy constants 147
— — Brillouin zones 97
— — energy of interfaces 300, 301
— — growth twins 116
— — lattice strains 195
— — specific heat 55
— — twins, crystallography 118

Debye temperature 45 *et seq*
Deformation texture 281
— twins 117, 121
Demagnetization factor 150
Diamagnetic substances 89
Diamond, specific heat 44
Diffusionless transformations (*see* Martensitic transformations)
Discontinuous precipitation 38
Dislocations 42, 76, 111, 136, 216, 300 *et seq*
— calculations 302 *et seq*
— grain boundaries 112
— limitations of model 305, 306
Domain pattern (*see* Ferromagnetic domain pattern)
Drude-Lorentz theory 50
Dulong and Petit's rule 43
Duralumin, strain/stress ratio 186
— x-ray intensities after rolling 212

Einstein's theory of specific heat 43, 44, 57, 83
Elastic constants 87–98
— — alkali metals 93
— — aluminium 94, 96, 97
— — beryllium, magnesium 95
— — body-centred lattices 93
— — copper, silver, gold 91, 93, 94
— — cubic metals 91
— — hexagonal metals 94, 95, 96
— — nickel 91, 94
— — tungsten 91, 94, 97
— — zinc 95, 96
— strain (*see* Strain)
Elastically strained aggregates 179 *et seq*
Electrical conductivity 55–65, 78 *et seq*
— — alkali metals 52, 56, 61, 62, 64, 65, 69
— — alkaline earth metals 56, 64, 66
— — anomalies 64, 66, 67
— — Einstein model 57
— — of gold, silver 66, 69

Electrical conductivity (*contd.*)
— — effect of electron-electron collisions 65, 66
— — Grüneisen formula 58
— — liquid helium 60, 69
— — ideal metal 57, 58
— — 'ideal' resistance of sodium and lithium 61, 62
— — of magnesium 66, 67
— — quantum theory treatment 57
— — round a dissolved atom 99
— — size effect 69
— — superlattices 71
Electron distribution 98–102
— levels 104, 106, 110
Electronic heat 49, 50, 84, 86
— — transition metals 86
— structure of solids 103 *et seq*
— — — — x-ray spectroscopy 103
Electrons, transition probabilities 106, 107
Energy of interfaces, copper 256
— — — and orientation 31, 38, 294, 298 *et seq*
— — — determination 268, 294 *et seq*, 306 *et seq*
— — — dislocation model 300 *et seq*
— — — driving force for grain growth 267 *et seq*
— — — in faulted crystal structure 34
— — — interpretations 300 *et seq*
— — — in martensitic transformations 3, 20
— — — specific energy of grain boundaries 223, 293
— — — twins 115, 116, 124, 135, 283 *et seq*, 288, 311
Entropy of a Debye solid 60
Exchange energy 141, 143 *et seq*
Excited states, lifetime 109, 110

Ferrite, orientation 29
Ferromagnetic crystals
— — anisotropy constants 143 *et seq*
— — exchange energy 145, 146
— — magneto-elastic energy 148, 151
— — magneto-static energy 145, 150 *et seq*
— domains 150 *et seq*
— — magneto-static energy, effect of inclusions 166
— — pattern 157, 158
— — — cobalt-nickel, iron-silicon, cobalt, nickel 157
— domain structure 145, 155 *et seq*
— — — cobalt 155
— — — iron 155, 158, 159
— — — iron-silicon 163
— — — polycrystalline material 170
— — — single crystal 158
— — wall 160 *et seq*
— — — movement 160
Ferromagnetism 81–83, 140 *et seq*
— and the periodic table 142
Free electrons 79, 84, 86, 88, 95
— energy of 'embryos' 255 *et seq*
Free electrons (*contd.*)
— — differences in martensitic transformation 23, 25, 26
— — — in slip processes 25, 26
Frequency of absorption edges in metals 105 *et seq*

Gold, cohesive energy 87
— elastic constants 94
— electrical conductivity, anomalies 66
— energy of the bottom of the Fermi distribution 102
— lattice distortions in filed metal 213
— — spacing changes, size of particles 199
— magnetic properties 81
— surface tension 307, 308, 309
— twins 121
— alloys, electron distribution 98
Gold-bismuth, superconductivity 68
Grain boundary migration 234, 244 *et seq*, 267, 269, 285
— — — activation energy 246 *et seq*
— — — entropy 246 *et seq*
— — — free energy 245 *et seq*
— — — — — dependence on inclusions 250, 251, 252
— — — theory 244 *et seq*
— growth 222 *et seq*
— — activation energy 234 *et seq*, 245 *et seq*, 272, 273
— — aluminium 237, 249
— — brass 237, 249
— — continuous 270, 272
— — copper 249
— — critical radius of 'embryos' 257
— — definition 222
— — dependence on composition 273
— — — on inclusions 278, 279
— — — on strain 237, 238
— — — on temperature 234 *et seq*, 272
— — driving force 246, 267, 268, 270
— — free energy 223, 248 *et seq*
— — — — dependence on strain 253
— — geometric 269, 270, 271
— — grain boundrary melting 267, 268, 269
— — grain size distribution 277
— — limiting grain size 274, 275, 278
— — mechanism 224 *et seq*, 265 *et seq*
— — orientation 233
— — quantitative observations 271
— — recovery anneal 238
— — after recrystallisation 265
— — rock salt 238, 241, 249
— — silver 249
— — effect of a free surface 277
— — theory 224 *et seq*
— — twins 286
Growth transformation 1, 2, 28 *et seq*
— — twins 116
— — cubic metals 116
— — zinc 116
Guinier-Preston zones 33
— aluminium-copper, beryllium-copper 33

Hafnium, superconductivity 67
Hardness, twins 120
Heat of solution in alloys 101
Hexagonal metals
— — anisotropy constants 147
— — Brillouin zone 95
— — elastic constants 94, 95, 96
High frequency resistance 70

Ideal electrical resistance 57, 62
Impurity scattering 56
Indium-lead, superconductivity 68
Indium-thallium, martensitic transformation 2, 16, 18, 19, 39
Interface energy (*see* Energy of interfaces)
Ions, exchange interaction 92
Insulators 80, 104
Iron, coercive force 167, 169
— ferromagnetic domain structure 151, 155, 158, 159
— grain growth 273
— lattice distortion in filed metal 213
— lattice strain 194
— magnetic properties 146, 154, 173
— recrystallisation 228
— saturation magnetization 144
— specific heat 51
— strain/stress ratio 185
— twins 121, 128
Iron-manganese
— — martensitic structure 3
— — strain transformation 25
Iron-nickel, anisotropy constants 147
— — martensitic transformation 5, 26, 27
— — orientation 29
— — recrystallisation 231, 237
— — strain transformation 25
— — twins 121
Iron-silicon, anisotropy constants 147
— — ferromagnetic domains pattern 157, 163
— — energy of twin interfaces 312
— — single crystal 295

Lattice distortions in filed metals 213
— — from x-ray lines intensities 211 *et seq*
— spacing, changes 197, 198, 199
— — — copper, molybdenum, nickel, silver 197
— — — size of particles 199
— strains 180 *et seq*
— — aluminium, copper 181, 194
— — cubic metals 195
— — iron, magnesium, nickel 194
— — residual 189, 190, 191, 192, 193, 194, 195, 196
— — steel 192, 195
Lead, interfacial energy 299, 303
— preparation of single crystals 295 *et seq*
Lead-silver, paramagnetic substances 103
Lifetime of excited states 109
Lithium
— absorption spectrum 107
— binding energy 88
Lithium (*contd.*)
— electrical conductivity 61, 62
— martensitic transformation 3, 28
— specific heat 53
— strain transformation 25
— transition state 34
— x-ray emission bands 108
Lithium-magnesium
— — martensitic transformation, faults 28
— — strain transformation 25
London-Heitler approximation 77 *et seq*

Magnesium, cohesive energy 90
— elastic constants 95
— electrical conductivity 66, 67
— lattice strain 194
— twins 117, 121–124
— x-ray emission bands 109
Magnetic hardness 172, 173
— properties 81 *et seq*
— — cobalt alloys 82
— — copper-magnesium 90
— — ferrites 83
— — transition metals 81, 82, 89, 146
— substructure 151 *et seq*
Magnetization, changes in dimensions 148
— direction 154
Magnetic substructure, 'Bloch walls' 151 *et seq*
Magneto-resistance effect 71
Magnetostriction 147, 148
Manganese, specific heat 51
— -selenide, -telluride, specific heat anomalies 55
Martensite, plates 19, 21, 24
— rate of formation 5
Martensitic dislocation distortion 24
— structures 3, 4, 5, 8
— transformation 1 *et seq*
— — activation energy 5, 22
— — aluminium-copper 4, 19
— — antimony-silver 3, 28
— — atom movements 5, 8, 9
— — cadmium-gold 19, 24, 26, 27
— — cadmium-indium 18
— — chromium-manganese 18
— — cobalt 3, 10, 28
— — copper-manganese 18
— — copper-silicon 3, 27, 28
— — distortion 23, 24
— — effect of cooling 2, 3
— — — — heating 2
— — — — — thermal and mechanical treatment 2
— — faults 27, 28
— — — free energy 27
— — — spontaneous transformations 27
— — — indium-thallium 2, 16, 18, 19
— — — iron-carbon 4, 16, 17
— — iron-nickel 5, 26, 27
— — lithium 3, 28
— — — lithium-magnesium 28
— — mechanism 3 *et seq*
— — orientation relationships 6, 8, 11, 13, 14

Martensitic dislocation distortion (*contd.*)
— — silver-tin 3, 28
— — strain energy 27
— — — transformations 25, 27
— — zirconium 5, 9
Matthiessen's law 56
Mercury, specific heat, anomalies 52
— twins, crystallography 133
Metallic conduction 76 *et seq*
Metastable states (*see* Transition states)
Molar heat capacities (*see* Specific heat)
Molybdenum, lattice spacing, changes after rolling 197
— x-ray intensities after rolling 212

NERNST's heat theorem 43
Nernst-Lindemann formula 44, 49
Nickel, anisotropy constants 147
— coercive forces, maximum of particles 169
— elastic constants 94
— ferromagnetic domain pattern 157
— lattice distortion in filed metal 213
— lattice strain 194
— lattice spaces after working 197
— magnetic properties 146, 154, 169
— saturation magnetization 144
— specific heat 50
— oxide, electrical conductivity 78, 79
Nucleation 1, 2, 28 *et seq*, 223 *et seq*, 239 *et seq*, 258
— and growth transformations 1, 20, 24, 28 *et seq*
— block hypothesis 259–263
— dependence on grain size 244, 258
— — — orientation 258, 280
— — — purity 243
— — — strain 242, 258
— — — temperature 241
— — — time 240, 258
— frequency 223 *et seq*
— inclusions at grain boundaries 264
— in secondary recrystallisation 264
— texture inhibition of grain growth 265, 279
— theory 224 *et seq*, 255 *et seq*

ORDER-DISORDER transition 55, 71
Orientation 29
— aluminium-silver 30
— bainite 29
— cobalt 30
— ferrite 29
— grain growth 233
— iron-nickel 29
— lattice strain 180, 196
— secondary recrystallisation 230
— single crystals 295 *et seq*
— stress 194

PALLADIUM, specific heat 51
Palladium-silver, diamagnetic substances 89
Paramagnetic substances 81, 88, 103
Pauli exclusion principle 57
Permeability, ferromagnetic 173
Planck's constant 43
Plastic deformation 2, 188 *et seq*
— — in precipitation 39
Plastically strained aggregates 186 *et seq*
Platinum, specific heat 51
Precipitation from solid solutions 28, 30, 31, 32, 33, 35, 36, 37
— aluminium-copper (silver, zinc) 37
— aluminium-iron-nickel 31, 35
— cobalt-copper-nickel 31, 36, 37
— copper-gold 36
— copper-nickel-iron, copper-silver 31

QUANTIZATION of energy 43
— Einstein model 43

RAMAN lattice theory 52
Rare earth metals, specific heat, anomalies 54
Recovery 220 *et seq*, 250
— anneals 243
— definition 220
— energy 223
Recrystallisation 220 *et seq*
— aluminium, cadmium, copper, iron, tin 228, 230
— definition 221
— dependence on impurities 239
— dependence on strain 252, 253
— distribution of nuclei 243
— iron-nickel, rock salt 231, 233, 236, 237
— laws 222
— nuclei 254 *et seq*
— textures 279–282
— — mechanism 279
— — oriented growth 279–282
— theory 223 *et seq*
— twins 120, 282, 283
Relief effects 5, 8, 10, 14, 18
Resistivity (*see* Electrical conductivity)
Rhodium, lattice distortion in filed metal 202, 213
Rubidium, low temp. anomalous behaviour 61, 63

SATURATION magnetization 144, 146, 171
Schrödinger equation 77
Secondary recrystallisation 221, 232 *et seq*, 278
— — copper, silver 230, 237
— — driving force 278
— — nucleation 264
— — orientation 230
Semiconductors 78, 79
Silver
— alloys, electron distribution 98
— cohesive energy 87
— diamagnetism 89
— elastic constants 94

Silver (*contd.*)
— electrical conductivity 66, 69
— energy of the bottom of the Fermi distribution 102
— grain growth 249
— growth twins 116
— interfacial energy 297 *et seq*
— lattice spacing after working 197, 215
— lattice spacing changes, size of particles 199
— magnetic properties 81
— secondary recrystallisation 237, 249
— surface tension 307, 309, 311
Silver-tin, martensitic transformation 3, 28
Single crystal preparation 295 *et seq*
Slip 25, 117, 119, 313, 314
— activation energy 314
Specific heat 42 *et seq*, 84 *et seq*
— — of alkali metals 47, 52, 53
— — anomalies 47–55
— — — beryllium, mercury 52
— — — diamond 43, 47
— — — manganese-selenide, -telluride 55
— — — internal transition 47
— — — and lattice structure 48
— — — rare earth metals 54
— — — Schottky function 47, 48
— — — sodium 52
— — — tin (grey) 47
— — cobalt, copper, iron, nickel, manganese, palladium, platinum, tin 50, 51
— — copper-nickel 86
— — Debye model 45 *et seq*
— — diamond 44
— — and frequency density 49
— — influence of lattice structure 48
Steel lattice strain 195
— stress/strain ratio 188, 189, 190 (*see* Iron)
Strain, elastic 32, 301, 302
— energy 31, 32, 257
— induced precipitation 38
— plastic effects 24 *et seq*
Strain/stress ratio 180 *et seq*
— — — comparison of experimental and theoretical values 185
— — — copper, duralumin, iron, steel 185, 186, 188, 189, 190
—transformations 25
Stresses, caused by etching 193
— dependence on orientation 194
— in thin layers 193
Superconductivity 67 *et seq*, 84
— cadmium, hafnium 67
— gold-bismuth, indium-lead 68
— solutions of sodium in ammonia 69
— upper limits 68
Surface tensions 294 *et seq*, 306 *et seq*
— — measurement (copper, silver, gold) 306 *et seq*
Susceptibility, paramagnetic substances 81

Tantalum, x-ray intensities after rolling 212
Thermal transformations (*see* Nucleation and Growth transformation)
Third law of thermodynamics 43
Tin, energy of interfaces 303 *et seq*
— preparation of single crystals 295 *et seq*
— recrystallisation 228
— slip 313, 314
— specific heat 51
— twins, crystallography 134
Transformations, classifications 1
Transition metals, cohesive energy 88, 89
— — specific heat 85
— probabilities of electrons 106 *et seq*
— states 34 *et seq*
Tungsten, elastic constants 94, 97
— grain growth 273, 274
— twins, crystallography 132
— x-ray intensities after rolling 212
— x-ray line broadening: impurities 216
Twin interfaces 311 *et seq*
— mechanisms of formation 121, 122, 136, 283 *et seq*
Twins (twinning) 115 *et seq*
— absence in cast metals 285
— aluminium, beryllium, cadmium, copper, iron, magnesium, zinc 120–128
— copper-zinc, iron-nickel 118, 121
— critical stress 127
Twins (twinning), crystallography, antimony, arsenic, bismuth, mercury, β-tin, tungsten 132, 133, 134
— — — beryllium, cadmium, copper, magnesium, zinc 120, 122, 124
— — — cubic metals 118, 121, 136
— — — hexagonal metals 122
— — — rhombohedral metals 133
— cubic metals 118, 121, 132
— definition 115
— deformation 124 *et seq*
— disappearance 286, 287
— energy 135
— faults 119, 121, 136, 284, 289
— grain boundary migration 254
— grain size 286
— growth 285, 286
— hardness 120, 134
— identification 117
— impurities 123
Twinning movement 129 *et seq*
— — mechanism 130 *et seq*
— physical conditions 115
— shear 125, 126
— silicon ferrite 129
— variation of intensity 289
— x-ray diffraction 135

Umklapp-Prozess 64, 65

Vacant lattice site energy 112

Wave function of a crystalline solid 77
Widmannstätten structure 30, 34

X-RAY diffraction lines
— — — broadening 186, 196, 200 *et seq*
— — — — aluminium 207, 216
— — — — brass 202, 208
— — — — causes 200–210
— — — — copper, nickel, rhodium 202
— — — — definition 201
— — — — experimental measurement 201
— — — — tungsten 203
— — — intensity 210 *et seq*
— — — — aluminium, copper 214
— — — — duralumin 212
— — — — molybdenum, tantalum, tungsten, 212
— — — — theoretical relations 211
— — — movement 187 *et seq*
X-ray diffraction lines (*contd.*)
— — — — peaks 179, 186, 187, 196, 198
— — — shape 178
— emission, alkali metals, aluminium, beryllium, magnesium 109
— — alloys 108

ZINC
— elastic constants 93, 96
— grain growth 266, 273
— growth twins 116
— recrystallisation 233
— twins 123, 124, 125, 127, 135
Zirconium, martensitic transformation 5, 9

VOL.
3

VOL
3

FOREWORD TO VOLUME I

The study of the physical properties of metals has developed through a number of stages. The first was that in which the mechanical properties were correlated empirically with the heat treatment to which the metal had been subjected and, sometimes, to the chemical composition. At this stage the successful treatment of metals was an art, in the sense that experience rather than understanding led to the most satisfactory results. The next stage, in which the internal structure of the metal was examined, was based originally on the use of the microscope and it was found that many experimental facts could be explained in terms of effects that were of the right size to be seen under magnifications of less than about two thousand. The development of the x-ray diffraction techniques allowed phenomena of a smaller order of magnitude to be examined, and much of the existing information was found to be comprehensible in terms of the geometry of the crystal structure of the various phrases that were visible under the microscope.

More recent development can perhaps best be discussed by a division of the field into what may be termed 'statics' and 'dynamics'. Under the former heading is the study of the conditions which govern the structure of a metal or alloy when it is in thermodynamic and mechanical equilibrium. The theories of the phrases that are present in equilibrium and of the elastic constants have made remarkable progress in terms of rapidly developing theory of the part played by electrons on the metal.

Under the heading 'dynamic' effects we may include both the conditions governing the approach to equilibrium in respect of the phrases that are present, in which diffusion plays an important part, and the response of a metal to forces which are sufficient to cause non-recoverable or plastic mechanical deformation.

These and associated subjects have advanced so rapidly that it has become difficult for research workers in one part of the field to remain up to date in other branches. It is the purpose of these volumes, which will appear as an annual series, to present authoritative reviews of the present state of knowledge in specialized aspects of the field that includes both physical metallurgy and metal physics. It is not intended that any one volume should form a complete textbook on these subjects. It is hoped rather that a few subjects of current interest should be discussed rather fully so as to cover, in the course of several years, all the more important aspects in which progress is being made. In order to make the series reasonably self contained it is proposed that the necessary 'historical' background should be included the first time a particular subject is discussed. Subsequent articles on such subjects will generally only cover the more recent progress.

B. Chalmers

ACKNOWLEDGMENTS

THE authors and the publishers wish to thank the many scientists, publishers and authorities concerned for permission to use previously published illustrations and data, a list of which (with authors and source) appears below. While every effort has been made to obtain permission in every case where copyright material has been used, it is hoped that any inadvertent omission from this list will be excused by those concerned.

American Institute of Mining and Metallurgical Engineers
DUNN, C. G. *Trans.* 185 (1949) 72 *Figure 2 f p 296*

Cambridge University Press
FOWLER, R. H. Statistical Mechanics, 1929 *Figure 1 and Table IV on pp 46/7*

Akademische Verlagsgesellschaft, Leipzig
MEISSNER, W. Handbuch der exper. Physik, 1935 *Figure 4 on p 59*

Nature
GARROD, R. I. 1950 (165) 241 *Figure 7 on p 190*
BRAGG, W. L. 1942 (149) 511 *Figure 9 on p 205*
PATTERSON, M. S. and OROWAN, E. 1948 (162) 991 *Figure 11 on p 209*

Institute of Physics
RACHINGER, W. A. *J. Sci. Instrum.* 25 (1948) 254 *Figure 1 on p 178*
STONER, E. C. *Rep. Progr. Phys.*, London 1948 *Figure 11 on p 161*

Institute of Metals
HALL, W. H. *J.* 1950 (75) 1130 *Figure 10 on p 206*
GREENOUGH, A. P. and KING, R. *J.* 79 (1951) 415 *Figure 5e on p 299*

Journal of Applied Physics
AVERBACH, B. L. and WARREN, B. E. 20 (1948) 1068 *Figure 13 on p 215*

Journal of Metals
DUNN, C. G. *et al.* (1950) 1245 *Figure 5a and b on p 298*

Oxford University Press
MOTT, N. F. and JONES, H. Theory of Properties of Metals and Alloys *Figure 7 on p 71*

Physica
BOZORTH, R. M. 15 (1949) 209 *Figure 9 on p 159*

Physcial Review
WEISS, P. R. 74 (1948) 1493 *Figure 1 on p 143*
BOZORTH, R. M. and WALKER, J. G. 79 (1950) 888 *Figure 7 f p 156*
KINKSTRA, L. J. and WERT, C. 79 (1950) 979 *Figures 17 and 18 on pp 167/8*
MARTIUS, U. M., GOW, K. V. and CHALMERS, B. 81 (1951) *Figure 8 f p 156*

Physical Society
BRINDLEY, G. W. *Proc.* 52 (1940) 118 *Figure 12 on p 212*

Reviews of Modern Physics
KITTEL, C. 21 (1949) 541 *Figure 3 on p 151; Figures 4–6 on pp 153–6; Figure 16 f p 166 and Table IV on p 169*

The Royal Society
SMITH, S. L. and WOOD, W. A. *Proc.* A.181 (1942–3) 76 *Figures 5 and 6 on p 188*
AUST, K. T. and CHALMERS, B. *Proc.* A.201 (1950) 210 *Figure 3 on p 296 and Figure 5c on p 298*
MACDONALD, D. K. C. and MENDELSSOHN, K. *Proc.* A.202 (1950) 116 *Figure 5 on p 63*
AUST, K. T. and CHALMERS, B. *Proc.* A.204 (1950) 364 *Figures 5d, 7 and 8 on pp 299 and 303*

Springer-Verlag, Berlin
SIMON, F. E. Ergebn. exakt. Naturwiss. 9 (1930) 222 *Figure 2 on p 48*

VOL 3

VOL.
3

VOL.
3

1

CRYSTALLOGRAPHY OF TRANSFORMATIONS

J. S. Bowles and C. S. Barrett

A WEALTH of information has been accumulated during the last twenty years on the crystallographic aspects of phase transformations in the solid state. The purpose of this paper is to give a general review of this work and to consider in detail the contribution it has made to our knowledge of the atom movements accompanying the transformations, in the transforming material, in the boundaries of the transforming regions and in the surrounding matrix.

It is customary to classify the transformations in metals into two types. In the one type, the so called martensitic transformations, the new crystal is formed from the parent crystal by atom movements which are so cooperative and regular that they produce a change in the shape of the transforming region. There is little or no interchange in the position of neighbouring atoms during the transformation. In the second type, the nucleation and growth transformations, the new phase grows from a nucleus by thermally activated diffusion of atoms from the parent phase to the new phase. Interchange of position of neighbouring atoms does occur as they cross the interphase boundary and there is no change in shape of the transforming region.

This classification is somewhat arbitrary, for the characteristics that have been chosen as the definitive ones may not represent the most fundamental differences between the two types. The final selection of the most appropriate definitions and names for the two types of transformations awaits a more complete understanding of the transformation mechanisms. The choice of terms used here is justified by their widespread use in the past. Martensitic transformations have also been called diffusionless and athermal; these names emphasize the idea that the transformation involves no thermally activated transfer of atoms at the interphase boundary and no composition change in the transforming region. Such names, however, encounter the objection that diffusion within the parent phase itself may in some cases be a controlling factor even though diffusion at the boundary is not. Nucleation and growth transformations have also been termed diffusion processes and thermal transformations, names which bring out the occurrence of thermally activated transfer of atoms to the growing phase.

Much attention in the present discussion is directed to the atom movements and lattice distortions in the two transformations, but this

is not intended to imply that these are necessarily the most convenient criteria for distinguishing in the laboratory one type of transformation from the other. An exceedingly useful criterion for this purpose is the fact that nucleation and growth processes go to completion isothermally, whereas martensite transformations rapidly come to a halt when the rate of cooling or heating is brought to zero, and the transformation process is resumed only if the temperature change is resumed. Other characteristics are listed in the following section.

MARTENSITE TRANSFORMATIONS

General Characteristics

The distinctive features of martensitic transformations, which have been reviewed in detail by TROIANO and GRENINGER[1] and others,[2–6] may be stated concisely.

1. Individual martensite crystals of plate shape, or of lens shape as in *Figure 1*, form on crystallographic planes. In most alloys the crystals form within times of the order of 10^{-4} seconds or less, even at low temperatures. The transformation occurs without change of composition of the transforming regions. Some examples have been observed in which the plates broaden relatively slowly, but even in these the original plate is observed to form very quickly (the indium-thallium transformation is an example[7]).
2. Transformation occurs only when the specimen is cooling and there is negligible transformation if cooling is stopped. In most instances the reaction proceeds only by the formation of new plates, not by continued growth of plates already formed.
3. The transformation begins at a temperature (M_s) that is not depressed by increasing the cooling velocity, but is dependent upon composition and prior thermal and mechanical history.
4. The low temperature phase reverts to the original high temperature phase in a similar manner during heating, unless competing reactions set in, such as nucleation and growth of the original phase.
5. The martensite crystals form in many specific orientations within a parent crystal, but on heating these revert to the original single crystal in which they formed.
6. Visible tilting and distortion of a polished surface is caused by the transformation.
7. Plastic deformation is effective in forming martensite above the M_s temperature, provided the temperature does not exceed a critical value (M_d). Cold work tends to suppress the transformation when a cold-worked specimen is subsequently cooled.

VOL 3

VOL.
3

Figure 1. Martensite crystals in a large grain of a partially transformed alloy of iron-30 per cent nickel (polished and scratched before transformation and unetched). The distortion from the transformation has bent the scratches and tilted the surface (Magnification 150 ×)

VOL
3

But cooling while a stress is applied increases the amount of transformation at each temperature, according to SCHEIL[8] and to CHANG and READ.[9] MCREYNOLDS[10] found no effect on M_s of stresses that were purely elastic.

8 Stabilization of the high temperature phase results in some alloys if cooling is sufficiently slow or if a specimen is held for a sufficient time in a suitable temperature range; the result of stabilization is to lessen the amount of transformation that occurs during cooling to a given temperature.

9 The crystal structure of a strain-induced martensite is not necessarily the same as that of the martensite which forms spontaneously in the same specimen, and the structure may vary slightly or even change completely with varying composition of the parent phase. Two different martensitic phases may co-exist in an alloy, as in copper-aluminium,[11] copper-tin[12] and iron-15 per cent manganese.[13]

10 Transformations to hexagonal close-packed or face-centred cubic structures and to some others have been found to yield an imperfect form of the structures in which faulty stacking of the atomic layers is frequent. This occurs in cobalt, where the transformation from face-centred cubic to hexagonal close-packed produces faults in the stacking of the basal planes on the average about ten to fourteen planes apart,[14] and in lithium, where the body-centred cubic to hexagonal close-packed transformation produces even more closely spaced faults.[15] Strain-induced precipitation in copper-silicon alloys is productive of much faulting and the same is true of certain alloys of the silver-tin and silver-antimony systems.[17] Each of these systems provides conditions such that faulty stacking does not require the formation of interfaces of high energy.

11 The curve of amount transformed as a function of temperature on cooling below M_s is not retraced on heating, for rapid reversion during heating begins only at temperatures higher than M_s. Thus there is marked temperature hysteresis of a magnitude that depends upon the strain energies and interface energies involved. Cooling again after partial reversion brings a new M_s into play (M_s') which is somewhat higher than the original M_s[18].

Diffusionless Characteristics—It is generally agreed that martensite transformations do not involve any interchange in the positions of pairs or rings of neighbouring atoms, the total displacement of any atom relative to its neighbours being smaller than the atomic radius. Of the considerable amount of experimental evidence available to substantiate

this view, possibly the most convincing is the persistence of ordered arrangements of atoms throughout the transformation. It is found, for example, that if the parent phase contains a superlattice the martensitic phase also contains a superlattice. The martensite transformation in the copper-aluminum alloys offers an example of this behaviour.[19]

This behaviour also applies to ordered arrangements of atoms in interstitial solid solution. It has been pointed out by LYMAN[20] and by JASWON and WHEELER[21] that the arrangement of carbon atoms on the interstitial sites in the body-centred tetragonal martensite of iron-carbon alloys is precisely the arrangement which is expected if the carbon atoms do not move from the interstices they occupy in the parent phase, face-centred cubic austenite.

In austenite the carbon atoms are situated at the midpoints of the cube edges and in the equivalent positions that are at the centres of the cubes. However, the face-centred cubic structure referred to different axes is identical with a body-centred tetragonal structure having an axial ratio of $\sqrt{2}$; referred to these axes the carbon atoms in austenite occur at the midpoints of the four longer edges of the unit cell and at the centres of the square bases, which are equivalent positions. It has been shown[22, 23] that these are also the positions occupied by the carbon atoms in body-centred tetragonal martensite so that the transformation from austenite to martensite can be regarded simply as a distortion of one body-centred tetragonal structure into another, the interstitial carbon atoms remaining in the same positions relative to the neighbouring iron atoms. This inheritance of the position of carbon atoms is undoubtedly the explanation of the tetragonality of martensite for in their inherited positions all carbon atoms tend to stretch every unit cell in a crystal of martensite in the same direction. If the carbon atoms had moved into all interstices at random during the transformation, the situation would be different—the resulting structure would be body-centred cubic.* The essential point is that not all equivalent interstices in a body-centred cubic structure are derived from equivalent interstices in the face-centred cubic structure.

Further evidence suggesting that martensite transformations only involve small displacements of atoms relative to their neighbours is found in the change in shape of the transformed volume. If a polished surface is prepared on a sample of the parent phase the transformation produces characteristic upheavals on the polished surface which effectively render the martensitic phase visible. These relief effects

* ZENER[24] has pointed out that martensite retains its tetragonality for times which are very much longer than the average time (about one second at room temperature) that a carbon atom stays in a particular interstitial position. He proposes that this is due to the martensite being an ordered interstitial superlattice, at a temperature below the critical ordering temperature *i.e.* the tetragonal unit cell has lower free energy than the cubic cell that would result from disordering.

will be considered in more detail later. For the present it will be sufficient to point out that any transformation in which the atoms do not interchange position must be accompanied by a change in shape of the transformed volume and it is this change in shape that is responsible for the observed relief effects.

The remaining evidence consists of observations which indicate that the activation energy for the unit process in the transformation, whatever its nature, is very small compared with the activation energy for diffusion at the same temperature. From this it is concluded that the atom displacements are smaller than an interatomic distance. These observations are *1* martensite transformations are not accompanied by any change in composition so there is no need for long range diffusion. *2* Martensite plates form with extreme rapidity even at temperatures at which the mean time of stay of atoms on the lattice points is very long. The times of formation of martensite plates in a 71 : 29 iron-nickel alloy and in zirconium have been measured by FÖRSTER and SCHEIL[25] who found values of less than $0{\cdot}7 \times 10^{-4}$ sec and $3{\cdot}4 \times 10^{-4}$ sec respectively. The maximum possible speed is of course the speed of propagation of a sound wave in the material and it may well be that this is the actual rate of formation. In any event, the transformations are in many cases accompanied by an audible click. This is true even at temperatures near 4°K.[26] *3* Martensite transformations do not proceed at constant temperatures as a thermally activated process does, but cease when cooling is arrested.*

Atom Movements—Since martensite transformations are accomplished without interchange in the positions of neighbouring atoms, it follows that the observed orientation relationships between the parent structure and the martensitic structure, and the observed change in shape of the transformed volume, are a direct consequence of the atom movements that occur during the transformation. The atom movements can therefore be deduced from the crystallographic data.

The first attempt to describe the shifting of atoms in a martensite transformation was made by BAIN,[27] who proposed a mechanism for the transformation from face-centred cubic austenite to body-centred tetragonal martensite in steel. Bain noted that this transformation could be regarded, as was pointed out previously, as a distortion of one body-centred tetragonal structure with an axial ratio of $\sqrt{2}$, into another having the axial ratio of martensite. He therefore proposed that the transformation merely involves a compression of the **c** axis, and an expansion of the **a** axis until the martensite axial ratio is reached. Bain also proposed from the observed dependence of the axial ratio on carbon content, that it is the interstitially dissolved carbon atoms which prevent the axial ratio from going completely to unity.

* However, see the comment on this point in the footnote on p 22.

Table I. Orientation Relationships and Habit Planes in Martensite Transformations

System	*Composition*	*Transformation on Cooling*	*Orientation Relationships*	*Habit Plane in Parent Phase*	*Remarks and References*
Fe-C	0–0·4% C	*FCC → BCT*	*Presumably as for 1·4%C*	*Laths ‖ {110}γ arrayed on the {111} γ planes*	28, 29 *This has been referred to as a {111} habit plane but is probably just a further degeneration of the {225} plates into needles*
	0·5–1·4%C	*FCC → BCT*	*{111}γ ‖ {110}α ⟨110⟩γ ‖ ⟨111⟩α This is known as the Kurdjumow-Sachs relationship*	*{225}γ With decreasing C% the plates degenerate into laths with axis ‖ ⟨110⟩γ*	28–32 *Orientations by pole figure method*
	1·5–1·8%C	*FCC → BCT*	*Unknown*	(259)	28 *Lattice relationships have not been determined in this range. A deviation from the low carbon relationship is suspected from the difference in habit plane*
Fe-Ni	27–34% Ni	*FCC → BCC*	*{111}γ ‖ {110}α ⟨211⟩γ ‖ ⟨110⟩α This is known as the Nishiyama relationship*	*Approx.* (259) *but wide scatter*	28, 32–34 *Orientation determination by pole figure method. The Kurdjumow-Sachs relationship is found above room temperature and Nishiyama below, according to* 34
Fe-Ni-C ..	1·2% C 11·5% Ni	*FCC → BCT*		*Approx.* (259)	28
	0·8% C 22% Ni	*FCC → BCT*	*As in Fig.* 4	*Approx.* (259)	35 *Precision orientation determination*
Fe-Mn ..	1–15% Mn	*FCC → BCC (α′)*	*Unknown*	*Unknown*	13
	13–25% Mn	*FCC → CP Hex. (ε)*	*Unknown*	*Unknown*	13
Cu-Zn ..	40% Zn	*BCC → Structure unknown*	*Unknown*	(155) *or* (166)	36
	40% Zn + 1% Pb + Sn	*BCC → FCT*	*Unknown*	*Unknown*	37
Cu-Sn		*BCC → Structure unknown*	*Unknown*	(199)	26

		β′ is a distorted CPH structure with the [001] 2° *from normal to the* (001) *plane. Angle between* (100) *and* (010) *differs by* 1° *from* 120°		*from* (110)	
	12·9–14·7% Al	*BCC → CPH γ′* *The CPH phase becomes distorted into an orthorhombic lattice with increasing* Al%	*As in Fig.* 6	*Approx.* (122) 20° *from* (110)	37–40, 19 *Precision orientation determination*
Lithium ..	*'Pure'*	*BCC → CPH* *The hexagonal layers are in faulty stacking sequence*	{110} ‖ {00·1}CPH ⟨111⟩ 3° *from* ⟨11·0⟩CPH	(144), *which is* 10½° *from* (110)	42, 15, 43
Au-Cd ..	47·5 *at.* %Cd	*BCC → Orthorhombic β′*	(011)*β* ‖ (001)*β′* [111]*β* ‖ [110]*β′*	(133)	9
Zirconium ..	*'Pure'*	*BCC → CPH*	{110} ‖ {00·1} ⟨111⟩ 0° to 2° *from* ⟨11·0⟩	*Unknown*	44
Cobalt	*'Pure'*	*FCC → CPH*	{111 ‖ {00·1} ⟨110⟩ ‖ ⟨11·0⟩	(111)	44, 45 *Habit plane is from unpublished work by the authors*
In-Tl	20·75 *at.* %Tl	*FCC → FCT*	*As in Fig.* 10	(110)	7 *Analogous transformations probably occur in the systems* In-Cd[46], Cu-Mn[47] *and* Cr-Mn[48]

* The directions lie in the parallel planes

Subsequent determination of the orientation relationship, habit planes, and change in shape of the transformed volume have shown quite clearly that this transformation does not occur in this way. However, it is interesting to note that the correspondence between lattice positions before and after transformation that was suggested by Bain has been retained as a common feature of all mechanisms that have since been suggested for the transformation.

The next stage in the development of theories of atom movements was the determination of the orientation relationships that exist between parent and martensitic phases, and the postulation of mechanisms which attempted to produce the correct martensite

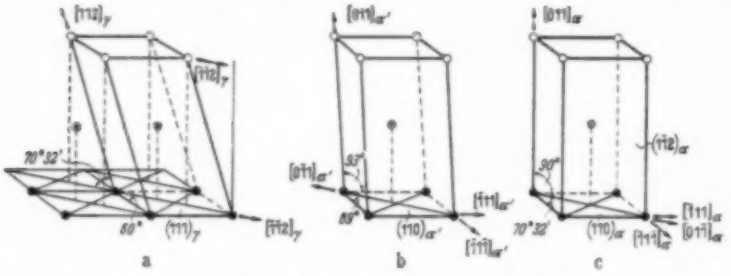

Figure 2. Atom movements postulated by Kurdjumow and Sachs for the transformation from A austenite (γ), to B tetragonal martensite (α′), and C to cubic ferrite (α). The bases of the cells indicated are (111) in γ and (110) in α′ and α

structures and the correct orientation relationships to the parent lattice. The available data on orientation relationships in martensite transformations are summarized in *Table I.*

KURDJUMOW and SACHS[31, 49] determined the orientation relationship between austenite and martensite in 1·4 per cent carbon steel, and proposed a transformation mechanism to account for this relationship. They proposed that martensite is formed by the two consecutive shears $(111)_A\ [\bar{1}\bar{1}2]_A$ and $(1\bar{1}2)_M\ [\bar{1}11]_M$. The movement of atoms produced by these shears is illustrated in *Figure 2.* This mechanism leads to the correct orientation relationship and to approximately the correct structure.* However, as was found subsequently, it is not consistent with the observed habit plane and relief effects on polished surfaces.

A slightly different orientation relationship was found in a 70 : 30 iron-nickel alloy by NISHIYAMA,[33] who accordingly proposed a somewhat different transformation mechanism. Nishiyama proposed that

* Certain readjustments of atom positions must occur before the new structure has the correct dimensions. Moreover, the later geometrical analyses of this transformation by JASWON and WHEELER[21] and by BOWLES[50] show that these two shears are not capable of producing an exactly body-centred cubic structure.

this transformation occurs by means of a single shear of 19° 28′ on $(111)_A$ $[\bar{1}\bar{1}2]_A$. This is the same as the first step of the Kurdjumow-Sachs mechanism. The Kurdjumow-Sachs second shear, although it would produce approximately the desired cubic structure, is not permissible in this case since in the Nishiyama relationship the $[\bar{1}\bar{1}2]_A$ direction is parallel to the $[1\bar{1}0]_M$ direction. Thus the enlargement of the basal angle of *Figure 2* from 60° to 70° 38′, which was accomplished by the second shear in the Kurdjumow-Sachs mechanism, must be

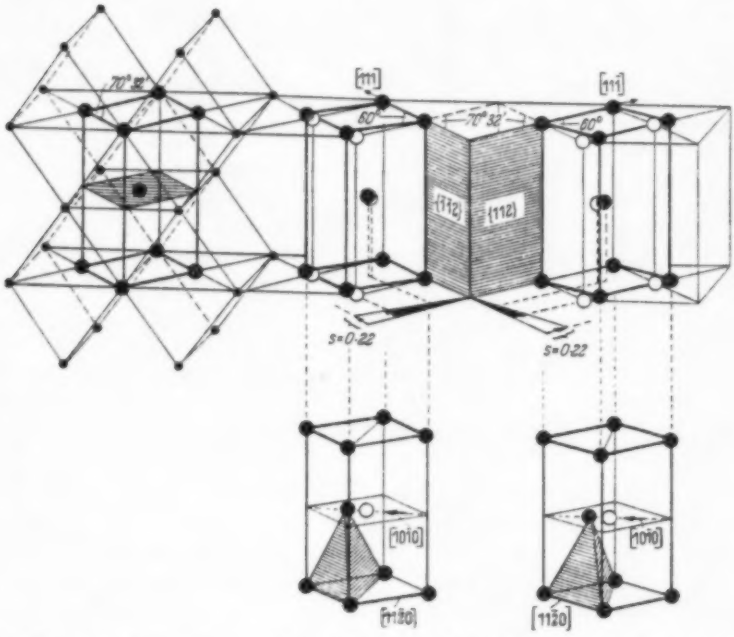

Figure 3. Atom movements postulated by Burgers for the body-centred cubic to close-packed hexagonal transformation in zirconium. On the left are body-centred cubic cells, and in heavy lines a cell having $(\bar{1}01)_{bcc}$ *as a base and* $\{112\}_{bcc}$ *as vertical sides, the latter serving as shear planes when the two hexagonal cells at the lower right are produced*

accomplished by 'readjustments' in the Nishiyama mechanism. This mechanism also leads to the observed orientation relationship but again is not consistent with the observed habit plane and relief effects.

From a study of the orientation relationship in zirconium (*Table I*) BURGERS[44] proposed that the martensite transformation of body-centred cubic (bcc) to close-packed hexagonal (cph) occurs by a heterogeneous shear on the system $(112)_{bcc}$ $[11\bar{1}]_{bcc}$. This distortion is illustrated in *Figure 3*. The crystallographic principle underlying this proposal is that the configuration of atoms in the (112) plane of a

body-centred cubic structure is exactly the same as that in the $(10\bar{1}0)$ plane of a close-packed hexagonal structure based on the same atom radius. The pattern on both these planes is a rectangle, $d \times (2\sqrt{2}/\sqrt{3})d$, where d is the atom diameter. Thus a hexagonal close-packed structure can be built up from a body-centred cubic structure by displacing the (112) planes relative to each other. It should be noted, however, that the array on the $(110)_{bcc}$ planes (see *Figure 3*) cannot be converted into an exact hexagonal array merely by the pure shear proposed by Burgers since the spacings of the $(112)_{bcc}$ planes and $(10\bar{1}0)_{eph}$ planes into which they transform are not equal. Nevertheless this mechanism leads to approximately the observed orientation relationship.

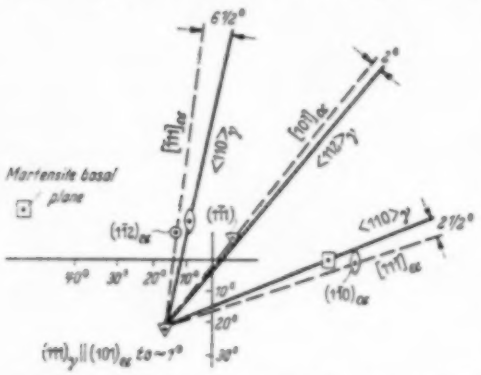

Figure 4. Orientation relationships in the martensite transformation, γ to α, in iron-0·8 per cent carbon-22 per cent nickel. Gnomonic projection with the plane of the martensite plate as the plane of projection (Greninger and Troiano)

BURGERS also proposed[44] a mechanism for the martensite transformation from the face-centred cubic structure to the close-packed hexagonal structure that occurs in cobalt. In this transformation, since the (111) planes in the face-centred cubic phase and the basal planes in the close-packed hexagonal phase have the same configuration of atoms, the change in structure could be produced by displacement of the (111) planes relative to each other. Burgers proposed that this transformation occurs by a shear on the system (111) $[\bar{1}\bar{1}2]$ as illustrated in *Figure 7*. This shear only occurs on alternate planes and so converts the ABCABC . . . sequence of (111) planes in the face-centred cubic structure with the ABABAB . . . sequence of basal planes in the close-packed hexagonal structure. This mechanism is consistent with the observed orientation relationship.

With the exception of the mechanism proposed for the face-centred cubic → close-packed hexagonal transformation, none of these transformation mechanisms has proved to be capable of explaining the observed habit planes and relief effects. Prior to the determination of the martensite habit planes it was generally believed that these planes would be the operative shear planes in the various mechanisms described above. However, the experimental determinations did not substantiate this prediction. In general, martensite plates do not form

parallel to the anticipated simple crystallographic planes, but parallel to planes of much higher indices, as will be seen from the available data on martensite habit planes, which are summarized in *Table I*. For example, GRENINGER and TROIANO[28] showed that the habit planes

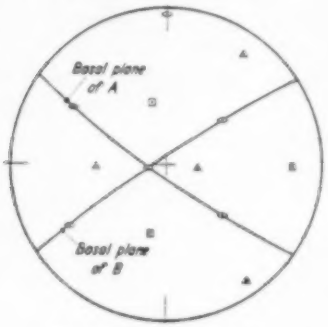

Figure 5. Orientation relationship between body-centred matrix, β_1, and martensitic β' in copper-aluminium alloy; the plane of stereographic projection is the plane of a set of martensite plates. Two β' orientations, A and B are present

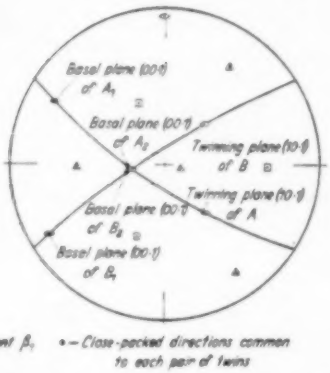
Basal plane (00·1) of A_1
Basal plane (00·1) of A_2
Twinning plane (10·1) of B
Twinning plane (10·1) of A
Basal plane (00·1) of B_2
Basal plane (00·1) of B_1

Figure 6. Orientation relationships between body-centred cubic matrix β_1 and close-packed hexagonal γ' in copper-aluminium alloys. Stereographic projection of the basal planes and the active twinning planes of the four γ' orientations contained in one set of parallel martensite plates are indicated; of these four, A_1 and A_2 are twins and likewise B_1 and B_2 (Greninger)

in carbon steels, ($< 1{\cdot}5$ per cent carbon), and high nickel steels are $\{225\}_A$ and $\{259\}_A$ in the austenite, respectively, and not $\{111\}_A$ as anticipated. Clearly, the transformation theories of Kurdjumow and Sachs and of Nishiyama are inadequate. Similarly, BOWLES[43] has

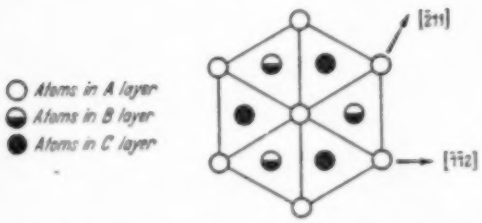

Figure 7. Face-centred cubic structure projected on the (111) plane; each layer is identical in atom pattern and the direction of shift for the Burgers mechanism of transformation to close-packed hexagonal is [$\bar{1}\bar{1}2$]

recently shown that the habit plane of lithium martensite has the indices {441}, differing widely from the {112} anticipated from Burgers' mechanism.

The first attempt to determine a transformation mechanism consistent with the observed irrational habit plane, as well as with the

observed structure and lattice relationships, was made by Greninger and Troiano. Working with an iron base alloy containing 0·8 per cent carbon and 22 per cent nickel, they made a study of the relief effects produced on a polished surface by the transformation, and concluded that these were produced by a shear on the martensite habit plane, $\{259\}_A$. Making this assumption they were able, from a goniometric analysis of the relief effects, to determine the direction and magnitude of the shear. Using a stereographic method they then applied this experimentally determined shear to the austenite lattice, and found that it did not accomplish the transformation to the martensite lattice. It did, however, generate from one of the {110} austenite planes a plane identical with the (112) martensite plane, and they found that the transformation could be completed by a second shear on the system $(112)_M\,[11\bar{1}]_M$. Greninger and Troiano therefore proposed that the transformation occurs in two stages, the first stage being a homogeneous shear on the habit plane and producing the observed relief effects; the second being a shear, homogeneous within narrow lamellae (not less than eighteen atomic planes in thickness on the average), but macroscopically heterogeneous and causing no observable change in the shape of the transformed volume. The second shear receives credence from the fact that it occurs on the martensite twinning elements, also martensite plates frequently show transverse markings which correspond to the traces of the $(112)_M$ plane.

This mechanism is consistent with the observed relief effects and explains the habit plane as being the plane of the first shear. It is also consistent, to a good approximation, with the observed structure and the orientation relationship, which in this case may be described as being midway between the Kurdjumow-Sachs and the Nishiyama relationships. However, since the proposed mechanism involves only shears, the predicted martensite dimensions are too small and it is necessary to propose that an anisotropic expansion occurs either before, during or after the shears. This expansion amounts to as much as 4·2 per cent in the $[100]_M$ direction. It is also inconsistent with the geometrical features of the transformation in steels of other compositions *e.g.* plain carbon steels containing less than 1·4 per cent carbon. In this case it is not possible to account for the Kurdjumow-Sachs relationship by a shear on the habit plane, which is now $\{225\}_A$, followed by a shear on the martensite twinning elements.

Jaswon and Wheeler have suggested[21] a somewhat different interpretation of the martensite habit plane. They point out that if the habit plane in austenite were an atomic plane that underwent a rotation during the transformation *i.e.* if the direction of its normal changed, large scale plastic distortion of the surrounding austenite would be necessary to accommodate the movement. Such an arrangement of the

plate would therefore be energetically less favourable than an arrangement in which the austenite plane parallel to the plate does not rotate. They therefore attempted to identify the habit plane with one of the crystallographic planes that do not rotate during the transformation.

In their analysis they considered the Kurdjumow-Sachs relationship and assumed that during the transformation each atom in the austenite moves to the nearest available position in the martensite structure. This represents the same correspondence between lattice positions in the two structures as proposed by Bain. Treating these minimum displacements as a homogeneous finite strain, they determined the planes that are not rotated by the strain. Three such planes were found: the $(111)_A$ plane, a plane which lies within 1° of $(111)_A$ and becomes coincident with it for zero carbon content, and a plane which lies within 1·5° of $(225)_A$. The last of these solutions demonstrates that the habit plane for plain carbon steel (< 1·5 per cent carbon) fulfills the anticipated requirement of zero rotation. It should be noted that this result means that each of the twenty-four crystallographically equivalent variants of the Kurdjumow-Sachs relationship has a specific $(225)_A$ plane as habit plane. (There is no direct experimental evidence that the particular variant considered by Jaswon and Wheeler does indeed have the $(225)_A$ plane as habit plane, and not any other plane of the form $\{225\}_A$.)

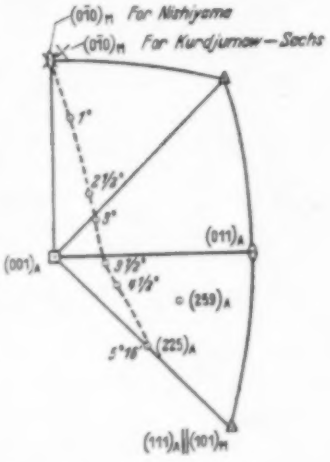

Figure 8. Stereographic projection showing variation of unrotated plane when orientation relationship is varied by different amounts from the Nishiyama to the Kurdjumow and Sachs relationship

It is implicit in the analysis of Jaswon and Wheeler that an orientation relationship different from the Kurdjumow-Sachs relationship would be characterized by different unrotated planes and therefore, in such cases, a different habit plane would be expected. Bowles (unpublished work) has repeated the Jaswon and Wheeler analysis for various orientation relationships of cubic martensite between those of Kurdjumow-Sachs and Nishiyama.* For all orientations, one of the unrotated planes is $(111)_A$ and another is close to $(111)_A$. The third solution is sensitive to the orientation relationship and varies from $(225)_A$ to $(\bar{1}01)_A$. *Figure 8* is a stereographic projection showing this variation of the third

* For body-centred cubic martensite, the Nishiyama relationship can be produced from the Kurdjumow-Sachs by a rotation of 5° 16′ about the $[101]_M$ direction.

unrotated plane as the orientation relationship is varied from the Nishiyama to the Kurdjumow-Sachs relationship; the projection shows austenite poles with the usual symbols of their symmetry, and a curve (broken line) along which the unrotated plane moves as the orientation relationship changes. The angles listed at points along this curve show the orientation relationship that leads to the unrotated plane indicated by the position of each point; each angle is the amount of rotation from the Nishiyama relationship toward the Kurdjumow-Sachs relationship about the normal to $(111)_A//(101)_M$, a rotation that increases from zero to 5° 16′ along the curve. (It is assumed in this graph that the Kurdjumow-Sachs variant is the usual standard variant.) Analyses for non-cubic martensite and for orientation relationships in which $(111)_A$ is not exactly parallel to $(101)_M$ have not been carried out.

Quite apart from such considerations of the generality of this concept of the habit plane as an unrotated plane, is the problem of explaining the relief effects. Jaswon and Wheeler's picture of the transformation as a simple homogeneous distortion of the lattice is not consistent with the observed relief effects. The relief effects produced by martensite transformations consist essentially of a simple tilting of the polished surface about its intersection with the habit plane; the line of intersection is not rotated. As Bowles has pointed out,[50] the homogeneous distortion proposed by Jaswon and Wheeler would not produce this kind of relief, for although the habit plane is not rotated, rows of atoms within this plane are rotated. This would lead to a rotation of the line of intersection of the polished surface and the habit plane by as much as 19°.

To produce relief effects of the observed type the habit plane must be a plane of zero *macroscopic* distortion *i.e.* there can be no macroscopic rotation of the habit plane, nor can there be any macroscopic rotation of rows of atoms within this plane. The Greninger-Troiano proposal[28] of a shear on the habit plane followed by a second heterogeneous shear fulfills this requirement. However, it should be noted that a shear is not the only kind of distortion that leads to an undistorted plane. The general requirement of homogeneous distortions that leave some plane undistorted is that every atom is moved in the same direction. This direction may or may not lie in the undistorted plane. In view of this, Bowles has generalized Greninger and Troiano's concept of resolving the total transformation strain into two shears,[50] to include distortions of this more general type. He has pointed out that if two consecutive distortions occur, each of which is characterized by an undistorted plane, certain relations must exist between the original and final lattice orientations. These permit the undistorted planes and directions of motion to be determined from the orientation relationship. For body-

centred cubic martensite in the Kurdjumow-Sachs relationship to austenite the anticipated relations were found to exist and the total atom displacement could be described by the two consecutive distortions with $(225)_A$ $[112]_A$ and $(112)_M$ $[11\bar{1}]_M$ as the undistorted planes and directions of motion, respectively. Tetragonal martensite may be produced by essentially the same distortions, the most significant difference being in the magnitudes of the two distortions; the resulting orientation relationship differs by only a few minutes of arc from the Kurdjumow-Sachs relationship.

It will be noted that the first of the above distortions is not a shear; the $[\bar{1}\bar{1}2]_A$ direction does not lie in the $(225)_A$ plane. This first distortion is analogous to Greninger and Troiano's first shear in that it generates the $(112)_M$ plane from the $(110)_A$ plane. In this case the structure generated by the first distortion is exactly half-way between two body-centred cubic twins and can be sheared in opposite senses on the system $(112)_M$ $[11\bar{1}]_M$ to produce two different martensite orientations. This accounts for the fact that whereas the Kurdjumow-Sachs relationship has twenty-four variants, the (225) plane only has a multiplicity of twelve.

This mechanism is consistent with the observed structures and orientation relationships. To account for the habit plane and relief effects, Bowles, like Greninger and Troiano, considers the first distortion to be homogeneous and to determine the shape of the plate, while the second is heterogeneous and produces no observable change in shape. The mechanism is therefore consistent with the observed habit plane and relief effects. A comparison of the observed and predicted angles of tilt of different austenite surfaces is shown in *Figure 9*.

This mechanism is also consistent with the observation that the long axes of the martensite needles in low carbon steel are parallel to $[1\bar{1}0]_A$ direction, for the $[1\bar{1}0]_A$ direction is the only direction that is not rotated either macroscopically, or on an atomic scale by this mechanism. The $[1\bar{1}0]_A$ direction is the intersection of the two undistorted planes.

It will be noted that since the close-packed row of atoms $[1\bar{1}0]_A$ is not distorted in this transformation the atom radius in the martensite is the same as in the parent austenite. Since the transformation is accompanied by a slight decrease in atom radius, it follows that the martensite dimensions predicted by this mechanism are slightly too large. An isotropic contraction must occur at some stage of the transformation.

The analogy between this mechanism and the Greninger-Troiano mechanism has already been commented upon. It will also be noticed that it only differs from the Kurdjumow-Sachs mechanism with respect to the first undistorted plane. The directions of motion,

$[\bar{1}\bar{1}2]_A$ and $[11\bar{1}]_M$, are the same in both cases and it is perhaps significant that these directions are the twinning directions in austenite and martensite respectively.*

Another geometrically consistent transformation mechanism has been worked out by Bowles, Barrett and Guttman for the diffusionless face-centred cubic to face-centred tetragonal transformation that occurs in certain indium-thallium alloys.[7] In this case the change in

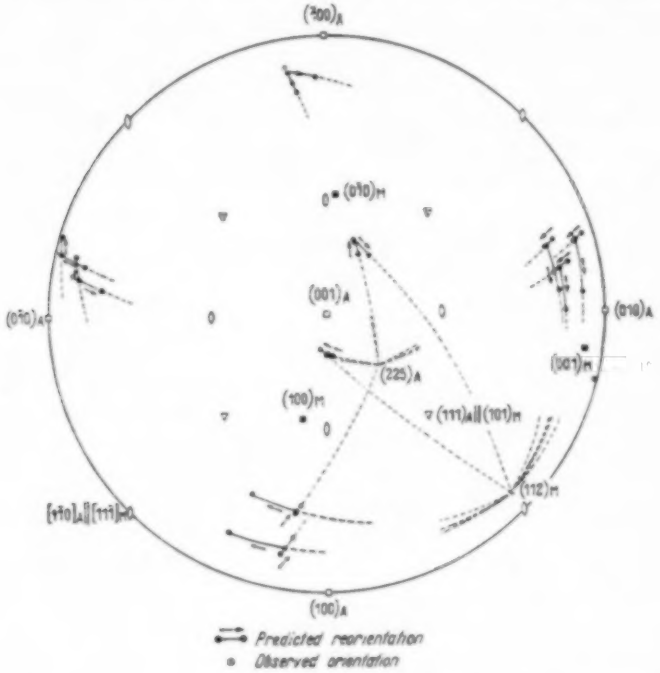

Figure 9. Comparison of the predicted and observed angles through which polished surfaces are tilted by the production of martensite plates in an iron-carbon alloy containing 1·35 per cent carbon. The data from thirteen experiments are rotated into the standard projection; the predicted reorientation of polished surfaces by first distortion (toward $(225)_A$) and by second distortion (toward $(112)_M$) is indicated and observed orientations are shown near the middle of the three positions to which they are to be compared

* The Bowles mechanism does not account for the {259} habit plane that is observed in 1·7 per cent carbon steels and in high nickel steels; none of the orientation relationships of *Figure 8* account for {259}. A preliminary report of work by E. S. Machlin (*J. Met.*, Oct. (1950) 1212) states that a {259} habit can be accounted for if $(259)_A$ is unrotated and undistorted by a first distortion in which the direction of motion is between $[0\bar{1}1]_A$ and $[\bar{1}\bar{1}2]_A$ and about 10° from $[0\bar{1}1]_A$; and if the second distortion leaves unrotated and undistorted a plane between $(112)_M$ and $(011)_M$ and $6\frac{1}{2}°$ from $(112)_M$, and involves a direction of motion that is coincident with $[1\bar{1}0]_A$ and that is about $2\frac{1}{2}°$ from $[11\bar{1}]_M$; and if the Greninger-Troiano orientation is assumed.

structure is achieved by means of two consecutive shears on two different {101} planes at 60° to each other. The shear directions are [101] directions. The first shear amounts to one third of that required for twinning the final tetragonal crystal on a (101) plane. This shear transforms the original face-centred cubic structure into a structure that can be described as being a third of the way between two tetragonal (101) twins. The second shear, which operates in either sense along a [101] direction, can produce two tetragonal orientations that are twins of each other. Occurring in one sense, this second shear is equal in magnitude to the first; in the opposite sense it is double the magnitude of the first. It should be noted that the directions of motion of atoms during transformation are twinning directions, as in the iron-carbon martensite transformation.

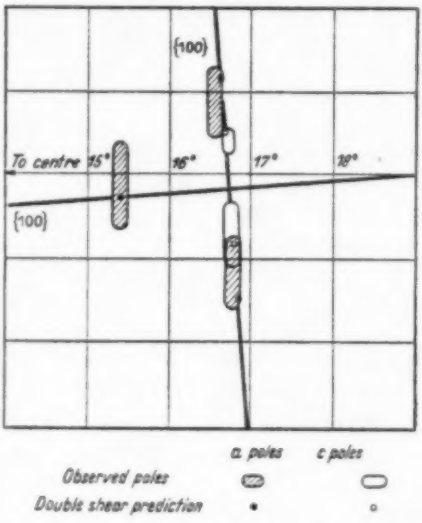

Figure 10. Pole figure of orientations of tetragonal indium-20·75 per cent thallium crystals clustered about the orientation of the original cubic crystal from which they formed. Predicted orientations of both a and c axes lie within the observed range of orientations of these axes, respectively, as determined by a precision Geiger counter X-ray spectrometer

Since there is a change of only about 2 per cent in the axial ratio in the indium-thallium transformation,[51] the shears involved are small and the tetragonal axes cluster very closely around the orientation of original cubic axes. In fact, precision determinations of the orientations are necessary to show that the tetragonal axes are not truly parallel to the cubic axes.[7] *Figure 10* is a pole figure of the cluster of tetragonal **a** and **c** poles at one of the cube poles* of a single grain that had been transformed with a single set of main bands; there is satisfactory agreement between the measured positions and the predictions of the double-shear theory.

This mechanism provides a complete explanation of the rather complicated microstructures arising from the indium-thallium transformation. The main bands in *Figure 11* are regions in which the first shear has occurred in opposite senses. The sub-bands within the main

* The cluster plotted in the figure surrounds a cube pole that is not parallel to the main bands; a different cluster is predicted and found about cube poles parallel to the main bands.

bands are the traces of the second shear planes. The second shear also occurs in opposite senses so that each set of sub-bands divides a main band into two twin orientations. The four different sub-bands in *Figure 11* thus represent eight different orientations. The sub-bands, as required by the transformation mechanism, are invariably the traces of {101} planes at 60° to the main bands. Moreover a single main band never contains more than two different sets of sub-bands and these are always at 90° to each other. This also follows directly from the transformation mechanism. The relief effects produced by this transformation present a very similar appearance to the polished and etched microstructure of *Figure 8* except that no signs of the sub-bands have been seen in the relief structures. Evidently the second shear is either heterogeneous on a very fine scale (*i.e.* there are closely spaced slip lines) or else the sense of the shear reverses frequently enough to prevent any observable change in shape. Thus, as in the iron-carbon transformation, the relief effects are produced entirely by the first distortion.

The indium-thallium transformation differs from most other martensite transformations in that the structure of the transformation product changes continuously on cooling below M_s. In the 20·75 atomic per cent alloy the axial ratio of the tetragonal phase varies from 1·020 to 1·0356 at room temperature. The transformation mechanism is flexible enough to accommodate this change, for the tetragonality can be increased simply by further shear on the same systems.

Transformations analogous to the indium-thallium transformation occur in several other solid solutions in tetragonal metals *e.g.* indium-cadmium, copper-manganese, and chromium-manganese. There is every reason to believe that these transformations occur by the same mechanism as the indium-thallium transformation. The microstructures produced are the same as in indium-thallium.

The essential difference between the earlier proposals and those of Greninger and Troiano, Bowles, and Bowles, Barrett and Guttman, is with respect to the mode of repetition of the distortion. These latter mechanisms recognize the fact that the unit distortion is not repeated throughout the lattice in a simple homogeneous fashion. It is from this fact that the necessity of describing the atom movements as a homogeneous distortion plus a heterogeneous distortion arises. Whether the directions of displacement specified by these distortions really describe the paths taken by the atoms during the transformation is an additional question, the answer to which can only come from a consideration of the mode of development of the martensite plate.

To place other martensite transformations on as sound a crystallographic basis as the transformations face-centred cubic to body-centred cubic or tetragonal, and face-centred cubic to tetragonal, it

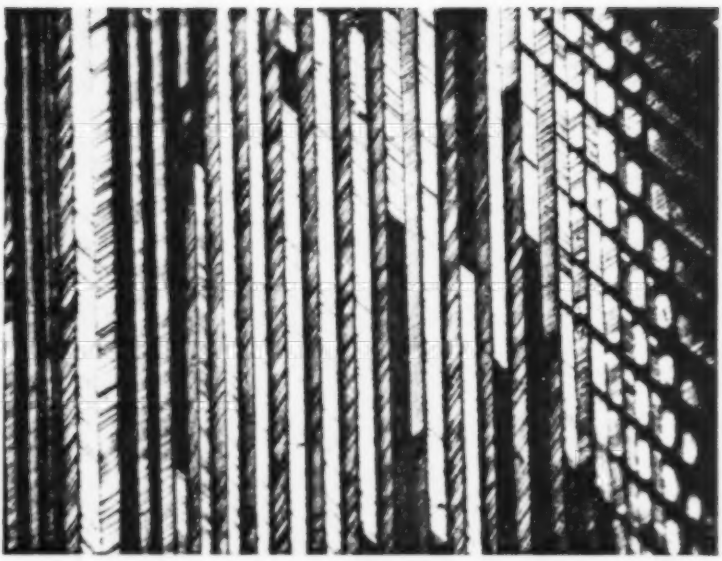

Figure 11. Microstructure of a grain of indium-20·73 per cent thallium after transformation from cubic to tetragonal. The first shear of the transformation establishes the boundaries of the main bands, and occurs in alternate senses in alternate bands; the second shear generates the sub bands, and occurs in alternate directions in adjacent sub bands of a given main band (Etched; polarized light; magnification 250 ×)

VOL
3

will probably be necessary to investigate the various ways in which the various unit cell distortions can be repeated throughout the lattice. For example, in the transformation body-centred cubic to close-packed hexagonal occurring in copper-aluminium alloys it has been shown[52] that the martensite possesses the superlattice anticipated on the basis of Burgers proposed atom movements. It will be necessary to determine how this distortion of the body-centred cubic structure (which, in this case, is a distortion that is heterogeneous) can be repeated to produce the observed irrational habit plane and the relief effects.

Mode of Development of Martensite Plates—The crystallographic analyses described above provide only a limited amount of information concerning the transformation mechanisms. Such analyses are capable of determining the correspondence between the initial and final positions of atoms in the two structures. They do not, however, give any information about the mode of development of the martensite plate *i.e.* they do not reveal the order in which different atoms make their displacements. Thus theories of the mode of formation of martensite plates, although they must be consistent with the crystallographic features of the transformation, must be based on other considerations.

Some of the controversial issues connected with theories of the development of martensite plates have been clarified by recent discoveries of martensite transformations in which the plates may be made to develop slowly. For this reason, instead of adopting a historical approach in this section, information that has been obtained by direct observation will be described first. Various problems connected with the formation of martensite crystals will then be discussed in the light of the theories that have been proposed.

So far two martensite transformations have been discovered in which the plates develop at an observable rate. These are the transformations in the gold-cadmium[9] alloys and the indium-thallium[7] alloys. In these alloys the transformation occurs by the formation of a thin plate nucleus which later widens. The plate nucleus extends completely across the crystal very rapidly and appears to form instantaneously; the thickening of the plate occurs at a rate sufficiently slow to photograph at successive stages. The development of martensite plates in this fashion, by the lateral propagation of an interface parallel to the habit plane, shows that at least some of the transformation distortions discussed previously occur at an interface. Information obtained from studies of the deformation of scratches by the production of martensite plates[53, 50] shows how this can occur. These studies have shown that scratches, although bent by the homogeneous distortion, remain continuous across the interface between the martensite plate and the matrix, as will be seen from *Figure 1*. This continuity of scratches shows clearly that during the widening the matrix on either side of the

developing plate is displaced. This behaviour is capable of a simple interpretation in terms of the crystallographic mechanisms that have been proposed. Consider the development of a martensite plate in an indium-thallium alloy, where the transformation occurs by the two shears (101) [$\bar{1}$01], (0$\bar{1}$1) [011]. Since the habit plane, (101) is not distorted by the first shear, the matrix can maintain perfect coherence with the developing plate as the shear occurs in successive atomic layers; the matrix is simply translated in the shear direction. When the first shear propagates in this way, each atom suffers only a small displacement as the migrating interface passes it. The macroscopic displacement of atoms, which is required by the fact that this shear is observed to be homogeneous, occurs while the atoms are still part of the untransformed matrix. The observed homogeneous distortion thus simply represents the integrated effect of the translational movements that have occurred in the matrix.

Since the atom displacements corresponding to the second shear are presumably also occurring at the interface, and since this second shear distorts the first shear plane slightly, it is clear that the two phases at the completion of the transformation cannot be perfectly coherent in the sense that the interface plane is a plane that is common to both structures. However, since the second shear occurs heterogeneously on a very fine scale, only small displacements of atoms need be involved and these can apparently occur without causing long range distortion of the matrix. A boundary between the phases which is irregular because of the heterogeneity in the second shear may well be a boundary of the low-energy type that has been discussed by SMITH.[54]

This picture of the development of martensite plates is consistent with all the observations and demonstrates clearly what seems to be the most fundamental difference between martensite type transformations and those which occur by nucleation and growth, namely, the extent of the coherence between the new phase and the matrix. In martensite transformations, since there is no interchange in the position of neighbouring atoms connected with the homogeneous component of the distortion, a change in shape must necessarily occur. It seems to be quite general that this change in shape is achieved by the additive effect of the translational movements of the matrix in the manner just described. Thus the homogeneous distortion that characterizes martensite transformations is a consequence of the shifting of the matrix to maintain as close a coherence as possible with the growing plate. In nucleation and growth processes this high degree of coherence is not maintained at the interface.

The proposed mechanism of growth of martensite plates brings an added significance to the crystallographic mechanisms described previously. Since part of the displacement of each atom occurs while

it is still in the untransformed matrix, as a translation in the first 'shear' direction, it is concluded that the crystallographic mechanisms do describe the paths taken by the atoms during transformation.

The existence of two martensite transformations in which the plates develop by the propagation of an interface parallel to the habit plane does not constitute proof that *all* martensites develop in the same way. However, since the translation of the matrix is observed in all martensite transformations in which it has been looked for, there is every reason to believe that the mode of development described above is typical.

The major problem remaining to be discussed is that of the production of the original plate nucleus. There are two conceivable ways in which the original thin plate could be produced. The transformation distortion could be imagined either as a simultaneous, nearly uniform distortion of the entire area of a thin plate-shaped region in the parent lattice, or by the propagation, in some manner, of a region of distortion through the parent lattice at the advancing rim of a plate. The first of these mechanisms can be ruled out, for it would require extremely long range forces between atoms. Many of the phenomena which characterize martensite transformations, although imperfectly understood at present, seem to indicate that martensite plates develop from nuclei. For example, when a martensite transformation is reversible, the plates that appear in a certain region during cooling reappear in the same form, in exactly the same region, during a second cooling cycle.[36] It has been concluded[53] from this that embryos exist in the parent phase that nucleates the reaction and that the sites of these embryos are not necessarily changed on reheating. Similarly, the nucleation concept promises to account for such phenomena as the absence of isothermal transformation in martensite transformations and perhaps also stabilization.

Although there is general agreement that plates develop from nuclei, there is considerable divergence of opinion on the nature of the distorted region serving as a nucleus and the manner in which it grows. FISHER, HOLLOMON and TURNBULL[55] suggest that the martensite transformation occurs by coherent growth of nuclei which were formed at higher temperatures and which have become supercritical in size because of the lowered temperature. They propose that the growth is accomplished by means of thermally activated atom movements, the activation energy being very small, thus permitting growth to occur with extreme rapidity. They state that the unit process involved is the movement of a single atom through a small distance, but a little consideration shows that this statement has to be qualified. It is a geometrical requirement that a region in which there is a continuous gradient of distortion must be propagated across the crystal in the

growth of a martensite plate. The distortion is that produced in the matrix by coherence. To maintain coherence, the movement of any given atom must cause displacements of neighbouring atoms in the austenite. This means in effect that the unit process must shift the whole strain gradient.

If there is even a small activation energy associated with the movement of the atoms at the austenite-martensite boundary, or with the shift of the distortion gradient, then the rate of propagation of the martensite plates should be a function of temperature and should become measurably slow at sufficiently low temperatures. If the activation energy were in the neighbourhood of 3,000 cal/mol, as might be estimated from the activation energy for self-diffusion, and if the time of formation of a martensite plate were, say, 70 μsec at $-$ 50°C, it would be 10 sec at liquid nitrogen temperatures, and 10^{146} centuries at liquid helium temperature (4°K). Even a process with a tenth of this activation energy would require centuries at 4°K if it were a 70 μsec process at liquid nitrogen temperature. It would therefore be expected that if the martensite reaction involves atom movements resembling self-diffusion and having an activation energy, it should be possible to see the slow growth of plates at low temperatures and, presumably, to suppress the transformation by rapid cooling. Kulin and Cohen have made a careful search for such effects in various nickel steels and in a 0·6 per cent carbon, 8 per cent manganese steel, but have found none.[26] The transformation continues in typical fashion down to 4°K, without suppression of the reaction due to rapid cooling, and plates form with characteristic rapidity even at 4°K. The report by KURDJUMOW and MAKSIMOVA[56] that the transformation in 0·6 per cent carbon, 6 per cent manganese steel could be suppressed by cooling to low temperatures was not confirmed.

In view of the results of Kulin and Cohen it is difficult to imagine that thermal vibrations play a significant part in determining the high rate of growth of martensite plates in steels. On the other hand, if a plate grew by a shear-like displacement of atoms in a cooperative movement, with the rate dependent upon the elastic constants of the metal, the rate should not be subject to marked retardation at low temperatures, because the elastic constants are far less dependent upon temperature than are diffusion processes.*

Cohen, Machlin and Paranjpe, in contrast with Fisher, Hollomon

* As this manuscript goes to press we are informed by J. H. HOLLOMON and R. CECH that they have observed dilatometrically an isothermal transformation of martensite in the alloy Fe + 8 per cent Mn + 1·6 per cent C at $-$ 190°C, and that recent work by Kurdjumow on Fe + 23 per cent Ni + 3·4 per cent Mn reveals what appears to be progressive transformation of individual martensite plates isothermally at an observable rate, with an activation energy of about 1,300 cal/mol.

and Turnbull, stress the cooperative nature of the atom movements necessary to create the nucleus, and the absence of diffusion-like atom jumps. They regard the nucleus as a strain centre or region of distortion in which the parent lattice is slightly displaced along the reaction path that leads to the martensite structure. These strain centres are visualized as existing in the parent structure until conditions become favourable for their propagation through the lattice to form a martensite plate.

For simplicity the transformation distortion is regarded as a simple shear and it is proposed that the variation of free energy with shear angle θ is of the type shown in *Figure 12*. The difference in free energies of the parent phase and the martensitic phase has been calculated for the iron-carbon transformation by ZENER,[24] by FISHER, HOLLOMON and TURNBULL,[55] and by COHEN, MACHLIN and PARANJPE.[53] These workers agree that at the transformation temperature the bulk free energy of martensite, neglecting the contribution of shear strain energy, is about 300 cal/mol less than that of austenite. The validity of the maximum in the free energy curve shown in *Figure 12* is confirmed by the work of McReynolds who has shown that the shear modulus and Young's modulus of austenite are both positive above and below M_s.[10] This indicates that the curve has an upward curvature at $\theta = 0$.

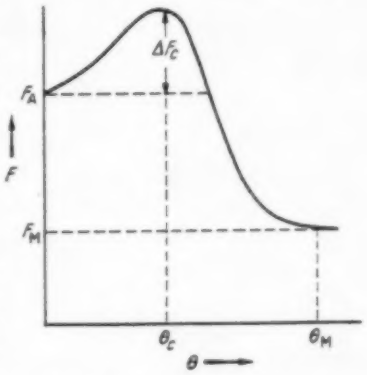

Figure 12. Free energy F, as a function of the shear strain, θ, along the path from the austenite structure through the critical strain of maximum free energy, θ_c, to strain corresponding to the martensitic structure, θ_M (Cohen, Machlin and Paranjpe[37])

The strain embryos proposed by Cohen, Machlin and Paranjpe (and the coherently growing nuclei of Fisher, Hollomon and Turnbull) can be regarded as being made up of regions in which the shear strain varies from zero up to the value corresponding to the final martensitic state. The curve of *Figure 12* thus gives the variation of free energy within the strain embryo. Since it is not possible to alter the shear strain in an elementary region of the strain embryo without changing the shear strain in the remainder of the embryo, it is clear that for the strain to be propagated spontaneously the free energy of the strain centre as a whole must be decreased by the moment. Therefore spontaneous propagation would be impossible in a strain centre that is represented only by that portion of the curve lying between the origin and θ_c. But if the strain centre includes the activation barrier on the

free energy curve, then during propagation elements with shear strains greater than θ_c decrease in free energy and elements with shear strain less than θ_c increase in free energy. If the decrease more than balances the increase, propagation occurs spontaneously, presumably with the velocity of an elastic wave, and produces a thin plate of martensite. The sudden appearance of a thin plate even in alloys in which the subsequent thickening of the plate is relatively slow has been observed in indium-thallium and gold-cadmium alloys. Mechanical twins, which are analogous in many respects, appear suddenly with their full length and subsequently thicken slowly, so it may be that the characteristic rate of thickening is always slower than the rate of propagation of the initial thin plate.

Cohen, Machlin and Paranjpe suggest that the strain centres are always present in the parent phase, propagating only when the temperature is lowered enough to make the strain exceed θ_c, the critical strain for spontaneous propagation. They further suggest that the strain centres are screw dislocations and that the habit plane of a martensite plate is determined by the direction of the singular line of a screw dislocation, which is the slip direction. Actually, the habit planes seldom conform to this proposed rule and at the present time any attempts to base habit theories on any one type of dislocation or group of dislocations would be highly speculative. Nevertheless, there may still be merit in the concept that the distortion associated with some group of dislocations has a large component in the direction of the transformation distortion. It is the transformation distortion that is propagated, not the dislocation distortion, and the habit plane need not perhaps be identified too closely with the geometry of the dislocations.

A difficulty arises when a theory based on extremely small strain centres is forced to account for the effect of grain size on M_s. To explain this effect, COHEN[3] proposed that the strain gradient stretches completely across the crystal and the potential nucleus thus becomes aware of the location of the crystal boundaries. But a strained region of this size is many orders of magnitude larger than one would expect around a dislocation or a small group of dislocations, and some modification of this theory or an alternate explanation seems to be required.

The general problem of nucleation merits a separate review and will not be discussed at length here. Either the strain centre nucleus proposed by Cohen, Machlin and Paranjpe, or the coherent embryo of Fisher, Hollomon and Turnbull can be imagined to extend itself by the diffusionless process that has been discussed.

Related Phenomena

Effects of Elastic and Plastic Strain—Since martensite transformations involve a homogeneous distortion of the parent structure it is expected

that externally applied elastic and plastic strains will play an important role and this aspect of the transformations has received some attention. It seems to be a general rule that isothermal formation of martensite can be induced by plastic strain at temperatures above M_s. Such strain transformations have been observed in the systems iron-nickel[8, 10], copper-zinc,[36] lithium,[57] lithium-magnesium[42] and gold-cadmium.[9] In addition, some martensitic phases are themselves transformed by cold work;[1] in the copper-aluminium alloys β'-martensite transforms to γ'-martensite with cold work and the ε-martensite in iron-manganese alloys can be similarly converted to α'-martensite.

The tendency towards martensite transformation by plastic strain diminishes as the temperature is raised above M_s, and the strain is accommodated by normal slip to an increasing extent. A certain maximum temperature exists (M_d) above which transformation cannot be induced by plastic strain. When slip has occurred the parent phase is stabilized to a certain extent against spontaneous transformation on cooling and M_s is depressed. Scheil has presented metallographic evidence to show that this effect is due to the slip bands acting as barriers in the same way as grain boundaries, and limiting the size of the martensite plates that can form. However, in unpublished work by Bowles and Clifton there is evidence to the contrary, for martensite plates in iron-nickel and iron-nickel-carbon alloys are seen to pass through slip bands and even through deformation bands. In the latter case the plate is bent at the deformation band so that it follows the trace of the habit plane in the differently oriented regions. Perhaps slip bands and sub-boundaries are semi-permeable barriers to the passage of martensite distortions.

The competitive nature of the slip and strain transformation processes has been portrayed schematically by Scheil[8] (*Figure 13*). With increasing temperature the shear resistance to slip, τ_{S_1}, decreases and the shear resistance to transformation, τ_{M_1}, increases. Below T_{B_1}, τ_{M_1} is negative implying that the parent phase is mechanically unstable and shears spontaneously to martensite. Above T_{B_1}, τ_{M_1} is positive but smaller than τ_{S_1} implying that when an external force is applied, transformation rather than slip will occur. At T_{A_1} this situation is reversed so that T_{A_1} corresponds to McReynold's M_d. The curves τ_{S_2} and τ_{M_2} are intended to describe the effects of work hardening on the shear resistance to slip and to transformation.

Scheil's picture of the interrelation of the processes of slip and transformation has been interpreted by Zener in terms of free energy as a function of shear (*Figure 14*) and McReynolds[10] has made a study of the predictions derived therefrom. In *Figure 14* the height of the potential hump between the minima, which must be surmounted, corresponds to the critical shear stress required for the transformation

and the curvature near a minimum represents the shear modulus. The curves T_1, T_2 *etc* represent the proposed effect of temperature and show how the parent phase could become first metastable and then unstable. This picture is in accord with the properties proposed by Scheil to account for his observations but leads to a number of predictions that have not been substantiated by the work of McReynolds. It is expected from this picture that the elastic modulus and yield stress of the parent phase should decrease as the temperature is lowered to M_s. Moreover, an applied stress in the elastic range should cause transformation to

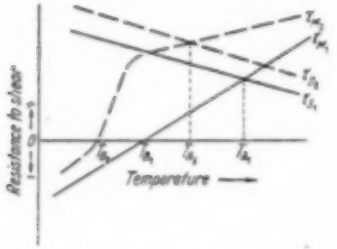

Figure 13. Scheil's theory of the relative resistance to shear by slip and by martensite transformation

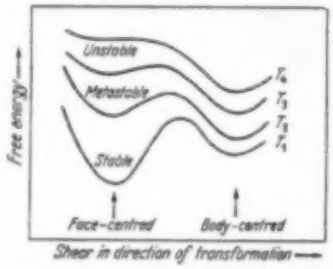

Figure 14. Free energy as a function of the shear for the transformation from face-centred cubic to body-centred cubic, at different temperatures (Zener)

occur at a higher temperature than it does in the absence of stress. Scheil's results on iron-29 per cent nickel alloy showed some indications of a slight decrease in elastic modulus with decreasing temperature, and of a slight increase of M_s when stress was applied. McReynolds, however, found no change in the modulus, and no effect of externally applied stress (within the elastic range) on the M_s temperature.[10] The yield stress did not decrease between M_d and M_s but actually increased to a maximum just above M_s. (It is not clear whether the 0·02 per cent plastic yield involved in these tests produced any strain-martensite.) The only other investigation of the effect of applied stress on a martensite transformation is that of Chang and Read who have shown[9] that in a gold-cadmium alloy (47·5 atomic per cent Cd) a stress corresponding to bending a $\frac{1}{2}$in. square cross section specimen over a span of 1·5 in. to give a displacement of 0·1 in. at the centre, produced an increase in M_s and a decrease in the temperature at which the reverse transformation began.

These data are apparently conflicting and a complete explanation cannot be given at present. It might be suggested that the absence of an effect of applied stress on M_s in iron-nickel alloys might be due to the fact that the strains at the strain centres which nucleate the transformation would need to be much greater than the ordinary elastic limit.

Thus an artificially induced strain might not have a measureable effect on M_s. According to Chang and Read the homogeneous shear involved in the gold-cadmium transformation is only about 3° compared with about 11° in the iron-nickel transformation. In gold-cadmium, then, the applied stress might produce a strain that is a greater fraction of the total strain required than in iron-nickel, and thus be more effective in producing the transformation.

Another possible explanation arises from the fact that Zener's picture does not include the effect of coupling between the different parts of a strain centre nucleus. The Cohen, Machlin and Paranjpe treatment has demonstrated that it is not necessary for the shear modulus to become zero for a mechanical instability to arise. Thus to predict the effect of an elastic strain it is necessary to consider its effect on the shape of the free energy curve as well as on the free energy of the metastable parent phase. If the shape of the curve is essentially unchanged, a detectable change in M_s is not expected. Plastic deformation, on the other hand, should be able to propagate strain centres (as it does dislocations) and cause transformation even above M_s.

Faults—The prevalence of faulty stacking of close-packed layers in phases formed by martensitic transformations has been mentioned (p 3). On the basis of our present understanding of the distortions accompanying these transformations it is natural to associate the faulting with the heterogeneous shears of the transformations. There is a close parallel, on this view, between faulty structures resulting from spontaneous transformations and those resulting from strain-induced transformations. In each case there is a shearing distortion which impinges on the neighbouring grains or the untransformed material of the given grain and which is relieved by the gliding process on irregularly spaced layers. The shear strain energy in the surrounding material, arising from the transformation distortion, surely increases as the distance between gliding layers increases, and would on this account tend to make the gliding lamellae (or the oppositely sheared lamellae) as thin as possible; but other factors act to increase the lamellar thickness. A lamella so thin that the surface layer is sheared less than half an interatomic distance would not produce a system of lower strain energy if glide took place within it. Furthermore, if glide (or reversed shear) results in an interface, the energy to produce the interface must be provided, and this would also tend to limit the total number of faults.

Faulting should be most frequent when the composition and temperature of a phase is such that other phases of the same composition of differing stacking arrangement have equal or lower free energy. Thus in the copper-silicon system, for example, any face-centred cubic alloy that can be cooled into a region where it would be stable with the

close-packed hexagonal structure is susceptible to faulting. On the other hand, the same alloy when heat treated to have a fault free hexagonal structure does not become faulted by deformation, judging by the experiments that have been tried;[16] in this case faulting would lead to an increase in free energy. The same situation apparently exists in silver-tin alloys near the maximum solubility of the silver-base solid solution, and in silver-antimony alloys as well.[17]

In cobalt, when the high temperature phase, which is face-centred cubic, is cooled below the M_s temperature, lamellae shift into the hexagonal stacking sequence because this has lower free energy even with very thin lamellae. Presumably a fault free hexagonal form would have still lower free energy than the faulted form and would be the equilibrium structure. In lithium and lithium-magnesium alloys, similarly, the low temperature phase contains many faults, not because the faulted structure is the structure of lowest free energy, but because it is the structure that can be reached by atoms moving out of the body-centred cubic high-temperature structure without setting up stress fields and interfaces of prohibitively high energy. In copper-silicon alloys of the range 5·1 to 5·4 per cent silicon, plastic flow produces a phase (γ') that is coherent with the face-centred cubic matrix and different in structure from the stable precipitate that forms slowly during eutectoid inversion.[16]

NUCLEATION AND GROWTH TRANSFORMATIONS

In this section an attempt is made to review the fundamental ideas and general principles that have been proposed concerning crystallographic relationships in nucleation and growth transformations. The extensive bibliographies that have recently appeared on the subject of precipitation from solid solutions,[58–62] which is properly within this field, have made a lengthy treatment and a comprehensive bibliography here unnecessary.

Reactions that proceed by the thermally activated movement of an interphase boundary differ from martensite reactions in a number of respects. At the advancing interface there is a more complete rearrangement of atom positions, a less orderly shift of position as an atom leaves one phase and joins another, and less cooperative movement of the atoms. A new phase may strain the old phase from which it forms, because it may not have the same specific volume as the old phase, but the homogeneous shear component of strain that is characteristic of martensitic transformations is absent. The crystallographically regular distortions of polished surfaces that are found after the martensite transformation do not exist. The interphase boundary moves in a way analogous to boundary migration in recrystallization

and grain growth, and not like the boundary movement in mechanical twinning.

Regardless of differences in types of reaction, a crystallographic relation in orientation between the parent crystal and the products of the transformation is observed in nearly all instances, and when the products have lamellar to lenticular shapes they are arranged on definite crystal planes of the parent phase.

Orientation Relationships—Orientation relationships and habit in nucleation and growth transformations may be controlled by factors that are not important in martensitic transformations, and as a consequence are less readily interpreted in fundamental terms. Nevertheless, some use has been made of the crystallographic data. Assuming that the orientations of the fully grown crystals resulting from eutectoid decomposition are identical with the orientations of their nuclei, it has been possible to use orientation data to indicate which of two phases nucleates the eutectoid reaction. SMITH and MEHL[30] found that the orientations of bainite formed in a crystal of 0·78 per cent austenite at 350°C and 450°C are identical with those for the precipitation of pro-eutectoid ferrite in low carbon steel, and concluded that since both are nucleation and growth processes, the same phase nucleates both, and thus that ferrite rather than cementite nucleates bainite.

The martensitic mechanism may be operative in the early stages of some transformations (including some cases of precipitation from solid solution) that are ordinarily classed as nucleation and growth transformations. This may be suspected when the newly formed phase is coherent with the matrix. It would be desirable to be able to conclude from orientation data whether or not the nuclei in nucleation and growth reactions form martensitically. If, for a given change in crystal structure, it were found that the orientations in nucleation and growth processes differed from those in martensitic transformations, this would strongly suggest a difference in the nucleation mechanism; but similarity in the orientations, on the other hand, would not necessarily mean similarity in the mode of nucleation.

Actual data seem to indicate that within the precision of the determinations the same orientation relationships result from both modes of transformation when the participating phases have the same structures or closely similar structures. For example, the orientations found by YOUNG[63] in iron-nickel meteorites differ little, if at all, from those obtained in artificial iron-nickel alloys that transform martensitically. Similarly, pro-eutectoid ferrite, formed from austenite by a diffusion process, has the same orientation relationship as the martensite produced on quenching low carbon steels. Close-packed hexagonal precipitates forming in face-centred cubic phases (for example, the phase precipitating from aluminium rich aluminium-silver alloys) are

oriented identically with close-packed hexagonal cobalt that has formed martensitically from face-centred cubic cobalt. The grounds for suspecting martensitic nucleation are best when the new phase is known to be coherent with the matrix during the early stages of growth, and particularly when the new phase is a metastable rather than an equilibrium phase, as, for example, in the aluminium-silver system where coherent metastable γ' precedes stable γ during precipitation. At the present time the theory seems attractive—to the authors at least—that nucleation is martensitic in many nucleation and growth reactions, and that the martensitic type of atom movements continue throughout the coherent growth stage of precipitation, thus straining the matrix as martensite does and causing hardening. The strains from this mode of precipitation, which could account for the distortion of the matrix that is frequently so pronounced in x-ray photographs of age hardening alloys, would continue to increase with increasing precipitation until either break-away or recrystallization relieved them.

If atom transfer to the nucleus across a boundary occurs by diffusion, the rate controlling factor in the growth of the new phase may be the rate of diffusion at the boundary, especially when transformation occurs without composition change. Little is known about grain boundary and interphase boundary diffusion rates at present, though activity in this field of research is increasing; but these rates are thought to be responsible for the orientation dependence of the rate of grain boundary migration.[64]

Habit—Precipitation from solid solution frequently produces crystallographic arrays of plate-shaped crystals similar, on a microscopic scale, to the 'Widmanstätten structure' of iron-nickel meteorites. Young noted[63] that in meteorites the body-centred cubic phase (kamacite) forms lamellae on the (111) plane of the face-centred cubic taenite, which presumably is the parent phase, with orientations such that one phase could have transformed to the other with minor shifting of rows of atoms and a very slight change in the density of packing of the atoms. Mehl and his collaborators investigated the Widmanstätten structure in a number of alloy systems and found a number of examples of precipitation in the form of plates, with the plates lying parallel to a plane of the parent solid solution that was identical or nearly identical with some plane in the precipitate. Yet exceptions were also observed, such as the precipitation of iron nitride from ferrite. It was learned, also, that precipitation could occur in some alloys by the formation of polyhedra, or sometimes needles which are parallel to directions of high indices in the matrix, or even less regular shapes, as well as plates. Simple rules also proved inadequate to cover plate-like precipitates in systems where matrix and precipitate both have the same structure and

VOL. 3

differ only in lattice constants. This occurs in the systems copper-silver, copper-cobalt, copper-nickel-cobalt and copper-nickel-iron, with both phases being face-centred cubic, and in iron-nickel-aluminium with both phases having body-centred cubic atom locations. In such cases, when the orientations of matrix and precipitate are the same, obviously the similarity in atomic pattern between any plane and the corresponding plane of the other phase is the same as for any other analogous pair, yet plate-shaped rather than equiaxial precipitates are found. There can be little doubt that the concept of similarity in atom pattern on the habit plane and the concept of minimum shifting of atoms in forming the new phase are to be regarded as approximations to more fundamental laws.

The precipitation of metastable phases prior to the appearance of stable phases is important in this connection. If a metastable structure comes out of solution in the shape of plates on a particular set of matrix planes, and if this subsequently transforms into a stable phase, it is natural to expect the shape of the stable phase to be dictated by the shape of its predecessor.

An important factor with all nuclei, coherent and incoherent, is the interface energy between matrix and precipitate. It is clear that there is a strong dependence of interfacial energy on the orientations at a boundary, as SMITH[65] has pointed out. Calculations of READ and SHOCKLEY[66] show that near certain orientations where a minimum interface energy exists there is a rapid change of energy with change in some (or probably all) of the five variables which specify the orientation of the interface in the two adjoining crystals, and experimental determinations of DUNN and co-workers[67, 68] and of AUST and CHALMERS[69] confirm this rapid change. Therefore the interfacial energy alone is capable of providing a precise orienting force favouring certain orientations of a boundary. When the atomic volume of a precipitate differs from that of the matrix in which it is embedded, there is reason to expect it to assume the shape of a thin disk, for as MOTT and NABARRO[70] have shown the strain energy in the matrix resulting from the volume change is less for this shape than for a sphere.

The total deformation energy for a matrix to accommodate clusters of atoms in the form of plates on different matrix planes should be a function of the difference in size of the segregating atoms, the alterations of interatomic distances, and the interatomic force as a function of the distance law. An approximate calculation along these lines, considering small clusters of atoms, was made by SMOLUCHOWSKI[71] for precipitation in the copper-silver system. Another approach to the same problem, by BARRETT,[72] was made by the following approximate method. A thin crystal having the anisotropic elastic constants of a macroscopic crystal was assumed to be strained to fit coherently with

the matrix on a certain plane. This determined two principal strains parallel to the surface of the disk. The third principle strain was determined by the requirement that the stress normal to the disk must be approximately zero. Then the elastic strain energy of the disk was computed and compared with the energy for coherence on other planes. In this computation, omitting strain energy in the matrix and assuming that infinitesimal strain theory applies, the result was obtained that in the copper-silver system the strain energy would be less for disks on {100} planes than on {111} planes, in agreement with

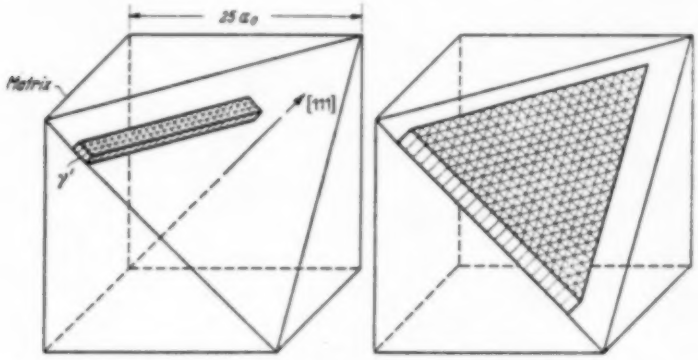

Figure 15. Manner of growth of precipitate (γ') in aluminium-silver matrix, according to Geisler and Hill. 'Stringlets', indicated at the left, develop into 'platelets' on {111} planes, indicated at the right

GEISLER's conclusions[58] regarding the actual habit at both ends of the copper-silver system.* In this computation no martensitic shear component was considered.

GEISLER and HILL[75] have found evidence that in aluminium-silver alloys aged for long times at room temperature the precipitation of platelets of the transition phase is preceded by a stage in which 'stringlets' are precipitated. The diffraction patterns are explicable in terms of particles having only one extended dimension (not two or three) which is along the close-packed rows, ⟨110⟩, of the face-centred cubic matrix. Judging by the diffraction patterns the stringlets grow into platelets on {111} planes, as indicated in *Figure 15*. Similar stringlets were found along ⟨100⟩ directions in aluminium-magnesium-silicon alloy at an early stage in the development of plates on {100} and {110} planes. There is a possibility that the diffraction streaks which appear to be caused by thin plates are actually caused by

* The habit is somewhat uncertain in copper-rich alloys; BARRETT, KAISER and MEHL[72] concluded precipitation was on {111} planes, but Geisler concludes that photographs of GAYLER and CARRINGTON[74] indicate {100} planes.

stacking faults, and it is unwise at present to exclude this possibility. Surely if the nucleation process were martensitic there would be ample reason to expect faults, for the structure change is the same as in cobalt. Conversely, the presence of faults would imply martensitic nucleation, for thermally activated atom transfer should produce an equilibrium structure, which would be a fault free one.

GUINIER[76] finds evidence of superlattices or periodic arrangements of atoms on the lattices of certain precipitating alloys. The aluminium-rich aluminium-silver alloys give superlattice reflections in the stage before a precipitate appears, indicating a period three times the normal spacing along [100]. In aluminium-copper alloys he finds there is a superlattice arrangement of atoms in the metastable precipitate phase θ'. The wavelength of this periodicity is equal to the spacing between seven (001) planes of θ' and also five (001) planes in the matrix, which led Guinier to suggest that interaction between the two structures gave rise to the periodicity.

The final stage in the precipitation is the transformation from θ' to the stable θ phase, with five groups of orientations of θ around each of the $\langle 001 \rangle$ axes of θ'. This sequence was characteristic of low temperature aging; with aging at higher temperatures only three of the five groups of orientations were found and no preliminary appearance of θ' preceded θ. Guinier concluded that the mechanism changed at the higher temperature and that θ nucleated directly. Guinier finds evidence of ordering in aluminium-rich aluminium-silver alloys also, in the stage before a precipitated phase appears, the period being three times the normal spacing along [100].

From the diffuse scattering of X-rays near the principal reflections and the direct beam, GUINIER[77] has studied the shape of segregated clusters of solute atoms in supersaturated solid solutions and has distinguished two types. In silver-zinc and aluminium-silver alloys he obtained diffraction effects from which it appeared that the clusters are equiaxial (roughly spherical) when they are about 30Å in diameter and 100Å apart. On the other hand, in aluminium-copper and copper-beryllium alloys the clusters appeared to be plate shaped, judging by their diffraction patterns, their size in a particular example (aluminium-4 per cent copper aged 24 hours at 100°C) being about 35Å in diameter and one or two layers thick. These 'Guinier-Preston Zones' are segregations of solute atoms in the solid solution prior to the appearance of the new phase. Guinier points to the correlation between the shape of these segregated clusters and the difference in the atomic diameters of solvent and solute atoms given in *Table II.* on page 34.

There is a basis here for believing that the disk shape is preferred, as suggested by Mott and Nabarro, when volume misfits are large, but that a spherical shape is preferred otherwise.[70] However, the shape of

Table II. Correlation between Shape of Nuclei and Difference in Atomic Diameter

Alloy	*Difference in Atomic Diameter*	*Shape of Nuclei*
	(*per cent*)	
Aluminium-Silver ..	+ 0·7	*Spheres*
Aluminium-Zinc	− 3	*Spheres*
Aluminium-Copper ..	− 11	*Plates*
Copper-Beryllium ..	− 20	*Plates*

these clusters in the matrix appears not always to determine the shape of precipitate particles that have grown to visible size, for aluminium-silver micrographs show a Widmanstätten figure of plate-shaped particles rather than spherical particles.

The many shapes that precipitated particles can have, their complex relation to the crystal structure of the matrix, the possible effects of ordering before or after precipitation, and the importance of any transition phases that form (even when these are so small in one or more dimensions that they lack full three-dimensional diffraction) may be summarized as the factors that could hardly be predicted by any simple theory. There has been, nevertheless, a steady increase in understanding of some aspects of the general problem, such as the importance of orientation dependent interfacial energy, shape dependent strain energy, and faulting.

Transition States—Metastable states resulting from transformations in pure metals are rare, but a few examples are known. Lithium and cobalt, as mentioned in earlier paragraphs, transform on cooling to structures that contain many faults in the stacking of close-packed layers, structures which are undoubtedly metastable with respect to equilibrium phases free from stacking disorders. The metastability of the faulted structure of lithium is indicated by the fact that its powder diffraction pattern resembles that of a faulted hexagonal close-packed structure, but cold work reduces the pattern to that of a face-centred cubic one, the cold work acting in much the same manner as thermal vibrations in 'shaking down' the structure toward equilibrium, just as cold work accelerates precipitation in a supersaturated alloy.

The suggestion has been made that the increased entropy of disordered hexagonal cobalt makes it a slightly more stable form than perfect hexagonal cobalt.[14] However, this reduction of free energy by entropy change is probably overbalanced by an opposing factor that raises the free energy of the faulted structure above that of the fault free structure: each fault introduces cubic-hexagonal interface energy. In any event, the faulted structure does not exist as a result of thermal

equilibrium, but because it was so formed during the transformation and has not had opportunity to reach true equilibrium.

Non-equilibrium conditions are doubtless common in pure metals as a result of supercooling or superheating of a phase. Even in iron of the highest purity there is a reluctance to nucleate a new phase, for the $\gamma \rightarrow \alpha$ and $\alpha \rightarrow \gamma$ transformation temperatures are several degrees apart even at the slowest heating and cooling rates.[78] When supercooling is great enough, as in rapid cooling, it may be that a martensitic process replaces a grain growth process. In such transformations the product of the martensitic change could be either the equilibrium phase or a metastable one that forms because it can grow by a faster mechanism (a cooperative movement, without diffusion) than the normal grain growth process, and because it is of lower free energy than the supercooled parent phase even though higher than the equilibrium phase. It has been suggested[42] that a martensitic transformation replaces the nucleation and growth transformation in iron under some conditions. This might account for some characteristics of the transformation curves observed by Rogers and Stamm and would neatly account for SAUVEUR and CHOU's[79] observation of a martensite-like microstructure that was visible on an unetched sample after quenching. If this interpretation is correct, ROGERS and STAMM's experiments[78] on irons of different purity imply that the choice between the competing modes of transformation is strongly dependent on purity.

Turning now from metals to alloys, we find non-equilibrium states and metastable crystal structures in considerable number. Some important and typical examples are discussed below.

When the CsCl type structure in the ternary iron-nickel-aluminium system transforms, BRADLEY and TAYLOR[80] found that two phases appear, one similar to the high temperature (ordered) phase, and one a disordered body-centred cubic phase richer in iron. When these were present in about equal amounts, they took the form of lamellae parallel to {100} planes of the parent phase and were coherent on these planes. It was concluded that the two phases formed a wave pattern of varying iron content with a wavelength of the order of a micron after 16 days annealing at 850°C.

A striking example of this wave-like precipitation was found by DANIEL and LIPSON[8] in Cu_4FeNi_3. The high temperature phase, of face-centred cubic structure, transforms into copper-rich and copper-poor phases, both face-centred cubic, but differing in parameter. Before the alloy reaches the equilibrium two-phase condition the diffraction lines become flanked by slightly diffuse side bands. Daniel and Lipson account for these by assuming that there is a sinusoidal variation in lattice spacing, with waves perpendicular to $\langle 100 \rangle$ directions and wavelengths increasing with increasing annealing times

from 100 to about 5,000Å. The Daniel-Lipson analysis of the intensity of the side bands for the different orders of diffraction indicates that changes in parameter caused by the segregation to copper-rich and copper-poor volumes are of predominant importance compared to the accompanying changes in the scattering factor.

This stage is followed by the appearance of two metastable tetragonal phases whose a dimensions are the same as that of the matrix and whose c/a ratios are greater and less than unity.[82] These metastable phases are coherent with the matrix on their basal planes, the fit being exact. Finally, the equilibrium phases appear.

HARGREAVES,[83, 84] in a study of these alloys by monochromatized x-rays concludes that a more satisfactory explanation of the observed intensities lies in a model for the periodic structure based on the occurrence of alternate lamellar volumes of the intermediate tetragonal phases rather than sinusoidal waves. The side bands appear in the diffraction pattern while these volumes retain completely their coherence with the matrix crystal so that the whole crystal diffracts with the phase relationships of a modulated lattice. The apparent movement of the side bands, attributed by Daniel and Lipson to an increase in the wavelength of the modulated structure, is explained by Hargreaves as being due to the superimposition of the various orders of side bands that may occur during an early stage of growth.

The later stages of annealing lead first to diffraction patterns from the lamellae of the tetragonal phases and subsequently from the equilibrium cubic phases. Metallographic evidence shows that the cubic phases retain the lamellar form. The three stages of precipitation are therefore considered to be the periodic stage involving completely coherent lamellae, the intermediate stage in which coherence is retained on one plane and the equilibrium stage in which the cubic phases appear and all coherence is lost.

There are also other examples in which coherence across interphase boundaries is involved. HARKER[85] has discussed this in the alloy gold-copper where the onset of long distance order introduces tetragonality. GEISLER and NEWKIRK[86] found an example in the copper-nickel-cobalt system where equilibrium precipitate and depleted matrix were both face-centred cubic in structure but had lattice parameters smaller and larger, respectively, than the parent phase. In the early stages of precipitation there appeared to be coherency such that both precipitate and depleted matrix were strained into tetragonal structures that fitted together exactly on (001) planes, as indicated in *Figure 16*. Hargreaves has suggested[83] that there is also evidence for the periodic type of structure in the x-ray patterns published by Geisler and Newkirk.

The structure that precipitates first from the aluminium-rich matrix

in the aluminium-copper system is tetragonal, with a basal plane that matches the {001} planes of the cubic matrix, but with no other obvious planes of good matching.[87] The equilibrium precipitate ($CuAl_2$) does not show this relationship.

In aluminium-silver alloys a close-packed hexagonal plane precipitates from the face-centred cubic matrix with exact matching at the interface, which is $(111)_{fcc}$ and $(001)_{hcp}$[88] At a later time the stable

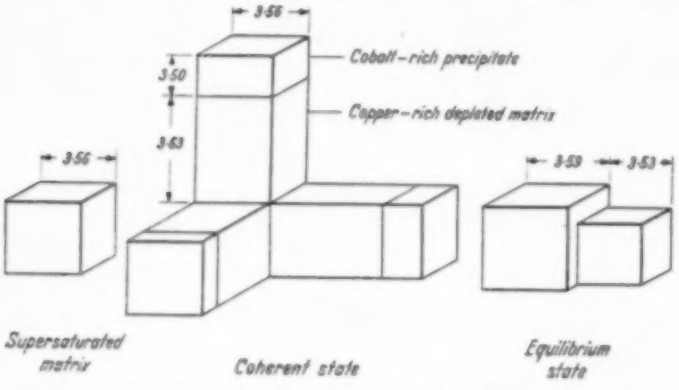

Figure 16. Stages in precipitation from a supersaturated copper-nickel-cobalt alloy (Geisler and Newkirk)

structure appears; this is also close-packed hexagonal, but it does not match the matrix (111) plane exactly—it has broken away from coherence. The precipitate is presumed to be in a strained condition when coherent, and when the stresses maintaining the coherence become intolerable it breaks away and assumes its equilibrium dimensions. MOTT and NABARRO,[70, 89] developed a theory of the thickness at which breakaway occurs, which accounted for the fact that the coherent condition lasts until the plates are many hundreds of Ångstroms thick in the aluminium-silver alloy, but are much thinner in other alloys where the misfit is greater, as in aluminium-zinc.[90] The formation of the transition precipitate involves merely an alteration in the stacking of the close-packed planes and requires merely a shifting on slip planes; similarly, the breakaway process is also assumed to be a movement of the same sort, and could be accomplished by the passage of dislocations over the interface.

The point of view adopted in these early discussions of coherency and breakaway is open to challenge. The assumption is made that the coherency stresses are merely biaxial, the principal stresses lying in the plane of the precipitate-plate. This would not be the case if the plate formed in such a way that shear strains of appreciable magnitude were set up *i.e.* if the nucleation was typically martensitic. Further, it has

been assumed that the strain free lattice dimensions of the precipitate are those characteristic of the stable phase, of equilibrium composition. Yet assurance is lacking that the composition of the precipitate, when in the coherent state, is the same as it is when in the stable state. If this is not true (and it would not necessarily be true if nucleation is martensitic) then the assumed stress free dimensions, computed stresses, and computed strain energies would be incorrect.

Coherence may also be broken by a mechanism quite different from the one discussed above; namely, by the moving of a non-coherent boundary across a grain (referred to by Mehl and Jetter as 'discontinuous precipitation'[62]). Smith points out that rapid diffusion must occur along the non-coherent boundary so as to transport the excess of one kind of atom from its position at the particles of the original precipitate to the new pearlite-like particles of precipitate in the recrystallized matrix.[65] Since the matrix ahead of the moving boundary is strained and the matrix behind it is recrystallized and strain free, a driving force for this mechanism is the strain energy resulting from the coherency strains that are believed to cause the hardening. This is then a mechanism for overaging, competitive with the more local breakaway process at each precipitate particle. Still another mechanism of overaging that can be imagined is the relaxation of strains in the matrix, independently of whether or not there is an accompanying decomposition of metastable precipitate into stable precipitate. Geisler has summarized[58] the various changes in physical properties that accompany aging and overaging and has correlated these with the structure changes in the various alloys. He emphasizes the variation, from one alloy system to another, in presence and absence or the relative importance of the various structural changes that can occur in overaging.

The discussion of transition states would not be complete without mention of states that form during plastic deformation. Strain-induced precipitation in the copper-silicon system is an example[16] (this and other examples have been discussed on pp 24–28). When applied stresses can aid in the atomic movement needed to nucleate a precipitate phase, of either stable or metastable type, it is easy to understand why plastic deformation should accelerate precipitation.

In conclusion, it has been emphasized that metastable phases often occur during transformations normally classed as nucleation and growth processes; these phases very commonly share a plane of atoms with the parent matrix and take up orientations and shapes dictated by this coherence. Even the crystal structure of these phases appears in some alloys to be controlled by this coherence. The importance of the low interface energy at the coherent boundary in influencing the crystallographic relations is obvious. But, in addition, it is suggested

VOL 3

that the systematic atom movements which characterize martensitic transformations may also occur in the early stages of precipitation in some age hardening alloys. The crystal structure of a precipitate in such alloys would then be that structure, of lower free energy than the parent, into which the parent structure can most easily slide, and may be a metastable phase quite different from the equilibrium phase in structure. The shears or shear-like distortions in the matrix that originate from this mode of precipitation would be severe enough to account for the distortions registered in diffraction patterns of age hardening alloys, and would constitute a major cause of the hardening. The role of plastic deformation in precipitation would in these cases be analogous to its role in strain-induced martensitic transformations—at least during early stage precipitation.

If martensitic precipitation of a metastable phase determines the orientation relationships and habit planes in certain alloys, it is not surprising that a universal theory that would account for all such Widmanstätten relationships has not yet been found. Prerequisites to this would be reliable data as to whether, on the one hand, only the static problem of equilibrium states is involved, or, on the other hand, the dynamic problem of martensitic transformation. If the latter, detailed and perhaps precision data would be required regarding any transition states that may exist, data upon which to base a detailed analysis of atom shifts analogous to those reviewed in the first half of this chapter that appear to account successfully for the orientations, habit, and distortions connected with martensite transformations in iron-carbon and indium-thallium alloys.

REFERENCES

[1] TROIANO, A. R. and GRENINGER, A. B. *Met. Progr.* 50 (1946) 303
[2] *Metals Handbook* Cleveland, 1948
[3] COHEN, M. *Trans. Amer. Soc. Met.* 41 (1949) 35
[4] KURDJUMOW, G. V. *J. Tech. Phys. U.S.S.R.* 18 (1948) 999. (Translations published by Henry Brutcher, Altedena, California)
[5] FISHER, J. C. *Trans. Amer. Soc. Met.* 41A (1950) 201
[6] COHEN, M. Cornell Conference of National Research Council, 1948 In press
[7] BOWLES, J. S., BARRETT, C. S. and GUTTMAN, L. *Trans. Amer. Inst. min. (metall.) Engrs* 188 (1950) 1478
[8] SCHEIL, E. *Z. anorg. Chem.* 207 (1932) 21
[9] CHANG, L. C. and READ, T. A. *Trans. Amer. Inst. min. (metall.) Engrs* 189 (1951) 47
[10] MCREYNOLDS, A. W. *J. appl. Phys.* 17 (1946) 823
[11] KURDJUMOW, G. *Bull. Acad. Sci. U.R.S.S. Chem. Series*, No. 2 (1936) 271
[12] ISAICHEV, I. and SALLI, I. *J. tech. Phys. U.S.S.R.* 5 (1935) 395. Reviewed in 4
[13] TROIANO, A. R. and MCGUIRE, F. T. *Trans. Amer. Soc. Met.* 31 (1943) 340
[14] EDWARDS, O. S. and LIPSON, H. *J. Inst. Met.* 69 (1943) 177; *Proc. roy. Soc.* 180 (1942) 268
[15] BARRETT, C. S. Cornell Conference of National Research Council, 1948 In press

[16] BARRETT, C. S. *Trans. Amer. Inst. min. (metall.) Engrs* 188 (1950) 123; *J. Met.* January (1950)
[17] —— and BARRETT, MARJORIE A. *Bull. Amer. phys. Soc.* 25 November (1950) 23; *Phys. Rev.* In press; BARRETT, C. S., Pocono Conference on Imperfections in Almost Perfect Crystals, National Research Council Committee on Solids, 1950 In press
[18] —— and CLIFTON, D. F. *Trans. Amer. Inst. min. (metall.) Engrs* 188 (1950) 1329; *J. Met.* November (1950) 1329
[19] KURDJUMOW, G. Discussion to A. B. Greninger *Trans. Amer. Inst. min. (metall.) Engrs* 133 (1939) 204
[20] LYMAN, T. Discussion to N. J. Petch *J. Iron Steel Inst.* 147 (1943) 221
[21] JASWON, M. A. and WHEELER, J. A. *Acta Crystallogr.* 1 (1948) 216
[22] PETCH, N. J. *J. Iron Steel Inst.* 147 (1943) 221
[23] LIPSON, H. and PARKER, A. M. B. *ibid* 149 (1944) 123
[24] ZENER, C. *Trans. Amer. Inst. min. (metall.) Engrs* 167 (1946) 550
[25] FORSTER, F. and SCHEIL, E. *Z. Metallk.* 32 (1940) 165
[26] KULIN, S. A. and COHEN, M. *Trans. Amer. Inst. min. (metall.) Engrs* 188 (1950) 1139; *J. Met.* September (1950) 1139
[27] BAIN, E. C. *Trans. Amer. Inst. min. (metall.) Engrs* 70 (1924) 25
[28] GRENINGER, A. B. and TROIANO, A. R. *Trans. Amer. Inst. min. (metall.) Engrs* 140 (1940) 307
[29] MEHL, R. F., BARRETT, C. S. and SMITH, D. W. *ibid* 105 (1933) 215
[30] SMITH, G. V. and MEHL, R. F. *ibid* 150 (1942) 211
[31] KURDJUMOW, G. and SACHS, G. *Z. Phys.* 64 (1930) 325
[32] WASSERMANN, G. *Mitt. K.-Wilh.-Inst. f. Eisenforsch.* 17 (1935) 149
[33] NISHIYAMA, Z. *Sci. Rep. Tôhoku Univ.* 23 (1934–35) 638
[34] MEHL, R. F. and DERGE, G. *Trans. Amer. Inst. min. (metall.) Engrs* 125 (1937) 482
[35] GRENINGER, A. B. and TROIANO, A. R. *ibid* 145 (1941) 291; 1949
[36] —— and MOORADIAN, V. G. *ibid* 128 (1938) 337
[37] ISARTSCHEW, I., KAMINSKY, E. and KURDJUMOW, G. Discussion to 36
[38] Private Communication
[39] GRENINGER, A. B. *Trans. Amer. Inst. min. (metall.) Engrs* 133 (1939) 204
[40] GAWRANEK, V., KAMINSKY, E. and KURDJUMOW, G. *Metallwirtschaft* 15 (1936) 370
[41] WASSERMANN, G. *ibid* 8 (1934) 133
[42] BARRETT, C. S. and TRAUTZ, O. R. *Trans. Amer. Inst. min. (metall.) Engrs* 175 (1948) 579
[43] BOWLES, J. S. *ibid* 191 (1951) 44
[44] BURGERS, W. G. *Physica* 1 (1934) 561
[45] TROIANO, A. R. and TOKICH, J. L. *Trans. Amer. Inst. min. (metall.) Engrs* 175 (1948) 728
[46] BETTERIDGE, W. *Proc. phys. Soc.* 50 (1938) 519
[47] WORRELL, F. T. *J. appl. Phys.* 19 (1948) 929; ZENER, C. *Elasticity and Anelasticity of Metals* Chicago, 1949
[48] CARLILE, S. J., CHRISTIAN, J. W. and HUME-ROTHERY, W. *J. Inst. Met.* 77 (1949) 169
[49] SACHS, G. *Z. Metallk.* 24 (1932) 241
[50] BOWLES, J. S. *Acta Crystallogr.* In press
[51] GUTTMAN, L. *Trans. Amer. Inst. min. (metall.) Engrs.* In press
[52] KURDJUMOW, G. and MIRETSKY, V. *J. tech. Phys. U.S.S.R. No. 22* (1938)
[53] COHEN, M., MACHLIN, E. S. and PARANJPE, V. G. *Trans. Amer. Soc. Met.* 42A (1950) 242

[54] SMITH, C. S. *Pocono Conference on Imperfections in Almost Perfect Crystals, National Research Council Committee on Solids*, 1950 In press
[55] FISHER, J. C., HOLLOMON, J. H. and TURNBULL, D. *Trans. Amer. Inst. min. (metall.) Engrs* 185 (1949) 691; *J. appl. Phys.* 19 (1948) 775
[56] KURDJUMOW, G. V. and MAKSIMOVA, O. V. *Doklady Akad. Nauk. U.S.S.R.* 61 (1948) 83
[57] BARRETT, C. S. *Phys. Rev.* 72 (1947) 245
[58] GEISLER, A. H. Cornell Conference of National Research Council, 1948 In press
[59] SMITH, G. C. *Progress in Metal Physics* 1 p 163 London, 1949
[60] HARDY, H. K. *J. Inst. Met.* 75 (1949) 707
[61] BARRETT, C. S. *Structure of Metals* New York, 1943
[62] MEHL, R. F. and JETTER, L. K. *Age Hardening of Metals Amer. Soc. Met.*, 1940
[63] YOUNG, J. *Proc. roy. Soc. A* 112 (1926) 630; *Phil. Trans. A* 238 (1939) 393
[64] BECK, P. A., SPERRY, P. R. and HU, H. *J. appl. Phys.* 21 (1950) 420
[65] SMITH, C. S. *Trans. Amer. Inst. min. (metall.) Engrs* 175 (1948) 15
[66] READ, W. T. and SHOCKLEY, W. *Phys. Rev.* 78 (1950) 275
[67] DUNN, C. G. and LIONETTI, F. *Trans. Amer. Inst. min. (metall.) Engrs* 185 (1949) 125
[68] ——, DANIELS, F. W. and BOLTON, M. J. *ibid* 188 (1950) 368
[69] AUST, K. T. and CHALMERS, B. *Proc. roy, Soc. A* 201 (1950) 210
[70] MOTT, N. F. and NABARRO, F. R. N. *Proc. phys. Soc.* 52 (1940) 86
[71] SMOLUCHOWSKI, R. *Physica* 15 (1949) 175
[72] BARRETT, C. S. Discussion to 58
[73] ——, KAISER, H. F. and MEHL, R. F. *Trans. Amer. Inst. min. (metall.) Engrs* 117 (1935) 39
[74] GAYLER, M. L. V. and CARRINGTON, W. E. *J. Inst. Met.* 73 (1947) 625
[75] GEISLER, A. H. and HILL, J. K. *Acta Crystallogr.* 1 (1948) 238
[76] GUINIER, A. *J. Phys. Radium* 3 (1942) 124
[77] —— *Physica* 16 (1949) 148
[78] ROGERS, B. A. and STAMM, K. O. *Trans. Amer. Inst. min. (metall.) Engrs* 150 (1942) 131
[79] SAUVEUR, A. and CHOU, A. *ibid* 84 (1929) 350
[80] BRADLEY, A. J. and TAYLOR, A. *Proc. roy. Soc. A* 166 (1938) 353
[81] DANIEL, V. and LIPSON, H. *ibid* 181 (1943) 368; 182 (1944) 378
[82] BRADLEY, A. J. *Proc. phys. Soc.* 52 (1940) 80
[83] HARGREAVES, M. E. *Acta Crystallogr.* 2 (1949) 259
[84] —— *ibid* In press
[85] HARKER, D. *Trans. Amer. Soc. Met.* 32 (1944) 210
[86] GEISLER, A. H. and NEWKIRK, J. B. *Trans. Amer. Inst. min. (metall.) Engrs.* 180 (1949) 101
[87] FINK, W. L. and SMITH, D. W. *ibid* 137 (1940) 109
[88] BARRETT, C. S. and GEISLER, A. H. *J. appl. Phys.* 11 (1940) 733; ——, —— and MEHL, R. F. *Trans. Amer. Inst. min. (metall.) Engrs* 143 (1941) 134
[89] NABARRO, F. R. N. *Proc. phys. Soc.* 52 (1940) 90; *Proc. roy. Soc. A* 175 (1940) 519
[90] GEISLER, A. H., BARRETT, C. S. and MEHL, R. F. *Trans. Amer. Inst. min. (metall.) Engrs* 152 (1943) 201

2

PROPERTIES OF METALS AT LOW TEMPERATURES

*D. K. C. MacDonald**

TO A 'PRACTICAL' metallurgist the suggestion in our title that low temperatures—by which we mean very approximately temperatures below 90°K, and more particularly below 20°K—should play a significant role in the properties of metals may well seem untenable. It is true that for commercial alloys, steels *etc*, the cohesion, strength and compressibility are not significantly altered at these low temperatures.† However, a fundamental understanding of these properties demands a knowledge, for example, of the behaviour of the conduction electrons in pure metals and alloys of varying composition; this in turn can only be investigated adequately by the inclusion of very low temperature research since, for example, the specific heat contribution of these electrons is obscured at normal temperatures by that of the metallic lattice. Furthermore, progress generally in our knowledge of the solid state depends most surely on a study of simple metals such as the alkalis which may afford a relatively simple theoretical model for study and for these certainly the behaviour at rather low temperatures is most significant.

It will not be our purpose here to attempt to relate directly the progress attained in fundamental research to practical problems of strength *etc*. For a survey of this nature the reader might turn in the first place to HUME-ROTHERY's *Electrons, Atoms, Metals and Alloys*,[1] and of course the recent work by MOTT[2] and his school on dislocation theory in metallic lattices also affords an excellent example of a direct relationship to a very practical field. We wish here to summarize recent progress in the observation of fundamental electrical and thermal properties, primarily in the low temperature region, and to discuss specific heats and electrical conductivity in particular.

Part I

SPECIFIC HEATS

Since the beginning of the century, the determination of specific heat and its variation at low temperatures has been a powerful tool in the

* Physics Division, National Research Council, Ottawa, Canada (lately of Clarendon Laboratory, University of Oxford).

† This is perhaps rather a sweeping statement; from the practical standpoint not inappreciable changes in the mechanical properties may occur, but little systematic work has as yet been done in this field.

study of the solid state. In the classical theory, each element of a lattice had a thermal energy $6 \times \frac{1}{2}kT$ (kinetic + potential), yielding a total energy per mol:

$$E = 3NkT = 3RT \quad \ldots\ldots (1)$$

and therefore a constant specific heat:

$$C_v = \frac{\partial E}{\partial T} = 3R \approx 6 \text{ cal/mol/°K} \quad \ldots\ldots (2)$$

For most elements, reasonable agreement with experiment at room temperature was shown by the empirical law of Dulong and Petit, although a notable exception was the case of diamond.

The Einstein Model—The recognition by EINSTEIN[3] of the relevance of the quantization of energy levels in a simple (Planck) oscillator given by:

$$\varepsilon = nh\nu^* \quad \ldots\ldots (3)$$

where h, Planck's constant $= 6{\cdot}55 \times 10^{-27}$ erg sec, showed that this classical result could only be expected to hold for temperatures not small compared with a characteristic temperature of the lattice, Θ_E, defined by

$$\Theta_E = h\nu/k \quad \ldots\ldots (4)$$

where k, Boltzmann's constant $= 1{\cdot}37 \times 10^{-16}$ ergs/°K. The lattice was simulated by an aggregation of N similar, independent, oscillators of frequency ν and Einstein showed:

$$E = 3RT\frac{h\nu/kT}{\varepsilon^{h\nu/kT} - 1} = 3RT\frac{\Theta_E/T}{\varepsilon^{\Theta_E/T} - 1} \quad \ldots\ldots (5)$$

and

$$C_v = 3R\,\frac{(\Theta_E/T)^2}{(\varepsilon^{\Theta_E/T} - 1)\,(1 - \varepsilon^{-\Theta_E/T})} \quad \ldots\ldots (6)$$

For $T \gg \Theta_E$ we have $E \approx 3RT$, and $C_v \approx 3R$ in agreement with 1 and 2, while if $T \ll \Theta_E$ then:

$$E \approx 3RT\left(\frac{\Theta_E}{T}\varepsilon^{-\Theta_E/T}\right) \quad \ldots\ldots (5a)$$

and

$$C_v \approx 3R\left(\frac{\Theta_E}{T}\right)^2\varepsilon^{-\Theta_E/T} \quad \ldots\ldots (6a)$$

thus the specific heat falls rapidly to zero as T diminishes. This theoretical deduction added great weight to NERNST's previous statement[4] of his Heat Theorem, now accepted as the Third Law of

* Ignoring the zero point energy contribution which does not affect the specific heat; more strictly $\varepsilon = (n + \frac{1}{2})h\nu$.

Thermodynamics from which a basic deduction in its present formulation is the vanishing of the specific heat at absolute zero.*

The vital feature is now the recognition of a temperature, Θ, characteristic for each substance, above which we may say that thermal energy blurs the individual features of each lattice structure, while below this temperature we may expect the specific heat (and many other observable parameters) to depend fairly critically on the precise energy-level pattern evinced by the particular solid lattice. The 'anomalous' specific heat of diamond on the classical theory is readily explained by the assumption of a high characteristic frequency, ν, such that the resulting Θ is large compared with room temperature; consequently the specific heat already lies well below the Dulong–Petit value.

Development of the Theory—It was soon recognized[6–9] that this 'Einstein model' was too crude an approximation to reproduce the low temperature specific heat sufficiently accurately. In particular the very rapid decay ($\sim \varepsilon^{-\Theta/T}$) for $T \ll \Theta$ arises because a minimum energy $\sim h\nu$ is necessary to excite the lowest mode of the Planck oscillator and the probability diminishes very rapidly as the temperature is lowered. NERNST and LINDEMANN observed from their experimental data that 'der Abfall der Atomwärme bei den untersuchten Elementen Pb, Ag, Zn, Cu, Al und ferner beim KCl bei tiefen Temperaturen *langsamer erfolgt*, als der Formel von Einstein entspricht'. They proposed a generalization of Einstein's formula:

$$E = 3RT\,\tfrac{1}{2}\left(\frac{\Theta/T}{\varepsilon^{\Theta/T}-1} + \frac{\Theta/2T}{\varepsilon^{\Theta/2T}-1}\right) \qquad \ldots\ (7)$$

with a corresponding expression for C_v, on quasi theoretical grounds that we need not discuss here. This yielded much better agreement with experiment down to temperatures $\sim 20°$K. The Nernst–Lindemann formula is regarded today as a very useful approximate expression and we shall speak of it again below.

In his original paper EINSTEIN identified the frequency ν with a sharp resonance absorption in the infra-red, but was later[10, 7] led to consider the general connection with the elastic vibrations of the crystal. Thus, other things being equal a high Θ would imply strong elastic binding, that is a more rigid solid. This conclusion is of general validity; as an instance beryllium has $\Theta \sim 1{,}000°$K while lead has $\Theta \sim 90°$K. Einstein himself also recognized[7]† that the coupling between neighbouring atoms would generally be so strong that the

* A valuable survey of the Third Law in modern terms is given, in particular, by SIMON.[5]

† A particularly interesting paper containing in addition a valuable discussion on approximate relations between solid parameters (such as the LINDEMANN[11] melting-point formula for Θ) which may be derived by dimensional considerations.

assumption of a monochromatic vibrational spectrum could only be regarded as a rough approximation.

The Debye Model—DEBYE's approach[8] was to consider the coupled vibrational modes of the atomic lattice—some $3N$ in all—as forming a continuum of elastic vibrations running from the longest wavelengths ($v \to 0$) to a short wavelength-limit of the order of the lattice structure. This model leads directly to a frequency density distribution:

$$\mathrm{d}n = \frac{4\pi}{C^3} v^2 \mathrm{d}v \qquad \ldots . \quad (8a)$$

where C is the velocity of elastic waves in the crystal assumed independent of v and isotropic. More generally:

$$\mathrm{d}n = \frac{4\pi}{3}\left(\frac{2}{C_t^3} + \frac{1}{C_l^3}\right) v^2 \mathrm{d}v \qquad \ldots . \quad (8b)$$

where C_t and C_l are the velocities of transverse and longitudinal waves, again assumed independent of v and isotropic. The weighting of 2 : 1 arises from the polarized transverse modes. Associated with each proper vibration we have the energy of a Planck oscillator and thus:

$$E = \frac{4\pi V}{C^3} \int_0^{v_m} \frac{h v^3 \mathrm{d}v}{\varepsilon^{hv/kT} - 1}$$

where $\frac{1}{C^3} = \frac{2}{C_t^3} + \frac{1}{C_l^3}$, V is the molar volume, and v_m is the maximum frequency, given by $v_m^3 = C^3 \left(\frac{9N}{4\pi V}\right)$

that is

$$E = 3RT.3\left(\frac{T}{\Theta_D}\right)^3 \int_0^{\Theta_D/T} \frac{x^3 \mathrm{d}x}{\varepsilon^x - 1} \qquad \ldots . \quad (9)$$

where a characteristic Debye temperature, Θ_D, is now defined by $\Theta_D = \frac{hv_m}{k}$

At high temperatures we have $E \approx 3RT$ again in agreement with the classical treatment, but at low temperatures:

$$E \approx 9RT^4 . \frac{1}{\Theta_D^3} \int_0^{\infty} \frac{x^3 \mathrm{d}x}{\varepsilon^x - 1} \qquad \ldots . \quad (9a)$$

and the specific heat:

$$\begin{aligned} C_v &\approx 233{\cdot}8R(T/\Theta_D)^3 \\ &\approx 464(T/\Theta_D)^3 \text{ cal/mol } ^\circ\text{K} \qquad \ldots . \quad (10) \end{aligned}$$

Almost simultaneously with Debye's work, BORN and v. KÁRMÁN[9] discussed the complete dynamical treatment of the proper vibrations of a lattice starting from the atomic force constants. Basically, the

problem was not new (*cf* BRILLOUIN's excellent book[12]). NEWTON[13] first attacked the analysis of the vibration of a one-dimensional lattice when considering the velocity of sound, and KELVIN was the first to consider a 'diatomic' lattice of large and small coupled masses. This then yields two distinct vibrational modes—the so-called 'acoustical' and 'optical' branches. Born's linear 'sodium chloride' lattice essentially duplicated Kelvin's problem.

In this approach the velocity of propagation is no longer constant nor necessarily isotropic and the simple vibrational frequency density

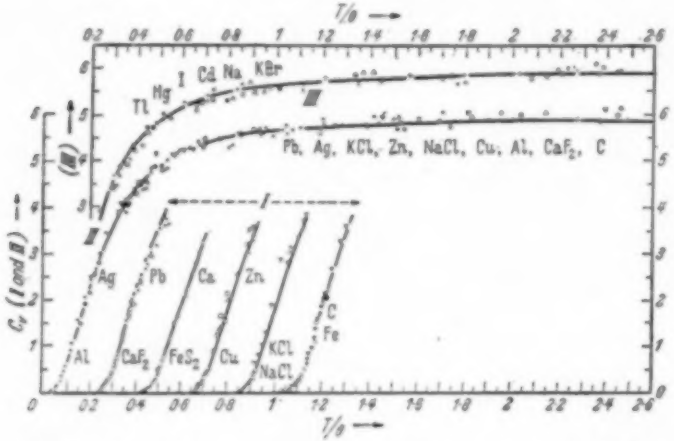

Figure 1. The molar heat capacities of various solids as functions of T/Θ_D *[Note—The curves I have been shifted horizontally, and the curve III vertically, for clarity]*

of equation 8 no longer obtains. The problem of analysing the true spectrum for a particular crystal is very complex and difficult to generalize; consequently Debye's much simpler and very elegant approximation has been widely applied to the analysis and comparison of experimental data, although more recently, as we shall see, the Born–v. Kármán analysis has come into prominence.

Many metals and crystalline solids are found to exhibit specific heats which agree quite closely with the Debye formula, and surveys will be found in EUCKEN,[14] FOWLER,[15] or FOWLER and GUGGENHEIM,[16] SCHRÖDINGER,[17] BORN[18] and MOTT and JONES.[19] We reproduce here *Figure 1* and *Table I* which are self-explanatory from Fowler (after Schrödinger).

In the Debye theory, Θ_D is of course a constant parameter by definition; however in presenting experimental data it has become conventional to derive values at various temperatures for an effective Θ_D necessary to 'force' agreement with the Debye theory and to plot

Table I. Data for Figure 1, studying the Law of corresponding states

Substance	Chemical symbol	Temperature range °K	Θ	Points in Fig. 1 Curves		
				I	II	III
Lead	Pb	14–573	88	×	×	
Thallium ..	Tl	23–301	96			○
Mercury ..	Hg	31–232	97			□
Iodine	I	22–298	106			×
Cadmium ..	Cd	50–380	168			+
Sodium	Na	50–240*	172			△
Potassium bromide	KBr	79–417	177			●
Silver	Ag	35–873	215		●	
Calcium	Ca	22–62	226	○		
Sylvine	KCl	23–550	230	▽	▽	
Zinc	Zn	33–673	235	□	□	
Rock-salt ..	NaCl	25–664	281	◇	◇	
Copper	Cu	14–773*	315	△	△	
Aluminium ..	Al	19–773	398		+	
Iron	Fe	32–95*	453	○		
Fluorspar ..	CaF_2	17–328	474	○	○	
Iron pyrites ..	FeS_2	22–57*	645	+		
Diamond ..	C	30–1169	1860	▼	▼	

thus a curve of Θ_D as a function of temperature. If a substance obeyed the Debye theory precisely then of course Θ_D would be constant. If this is not the case within experimental error, strictly one may only say that the Debye theory is inapplicable, but in fact this approach is of considerable value when certain types of variation common to a number of substances can be recognized.

ANOMALOUS SPECIFIC HEATS

Effect of an Internal Transition—After the initial remarkable success of the Debye theory, deviations in a greater or lesser degree have been found in quite a number of solids and these are still of considerable interest today. SIMON[20, 5] proposed that deviations in grey tin, silicon, diamond and the alkali metals might be ascribed to an 'internal transition', giving rise to a SCHOTTKY anomaly[21] in the specific heat. If we assume that the atomic constituent of the lattice may exist in two internal states separated by an energy difference U, then at absolute zero all atoms will be in the ground state, while at very high temperatures half will be in the excited state. In the region of an intermediate temperature defined by $\Theta_S = \frac{U}{k}$ a transitional energy $E = \frac{N}{2}U = \frac{R\Theta_S}{2}$,

* For Na, Cu, Fe, FeS_2, C_V rises *above* the curve after these temperatures.

with a corresponding entropy content $R \log_e 2$ will have to be supplied. At any temperature, T, the occupational probabilities will be $\frac{\varepsilon^{-\Theta_s/T}}{1+\varepsilon^{-\Theta_s/T}}$; $\frac{1}{1+\varepsilon^{-\Theta_s/T}}$ leading to a specific heat contribution:

$$\Delta C_v = R\left(\frac{\Theta_s}{T}\right)^2 \frac{\varepsilon^{-\Theta_s/T}}{(1+\varepsilon^{-\Theta_s/T})^2} \quad \ldots . \quad (11)$$

Figures 2a and 2b show how Simon applied his theory to grey tin, proposing an underlying lattice temperature, $\Theta_D = 260°\text{K}$, with a transition temperature, $\Theta_S = 69°\text{K}$ corresponding to $U = 6 \times 10^{-3} ev$. The case of the alkalis will be discussed later (see p 61).

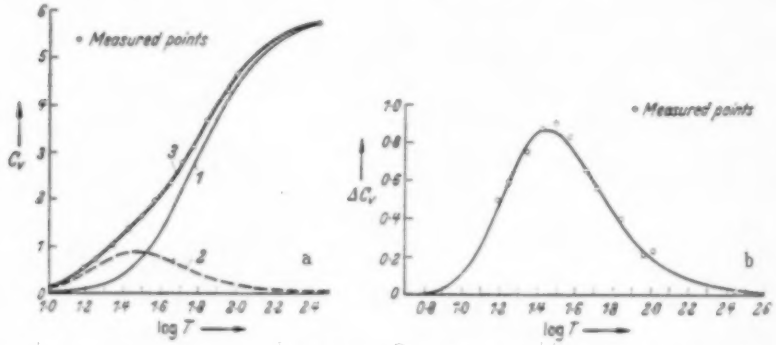

Figure 2a. *Atomic heat of grey tin: 1 Debye function,* $\Theta_D = 260°K$, *2 Schottky function* $\Theta_S = 69°K$, *3 Sum of 1 and 2*

Figure 2b. *Anomaly in the atomic heat of grey tin: Shottky function,* $\Theta_S = 69°K$

The general validity of Simon's hypothesis in interpretation of low temperature data must be regarded as less certain today in view of the relatively recent work of Blackman and pupils of Born on the detailed vibrational lattice spectrum following the Born–v. Kármán foundation. However, it is also possible that in some cases the anomalous increase in C_v over the value $3R$ observed at high temperatures may be ascribed to the onset of such a transition, rather than to anharmonicity of atomic vibrations. Since thermal expansion is also intimately related to the latter effect, it offers another source of experimental data in examining the significance of specific heat anomalies.

Influence of Lattice Structure—BLACKMAN* resumed study[22, 23] of the crystalline lattice problem, particularly in contrast with the Debye continuum. He made very marked progress in a series of papers finding, in general, that many features of specific heat data hitherto regarded as anomalous must be regarded rather as a direct consequence of fundamental lattice theory. He starts first with the one-dimensional

* Blackman has published an excellent review.[21]

problem and finds that '. . . The main difference between the linear lattice of equal masses and the continuum lies in the heaping up of vibrations near the maximum frequency'. Extension to two-dimensional and three-dimensional structures showed that the periodic lattice evinced a spectrum differing very markedly, in general, from that of the Debye continuum. Considerable dispersion occurs in the lattice and there is also the complication, mentioned earlier, of acoustical and optical modes of vibration. The greatest drawback is simply the complexity of the detailed spectrum problem but it appears general that the frequency density will exhibit two or more maxima. This behaviour was first found by Blackman in the two-dimensional lattice but later investigations *e.g.* KELLERMAN[24] on sodium chloride and SMITH[25] on diamond, have always confirmed this in solid lattices. This characteristic provides an *a posteriori* justification for the Nernst–Lindemann formula, which may then be regarded as approximating to the true vibrational spectrum by two monochromatic components (Einstein functions) at these maxima.

Variation of Frequency Density—It also appears to be a general property, although no general proof has yet been obtained, that the frequency density, which starts off as a ν^2 law for long wavelengths (as in the Debye spectrum), rises faster than ν^2 as soon as the continuum region is passed. This has a very important consequence. For sufficiently low temperatures (and Blackman suggests $< \Theta_D/50$ or even $< \Theta_D/100$) the specific heat should obey strictly the simple Debye T^3 law (*cf* equation 10) since physically for long enough wavelengths the solid must behave effectively like a continuum. The increase of frequency density will then, however, call forth a rise in the specific heat over the expected Debye value as the temperature is increased, or, interpreting this as a variation of characteristic temperature, Θ_D will then fall. If moreover as frequently happens, the general trend is for Θ_D to fall somewhat from the high temperature end, then the $\Theta_D : T$ curve will exhibit a minimum region wherein then, as Blackman says, a 'pseudo-T^3 law' will be exhibited, although the true continuum behaviour has not yet been attained. Recognition of this factor has enabled a number of discrepancies to be removed between the calculations of Θ_D from elastic constants on the one hand and thermal data on the other. It makes very evident the necessity for thermal data in the region of only one or two degrees above the absolute zero in order that one may be certain that the true theoretical T^3 law should obtain.

Contribution of Electronic Specific Heat—In the case of the electronic contribution to the specific heat in metals this requirement does not perhaps seem to have been fully recognized always. It will be remembered that on the classical theory the thermal status of the free or conduction electrons was very unsatisfactory; on the one hand, the

concept of an electron 'gas' in the Drude–Lorentz theory of thermal and electrical conductivity seemed very appropriate while, on the other, such a classical gas should have contributed an additional specific heat $\frac{3}{2}nR$ cal/gm atom where n is the number of free electrons per atom. To explain the magnitude of the conductivities a value of $n \approx 1$ was necessary for simple metals, while no corresponding specific heat was observed.

Modern quantum theory, in particular the application of the Pauli exclusion principle in Fermi–Dirac statistics, showed, however, that except at very high temperatures only a very small fraction of the conduction electrons (those on the surface of the Fermi sphere) can interchange thermal energy with the lattice; consequently at normal temperatures, the electronic specific heat is negligible and the electron gas is said to be degenerate. More generally, however, SOMMERFELD[26] has shown that the free electrons should exhibit a specific heat linear in T at low temperatures; this consequently should become significant at sufficiently low temperatures where the lattice contribution is falling roughly as T^3. The actual magnitude of the linear term will clearly depend on the density of electron states near the top of the Fermi distribution and information about the whole energy-band can only be obtained if measurements can also be made at sufficiently high temperatures and for all the electrons to contribute essentially (see also the paper by STONER[27]). This depends of course on the actual degeneracy temperature and if this can be approached, so that the electron gas tends to become Maxwellian, then an electronic specific heat of the order of $\frac{3}{2}R$ should manifest itself in addition to the classical lattice heat. This increase is observable in some metals, particularly the transition elements*, but in a simple metal the degeneracy temperature is too high *e.g.* in sodium $T_{deg} \sim 36{,}000°K$.

It is clear that, to separate out the electronic heat at low temperatures, the lattice heat must be known accurately and it has been customary, for this purpose, to express the specific heat in the form:

$$C_v = \gamma T + 464(T/\Theta)^3 \qquad \ldots \quad (12)$$

where the validity of the Debye law for the lattice heat is implicit in the second term. Thus:

KEESOM and CLARK[29] found for nickel in the range 1° to 10°K:

$$C_v = 1{\cdot}74 \times 10^{-3}T + 464(T/413)^3$$

* See, for example, CLUSIUS and SCHACHINGER[28] where the case of palladium is carefully analysed from $\sim 2°K$ to room temperature. They find, in particular, that the electronic specific heat is well represented throughout by a term $\sim \chi_s T$ where χ_s is the magnetic susceptibility.

KOK and KEESOM[37] for platinum and copper (1·2° to 20°K) respectively:

$$C_v = 1{\cdot}6 \times 10^{-3}T + 464(T/233)^3$$
$$C_v = 1{\cdot}78 \times 10^{-4}T + 464(T/335)^3$$

KEESOM and VAN LAER[30] found for tin between ~ 1°K and ~ 3°K:

$$C_v = 4 \times 10^{-4}T + 464(T/185)^3$$

DUYCKAERTS[31] for cobalt between 2° – 18°K finds:

$$G_v = 1{\cdot}2 \times 10^{-3}T + 464(T/443)^3$$

KEESOM and KURRELMEYER[32] for iron between 1·1° – 20·4°K:

$$C_v = 1{\cdot}2 \times 10^{-3}T + 464(T/462)^3$$

and DUYCKAERTS[33] a very similar result.

ELSON, SMITH and WILHELM[34] for manganese between 16° – 22°K:

$$C_v = 4{\cdot}2 \times 10^{-3}T + 464(T/410)^3$$

PICKARD[35] and PICKARD and SIMON[36] for palladium between 2° and 22°K:

$$C_v = 3{\cdot}1 \times 10^{-3}T + 464(T/275)^3$$

In most cases, in fact, the experiments have been made at temperatures sufficiently low to assume reasonably that the Debye continuum has been reached, but data in so limited a region as those of ELSON *et al*[34] would seem of rather doubtful value. The Sommerfeld free electron gas theory predicts $\gamma \approx 10^{-4}$ and it appears therefore quite justifiable, on the one hand, to conclude from this data—in general agreement with theory (*cf* MOTT and JONES[19])—that the density of states for certain bands is much higher in the transition metals *e.g.* Pt, than for a 'simple' metal like Cu; more data on the specific heat of alkali metals at very low temperatures appear very desirable from other points of view as well (*vide infra*). On the other hand, too detailed quantitative conclusions seem unwarranted in the present position particularly when we note that Keesom and van Laer (*loc cit.*) say in the case of tin that '. . . It is worth, however, to be noted that with a γ-value less than $4{\cdot}0 \times 10^{-4}$ and another corresponding value of Θ_D one can get a rather good agreement too'.

Sommerfeld's 'free-electron' formula may be written:

$$\gamma = 3{\cdot}26 \times 10^{-5} \times V^{\frac{1}{3}} \times n^{\frac{1}{3}}$$

where V is the atomic volume, and n 'the number of free electrons per atom'. Certain authors express experimental γ-values, consequently, as an effective number of free electrons. Except in the case where $n \approx 1$ (as in Cu), thus justifying a free-electron assumption, this seems

very misleading, particularly in contrast to values of effective electron freedom derived from measurements of conductivities.

In the case of sodium, which might appear an ideal case (*vide infra*) for testing the Sommerfeld model, PICKARD and SIMON[36] found, however, definitely anomalous behaviour at low temperatures; the specific heat goes through a definite maximum* around 7°K, similar to that observed in beryllium by CRISTESCU and SIMON[38] around 11°K. The entropy content of these anomalies is small ($\sim 10^{-2}R$ for Na, $\sim 10^{-3}R$ for Be) and the possibility of a connection with the conduction electron properties was partly responsible for the investigation of the electrical conductivity of the alkali metals by MACDONALD and MENDELSSOHN[39, 40] The anomalous increase in the specific heat of mercury at low temperatures also found by Simon and Pickard is of a less dramatic nature and it appears quite possible that lattice theory may be adequate to account for it—Blackman's[22] view point is '. . . *As long as there is no actual maximum in the specific-heat curve* . . . no reason to suppose that . . . lattice theory alone will not account. . . .' These complications in metals due to the conduction electrons should also make abundantly clear why experiments on typical crystalline insulators such as rock-salt and sylvine (KCl) are vital to the general problem.

The Raman Lattice Theory—Although it might be felt that the crystal lattice analysis together with the Debye approximation, were now well established, a new theory was proposed by RAMAN[41] together with much fresh examination of specific heat data. The theory is, unlike Born's, not a detailed mathematical analysis of a definite physical model. It is a rather dogmatic concept, to which Raman was led by his observations on the phenomenon of scattering of light in crystals which goes by his name. He divides the crystal-vibrations into two classes (somewhat arbitrarily). Those '. . . *of the first class* are on a relatively large scale and may be described without any reference to the fine structure of the solid. These are the elastic vibrations of the crystal . . . (Those) . . . *of the second class* are essentially dependent on the fine structure of the crystal.' Raman says that the elastic vibrations of a macroscopic crystal give a continuous spectrum, but then states —without evident analytical support—that the vibrations of the second class appear as a set of '*discrete and enumerable monochromatic frequencies in the infra-red region of the spectrum*'. He maintains then that the energy associated with the elastic vibrations of the first class may be entirely ignored, summing up his viewpoint specifically thus: 'In evaluating the thermal energy of a crystalline solid, we are only concerned with the discrete or monochromatic frequencies appearing in its infra-red spectrum which owe their origin to the displacements of the atoms from their positions of equilibrium in the characteristic structure of the

* And therefore certainly not explainable by lattice theory (*cf* BLACKMAN[22]).

crystal: the elastic vibrations which involve only a general distortion of the lattice may be left out of account altogether.'

This interpretation of lattice behaviour, as Raman appreciates, is in direct contradiction to the Born and Debye concepts; if accepted, it leads immediately to a lattice specific heat expressible as a weighted sum of Einstein terms, the weights depending on any degeneracies assumed to be present. In a series of papers, following his primary thesis, Raman's pupils have calculated specific heat functions for many substances in this way: NORRIS[42]–White P; DAYAL[43]–Li, W, Au, Si, grey Sn; ANAND[45]–diamond; DAYAL[44]–Mg, Zn, Cd; NORRIS[46]–quartz; and VENKATESWARAN[47]–NaCl, KCl. In some cases, estimates for the characteristic frequencies to be employed are obtained from spectroscopic data; thus Anand (*loc. cit.*) uses certain features, somewhat arbitrarily, of the fluorescent and ultraviolet absorption spectra of Nayar on diamond to procure these frequencies. On the other hand, as Dayal (*loc. cit.*) has done '. . . the frequencies can be evaluated from the specific heat data themselves'. One can hardly adduce any real support for the Raman theory from such a course particularly if one recalls the remarkably good agreement obtained by Nernst and Lindemann with a less arbitrary formula of only two monochromatic terms.

A definite conflict between the two schools lies clearly in the form of the specific heat curve at sufficiently low temperatures. Debye and Born–Blackman predict T^3 (in the absence, of course, of electronic contributions) while Raman must have then $C_v \sim \varepsilon^{-\Theta_0/T}$ (*cf* 6a) where Θ_0 is characteristic of the lowest discrete frequency. Thus, for Li, Dayal gives essentially:

$$E = 3R\left\{\frac{1}{2}\left(\frac{406/T}{\varepsilon^{406/T}-1}\right)+\frac{7}{16}\left(\frac{224/T}{\varepsilon^{224/T}-1}\right)+\frac{1}{16}\left(\frac{89/T}{\varepsilon^{89/T}-1}\right)\right\}$$

At sufficiently low temperatures (say $< 10°$K) only the last term can contribute appreciably; unfortunately data are only available[48] down to $\sim 15°$K, although even there the calculated value is already significantly less than that observed. Future work on the specific heat of the alkali metals at very low temperatures being undertaken at the Clarendon Laboratory may serve incidentally to aid the final experimental resolution of the controversy. In this connection BORN[49] himself has given detailed analytical support of lattice theory in relation to x-ray scattering to which Raman had also applied his theory, and Blackman has pointed out[23] (1942) that the calculated specific heats from detailed lattice theory where the spectrum has been determined show in fact considerably better agreement with experiment than the results of Raman and his school. It appears, then, that the Raman theory can only be regarded as a convenient extension of the

Nernst–Lindemann approximation which may be expected to break down at very low temperatures.

Rare Earth Metals—Since the war, PARKINSON, SIMON and SPEDDING[50] have extended the field of measurements to the rare earth metals. Because of their very similar chemical properties one would expect

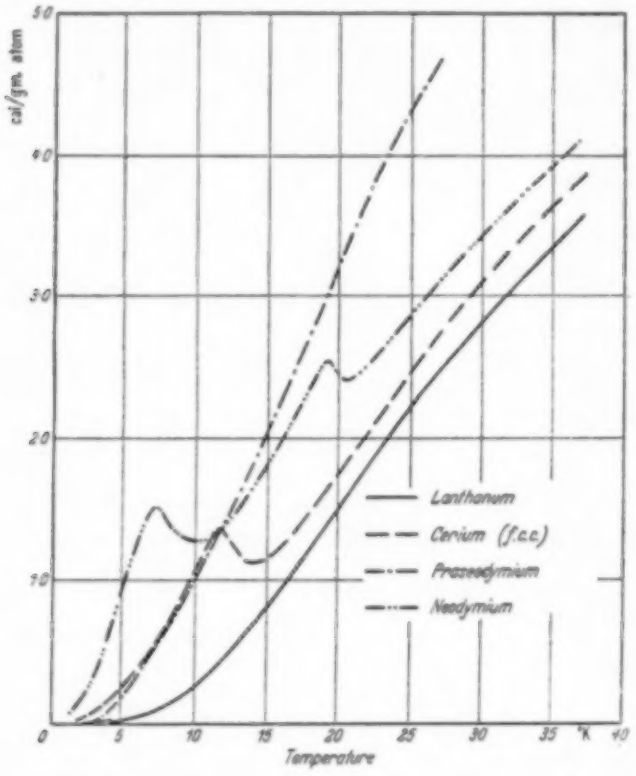

Figure 3. Low temperature anomalies in the specific heats of rare earth elements

a priori that any particular anomalous features might be attributed to the behaviour of the inner unfilled electronic shell thus shedding light perhaps on the Simon–Schottky hypothesis. The metals La, Ce, Pr and Nd were investigated down to $\sim 2°K$ and anomalous behaviour of considerable interest was found in the low temperature region particularly in Nd and Ce. (*Figure 3* is reproduced from Parkinson's thesis.) The low temperature anomaly in Ce appears, moreover, to be related to a relatively high temperature anomaly (around 170°K) known to exist in earlier work (*e.g.* TROMBE[51] and FOEX[52]). It appears very probable that the high temperature anomaly corresponds to an

effective change in phase of the metal produced by a change in electronic configuration. On the assumption that the low temperature anomaly will only be observed in *one* of these 'phases', an obvious connection arises, dependent on whether or not the high temperature transition is carried to thermodynamic completion.

It appears possible that a similar relationship exists between anomalous behaviour of the electrical resistance of Cs in the helium-hydrogen range[40] and a large anomaly observed in the region of − 20° to − 30°C. Bridgman has found a large volume transition in this metal at about 45,000 atm at ambient temperature, which may correspond to the latter anomaly, and theoretical calculation[53] suggests that an electronic transition is again responsible here; roughly speaking, the 6*s* 'valence' electron is forced into the 5*d* level.

Conclusion—It has not of course been possible here to discuss—or even mention—all relevant measurements of specific heats. We should certainly, however, note the work of Giauque and his associates *e.g.* GIAUQUE and MEADS[54] and MEADS, FORSYTHE and GIAUQUE.[55] In these two papers, particularly, specific heats of four metals (Al, Cu, Ag and Pb) all of face-centred cubic structure are determined carefully from 15° to 300°K. The expressed intention was the provision of data which would be useful in a comparison of metals in the same crystallographic class rather than a discussion of any particular theory.

Finally we ought to mention the power of specific heat measurements in observing transitions in alloys.* Such transitions, particularly the order-disorder transition, are not of course specifically low temperature phenomena; the critical temperature will depend on the net atomic energy of interaction tending to produce order. On the one hand this may be so great that the (virtual) transition temperature will lie above the melting point; an example is AuZn. Or, if small, the transition will only occur in the low temperature region. KELLEY[57] has observed anomalies in the specific heats of MnSe and MnTe in the room temperature region which may be attributable to this source.

Part II

ELECTRICAL CONDUCTIVITY OF METALS AND ALLOYS

While a basic understanding of the low temperature ($T < \sim \Theta$) behaviour of the specific heat of solids was achieved very shortly after the discovery of the quantum, it was not until some twenty years later *c* 1927–8 that an analysis of the low temperature electrical conductivity could be essayed. This is because electrical resistance is essentially a lattice-*scattering* phenomenon; the quantum mechanical analysis of

* The article by NIX and SHOCKLEY[66] is a valuable survey of this field.

such a process was naturally a much later development than the bare specification of the lattice energy levels sufficient for the specific heat.

WILSON[58] has said in fact: '. . . It is perhaps unfortunate that so much attention has been paid to the resistance of metals, since it is probably one of the least characteristic properties of the substance, and depends upon the electronic distribution and the elastic constants in a very complicated way . . . It is only to a second approximation that there is any interaction between electrons and lattice vibrations, so that we may say that the resistance is a second order quantity'. Without taking issue here over the precise significance of the phrase 'least characteristic properties', we would suggest that it might rather be regarded as quite fortunate that such 'second-order interactions' can be examined experimentally with relative ease through the electrical conductivity. Thus the fact that strontium exhibits much poorer relative conductivity than rubidium, shows immediately that the simple classical electron-gas model cannot be adequate, while the very existence of metallic conductivity in the former suggests immediately that the valence electrons must 'spill over' into the second Brillouin zone of the band theory of metals.

It is of course true that for more detailed knowledge of the influence on the conduction electrons of such zone structure it is, in general, necessary to turn to some more elaborate type of measurement such as the soft x-ray spectra. This seems, however, a parallel situation to that which occurs in the study of the lattice itself by specific heats on the one hand and x-ray crystallography on the other.

We shall see that a perfectly regular lattice cannot scatter electrons and hence produces no electrical resistance. The type of lattice deformation which can cause scattering can be classified into:

i Thermal vibration of the lattice;

ii static perturbation due, for example, to the presence of a foreign atom ('impurity') or variation of long-range order as in an alloy.

Although these two effects are not necessarily independent it is frequently the case experimentally and Matthiessen's law[59, 60] (which postulates the direct additivity of the two components of resistance considered independently), is generally assumed true with good approximation (*cf* MOTT and JONES[61]) although deviations do exist and are of interest theoretically. Consequently, with this assumption, the scattering of type *ii* is not a low temperature effect specifically; however, with small amounts of impurity present this resistance component may only become appreciable at low temperatures and ultimately will form the 'residual' temperature-independent component of resistance.*

* NORDHEIM[62] first discussed impurity scattering quantitatively (*cf* also MOTT and JONES[63]) and showed that the resistivity due to a disordered solid solution should vary with the fractional concentration, x, as $x(1-x)$, being zero consequently for $x = 0, 1$ and reaching a maximum at $x = 1/2$.

Quantum Theory Treatment—The first detailed treatment of electrical resistance on a quantum basis is due to HOUSTON.[64] The fundamental difference from a classical treatment lies in the analysis of the interaction of a 'free' electron with a repetitive, periodic lattice. In both cases, if an electron 'collides' with a single ('free') atom (whose mass is large compared with that of the electron) then it will be scattered almost elastically, the amount of energy transferred to the atom being a negligible fraction of that of the incident electron. If we then turn to a periodic lattice structure the classical picture is now simply one of multiple quasi-elastic collisions and if we also assume (classically) that the vibrational lattice energy is proportional to the temperature, T, then we arrive readily at the conclusion that: $\rho \propto T$ which in fact does prove to be true for high temperatures ($T \gg \Theta$), as we might expect. In the quantum mechanical treatment, however, a coupled lattice structure will now only have a certain set of energy levels which it may assume. If, for simplicity, we adopt the Einstein model (*vide* p 43) then only those states with $\varepsilon = nh\nu$ (or strictly $(n + 1/2)h\nu$) are permissible for the 'lattice oscillators'. Consequently interaction and scattering will only be possible under the transfer of one or more quanta, $h\nu$, from electron to lattice or *vice versa*. For an electron then to gain a quantum, a lattice oscillator must at least be in the first excited level and the probability of this $\sim \varepsilon^{-h\nu/kT}$ which clearly falls rapidly to zero as $T \to 0$. For an electron to lose a quantum there must, by the Pauli exclusion principle, be a lower energy state empty into which it may fall. If we assume that the electron gas is effectively also at temperature T during the passage of a current* then this probability diminishes as $1/(\varepsilon^{h\nu/kT} + 1)$. Thus the electric resistance of an ideal metal (without scattering of class *ii*) must fall to zero with $T \to 0$ as a consequence of the fact that both the lattice oscillators and the electrons must already both be in their lowest energy states. One sees immediately that the 'zero-point vibrations' of the lattice, characterized by a lowest quantum state $\varepsilon = \frac{1}{2}h\nu$, cannot lead to electrical resistance since the lattice cannot 'donate' any of this energy to the electrons. If we adhered to the Einstein vibration spectrum we should find approximately that:

$$\rho \sim \frac{1}{\varepsilon^{h\nu/kT} - 1}, = \frac{1}{\varepsilon^{\Theta/T} - 1}\dagger$$

and therefore for $T \gg \Theta$,

$$\rho \propto T \qquad \ldots . \quad (13)$$

in agreement with the classical result; while for $T \ll \Theta$:

$$\rho \propto \varepsilon^{-\Theta/T} \qquad \ldots . \quad (14)$$

* This is a fundamental assumption in the theory of electrical resistance which assumes that the applied electric field is only a small perturbation.

† For a more detailed analysis see CORNISH and MACDONALD.[130]

Development of the Theory—The introduction of the Debye spectrum for the lattice vibrations leads again to 13 for high temperatures but the decay of resistance, like that of the specific heat, at low temperatures is now slower, following a law:

$$\rho \propto T^5 \qquad \ldots . \quad (15)$$

Houston's work already provided these limiting laws, but his analysis was not wholly satisfactory since he employed, by direct analogy, scattering laws taken from x-ray analysis and then included *a posteriori* the characteristics of electron–lattice interaction (such as discussed above) in a rather *ad hoc* manner.*

Bloch[65] then undertook afresh a comprehensive analysis of the problem and the approximations necessary for a strict solution became apparent. Roughly speaking, these are based on three assumptions:

1 The 'gas' of 'valence' electrons is composed of practically free electrons of isotropic characteristics.
2 The interaction of the electrons with the lattice is very weak.
3 The lattice and electron gas remains essentially in thermal equilibrium at temperature T.

These premisses are evidently not wholly independent. In addition the lattice spectrum is assumed to obey Debye's law, and no quantitative work has yet been done on the question of the effect of the true crystal lattice spectrum on the electrical resistance.

Even under these assumptions, a strict solution in closed form is only possible at high and low temperatures. However, more recent theoretical investigations of varying rigour *e.g.* those of Supek,[66] and Kohler,[67] have shown that a relatively simple integral expression occurring in Bloch's analysis for low temperatures may be taken as essentially valid for the resistance of the 'ideal' metal at all temperatures.† Grüneisen[69] was the first to suggest on heuristic grounds the general use of this formula, namely:

$$\rho \propto \left(\frac{T}{\Theta}\right)^5 \int_0^{\Theta/T} \frac{x^5 \mathrm{d}x}{(\varepsilon^x - 1)\,(1 - \varepsilon^{-x})} \qquad \ldots . \quad (16)$$

For $T \gg \Theta$ the integral $\approx 1/4(\Theta/T)^4$, and thus $\rho \propto T$ again, while for $T \ll \Theta$, the upper limit of the integral may be set as infinite and therefore $\rho \propto T^5$ in agreement with 15.

Experimental Support of Theory—The first quantitative comparisons of experiment and theory were remarkably encouraging. Thus Grüneisen[70] (or see Meissner[71]) gave a table in which values of Θ_D, deduced

* See, however,[120] where deviations from the Debye spectrum are investigated.

† Current analyses by Rhodes[68] and Sondheimer[121] suggest, however, that not inappreciable deviations (up to ~ 10 per cent) from this expression may occur in the range: $\sim 0{\cdot}4\,\Theta > T > \sim 0{\cdot}1\Theta$.

from specific heat data (in comparison with the Debye law), and of Θ_e, say, deduced from 16 were compared. Part of this table appears below, and *Figure 4*[71] shows the variation of normalized resistance (ρ/ρ_Θ) as a function of temperature for a number of metals.

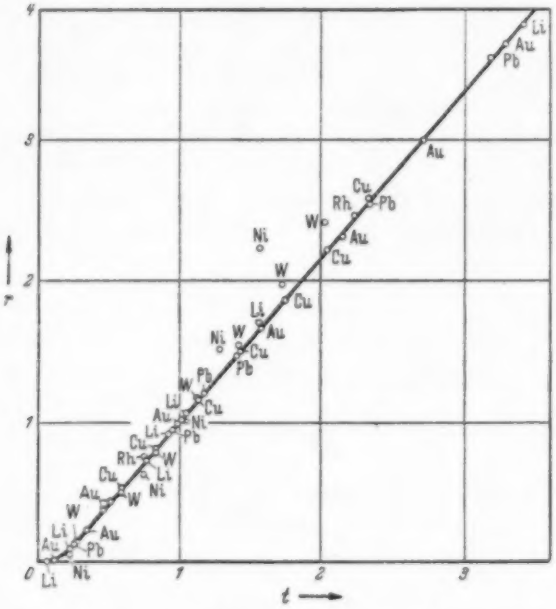

Figure 4. Normalized resistance $r(= \rho/\rho_\Theta)$, as a function of normalized temperature $t(= T/_\Theta)$, for various metals

Table II. Comparison of Θ_D obtained from Specific Heat Data and Θ_e deduced theoretically

Metal	Na	Cu	Ag	Au	Al	Pb	W	Ta
Θ_D (°K)	159°	315° – 330°	210° – 225°	163° – 186°	390°	82° – 88°	305° – 337°	245°
Θ_e (°K)	202°	333°	223°	175°	395°	86°	333°	228°

Apart from the case of sodium, to be discussed below, the agreement seems to leave nothing to be desired. In fact, if we consider metals such as Al and Pb, it seems rather surprising that the underlying theoretical assumptions mentioned above should have been adequate. However, one must now remark that the table of Θ_e is based generally

on the comparison of data which are significant down to the hydrogen point (20·4°K) only.

Since the energy (or entropy) of a Debye solid deviates appreciably from classical behaviour only below say, $T \sim 0{\cdot}4\Theta$ to $0{\cdot}5\Theta$, and correspondingly the electrical resistance only departs significantly from linearity with temperature for $T \sim 0{\cdot}2\Theta$ to $0{\cdot}3\Theta$, one can in fact only regard experimental data below this region as really significant in testing the detailed validity of the theory although useful estimates of Θ may be obtained otherwise. Thus, since most metals have Θ in the order of 100°K, it is clear that continuous measurements below say 20°K will be called for. On the other hand, however, the 'residual' resistance (*vide supra*) imposes a limitation of a kind not generally met with in calorimetric measurements. At very low temperatures (say < 4°K) the thermal lattice scattering has generally become small in comparison with class *ii* scattering which therefore now dominates the measurements. Consequently, although before the war a great deal of data was already available on the electrical resistance at isolated temperatures (generally ~ 290°K, ~ 90°K, ~ 20°K (sometimes ~ 14°K), and in the liquid helium range ($\leqslant 4$°K), this is not really adequate for a close investigation; it was nonetheless, of course, of the greatest value in checking the earlier developments of metallic resistance theory particularly in the years 1928–35. We should mention particularly the comprehensive studies of MEISSNER and VOIGT[72] and of the Leiden school; a brief synopsis of the latter work is given[73].

Measurements in the Region of 4°K to 20°K—A detailed study of a number of selected metals (Pt, Ag, Au, Cu, Pb, Cd, Tl, Sn, K, W) in the vital region between 4°K and 20°K has also been carried out by DE HAAS, DE BOER and VAN DEN BERG* [74–8]; the usual method of empirical data analysis has been to plot the resistance as a function of temperature logarithmically and determine to what extent a law of the type $R = AT^B$ will fit. This temperature region presents peculiar difficulties of technique since no liquid exists between 5°K and 14°K and more recently MACDONALD and MENDELSSOHN,[39, 40, 79] using a modified Simon helium liquefier,[80] have been able to cover the whole range continuously. A systematic study has been made so far of the alkali (Li, Na, K, Rb, Cs) and alkaline earth metals (Be, Mg, Ca, Sr, Ba); the work is being extended to other groups, but the 'simple' metals are of primary theoretical interest since it is there that one would hope for the closest approximation *a priori* to a theoretical model. The alkalis, in particular, would be expected to lend themselves most readily to a simple free-electron model. On the one hand, the low binding energy of the valence electron should obviously tend most

* Or see: van den Berg: Thesis, 'De electrische Weerstand van zuivere Metalen bij lage en zeer lage Temperaturen,' Leiden, 1938.

easily to the formation of an electron gas of weak interaction while the monovalent character suggests that the influence of the specifically periodic lattice field on the otherwise free motion of the electron should be small. For when N atoms are brought together to form a metal crystal each valence state in the original atom contributes 2 (because of spin) energy states to the range ($2N$ in all therefore) available for conduction in the solid metal. In a monovalent metal, therefore, only about half—the lower half—of this range of states is occupied by electrons. Now these relatively low energy electrons have fairly *long* quantum mechanical wavelengths ($\lambda \sim h/mv$) and consequently the intrinsic lattice structure should not be of great significance; electrons having energies, however, near the top of the energy range, as will arise in a divalent metal, will be strongly affected because of their short wavelengths and will suffer continual intense diffraction by the lattice structure. The situation is a direct parallel to the propagation of elastic waves through a crystal (see p 52) and the first zone (Brillouin zone) of electron energy states considered here is the immediate analogue of the zone of acoustic vibrations whose spectrum is that of a non-dispersive continuum at *long* wavelengths but is strongly distorted by the specific lattice structure at the *short* wavelength end.*

Electrical Conductivity of the Alkali Metals—The results for the alkali metals show that sodium appears to conform almost perfectly to the ideal free-electron model, the resistance following equation 16 very closely from room temperature to the lowest temperatures with a value of $\Theta_e \approx 200°K$ throughout. *Table III* gives collected data on the 'ideal' resistance (*i.e.* with the residual resistance, due to class *ii* scattering, subtracted). On the other hand deviations are found in all the other alkalis, becoming particularly severe in the case of Rb and Cs. (These conclusions are also borne out by comparative measurements[122] of the magneto-resistance; the relative magnitude of this quantity may be considered as a measure of the departure from ideality of the electron gas.) *Table IV* details the conductivity values for Li, a value $\Theta \approx 360°K$ being chosen to make the higher temperature values agree reasonably (*cf* also GRÜNEISEN[70]). In the case of Rb the discrepancy is so great that tabular comparison is of little value and therefore a graph of 'apparent' Θ_e against T has been derived (*cf* the presentation of specific heat data) which shows the enormous variation (see *Figure 5*).

The case of sodium already calls for comment in that $\Theta_e \approx 200°K$, while $\Theta_D \approx 150°K$ (see *Table II*). SIMON[5, 20] had earlier suggested on the basis of the available data that the true lattice vibrational spectrum was characterized by $\Theta \approx 200°K$ while the inclusion of a 'Schottky' internal transition with a characteristic temperature

* This is of course a somewhat heuristic description and a more rigorous analytic discussion of Brillouin zone structure is not possible here.

Table III. 'Ideal' Resistance, r (i.e. with residual resistance subtracted), of sodium normalized to Unity at 273°K

T °K	r calc Θ = 202°K	r obs		
		1	2	3
273·2	1·0000	1·0000	1·0000	1·0000
170·9	0·5672	—	0·5672	—
108·7	0·3135	—	0·3168	—
90·0	0·2600	—	—	0·2420
87·8	0·2279	0·2279	—	—
77·6	0·1860	0·1849	—	—
56·77	0·1022	—	0·1055	—
20·4	0·00327	0·0034	—	0·00326
15·95	0·00100	—	—	0·00098
14·1	0·00055	—	—	0·00051
13·1	$0{\cdot}00038_4$	—	—	$0{\cdot}00036_8$
11·05	$0{\cdot}00015_4$	—	—	$0{\cdot}00017_2$
9·65	0·00009	—	—	$0{\cdot}00010_2$
8·1	0·00004	—	—	0·00005
4·2	0·00000	—	—	0·00000

1 Meissner and Voigt[73]
2 Woltjer and Kamerlingh Onnes[61]
3 MacDonald and Mendelssohn[40]

Table IV. 'Ideal' Resistance, r, of Lithium

T °K	r calc Θ = 363°K	r obs		
		1	2	3
374·5	1·433	1·443	—	—
329·7	1·243	1·247	—	—
273·2	1·0000	1·0000	1·0000	1·0000
90·9	0·1692	—	0·1621	—
90·0	0·166	—	—	0·171
86·3	0·1492	—	0·1464	—
80·1	0·1236	—	0·1252	—
77·7	0·1139	—	0·1169	—
20·4	0·0004	—	0·0013	$0{\cdot}0013_3$
17·8	$0{\cdot}0002_1$	—	—	$0{\cdot}0007_6$
16·05	0·00015	—	—	$0{\cdot}0004_6$
14·8	0·00011	—	—	0·00029
13·55	0·00008	—	—	$0{\cdot}0002_1$
12·3	0·00004	—	—	$0{\cdot}0001_4$
11·4	$0{\cdot}00002_1$	—	—	0·00009

1 Meissner[68]
2 Meissner and Voigt[73]
3 MacDonald and Mendelssohn[40]

$\Theta_S \approx 95°K$ would yield an effective specific heat value of $\Theta \approx 150°K$. This explanation is attractive since one would not expect an internal transition to contribute to electron scattering, *i.e.* Θ_e would equal 200°K. On the other hand, of course, the apparently constant Θ values may be spurious, the vibrational spectrum deviating markedly from the Debye law. The prime difficulty in this matter lies in our relative ignorance of

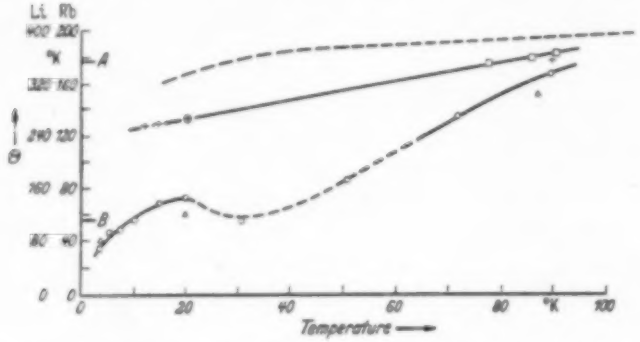

Figure 5. Variation with temperature of Θ deduced from electrical conductivity measurements. The top dashed line represents Θ for lithium as deduced from specific heat data. A is the limiting value of Θ for Li deduced from the elastic constants and B is the value of Θ for ribidium deduced from Lindemann's melting-point formula

	MacDonald and Mendelssohn[40]	Data of Meissner and Voigt[72]
Rb	○	△
Li	+	□

the effective lattice bonding forces (including the influence of the conduction electrons) as compared for example, with the simple ionic lattices; FINE[83] did in fact estimate the spectrum for tungsten (body-centred cubic) on the assumption of central forces and isotropicity, since tungsten does satisfy the Cauchy elastic relations although the assumption of central forces must be only very approximate.* It will be necessary also in a fuller treatment when considering the effect on electrical resistance, to remember that only the longitudinal lattice waves are effective in electron scattering. (See further a recent discussion by Blackman[133] on this problem.)

If in Rb, for example, the remarkable variation in Θ (*Figure 5*) is directly ascribable to the character of the lattice spectrum then we should certainly expect that low temperature specific heat measurements will be of the greatest interest. However, we believe that the anomalous behaviour of Rb and Cs particularly is due primarily to the

* *Cf* also Leighton's work[84] on the spectrum of a face-centred cubic crystal (applied to Ag).

nature of the electron lattice interaction; this also concords with the fact that sodium has the highest 'normalized' conductivity of the alkali metals.

Anomalous 'kinks' were also observed in the low temperature resistance of K and Cs; there is some evidence to suggest that, at any rate in K, these *may* be related to the presence of small Na impurities although the physical mechanism involved is as yet quite unknown. On the other hand, it seems quite probable that these may be characteristic of a low temperature electronic modification of these metals (see p 55).

Electrical Conductivity of the Alkaline Earths—The metals of the second column of the periodic table are also of fundamental interest since, for example, Ca (f.c.c.), Sr (f.c.c.) and Ba (b.c.c.) each have a first energy zone which could contain just two electrons per atom; if then the first and second zones were separated by an energy gap everywhere, the first would just be filled leading to a 'perfect' insulator. However the presence of (rather poor) metallic conductivity in these metals shows that there must be a slight overlap into the second zone in some directions in momentum space and we therefore have the simplest case of a metal with conduction due to a few free electrons and an equal number of positive holes (although of less mobility). Such a model indicates immediately a much greater magneto-resistive effect, for example, than could be expected in the alkalis and this is in fact confirmed.

Inhibition of Quantum Transfer—Apart from the general comparison of experiment with the Bloch–Grüneisen law, the ultimate behaviour of the resistance at very low temperatures ($T \ll \Theta$) is of interest; if electron-electron collisions can be neglected then one should expect that $\rho \propto T^5$ ultimately, independent of any particular assumptions (*cf* $C_v \propto T^3$ in the true lattice-continuum region). There are, however, at least two possible causes for deviation. It is a customary assumption (the *Bloch'sche Annahme*) in the theory of resistance that the lattice vibrations may always be considered as having a distribution characteristic of true thermal equilibrium at a given temperature. That is to say, one assumes that the electron-phonon collisions do not appreciably perturb the thermal distribution of the 'phonon-gas'. PEIERLS[85] however pointed out that in an ideal metal lattice at low temperatures the lattice-wave relaxation time would be very long; consequently on initiating an electron current the first transfer of quanta from electrons to lattice vibrations would 'load up' the lattice waves with momentum in the direction of the electron current. Future transfer of quanta would thus be inhibited and Peierls suggested that only *Umklapp-Prozesse* which are of relatively rare occurrence at low temperatures could provide the resistance mechanism.

In an *Umklapp-Prozess* an electron suffers simultaneously a favourable lattice collision *i.e. absorption* of a quantum which raises its energy to that of the Brillouin zone boundary, where it then effectively suffers momentum reversal by Bragg reflection (due to strong diffraction by the lattice). If we are dealing with a monovalent metal and the maximum electron energy (at the top of the 'Fermi surface') is say $\sim \Delta E$ less than that of the zone boundary then the probability of each of the occurrences will be proportional to $\varepsilon^{-\Delta E/kT}$ thus falling off rapidly for $T < \sim \frac{\Delta E}{k}$. That is to say, somewhere below such a temperature the resistance due to thermal scattering would decay with very great rapidity. Since this has not been observed experimentally Peierls concluded that the Fermi surface must at least touch the first plane of energy discontinuity. The only experimental evidence which favours such a tenet in the alkali metals lies in the soft x-ray emission studies of SKINNER.[86] Both Li and Na are found to show departures from the energy spectrum expected for free electrons. Skinner himself says, 'the alkali metals have one (valence) electron per atom, and this is enough to fill only half of the volume of the first Brillouin zone. Hence it has often been supposed that the value of **k** (the wave-number) corresponding to the maximum energy of the conduction electrons would be too small to touch the bounding planes, the energy contour in **k**-space therefore remaining approximately spherical. . . . (However,) the kink of the . . . (observed x-ray) curve for Na . . . shows that the **k**-vector has not only touched, but also penetrated, the boundaries of the first zone, before the energy has reached the value E_{max}.'

Although other experimental evidence (as, for example, optical properties and the conductivity) indicates in fact that the electrons in sodium are practically ideally free* and Peierls himself has suggested more recently (private communication) that binary electron-collisions (*cf* also HOUSTON[88]) may yield the necessary *Umklapp-Prozess* without requiring deformation of the Fermi surface, yet further experimental data on the character of the Fermi surface appear very desirable.

Effect of Electron-Electron Collisions—The second specific feature affecting the ultimate law of the resistance is the possibility of electron-electron collisions. BABER[89] has analysed this problem theoretically using MOTT'S[90, 91] two-zone model particularly appropriate to the transition metals, and has shown that a component of resistance proportional to T^2 should arise at sufficiently low temperatures, like the linear component of electronic specific heat; this, however, would only be expected to be of significance in the hydrogen-helium range if the density of electron states is abnormally high as is the case in

* As do also the theoretical calculations by SLATER[87] of the form of the surfaces of constant electron energy.

the transition metals. This is borne out by the experiments of DE HAAS and DE BOER[92] on platinum, who find a dominant T^2 component below 20°K, and also by the fact that on the other hand, our work on the alkalis shows that at sufficiently low temperatures all these metals, with the possible exception of Cs, do approach a T^5 law closely.

The question also appears of interest in relation to the Fröhlich theory of dielectric breakdown in solids.[93, 94] This is based essentially on the possibility of 'run-away' electrons whose lattice-collision relaxation times vary with energy in such a manner that they can acquire energy from an applied electric field more rapidly than they can dissipate it to the lattice. Fröhlich opens the second of these papers, '. . . it will be shown that no stationary state can be reached on the assumptions conventionally made in calculating the electron current in solids. According to these assumptions, the conduction electrons are considered as free except for their collisions with lattice vibrations and other lattice imperfections. Collisions between electrons are considered as unimportant. *While this latter condition can hardly be true for good conductors.* . . '. The confirmation of the T^5 law in simple metals (also given by VAN DEN BERG[95]) however, suggests a possible contradiction—with its consequent corollary—of this last statement.

Anomalies in Resistance—The above-mentioned work of van den Berg and de Haas on gold, particularly, revealed a most interesting behaviour. At low temperatures ($< \sim 10$°K) the resistance passed through a definite minimum and the position of this minimum was found to depend on the effective impurity content (chemical and physical); van den Berg also reported the phenomenon in silver but in this case the effect was much smaller and not observed in all specimens. MACDONALD and MENDELSSOHN[79] have observed the same effect in magnesium. The dependence on impurity is qualitatively similar—the temperature of the minimum being lowered with reduction of impurity. A considerable amount of work has recently been published in this field by MENDOZA and THOMAS,[134] MACDONALD and TEMPLETON,[135] and GERRITSEN and LINDE.[136] The whole subject was reviewed and discussed at the 1951 Low Temperature Conference in Oxford.[137]

Some workers favour the view that the resistance will rise towards infinity as $T \to 0$. This would then conform with Gorter's proposal[96] that all irreversible processes vanish at $T \to 0$; thus in the case of a metal the resistance would either have to vanish completely as in fact occurs in the class of superconductors (*vide infra*) or become infinite. If true thermodynamic equilibrium obtained then the 'theorem' would appear very reasonable*; presumably all metals would become perfect ideal crystals, all impurity atoms having to

* Gorter himself suggested that this theorem may only be valid under the same conditions as govern the Third Law *i.e.* essentially true thermodynamic equilibrium.

take up positions of perfect order as in a superlattice or else being precipitated on to the surface of the crystal. Consequently one would expect all scattering of class *ii* to vanish and, as we have seen, thermal scattering will disappear as $T \to 0$. However in actual metals these conditions of course cannot obtain as is evidenced by the very existence of residual resistance.

The writer does not believe that the presently available experimental data provide in fact serious confirmation of a tendency towards infinite resistance. Furthermore, the diminution of the minimal temperature with impurity indicates that a highly peculiar situation would arise in specimens of vanishingly small impurity. However, further experimental data at very low temperatures* seem most desirable.

In divalent magnesium one might suggest that a peculiarity of the overlapping Brillouin zone structure of the valence electrons was responsible, but nothing of this character seems feasible in the case of gold which has a single valence electron outside completed inner shells. The writer believes that the inclusion of ferro-magnetic impurities may be the source of the effect, and experiments on appropriate gold alloys are in progress to test this hypothesis. This work, together with a detailed experimental investigation of a range of copper specimens,[137] does not support this hypothesis. A severe problem in attempting to relate the phenomenon to impurity content in detail is that spectrographic analyses (on the Cu specimens in particular) show that only extremely small impurities are present.

Superconductivity—We have mentioned above the phenomenon of superconductivity. This was first discovered by Kamerlingh Onnes in mercury in 1911. The essential features in a pure unalloyed metal are that the electrical resistance *entirely* disappears abruptly at some temperature (T_c) characteristic of the particular metal; this transition temperature is lowered by the presence of a magnetic field and in that case the appearance of superconductivity is marked by the expulsion of the magnetic induction (B);[97] thereafter the superconductive metal behaves as an ideal diamagnetic body ($B = 0$; $\chi = -1/4\pi$). Superconductivity in itself presents a wide field for theoretical and experimental research[98–100] and can only be discussed here very briefly.

From our present point of view, perhaps the most interesting question is to ask what determines whether or not a particular metal is a superconductor. Alternatively, we may ask: do all metals ultimately become superconductive? Remarking that hafnium and cadmium, for example, have been found to become superconductive as low as 0·54°K and 0·35°K respectively[101] it appears impossible to

* Further work on Mg in the region below 1°K is projected at the Clarendon Laboratory and it is understood that work on Au, Ag and Cu is in progress at Bristol. (The Bristol work is now published.[184])

say categorically that a given metal will not become superconductive as and when regions of lower temperature become accessible. However, it is a general feature that the known simple superconductors lie in a fairly well defined region of the periodic table and, in particular, it seems very unlikely that an alkali or noble metal will become superconducting. The theory of BORN and CHENG[102] relates the incidence of superconductivity to metals where the Fermi surface is particularly close to corners of a Brillouin zone; on the other hand, Heisenberg's theory[103], based on the evolution of an ordered state in the electrons on the surface of the Fermi sphere due specifically to the Coulomb interaction predicts that, with the exception of ferromagnetics, all metals must become superconductors. Again, a most recent theory due to FRÖHLICH,[104] based on the interaction (**via** the lattice) of electrons on the Fermi surface whose momentum difference is related to the velocity of sound in the crystal, introduces consequently lattice parameters which provide a criterion for the existence of superconductivity between different metals.

Quite a wide range of compounds and alloys become superconducting; for example the In–Pb system shows a continuous variation of transition temperature between that of pure In (3·4°K) to that of pure Pb (7·3°K). Cases also exist of a compound of two *normal* conductors which exhibits superconductivity *e.g.* Au_2Bi ($T_c = 1{\cdot}7$°K) and CuS (1·6°K). The occurrence of a superlattice in an appropriate alloy with its attendant Brillouin-zone structure would appear to provide an interesting test of the Born–Cheng theory. Superconductive alloys generally differ markedly in their behaviour from pure metals; in particular the magnetic flux is not completely expelled at the transition (*cf* Meissner–Ochsenfeld effect in pure metals), being 'frozen-in' to a considerable extent. MENDELSSOHN[105] has suggested that the structure of an alloy resembles that of a 'sponge' whose meshes have a much higher critical magnetic field than the enclosed material. This interpretation allows a number of the properties of superconductive alloys to be correlated, but the precise physical nature of these meshes is not yet clear.

The upper limit of superconductivity is naturally also of considerable importance. The highest transition temperature for a pure metal is 9·2°K for Nb (Cb) and for compounds 13°K (NbH) and 15°K (NbN). The latter is notable since it can be reached easily with liquid hydrogen boiling under reduced pressure; much work has recently been done in this field by ANDREWS and his associates[106, 107] particularly in connection with the development of a high sensitivity bolometer based on the very rapid variation of electrical resistance with temperature around the transition point.

A claim by OGG[108] to have discovered superconductivity in solutions

of sodium in ammonia at temperatures as high as $\sim -100°C$ naturally aroused great interest. The claim was not, however, substantiated by independent experiments[109–111] and Ogg's conductivity measurements could in fact be explained through an appreciation of the formation of the highly conducting $Na–NH_3$ eutectic* around $-110°C$ and of the character of the phase-concentration diagram.[112] These 'dilute metals' provide in fact useful models in the theory of metals since one may effectively alter the concentration of the free electron 'gas' and so vary the degeneracy temperature (*cf* p 50).

Effect of Size on Resistivity—Thus far we have been concerned solely with metals in bulk but low temperatures have also enabled fresh advances to be made in the realm of size effects. Since late in the last century it has been known that very thin metallic specimens exhibited a higher specific resistivity than the same metal in bulk. J. J. THOMSON[113] first analysed how such an effect could arise because of the limitation of electron free path by the geometrical size rather than purely by atomic collisions. Much work has been done subsequently in this field but suitable metallic films must clearly be very thin when we observe that at room temperature the electronic mean free path in silver is only about 10^{-5} cm. Additional complication then enters because of the specific structural properties compared with true bulk metal[114, 115]. However, in liquid helium the conductivity of pure metals rises by a factor of about 10^3 generally, and consequently specimens between $\sim 10\mu$ and $\sim 100\mu$ should exhibit the effect strongly while yet having essentially bulk structure.

Size–effect data should yield information directly on the mean free path and also on the law of electron scattering at the surface of the specimen (the two limits being those of wholly diffuse, or purely specular, reflection—in the latter case no size effect would occur). FUCHS[116] gave a fundamental analysis for thin films on the assumption of an ideal free electron gas, and this has also been extended by DINGLE,[117] CHAMBERS[118, 119] and MACDONALD and SARGINSON.[120] ANDREW[121] carried out measurements between 1·5°K and 20°K on a wide range of tin and mercury specimens at helium temperatures and deduced values of $\sim 0{\cdot}4$ and $\sim 0{\cdot}6$ respectively for the effective number of free electrons per atom for these metals; the assumption of purely diffuse scattering was found to be consistent with the experimental results.

Since metals like tin and mercury cannot be regarded in bulk as a close approach to the ideal free-electron model, MACDONALD[122] undertook measurements on specimens of sodium. An additional effect was then also found in the tendency for the resistivity in a given specimen to *fall* towards the bulk value on the application of a magnetic field

* The conductivity is in the same order as that of a pure metal.

as a consequence of the change in the electron orbits. This effect can yield direct knowledge of the intrinsic electron momentum and again information on the scattering law. Theory has been developed by SONDHEIMER,[123] MACDONALD and SARGINSON[120, 124] and CHAMBERS[118] and the latter has also contributed experimental data. We may note that MacDonald's experiments on the simple size effect in sodium do indicate a variation of scattering law with specimen size; the surface reflection in this case only appears to tend to complete randomness for size $< \sim 20\mu$.

Effect of Temperature on High-Frequency Resistance—Not unrelated to these experiments is the work of PIPPARD[125] on the variation with temperature of the high frequency resistance of metals. At very high frequencies (1,200 Mc/s; $\lambda \sim 25$ cm). the electromagnetic field can only penetrate for a very short distance into the metal and it can thus arise that this region becomes smaller than the classical electron mean free path, particularly at low temperatures when the mean free path becomes relatively long. A limitation (additional now to that of the classical skin-depth effect) is thus imposed rather analogous to that of the simple size effect in a geometrically restricted conductor, and again information may be obtained on the scattering law at the surface. Pippard worked both on 'normal' metals and superconductors; in the latter case, following LONDON's[126] earlier work, the high-frequency (eddy-current) component of resistance, although found to drop abruptly at the transition point, does not vanish entirely and its progressive decrease with further temperature reduction is of importance in assessing the effective proportion of the conduction electrons which take part in the superconductive process. Purely direct-current resistive measurements alone cannot yield directly this information since even a small number of superconductive electrons will 'short-circuit' the metal and prevent any electric field whatsoever being set up to interact with any 'normal' electrons which are present.*

An approximate theory of the high-frequency resistance in the normal metal was given by Pippard himself and REUTER and SONDHEIMER[127] have also analysed the phenomenon in terms of the fundamental statistical electron theory of metals. CHAMBERS[119] has made a careful experimental study of the surface conditions in similar experiments and has concluded that for Sn, Cu and Ag the electron reflection may be assumed to be completely diffuse at all temperatures. The actual magnitude of the high-frequency resistance is found to be strongly affected by polishing *etc* and Chambers concludes that the surface layer responsible extends for $> 2 \times 10^{-5}$ cm into the body of the metal.

Effect of Superlattice Structure—The determination of long-range order

* It should be appreciated that the reference to 'normal' and 'superconductive' electrons must be interpreted statistically.

(superlattices) in alloy structures by observing the electrical resistance is now well known. On the one hand a graph of resistance as a function of composition will exhibit more or less sharp minima, superimposed on the normal curve of impurity scattering (type *ii* *cf* p 56), where ordered structures occur (*cf Figure 6*); on the other hand observation of the variation of resistance with temperature will generally show up clearly the critical point where an order–disorder transition occurs (*cf Figure 7*). This is not of course a specifically low temperature phenomenon any more than the corresponding observation of a specific heat anomaly at the transition point.

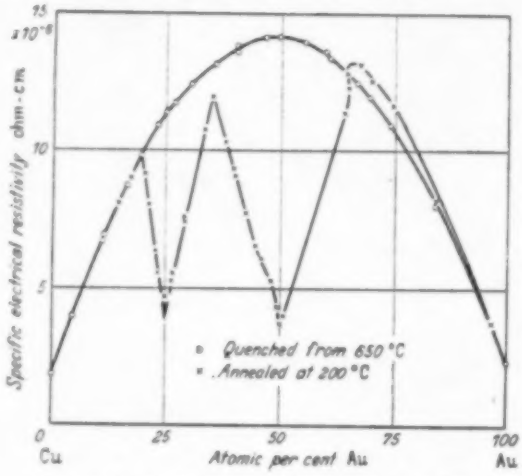

Figure 6. Variation of resistance with composition in Cu-Au alloys

Magneto-Resistance Effect—However, the inception of a new superstructure can produce an additional effect as yet not widely investigated. A well developed superlattice will evoke new Brillouin zones characteristic of the additional symmetry now present and these may give rise to strong additional diffraction of the free electrons *i.e.* distortion of the energy states from that characteristic of free electrons (*cf* p 65). This is a separate effect to be distinguished from the general reduction in scattering (increase of *relaxation time*) which will have occurred due to the additional lattice order.

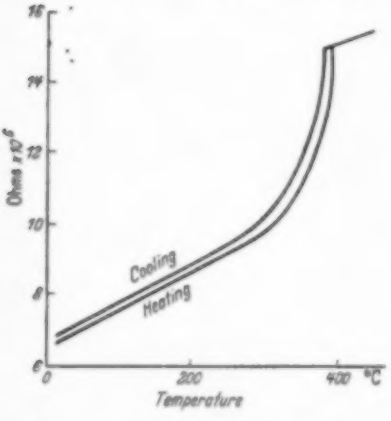

Figure 7. Variation of resistance with temperature of the alloy Cu_3Au

Now the magneto-resistance effect, as mentioned earlier, may be regarded in essence as a measure of departure from purely free electron behaviour. Consequently under these conditions an intrinsic alteration

would be expected in this effect, which in turn shows itself very much more strongly at low temperatures since it depends roughly on the square of the conductivity, other things being equal. Thus KOMAR[128] observed the magneto-resistance of $AuCu_3$ at room temperature and $\sim 80°K$ as a function of the temperature (the degree of order being 'frozen-in' by quenching) and found a large relative change in magnitude when the superlattice is established. A reversal in the sign of the Hall effect[129] around the transition also indicates the establishment of new nearly occupied zones as a result of the superlattice formation. Further work in this field would appear most valuable.

REFERENCES

[1] HUME-ROTHERY, W. *Electrons, Atoms, Metals and Alloys*, Iliffe and Sons, London 1948
[2] MOTT, N. F. *Physica* 15 (1949) 119; *Research* 2 (1949) 162
[3] EINSTEIN, A. *Ann. Phys., Lpz.* 22 (1907) 180, 800
[4] NERNST, W. *Göttingen Nachr.* 8 (1906) 1; *S.B. preuss. Akad. Wiss.* (1906) 933
[5] SIMON, F. E. *Ergebn. exakt. Naturw.* 9 (1930) 222
[6] NERNST, W. and LINDEMANN, F. A. *S.B. preuss. Akad. Wiss.* 22 (1911) 494
[7] EINSTEIN, A. *Ann. Phys., Lpz.* 35 (1911) 679
[8] DEBYE, P. *ibid* 39 (1912) 789
[9] BORN, M. and v. KÁRMÁN *Phys. Z.* 13 (1912) 297; 14 (1913) 15
[10] EINSTEIN, A. *Ann. Phys., Lpz.* 34 (1911) 170
[11] LINDEMANN, F. A. *Phys. Z.* 11 (1910) 609
[12] BRILLOUIN, L. *Wave Propagation in Periodic Structures* New York, 1946
[13] NEWTON, I. *Principia, Book II*, 1686
[14] EUCKEN, A. *Handb. exp. Phys.* 8 Part 1 (1929) 239
[15] FOWLER, R. H. *Statistical Mechanics* Cambridge, 1929
[16] —— and GUGGENHEIM, E. A. *Statistical Thermodynamics* Cambridge, 1939
[17] SCHRÖDINGER, A. *Handb. der Physik.* 10 p 304 Springer, Berlin, 1926
[18] BORN, M. *ibid.* 24 part 2, p 623 (1933)
[19] MOTT, N. F. and JONES, H. *Theory of Properties of Metals and Alloys* London, 1936
[20] SIMON, F. E. *S.B. preuss. Akad. Wiss.* 33 (1926) 477
[21] SCHOTTKY, W. *Phys. Z.* 22 (1921) 1; 23 (1922) 9, 448
[22] BLACKMAN, M. *Reports on Progress in Physics* 8 p 11 London, 1941
[23] —— *Proc. roy. Soc. A* 148 (1935) 365, 384; 149 (1935) 117, 128; *Proc. phys. Soc.* 54 (1942) 377
[24] KELLERMAN, E. W. *Phil. Trans. A* 238 (1940) 513
[25] SMITH, H. J. *ibid* 241 (1948) 105
[26] SOMMERFELD, A. *Z. Phys.* 47 (1928) 1
[27] STONER, E. C. *Phil. Mag.* 25 (1938) 899
[28] CLUSIUS, K. and SCHACHINGER, L. *Z. Naturforsch.* 2*A* (1947) 90
[29] KEESOM, W. H. and CLARK, C. W. *Physica* 2 (1935) 513
[30] —— and VAN LAER, P. H. *Commun. phys. Lab. Univ. Leiden* 252b (1938); *Physica* 5 (1938) 193
[31] DUYCKAERTS, G. *Physica* 6 (1939) 817
[32] KEESOM, W. H. and KURRELMEYER, B. *Commun. phys. Lab. Univ. Leiden* 257a (1939); *Physica* 6 (1939) 633
[33] DUYCKAERTS, G. *C.R. Acad. Sci., Paris* 208 (1939) 979; *Physica* 6 (1939) 401
[34] ELSON, R. G., SMITH, H. G. and WILHELM, J. O. *Canad. J. Res. A* 18 (1940) 83

[35] PICKARD, G. L. *Nature, Lond.* 138 (1936) 123
[36] —— and SIMON, F. E. *Proc. phys. Soc.* 61 (1948) 1
[37] KOK, J. A. and KEESOM, W. H. *Commun. phys. Lab. Univ. Leiden* 245a (1936); *Physica* 3 (1936) 1035
[38] CRISTESCU, S. and SIMON, F. E. *Z. phys. Chem. B* 25 (1932) 273
[39] MACDONALD, D. K. C. and MENDELSSOHN, K. *Nature, Lond.* 161 (1948) 972
[40] —— —— *Proc. roy. Soc. A* 202 (1950) 103
[41] RAMAN, C. V. *Proc. Indian Acad. Sci. A* 14 (1941) 459
[42] NORRIS, R. *ibid* 14 (1941) 468
[43] DAYAL, B. *ibid* 14 (1941) 473
[44] —— *ibid* 14 (1941) 492
[45] ANAND, V. B. *ibid* 14 (1941) 484
[46] NORRIS, R. *ibid* 14 (1941) 499
[47] VENKATESWARAN, C. S. *ibid* 14 (1941) 508
[48] SIMON, F. E. and SWAIN, R. C. *Z. Phys. chem. B.* 28 (1935) 189
[49] BORN, M. *Proc. phys. Soc.* 54 (1942) 362
[50] PARKINSON, D. H., SIMON, F. E. and SPEDDING, F. H. *Proc. roy. Soc. A* 207 (1951) 137
[51] TROMBE, F. *C.R. Acad. Sci., Paris* 198 (1934) 1591
[52] FOEX, M. *ibid* 219 (1944) 117
[53] STERNHEIMER, R. *Phys. Rev.* 78 (1950) 235
[54] GIAUQUE, W. F. and MEADS, P. F. *J. Amer. chem. Soc.* 63 (1941) 1897
[55] MEADS, W. R., FORSYTHE, W. R. and GIAUQUE, W. F. *ibid* 63 (1941) 1902
[56] NIX, F. C. and SHOCKLEY, W. *Rev. Mod. Phys.* 10 (1938) 1
[57] KELLEY, K. K. *J. Amer. chem. Soc.* 61 (1939) 203
[58] WILSON, A. H. *Theory of Metals*, Cambridge, 1936 Cap 6
[59] MATHIESSEN, A. *Ann. Phys. Chem., Lpz.* 110 (1860) 190
[60] —— and VOGT, G. *Ann. Phys., Lpz.* 7 (1864) 761, 892
[61] MOTT, N. F. and JONES, H. *Theory of Properties of Metals and Alloys* 287, 300 London, 1936
[62] NORDHEIM, L. *Ann. Phys. Lpz.* 9 (1931) 607
[63] MOTT, N. F. and JONES, H. *Theory of Properties of Metals and Alloys* 286 *et seq* London, 1936
[64] HOUSTON, W. V. *Z. Phys.* 48 (1928) 449; *Phys. Rev.* 34 (1929) 279
[65] BLOCH, F. *Z. Phys.* 53 (1929) 216; 59 (1930) 208
[66] SUPEK, I. *ibid* 117 (1940) 125
[67] KOHLER, M. *ibid* 125 (1949) 679
[68] RHODES, P. *Proc. roy. Soc. A* 202 (1950) 466
[69] GRÜNEISEN, E. *Interference of Electrons* Ed. P. DEBYE London, 1931
[70] GRÜNEISEN, E. *Ann. Phys., Lpz.* 16 (1933) 530
[71] MEISSNER, W. *Handb. exp. Phys.* 11 part 2 (1935) 50 *et seq*
[72] —— and VOIGT, B. *Ann. Phys., Lpz.* 7 (1930) 761, 892
[73] *Commun. phys. Lab. Univ. Leiden* 160a (1922) Tl [Liq. He range]; 160b (1922) Pb, U–Pb [< 14°K]; 167a (1923) In [Liq. He range]; 173a (1924) Na, K [Liq. He range]; Suppl 58 (1926) General data survey for Int. Crit. Tables; 194a (1928) Ni–Cu alloys; 194c (1928) Hf, Zr [> 1·3°K]; 196b (1929) Various metals; 212d (1931) In, Ga, Tl [< 20°K]
[74] DE HAAS, W. J., DE BOER, J. *Physica* 1 (1934) 609
[75] — — and VAN DEN BERG, G. J. *ibid* 1 (1934) 1115
[76] — — — *ibid* 2 (1935) 453
[77] — and VAN DEN BERG, G. J. *ibid* 3 (1936) 440
[78] — — *ibid* 4 (1937) 683
[79] MACDONALD, D. K. C. and MENDELSSOHN, K. *Proc. roy. Soc. A* 202 (1950) 523

[80] SIMON, F. E. Act. 7 int. Congr. Refrig. 1 (1936) 367
[81] WOLTJER, H. R. and KAMERLINGH ONNES, H. *Commun. phys. Lab. Univ. Leiden* 173a (1924)
[82] MEISSNER, W. *Phys. Z.* 2 (1920) 373
[83] FINE, P. C. *Phys. Rev.* 56 (1939) 355
[84] LEIGHTON, R. B. *Rev. Mod. Phys.* 20 (1948) 165
[85] PEIERLS, R. *Leipzig Vorträge* p 75, 1930
[86] SKINNER, H. W. B. *Phil. Trans. A* 239 (1940) 95
[87] SLATER, J. C. *Phys. Rev.* 45 (1934) 794; *Rev. Mod. Phys.* 6 (1934) 210
[88] HOUSTON, W. V. *Phys. Rev.* 55 (1939) 1255
[89] BABER, W. G. *Proc. roy. Soc. A* 158 (1937) 383
[90] MOTT, N. F. *ibid* 147 (1935) 571
[91] —— *ibid* 153 (1936) 699
[92] DE HAAS, W. J. and DE BOER, J. *Physica* 1 (1934) 609
[93] FRÖHLICH, H. *Proc. roy. soc. A* 188 (1947) 521
[94] —— *ibid* 188 (1947) 532
[95] VAN DEN BERG: Thesis "De electrische Weerstand van zuivere Metalen . . .," Leiden, 1938
[96] GORTER, C. J. *Physica* 5 (1938) 483
[97] MEISSNER, W. and OCHSENFELD, R. *Naturwissenschaften* 21 (1933) 787
[98] JACKSON, L. C. *Rep. Progr. Phys.* 6 (1939) 335
[99] MENDELSSOHN, K. *ibid* 10 (1946) 358
[100] SHOENBERG, D. *Superconductivity* Cambridge, 1938
[101] KÜRTI, N. and SIMON, F. *Nature, Lond.* 133 (1934) 907, 135 (1935) 31
[102] BORN, M. and CHENG, K. C. *ibid* 161 (1948) 968, 1017 (1948)
[103] HEISENBERG, W. *Z. Naturforsch.* 2a (1947) 185; 3a (1948) 65
[104] FROHLICH, H. *Phys. Rev.* 79 (1950) 845
[105] MENDELSSOHN, K. *Proc. roy. Soc. A* 152 (1935) 34
[106] ANDREWS, D. H., MILTON, R. M. and DE SORBO, W. *J. opt. Soc. Amer.* 36 (1946) 518
[107] ANDREWS, D. H. *Report of Cambridge Conference on Low Temperatures* p 56 London, 1947
[108] OGG, R. A. *Phys. Rev.* 69 (1946) 243, 544; 70 (1946) 93
[109] BOORSE, J. A., COOK, D. B., PONTIUS, R. B. and ZEMANSKY, M. W. *ibid* 70 (1946) 92
[110] DAUNT, J. G., DESIRANT, M., MENDELSSOHN, K. and BIRCH, A. J. *ibid* 70 (1946) 219
[111] MACDONALD, D. K. C., MENDELSSOHN, K. and BIRCH, A. J. *ibid* 71 (1947) 563
[112] BIRCH, A. J. and MACDONALD, D. K. C. *Trans. Faraday Soc.* 43 (1947) 792
[113] THOMSON, J. J. *Proc. Camb. phil. Soc.* 11 (1901) 120
[114] LOVELL, A. C. B. *Proc. roy. Soc. A* 157 (1936) 311
[115] APPLEYARD, E. T. S. and LOVELL, A. C. B. *ibid* 158 (1937) 718
[116] FUCHS, K. *Proc. Camb. phil. Soc.* 34 (1938) 100
[117] DINGLE, R. B. *Proc. roy. Soc. A* 201 (1950) 545
[118] CHAMBERS, R. G. *ibid* 202 (1950) 378
[119] —— *Nature, Lond.* 165 (1950) 239
[120] MACDONALD, D. K. C. and SARGINSON, K. *Proc. roy. Soc. A* 203 (1950) 223
[121] ANDREW, E. A. *Proc. phys. Soc. A* 62 (1949) 77
[122] MACDONALD, D. K. C. *Nature, Lond.* 163 (1949) 637
[123] SONDHEIMER, E. H. *ibid* 164 (1949) 920; *Phys. Rev.* 80 (1950) 401
[124] MACDONALD, D. K. C. and SARGINSON, K. *Nature, Lond.* 164 (1949) 921
[125] PIPPARD, A. B. *Proc. roy. Soc. A* 191 (1947) 370, 385
[126] LONDON, H. *Nature, Lond.* 133 (1934) 497; *Proc. roy. Soc. A* 176 (1940) 522
[127] REUTER, G. E. H. and SONDHEIMER, E. H. *Nature, Lond.* 161 (1948) 394
[128] KOMAR, A. *J. Phys. U.S.S.R.* 4 (1941) 547
[129] —— and SIDOROV, S. *ibid* 4 (1941) 552

[130] CORNISH, F. H. and MACDONALD, D. K. C. *Phil. Mag.* (1951). In press
[131] SONDHEIMER, E. H. *Proc. roy. Soc. A* 203 (1950) 75
[132] MACDONALD, D. K. C. *Proc. phys. Soc. A* 63 (1950) 290
[133] BLACKMAN, M. *ibid A* 64 (1951) 681
[134] MENDOZA, E. W. and THOMAS, J. G. *Phil. Mag.* 42 (1951) 291
[135] MACDONALD, D. K. C. and TEMPLETON, I. M. *ibid* 42 (1951) 432
[136] GERRITSEN, A. N. and LINDE, J. O. *Physica* 17 (1951) 573, 584
[137] *Proc. Int. Confce. on Low Temp. Phys.* Oxford (1951)

OL.
3

3

RECENT ADVANCES IN THE ELECTRON THEORY OF METALS

N. F. Mott

THE most striking advances towards the understanding of metals that have been made since the war are probably in the theory of defects. An analysis of a particular type of defect, the dislocation, has given an insight into many aspects of plastic deformation and mechanical strength, crystal growth and the behaviour of grain boundaries. At the same time the concept of the vacant lattice site, capable of moving about within the crystal, has helped to correlate the phenomena of diffusion, thermal recovery and creep.* The advances in electron theory in the last few years have been less striking; no new concept, like that of the dislocation, has been introduced which has shed light on any large number of problems hitherto obscure. At the same time, the advance in the theory of defects has presented the electron theory with a number of new problems. In particular, it has refocused interest on the elastic properties of metals, since the energies of dislocations and of grain boundaries are deduced from these quantities. In addition, it has raised again the problem of the distribution of charge round singularities in metals such as vacancies and dissolved atoms.

This article will describe particularly those advances in electron theory which are relevant to these problems. First, however, we give an account of the difference, from the point of view of wave mechanics, between a metal and a non-metal, a subject which we believe has not been quite correctly treated in previous articles.[6, 7] This leads to some discussion of the magnetic and thermal properties of the electrons in metals. We then discuss metallic cohesion, with particular reference to the transition metals. The next section deals with elastic constants. We then turn to alloys, and in particular to the distribution of charge round a dissolved atom; this leads to a discussion of the information to be obtained from the spectroscopy of soft X-rays. A final section gives a brief review of some applications of electron theory to particular kinds of lattice defect.

THE NATURE OF A METAL

In this section an account will be given of the conditions under which metallic conduction is to be expected; by the statement that a solid

* See, for instance, Cottrell's article on dislocations,[1] the author's Guthrie lecture on mechanical properties[2] and the articles on crystal growth by FRANK and his co-workers.[3–5]

shows metallic conduction we mean that the resistance remains bounded as the temperature tends to zero. If this is the case, free electrons must be present at the absolute zero. We have then to consider the proper description of the free electrons in a metal, and to ask under what conditions they will occur. The account given here is a development of that published previously by the present author.[8]

We must emphasize first of all the validity and physical significance of the well known theorem of Bloch; this states that the solutions of the Schrödinger equation:

$$\nabla^2\psi + \frac{2m}{\hbar^2}\{W - V(x, y, z)\}\psi = 0 \qquad \ldots . \quad (1)$$

where V is a periodic function of position, are of the form

$$\psi_k = e^{i(kr)}\, u_k(x, y, z) \qquad \ldots . \quad (2)$$

where $u_k(x, y, z)$ is periodic with the period of the lattice. This means that an extra electron introduced into an otherwise perfect non-conducting crystal has a wave function extending through the lattice. It is able to move through the crystal, and electric resistance will arise only on account of departures from the periodic field due to lattice vibrations or impurities. It is certainly true that wave functions of type 2 give the correct description of the electrons which carry the current in photo- and semi-conductors, each such electron being treated to a good approximation independently of all the other electrons in the solid.

To describe all the properties of a crystalline solid, however, we must use a wave function which is a function of the coordinates of all the electrons in it. Two approximations to these wave functions may be used for solids; these are:

a The collective electron treatment, in which each electron is described by a wave function of type 2 extending through the lattice.*

b The London–Heitler–Heisenberg (L.H.H.) approximation in which each electron is described by a wave function localized on or around one particular atom. Such wave functions will be denoted by $\psi_a(r)$, $\psi_b(r)$, the suffixes a, b, denoting lattice points. An extension due to LENNARD-JONES and his co-workers[9, 10] may be mentioned, in which a series of orthogonal wave functions are formed from these, which none the less describe wave functions on or near individual atoms.

In either case, a wave function antisymmetric in the coordinates of all the electrons must be set up to describe the solid.

Starting from the collective electron treatment, the periodic field of

* In molecular theory this is known as the method of molecular orbitals.

the lattice leads to a separation of the permissible states (those for which a solution of 1 of type 2 exists) into zones; the energy $W(\boldsymbol{k})$ of the state suffers a discontinuity in going from one zone to the next. WILSON[11] pointed out that if a crystalline solid can be correctly described by a wave function in which all zones are either full or empty, it cannot carry a current. He suggested that it might be legitimate to describe all crystalline solids by means of the collective electron treatment; insulators would be substances for which all zones are full or empty, metals those in which at least one zone is partly occupied.

It has been pointed out by various authors that there are substances with properties which do not agree with this classification. Nickel oxide (NiO) is one of them. This has a cubic structure; the 3*d* state may therefore be split by the field of the surrounding atoms into two zones, with 4 and 6 states per atom respectively. Since the nickel ion Ni^{++} contains eight 3*d* electrons, the zones cannot all be full or empty. According to Wilson's classification, then, NiO should show metallic conduction. Actually the substance when pure is a fair insulator and transparent, though with impurities which introduce Ni^{+++} ions it is a semi-conductor,[12] showing that electrons or 'holes' (the point where an electron is absent) have no difficulty in jumping from ion to ion.*

The present author[8] has suggested that it is not legitimate to use the collective electron model for such substances, and that the London–Heitler model, or Lennard-Jones' modification, must be used. We shall therefore discuss the properties of this model. It will be sufficient for our purpose to consider a cubic lattice of atoms each containing one electron, since such a material treated by the collective electron model would lead to a half-filled zone.

Suppose first that no ionized states are included in the wave function. Then with this approximation the material will have the following properties:

i It cannot carry a current; the electrons can change places, but no transport of charge is possible.[14]

ii It will be antiferromagnetic if the exchange integral is negative, as is normally and perhaps always (*cf* ZENER[15]) the case, and ferromagnetic at low temperatures, as in HEISENBERG'S[16] original model put forward in 1928, if the exchange integral is positive.

Consider now the introduction of ionized states. By this we mean, the addition to a wave function consisting of products of the type:

$$\psi_a(\boldsymbol{r}_1)\ \psi_b(\boldsymbol{r}_2)\ \psi_c(\boldsymbol{r}_3)\ \ldots,$$

and thus denoting one electron on each atom, of terms describing a state of affairs in which one or more atoms are without an electron,

* According to ZENER[12] this type of transition can take place through the oxide ion.

and an equal number carry two electrons. Such terms are familiar in the theory of molecules. They are always present to a greater or lesser extent, since the calculated energy of a state will always be lowered when they are introduced into a wave function. The same will be true of solids; but if a solid is to carry a current, the positive and negative charges must be separated by a large distance, so that they are effectively free of each other.

One can now state the following theorem: if one starts with the simple London–Heitler approximation (no ionized states), and adds to it terms representing states in which one electron is separated from a positive charge by a distance R, the coefficient $A(R)$ of this term will tend to zero as R tends to infinity if it is chosen in such a way as to minimize the energy. Or, alternatively, if one writes down a wave function describing a state in which there is just one widely separated electron and positive hole,* this will have higher energy than the state with none.

The proof depends on a theorem familiar in the study of semiconductors. The electron and positive hole will attract each other with a force of which the potential energy for large r is of the type:

$$V(r) = -e^2/\kappa r,$$

where κ is a dielectric constant. In this field, there necessarily exists a series of stationary states, leading up to a limit. Thus, in our wave function, to remove an electron from a bound state to a free state, will necessarily require energy.

Looked at from this point of view, the cause of the absence of conductivity in NiO is simple. If pure NiO is to conduct, it must contain current carriers, namely ions with electron configurations Ni^{+}, Ni^{+++}, far enough from each other to move freely. To form such ions would require energy amounting to several electron volts for each pair.

For such a material, or for our idealized lattice of monovalent atoms, we may attempt to plot the energy W (at the zero of temperature) against the number n of free electrons. By this we mean the calculated energy if a wave function is written down describing a state of affairs in which there are n free electrons—*i.e.* n widely separated pairs. Now no calculations of this type have in fact been carried out. But we suggest tentatively that, if they were, the result would be as in *Figure 1*. As we have seen, the energy must rise initially. We make the hypothesis that, if the overlap between atoms is not too small, the energy will eventually fall and may drop below the value for $n = 0$. Appealing to experiment, we may say that this must occur, because metals exist. On the theoretical side we may say that the argument

* The electron and positive hole being free to move must both be described by wave functions of type 2, although the rest of the lattice is described by wave functions of the London–Heitler type.

that W must increase with n no longer applies when n is comparable with the number of atoms.

Insulators, then, are substances for which the curve is as in *Figure 1*, curve *1*; metals are substances for which the energy behaves as in curve *2*. For metals, starting with the London–Heitler approximation, there will be in the state of lowest energy a large number of free electrons. Metals are thus best described by the collective electron approximation.

In view of these considerations, then, we believe that crystalline substances may be classified as follows:

I In substances in which, according to the collective electron treatment, all zones are full or empty, the collective electron or the London–Heitler methods are alternative and legitimate approximations

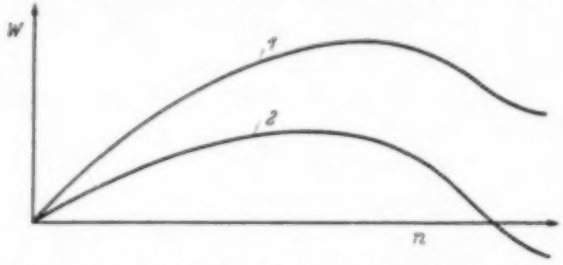

Figure 1. Suggested form of the energy W of a crystal as a function of n, the number of free electrons

to the exact wave function. Both predict an absence of current, and either could be used to obtain approximate values for the energy.

II In substances in which, according to the collective electron treatment, one or more zones are partly full, the two approximations are not alternatives. In non-conductors (NiO) the London–Heitler approximation or Lennard-Jones' modification must be used;* in metals the collective electron approximation is the only correct one. It would, of course, be possible to describe a metal by the London–Heitler approximation with the introduction of a large number of ionized states; but as the electrons in these states will be described by Bloch wave-functions, this amounts to the use of the collective electron treatment.

* SLATER[17] in a recent paper has made the suggestion that the absence of conductivity in an antiferromagnetic such as NiO can be explained using the collective electron model as follows. Owing to exchange forces, the effective potential energy of an electron in a given atom will depend on whether its spin is parallel or antiparallel to those in the atom under discussion. Thus in an antiferromagnetic material, in which the spins form a superlattice, the outermost Brillouin zone will be split in two. Slater considers that one half might be full and the other empty, a state of affairs in which no current would be possible. The suggestion is interesting; but if a complete description were possible along these lines, the antiferromagnetics would be bound to show metallic conduction above their Curie points. This is not the case.

We may contrast the behaviour of substances in class *II* of the two types, non-conducting and metallic.

a Magnetic properties

Non-conducting substances of class *II*, if the exchange integral is negative, will be antiferromagnetic. This means that electrons having the two spin directions will form a superlattice. No real theoretical proof of this has been given, but it seems plausible and in agreement with the experimental facts. The exchange integral leading to antiferromagnetism may be a direct exchange integral, or a super-exchange integral, that is the interaction between two atoms each with a spin moment via an oxygen ion (*cf* KRAMERS[18], VAN VLECK[19]). The curve

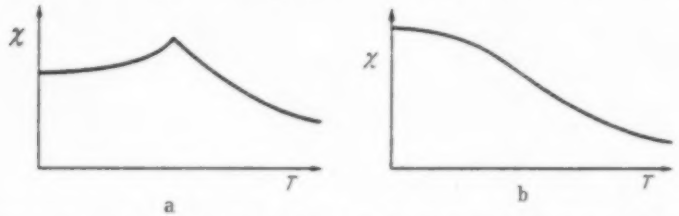

Figure 2. Curves showing the susceptibility (χ) of a magnetic substance as a function of temperature (T); a *Antiferromagnetic,* b *Paramagnetic*

showing susceptibility against temperature, for an anti-ferromagnetic is as in *Figure 2*a (see also the curves for CoO published by TROMBE[20]).

If the exchange integral is positive, the substance will be ferromagnetic, the saturation moment I depending on temperature according to the law:[21]

$$I_0 - I = \alpha T^{\frac{1}{2}} \qquad \ldots\ (3)$$

It is not certain, however, that such substances exist; ferromagnetic substances which do not show metallic conduction having, in general, structures in which the magnetic ions occupy two non-equivalent lattice sites, with more sites in one class than the other. The magnetic ions, by setting themselves anti-parallel to their nearest neighbours, thus give rise to a resultant magnetic moment.

Substances possessing metallic conductivity which are paramagnetic can be treated according to the conventional method for a Fermi gas,[6] and exhibit a susceptibility depending on the temperature as shown in *Figure 2*b.

The transition metals form a particularly interesting case. These are conventionally described by overlapping *d* and *s* bands.[6] We say that in Ni and Pd the *d* band is incomplete, with about 0·6 vacancies per atom, while for Cu and Ag it is full. The striking difference in properties between the (magnetic) metals Ni, Pd and Pt and the noble metals Cu, Ag and Au suggests that this statement corresponds closely

to some property of the exact wave functions. In other words, the state $3d^9 4s^2$ of the copper atom occurs very weakly in the exact wave function of copper metal. Clearly the conduction electrons, the electrons in the *s*-band of metals like nickel, must be described by the collective electron treatment. The important question then arises as to how we should treat the *d* electrons. The above considerations show clearly that in Ni, Pd, Pt, at any rate, and probably also Co, the *d* electrons—or better the vacancies or positive holes which are the magnetic carriers—must be treated by the collective electron method also. The reason is that their number per atom is non-integral. The metal may be thought of as a mixture of atomic cores in the states $3d^{10}$, $3d^9$ and perhaps $3d^8$, so that the vacancies must be free to move from atom to atom; we have no alternative but to treat them by the collective electron model. If the number of carriers per atom was one (or any integer) the question would be open; whether the carriers were mobile and contributed to the conductivity or whether they behaved as in a ferrite would depend on the overlap.

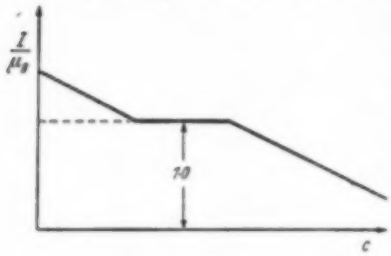

Figure 3. Hypothetical behaviour of a magnetic series of alloys at the composition where the magnetic moment I per atom is equal to one Bohr magneton (μ_B)

It is worth mentioning that in a series of alloys of cobalt with any element such as Cu, Zn, Ga, if the number of electrons in the *s* band tends to remain equal to 0·6, the number of vacancies in the *d* band should for some composition be equal to 1 per cobalt atom. If—as is probable—the *d* bands at this composition should be described by the London–Heitler approximation, we should expect at this composition a discontinuity in the energy change when an electron is transferred from the *d* to the *s* band. If the saturation moment *I* were plotted against composition *c* of, for instance, copper atoms, a variation as in *Figure 3* should be obtained. Unfortunately stable alloys in the required region have not been obtained.*

A number of papers on the properties of ferromagnetic materials, when described by the collective electron treatment, have been published by STONER and his co-workers.[23–25] As already stated, we consider this approach essentially correct for magnetic metals in which

* WENT[22] has examined the saturation moments of alloys of nickel and cobalt, and no discontinuity is observed at the composition for which the moment per atom is one Bohr magneton. However for such an alloy one would expect a mixture of nickel ions with one or no vacancies and cobalt ions, some of which would have more than one vacancy; so in this case no discontinuity is to be expected.

the number of carriers is non-integral. In Stoner's earlier treatments[23] an 'exchange' term is arbitrarily introduced into the free energy of the system, of the form $-\frac{1}{2}\nu I^2$. This is the same as the molecular field introduced into the theory by WEISS, and Stoner's work differs from Weiss's only in that the carriers form a degenerate gas obeying Fermi statistics. More recently the exchange term has been calculated by WOHLFARTH.[26]

An interesting and somewhat different suggestion as to the origin of this term has recently been put forward by Zener.[15] It was formerly considered that ferromagnetism occurred owing to a change in the sign in the exchange integral between *d* shells which was supposed to occur when the overlap between them becomes small. Two objections may be made against this:

i It has never been shown that the exchange integral does change sign.

ii The Heisenberg theory, based on an exchange integral, is appropriate to ferrites, where the carriers are not moving about, but it is not obviously appropriate to metals.

Zener suggests that the exchange integral (in the London–Heitler approximation) is always negative and tends to keep the electrons anti-parallel. Or, using the collective electron treatment, we may say that the Fermi energy ensures that, when we have to deal with electrons in states in a single zone, the resultant spin moment should be zero. In ferromagnetic metals, however, we have an incomplete *d* band which is narrow, owing to the small overlap between the *d* shells, and a wide *s* band. Zener suggests that the interaction between electrons in these two zones may ensure that the electrons in the *d* band produce their saturation moment, that is to say the largest magnetic moment possible, and the *s* band a small moment in the same direction. The proposed interaction is the same as that which ensures that for electrons in atoms in different orbital states the energy is a minimum when the spins are parallel. This in its turn arises, at any rate partly, from the fact that electrons with parallel spin are described by a wave function which is antisymmetrical in the space co-ordinates; therefore the wave function becomes small when they are close together, so that the positive contribution of the interaction e^2/r_{12} is minimized.*

Stoner's treatment does not yield formula 3 for the saturation moment at low temperatures. In this, according to HERRING and KITTEL[27], the method is incorrect, much in the same way as Einstein's theory of specific heat is sufficiently accurate in the neighbourhood of the characteristic temperature but has to be replaced by Debye's at low temperatures. Bloch's formula 3 is based on the theory of spin waves,

* ZENER[15] has also considered ferromagnetic compounds of manganese in this connection.

and their existence does not depend on any model, but, as shown by Herring and Kittel, simply on the assumption that the energy of a magnetized medium, in which the magnetization I is constant in magnitude but varies with direction, is of the form:

$$\tfrac{1}{2}\beta(\text{grad } I)^2,$$

where β is a constant.

SPECIFIC HEATS OF METALS

The specific heat of a degenerate Fermi gas, when the interaction between the electrons is neglected, is linear in the temperature. Its value per gram atom is

$$C_{el} = \tfrac{2}{3}\pi^2 k^2 T N(E_{\max})$$

where $N(E_{\max})$ is the number of electronic states per unit energy range at the surface of the Fermi distribution, for one gram atom of the material. Alternatively, if the electrons behave as if free, this can be written

$$C_{el} = \tfrac{1}{2}\pi^2 n_0 R T/T_0 \qquad \ldots . \quad (4)$$

where n_0 is the number of electrons per atom and $kT_0 = E_{\max}$, so that

$$T_0 = \frac{\hbar^2}{8mk}\left(\frac{3n_0}{\pi\Omega}\right)^{\frac{2}{3}} \qquad \ldots . \quad (5)$$

where Ω is the atomic volume.

The existence at low temperatures of a term in the specific heat linear in the temperature was a striking confirmation of correctness of the collective electron model. Unfortunately, however, when one tries to improve the approximation by taking into account the interaction between electrons, one finds at low temperatures a modified formula of the type

$$C_{el} = \text{const.}\, T/\log_e T$$

This was first pointed out in short notes by BARDEEN[28] and by WIGNER,[29] and treated fully by KOPPE,[30] whose algebra was corrected by WOHLFARTH.[31] According to Wohlfarth, the logarithmic term is definitely not in agreement with experiment. The trouble arises through the slow fall-off of the Coulomb interaction energy e^2/r between two electrons, which leads to large terms and in fact to a divergence in the interaction between electrons near the surface of the Fermi distribution. It was these divergencies which led HEISENBERG[32] to formulate a theory of superconductivity based on them.*

* In view of more recent work by FRÖHLICH[33, 34] and BARDEEN,[35] who ascribe superconductivity to a particular type of interaction between electrons and lattice vibrations, it is probable that this theory is incorrect.

Wohlfarth points out that the logarithmic term, and the divergence remarked by Heisenberg, disappear if one takes for the interaction between two electrons not e^2/r but $(e^2/r)\exp(-qr)$, in other words a screened Coulomb field. A value of q of the order 10^8 cm^{-1} is necessary in order to bring the results into agreement with experiment. It is thought that the term $\exp(-qr)$ represents the screening of the interaction between any two electrons due to all the other electrons. We do not know how to bring such a term formally into the theory here; but in the case of the interaction of the electrons in a metal with a fixed charge (*e.g.* a dissolved proton), such a term appears naturally (see p 98). In considering the effect of collisions between electrons on the lifetimes of excited states in metals, LANDSBERG,[36] too, has found it necessary to introduce such a term, for which LEE-WHITING[37] has been able to give a theoretical derivation (see p 110). BOHM[38] in a preliminary note has given another derivation of a screening constant. In what follows, then, we shall assume that formula 4 is

Table 1. Atomic Heats at 1° K, × 10^{-4} cal/°K/gm atom

Non-transition Metals	n_0	C_{el} *calculated*	C_{el} *observed*	*Method*	*Reference*
Cu	1	1·20	1·7	*T*	39
Ag	1	1·54	1·6	*T*	40
Zn	2	1·80	1·50	*T*	41
			1·36	*M*	
Cd	2	2·26	0·75	*M*	
Hg	2	2·35	3·75–4·5	*M*	
Al	3	2·2	3·48	*T*	42
			2·59	*M*	
Ga	3	2·44	0·8–1·5	*M*	
In	3	2·94	3·5–3·6	*M*	
Tl	3	3·10	2·8–3·4	*M*	
Sn	4	3·35	4·0	*T*	43
			3·45–3·95	*M*	
Pb	4	3·65	7·1	*M*	
Th	4	3·4	7·1	*M*	
Transition Metals					
Mn			42·0	*T*	44
Fe			12·0	*T*	45, 46
Co			12·0	*T*	45
Ni			17·4	*T*	47
Nb			70·0	*M*	
Pd			31·0	*T*	48
Ta			14·1	*T*	49
W			51·1	*T*	41
Pt			16·0	*T*	47

approximately right, and may be used to deduce values of $N(E)$ from experiment.

In *Table I* we give experimental values, either measured directly or for superconductors deduced from magnetic threshold curves. Values marked T are obtained from thermal measurement; those marked M from the magnetic threshold curve of superconductors, the values being taken from DAUNT.[50] C_{el} (calculated) is obtained from formulae 4 and 5.

It will be noticed that for the non-transition metals there is good agreement between the observed values and the order of magnitude of those calculated assuming free electrons. The observed values are usually higher than those calculated. This may be an example of the tendency quoted on p 87 for metals to take up a structure for which $N(E)$ exceeds the free-electron value.

For copper JONES[51] has made detailed calculations of the form of $N(E)$; it is thus possible to calculate the electronic specific heat, and JONES and MOTT[52] find

$$C_{el} = 1{\cdot}66 \times 10^{-4} T$$

in excellent agreement with the observed value.

For the transition metals C_{el} is in general much higher. For Ni, Pd, Pt and probably Co and Fe this was first ascribed by MOTT[53] to holes in the d band. The d band is comparatively narrow owing to the small overlap between the d shells, and this gives rise to a high density of states. For nickel calculations of the form of the d band by the cellular method have been made by SLATER[14] and by the method of tight binding by WOHLFARTH,[54] and both agree that the order of magnitude of $N(E)$ corresponds with the observed specific heat. In addition KEESOM and KURRELMEYER[55] have measured the specific heat of a number of copper–nickel alloys, and WOHLFARTH[56] finds close correlation between these results and theory, at any rate for the ferromagnetic nickel-rich alloys. There remain, however, some unexplained facts about the copper-rich alloys, which show a larger specific heat than pure copper and are paramagnetic. Neither of these facts is consistent with the hypothesis that the nickel is present in the state $(3d)^{10}$; it is just possible that it is present as $(3d)^8\ (4s)^2$ but that the s electrons are in bound states below the surface of the Fermi distribution, in the sense discussed on p 99.

The high values of the electronic specific heat for Mn and particularly for W are very hard to understand. The calculation of the band structure by MANNING and CHODOROW[57] does not reveal any such effect; and if ZENER[15] is right and in tungsten the cohesion is very largely due to exchange interaction between d shells, a narrow d band could certainly not be expected.

COHESIVE ENERGY

The basis of our understanding of the cohesive forces in metals was laid by Wigner and Seitz for the alkali metals and by Fuchs for the noble metals (for a review see MOTT and JONES,[6] Chapter IV). The collective electron model is used; the positive ions are pictured as floating in a sea of negative charge, and the cohesive energy is due to the attraction between each ion and the surrounding charge. In copper, silver and gold the positive ions, with configuration $(nd)^{10}$, are brought into such close contact that the ions overlap; the resulting sharp interaction is what keeps the ions apart, and leads to a close-packed structure. In

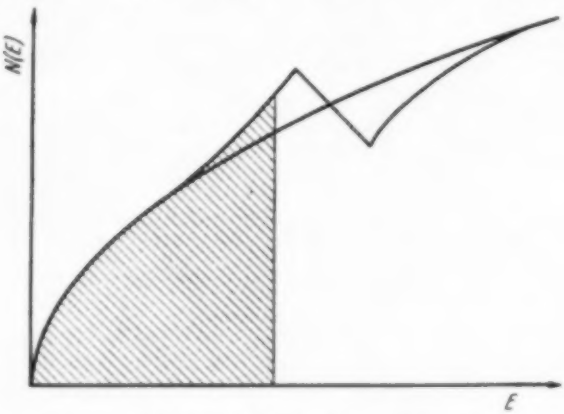

Figure 4. Showing the density of states in a metal: occupied states, as they will normally be for a stable structure, are shown shaded

the alkalis the overlap is negligible and the repulsive forces are due to the Fermi energy, which increases as $V^{-2/3}$ as the volume V decreases and to the oscillations in the wave function at the centre of the ion, which lead to a minimum in the curve when energy is plotted against volume, even in the absence of the Fermi energy (*Figure 5*).

The small corrections to the Fermi energy, which arise through the interaction of the electrons with the reflecting planes of the lattice, have little effect on the total energy. They are important, however, for:

a The elastic constants of polyvalent metals; these will be considered in the next section.

b The determination of the crystal structures of metals and alloys with more than one electron per atom; this is the basis of the work of JONES[58] on alloys obeying the Hume–Rothery rule. It is perhaps correct to say that, other things being equal, a metal or alloy will choose a structure for which $N(E)$ is as big as possible at the surface of the Fermi distribution. The reason is illustrated in *Figure 4*, which

depicts the variation in $\mathcal{N}(E)$ near the surface of a zone. $\mathcal{N}(E)$ first rises above the free electron value, and then sinks. If the surface of the Fermi distribution is in the region where $\mathcal{N}(E)$ is large, it will be able to sink to lower values of E. This may explain why the electronic specific heat is usually greater than the value computed for free electrons (p 86).

For the alkalis, as already stated, overlap (exchange) forces between the ions are not important. These are thus the metals for which accurate theoretical calculations of the lattice energy, lattice constants and compressibility are most feasible. Particularly detailed calculations have been made for lithium by SILVERMAN and KOHN[59] and by HERRING.[60] Very good agreement with experiment is obtained, the theoretical value of the binding energy being 36·0 kcal/gm atom compared with an experimental value of 36·5. We may also mention the work of KUHN and VAN VLECK,[61] who have proposed a simplified method by which the energies of the alkali metals can be estimated successfully, and also that of STERNHEIMER[62] who has given an explanation of the discontinuity in the volume of caesium observed at pressures of 45,000 kg/cm^2 in terms of an overlap of electrons into the empty $5d$ band. For the noble metals, it is very difficult to calculate from first principles the interactions between the closed shells. A way of estimating them empirically is given in the next section.

Our present ideas about metals of other types are as follows: considering first transition metals, it is reasonable to suppose that in Ni, Pd and Pt and perhaps cobalt the cohesion is similar to that in Cu, Ag and Au. Nearly full d shells, between which the interaction is repulsive, are in contact, the repulsion leading to a close-packed structure.* Metallic nickel, for instance, in which all the ions were in the state $(3d)^9$, would probably have binding energy very similar to that of copper. In fact, however, there is much evidence (MOTT and JONES,[6] Chapter VI) to show that there are 0·6 electrons per atom in the d band, or, in other words, a mixture of ions in the states† $(3d)^9$ and $(3d)^{10}$ in the ratio 6 : 4. The reason why the energy is lowered

* The estimate of the elastic constants given in the next section seems to confirm this for nickel.

† It has been suggested (MOTT and JONES,[6] p 222) that the magnetic carriers in nickel are not single holes, as stated here, but double holes, that is to say, ions in the triplet state of configuration $(3d)^8$. This suggestion was made in order to account for the paramagnetic behaviour of nickel above the Curie point, the slope of the line $(1/\chi$ as a function of $T)$ agreeing with the hypothesis that the elementary magnets have spin quantum number unity instead of $\frac{1}{2}$, g of course remaining equal to 2. But it is clear now[6] that this hypothesis is inadmissible, because coupled spins would obey Einstein–Bose rather than Fermi–Dirac statistics, and thus would give an electronic specific heat proportional to $T^{3/2}$ instead of the observed T. Wohlfarth has shown[56] that the observed paramagnetic behaviour can be explained in terms of the collective electron treatment without making any assumptions about coupled spins; one would have to go to higher temperatures than are actually possible to obtain a true paramagnetic magneton number.

when electrons are transferred from the *s* band to the *d* band is presumably as follows: the positive holes in the *d* band move slowly compared with the *s* electrons; to a very rough approximation one can suppose that the latter move in the field of a mixture of ions of types $(3d)^{10}$ and $(3d)^{9}$, their positions changing relatively slowly. There will thus be an electrostatic term arising from the attraction of the atoms carrying different charges, as in alkali halide crystals. No calculation has, however, yet been given from which the figure of 0·6 can be deduced.

In transition metals such as chromium and tungsten, an attractive interaction between the *d* shells probably plays the most important part in the cohesion. ZENER[15] has made the interesting suggestion that the spin moments of the *d* shells in these body-centred metals may be antiferromagnetic, a large negative exchange integral giving cohesion as well as holding the spins antiparallel. The body-centred structure is thus chosen because with this structure each atom is entirely surrounded by atoms with the opposite spin.

We shall return to this assumption of Zener's in discussing the elastic constants of tungsten. We may remark here, however, that if we take for the wave function of a body-centred antiferromagnetic an antisymmetrical determinant describing a definite spin on each atom, the contribution made by the exchange energy to the cohesion is zero. Doubtless in higher approximations, in which the reversal of the spins of neighbouring pairs was included in the wave function, a contribution leading to an attraction would arise.

It is, of course, a feature of the more chemical attempts to explain chemical binding[63–67] that cohesion in the long periods (Sc to Fe *etc*) is due to resonance between hybridized *s*, *p* and *d* orbitals. We are fully in agreement with this point of view, which in our opinion does not conflict with Zener's ideas. In considerations of this type, however, one always has to ask what properties of the model (a one-electron model of some type or another) can be considered properties of the exact wave function which describes the metal. We are very doubtful if non-integral valencies, as used by Pauling, can be so described, and we consider that the usefulness or otherwise of these non-integral valencies is and must remain largely a matter of opinion. On the other hand, the statement made in the collective electron model that a zone is full, or partially full, does seem to correspond to some property of the exact wave function. For instance, the fact that silver and silver–palladium alloys are diamagnetic up to a certain composition is explained on the model by saying that the *d*-band is full up to that composition; the most striking difference between Ni, Pd and Pt and Cu, Ag and Au is in their magnetic properties, so the description of the *d* band as full or not full must correspond to something real.

Similar sharp differences when overlap into a new zone begins are shown by magnesium–copper alloys, as JONES[68] has shown. This does not, of course, mean that the wave functions in *d* bands, for instance, are purely of *d* symmetry. As shown by JONES, MOTT and SKINNER[69] in 1934, the wave function in a given zone can be very hybridized. In view of these considerations, we very much doubt whether Pauling's attempt to describe cohesion in Ni, Cu, Zn, *etc* by means of resonating *d* orbitals is useful. The *d* band in Cu, for instance, is certainly full. Although the *d* shells will make a considerable van der Waals contribution to the cohesion, we do not think that it is correct to describe them by means of resonating bonds.

Attempts to calculate the cohesive energy of divalent metals have been made for beryllium by HERRING and HILL[70] and for magnesium by RAIMES.[71] These are fairly successful in obtaining values for the cohesive energy, lattice parameter and compressibility, but the calculations are complicated and it is difficult to form any physical model of the nature of the forces. JONES,[72] however, has made a useful comparison between the measured bulk modulus K of a number of metals and the contribution

$$K_F = \frac{1}{9}\frac{r^2}{\Omega}\frac{\mathrm{d}^2 E_F}{\mathrm{d}r^2}$$

due to the Fermi energy E_F alone. r is here the radius of the atomic sphere defined so that $4\pi r^3/3 = \Omega$, and E_F is given by

$$E_F = \frac{3}{5}\left(\frac{3}{\pi}\right)^{\frac{2}{3}}\frac{\pi^2\hbar^2}{2m}\left(\frac{n}{\Omega}\right)^{\frac{2}{3}}$$

where n is the number of electrons per atom. The values are given in *Table II.*

Table II. Bulk Modulus in dyne/cm² × 10¹¹

Metal	*n*	K_F	K *observed*	*Metal*	*n*	K_F	K *observed*
Cu	1	3·85	13·7	Mg	2	3·96	3·23
Ag	1	2·09	10·0	Zn	2	8·03	6·06
Au	1	2·11	16·7	Cd	2	4·47	5·06
Na	1	0·515	0·504	Al	3	13·6	7·75
K	1	0·172	0·401	Pb	4	8·06	4·33

These values may be interpreted as follows. The energy of the crystal may be divided into the Fermi energy, E_F, the energy of the lowest state E_0 (*Figure 5*), and the exchange interaction between the ions. If the interaction between the ions is negligible—as it must be for all these metals, except Cu, Ag and Au, the Fermi energy alone will give

the compressibility if the equilibrium value of the total energy coincides with the point of inflection, X in *Figure 5*, of the curve plotting E_0 against r. We see from the results of *Table II* that this must be so, approximately, for the divalent metals; for the monovalent metals sodium and potassium the Fermi energy is less important, the minimum in the total energy is near or to the left of X, and K is equal or greater than K_F.

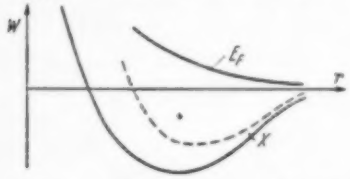

Figure 5. Contributions to the binding energy of a metal

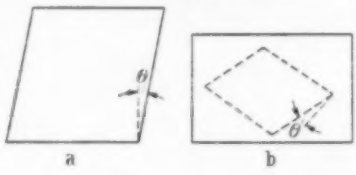

Figure 6. Deformation for which resistance to shear is given by a $C\theta$, *and* b $C'\theta$

For Al and Pb the reverse is the case. For the noble metals K is much greater than K_F on account of the interaction of the ions.

ELASTIC CONSTANTS

It is convenient, following MOTT and JONES[6] and ZENER,[73] to define for cubic crystals the following quantities:

a The bulk modulus, K, defined in terms of the elastic constants by $K = \frac{1}{3}(c_{11} + 2c_{12})$.

b The constant $C = c_{44}$, which measures the resistance to deformation with respect to a shearing stress applied across the (100) plane in the [010] direction. In a simple cubic structure of hard balls this resistance would be zero.

c The constant $C' = \frac{1}{2}(c_{11} - c_{12})$. This measures the resistance to

Table III. Elastic Constants of Cubic Metals, in dyne/cm² × 10¹¹

Metal	K $\frac{1}{3}(c_{11} + 2c_{12})$	C c_{44}	C' $\frac{1}{2}(c_{11} - c_{12})$
Cu	13·7	7·5	2·3
Ag	10·0	4·36	1·8
Au	16·7	4·20	1·5
Al	7·7	2·84	2·3
Pb	4·33	1·44	0·35
Ni	19·0	11·85	4·5
Cu + 25% Zn ..	12·3	7·2	1·8
Na (80°K)	0·504	0·593	0·072
K (83°K)	0·401	0·263	0·043
α-Fe	17·3	11·60	4·8
Mo	27·3	10·9	14·0
W	29·9	15·14	15·1

deformation applied across the (110) plane in the $[1\bar{1}0]$ direction. This resistance is zero for a body-centred cubic lattice of hard balls.

The two types of shear are shown in *Figure 6*. Values of these constants and of the compressibility, calculated from the data of BOAS and MACKENZIE,[76] are shown for a number of metals in *Table III*.

Calculations of the constants C and C' for metals were first made by FUCHS.[74] His and subsequent calculations are based on the following assumptions:

i The positive ions may be treated as point charges in a uniform electron gas. In deformations where the volume is unchanged the kinetic energy of this electron gas is unaltered (except for the terms considered under *iii*). The change in the potential energy may be treated as the change in the electrostatic interaction between the ions and the gas. The charge on each ion should be taken to be fe, where fe/Ω is the average charge density midway between the ions. For monovalent metals evaluation of the wave functions shows that $f \sim 1$; for polyvalent metals f takes some value between the valency of the ion and unity, which also can only be estimated by direct integration of the wave equations. The calculated values shown in *Table IV* are in multiples of $e^2f^2/2a\Omega$, where a is the lattice parameter and Ω the atomic volume.

Table IV. Calculated Values of C, C' in units of $e^2f^2/2a\Omega$

Structure	C	C'
f.c. cubic	0·9479	0·1057
b.c. cubic	0·7422	0·0997

ii A term contributed by the direct exchange interaction between the ions. This is negligible for the alkalis, aluminium, *etc* but is the predominating term for the noble metals. If $W(r)$ is the interaction energy of a pair of ions distant r apart, and if only interaction between nearest neighbours has to be considered, the contributions are as listed in *Table V*. We add also a value for K, the bulk modulus.

Table V

Structure	$C\Omega$	$C'\Omega$	$K\Omega$
f.c. cubic	$\frac{1}{4}r^2W'' + \frac{3}{4}rW'$	$\frac{1}{4}r^2W'' + \frac{3}{4}rW'$	r^2W''
b.c. cubic	$\frac{3}{8}r^2W'' + \frac{5}{8}rW''$	$\frac{1}{8}rW''$	$\frac{3}{8}r^2W''$

iii The contribution to the elastic constants which arises from the distortion of the Fermi distribution by the boundaries of the zones. This is assumed negligible in monovalent metals, but as we shall see it is of major importance in other metals.

It is of interest to consider the limiting case of a substance formed of hard spheres, so that W'' outweighs all the other terms. Then the elastic constants are in the ratio $K = 1$; $C = \frac{1}{2}$; $C' = \frac{1}{4}$ for face-centred cubic and $K = 1$; $C = \frac{2}{3}$; $C' = 0$ for body-centred cubic. For the face-centred cubic an anisotropy $C/C' = 2$ is to be expected in this case. In real materials the effect of W', which is negative, will diminish C' more than C. Also the electrostatic term is markedly anisotropic. It would thus seem typical—unless term *iii* is of great importance—that C' should be much smaller both than C and K. Reference to *Table III* will show that this is in fact the case, only Al and W (which is body-centred) being exceptions. These two metals will be discussed later in this section.

If terms of type *ii* are important, body-centred lattices should be very anisotropic. ZENER[75] has attributed the anomalously low value of C' for β-brass to this cause.

The metals for which the simplest comparison between theory and experiment can be made are the alkalis, because the ions are so far apart that only the electrostatic term (*Table IV*) need be considered. The comparison is as follows, in dyne/cm^2 $\times$ 10^{11}:

	$C(=c_{44})$	$C' = \frac{1}{2}(c_{11} - c_{12})$
Na (80°K, obs.) . . .	0·593	0·0725
Na (0°K, extrapolated) . .	0·656	0·0747
Na (calc., lattice parameter a extrapolated to 0°K) . .	0·580	0·070
K (obs., room temp.) . .	0·263	0·043
K (calc., room temp.) . .	0·26	0·030

The experimental values are taken from an article by BOAS and MACKENZIE.[76] The calculations refer to the absolute zero, so the comparison is most interesting for Na. Considering the nature of the approximations, the agreement may be said to be good.

Turning now to the noble metals, FUCHS[77] attempted for copper to calculate the overlap or exchange interaction between the ions. He showed that both for the elastic constants and for the compressibility, this interaction made the major contribution. We do not, however, consider that calculations of this interaction by the methods used by Fuchs are likely to be very reliable. In this report we assume a form

$$W'(r) = Ae^{-\mu r}$$

for the exchange interaction of a pair of ions, with μ large enough to

ensure that $rW' \ll W''$. We assume that the elastic constants C, C' are made up of the two terms indicated in *Tables IV* and *V*, and deduce W'' from the observed values of C, C'. We then assume that the bulk modulus K is the sum of the term given in *Table V*, namely r^2W'', and K_F, the term due to the Fermi energy. Using W'' deduced from the shear modulus, we can deduce K. The agreement with experiment shown in *Table VI* is quite good except for gold. The calculations have also been carried out for nickel (assuming one free electron per atom).

Table VI. Elastic Moduli in dyne/cm² × 10¹¹

Metal	C (obs)	C' (obs)	K (calc)	K (obs)
Cu	7·53	2·35	12·0	13·9
Ag	4·36	1·51	7·2	10·0
Au	4·20	1·45	6·9	16·7
Ni	11·85	4·5	20·4	19·0

We turn now to a consideration of the polyvalent metals. Referring to *Table III*, we see that tungsten and aluminium differ strikingly from the monovalent metals in being isotropic ($C = C'$). In tungsten, according to ZENER,[15] the binding forces are not of the typically metallic type; but to understand aluminium—and for that matter other polyvalent metals—we certainly have to consider point *iii* above, namely the effect of the crystal structure on the Fermi energy. Considerations of this type were first introduced by JONES[78] in his explanation of deviations from close-packing in divalent hexagonal crystals, and also in his discussion of HUME-ROTHERY and RAYNOR'S[79, 80] results on the lattice parameters of magnesium when various metals are taken into solid solution. They have been applied to the elastic constants of aluminium by LEIGH.[81] These authors made use of the principle that if in k-space there is an overlap across some plane boundary of a zone, as at P and Q in *Figure 7*, the overlapping electrons tend to deform the crystal in such a way that the regions in k-space that they occupy approach the origin O; energy is gained if this occurs. We shall apply this idea, first to the ratio c/a of hexagonal alloys, then to the elastic constants of aluminium.

Figure 8 shows the first Brillouin zone for the hexagonal close-packed structure. The first zone contains

$$2 - \frac{3}{4}\left(\frac{a}{c}\right)^2\left\{1 - \tfrac{1}{4}\left(\frac{a}{c}\right)^2\right\} \text{ electrons per atom}$$

When c/a is equal to 1·63 (close-packing), this is 1·73; when $c/a = 1{\cdot}856$ (as for zinc), it is 1·63.

The properties of a hexagonal metal will depend on whether overlap is at *B*, *A*, or both. The energies at these two points, assuming that the electrons behave as free electrons, are given in MOTT and JONES,[6] (Chap. V) and are reproduced in *Table VII.*

Table VII. Energies E_A, E_B in ev

Element	*c/a*	*n*	E_A	E_B
Zn	1·861	1·799	7·125	6·171
Cd	1·890	1·805	5·668	4·766
Be	1·585	1·731	9·594	11·476
Mg	1·625	1·743	4·882	5·547

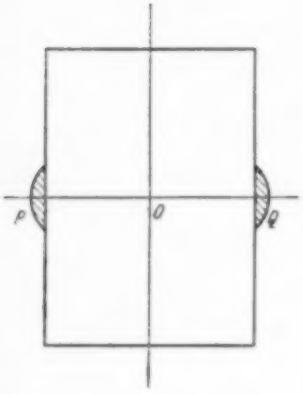

Figure 7. A region in k-space

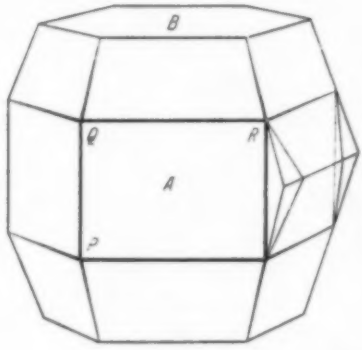

Figure 8. The first Brillouin zone for the hexagonal close-packed structure

One would suppose that for zinc and cadmium the overlap would be mainly at *B*, and that this would account for the large deviation from hexagonal close-packing. For Be and Mg the overlap will be at *A*. Why the two classes should differ in this way is not entirely clear. Probably the energy gaps in zinc and cadmium are larger than in Be and Mg; energy may be gained by a large deviation from hexagonal close packing; but why more energy is gained by an overlap at *B* than at *A* is not known. Perhaps the energy gap is greater at *B*.

The investigation of the lattice parameters of the Cu–Zn alloys by OWEN and PICKUP[82] affords evidence of the correctness of this interpretation for zinc. As copper is added to zinc, we should expect the number of electrons to decrease, the overlap to become smaller, the points *B* in *Figure 8* to move away from the origin, and thus the

c/a ratio to decrease. The following values obtained by OWEN and PICKUP[82] show that this is so.

		c/a
η-phase	end (pure Zn)	1·856
	beginning (97·3 per cent Zn)	1·804
ε-phase	end (86·8 per cent Zn)	1·554
	beginning (78·6 per cent Zn)	1·570

For higher concentrations another hexagonal phase, the ε-phase, appears, with c/a ratio closer to that for hexagonal close-packing. In this phase overlap will be at A. Since considerable deviation from close-packing is necessary before overlap at B occurs, it is natural that this can only occur when the number of electrons is sufficient to give a considerable overlap. For the ratios of electrons to atoms of alloys in the ε-phase, this presumably is not so.

It will be noticed that as the electron–atom ratio decreases in the ε-phase, the overlap at A thus decreasing, the c/a ratio approaches the value for hexagonal close-packing (1·63). It will be noticed also that the effect on c/a of a given change in the number of electrons is less than in the η-phase, thus confirming our guess that overlap at B has a greater effect in distorting the lattice than overlap at A.

A further set of alloys to which considerations of these kinds have been applied are those of Mg with In, Cd, Pb *etc.* Since, however, a detailed account of this work has already been given by RAYNOR[83] in Volume I of this Series, it will not be treated further here.

Turning now to the behaviour of aluminium, LEIGH[81] argues as follows: the quantity that we have called f, so that fe is the effective charge on each ion, though perhaps less than 3 is certainly greater than 1; he estimates $f^2 \sim 6{\cdot}75$, which, taking the electrostatic terms alone, gives the values below, shown in the second row (electrostatic).

	C(dyne/cm^2 × 10^{11})	C'(dyne/cm^2 × 10^{11})
Observed	2·9	2·9
Electrostatic	11·1	1·2
Boundaries of full zone	4·5	1·5

It will be noticed that the calculated value of C is much greater than the observed value. He then estimates the contribution that arises, if one assumes that the first zone is full, so that the surface of the Fermi distribution is constrained to move with the boundaries. The contribution, for any face-centred cubic metal for which this is so, is, according to Leigh:

$$C = h^2/ma^5 \quad C' = h^2/3ma^5$$

these are also tabulated above, in the third row. The contribution is necessarily positive, since by subjecting the surface of the Fermi

distribution to a constraint, the work done to deform the lattice must be increased.

A negative contribution to the elastic energy can only occur when, firstly, there is overlap into a second zone or vacancies in a first zone, and when as a result of the deformation there is a transfer of electrons from one point in k-space to another. We can illustrate this by the case of an (idealized) simple cubic alloy containing rather more than 2 electrons per atom, so that the first zone is full and there is some overlap into the second.

The Brillouin zone is shown in *Figure* 9a, there being overlap at A, B, C, D. If the cubic cell is sheared in the [010] direction across the (100) plane (*Figure* 9a), the zone is deformed as in *Figure* 9b;

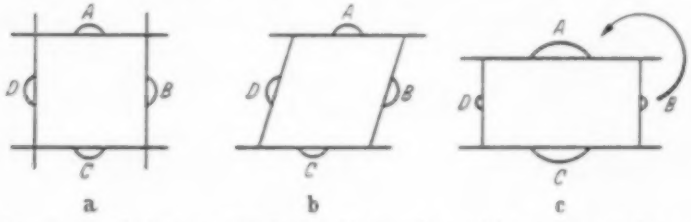

Figure 9. Brillouin zones of a simple cubic crystal, containing rather more than two electrons per atom, when subjected to shear

there is then no first order change in the energies of the points ABCD, so there is no flow of electrons from one to the other. The overlapping electrons thus make only a small positive contribution to the shear modulus $C(=c_{44})$. But if it is sheared in the [110] direction across the (110) plane, the zone deforms as shown in *Figure* 9c. The points B, D have a higher energy than A, C, electrons are transferred as shown by the arrows, and this leads to a considerable negative contribution to $C'[=\frac{1}{2}(c_{11}-c_{12})]$.

If the number of electrons had been slightly less than 2, so that there were holes in the first zone instead of electrons in the second, the position would be reversed; one would get a negative contribution to C.

Turning now to aluminium, which has the face-centred structure and three electrons per atom, Leigh suggests that the first zone is completely (or nearly) full, and that overlap into the second zone is what is important. Overlap will first occur across the (111) planes. A shear of type b (*Figure* 9) does not alter the distance of the mid-points of these from the origin; thus it is from C that a considerable negative contribution must be subtracted. Leigh shows that plausible assumptions about the overlap may be made that give a contribution which reduces C to the observed value; he also suggests that there

must be a small overlap over the (100) faces, in order to reduce C' to the observed value.

It seems probable that a description of this kind must be given for the elastic constants of all metals (other than transition metals) with more than one electron per atom. The purely electrostatic term will be too big, and must be reduced by a consideration of overlap.

Turning now to tungsten, an account of the elastic constants has been given by ISENBERG.[84] He concludes that the value is properly explained by Zener's hypothesis, that the cohesion is mainly due to exchange interaction between the *d* shells.

DISTRIBUTION OF ELECTRONS IN ALLOYS

In this section we shall review some recent work by FRIEDEL[85] on the distribution of electrons in dilute solid solutions of metals such as nickel, zinc, gallium, tin or arsenic in copper, silver or gold. The point at issue is the following: since the introduction of Hume-Rothery's rule and its explanation by JONES,[58] we have been accustomed to think that in these alloys one to four valence electrons from the metals zinc to arsenic respectively leave their atoms and join the conduction electrons of the alloys. On the other hand, we know that the charge contributed by these electrons is distributed in such a way as to screen the positive charge of the ion. If ze is the charge on the core with configuration $(3d)^{10}$ for the dissolved atom ($z = 0$ for Ni, $z = 2$ for Zn *etc*), the potential energy round an electron is of the form:

$$\frac{(z-1)\,e^2}{r}\exp(-qr) \qquad \ldots\ldots (6)$$

This is shown most directly from the observed electrical resistance of these alloys (MOTT and JONES,[6] p 293). The calculated value is infinite in the absence of a screening constant; from a comparison between observed and calculated values it is estimated that q is about 10^8 cm^{-1}.

There are two ways in which screening of this type can occur. One is that the wave functions of all the electrons should be modified in the neighbourhood of the dissolved atom in the way suggested in *Figure 10*, the total excess charge being equal to $(z-1)e$. Alternatively, in the field of the dissolved atom, there may exist bound states below the surface of the Fermi distribution. In the latter case the screening will be provided by the bound electrons; any modification in the charge density of the free electrons must be such as to keep unchanged their contribution to the charge round the impurity (*Figure 10b*).

The correct description can only be determined by a calculation of the energy using wave functions of the two types. It should be pointed out, however, that the two descriptions are not alternative

mathematical approximations to the same exact wave function for the whole system of electrons. An experiment exists which can show which is the correct form. This is the investigation of the x-rays emitted by the dissolved element when the alloy is used as an anti-cathode. In case *a* the band emitted when electrons jump from the conduction band to a lower level will have the same width as for the matrix (*e.g.* Cu). In case *b* a line (broadened by Auger effect) will appear on the low frequency side of this band. We shall return to this point in connection with x-ray emission from alloys.

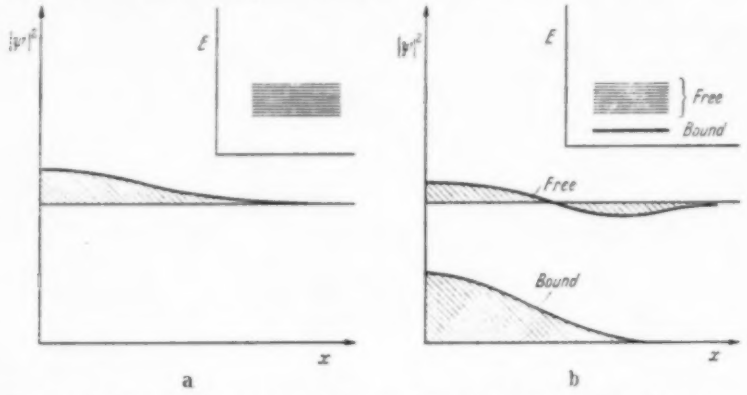

Figure 10. Charge distribution round a dissolved atom in an alloy **a** *without bound states,* **b** *with bound states, showing the contributions from the free and bound electrons: the inset diagrams show the energy levels in the two cases*

The treatment of this problem will be in terms of the Hartree–Fock approximation, in which each electron has its own wave function, and in which each wave function satisfies the Schrödinger equation for an electron moving in a field of potential $V(r)$. $V(r)$ need not necessarily be the same for all electrons: for electrons in the conduction band, it will be of the type *6*, that is, a screened field; if a bound state exists, the bound electron will be in an unscreened field of type e^2/r. We must therefore carry out a self-consistent calculation by firstly making an estimate of q and secondly determining whether or not there are any bound states for this value of q. If not the total shift of charge (the shaded area in *Figure 10***a**) must be determined. This should be equal to unity (if $z - 1 = 1$). This condition determines q. Thirdly if there is a bound state, then we know that the description of the electrons by wave functions in the Fermi distribution does not correspond to the state of lowest energy. We must put an electron into a bound state. To a first approximation, then, we should imagine a copper ion of the lattice replaced by an ion Zn^+, Ga^+, Sn^+ or As^+—that is, by a monovalent ion. The free Fermi electrons will then be

slightly perturbed by the stronger field round these ions; but the perturbation must be of type b in *Figure 10*, giving no heaping up of charge.

In order to discuss the heaping up of charge, and the existence of bound states, a few formulae are required. An electron moving in the field 6 will be described by a wave function with the asymptotic form

$$r^{-1} \sin (kr + \eta_l - \tfrac{1}{2}l\pi)\ P_l\ (\cos \theta)$$

where the phase η_l is itself a function of k.

The test for bound states is to plot η_0 against k as in *Figure 11*. Starting from large values of k, η_0 will increase as k is decreased. For large

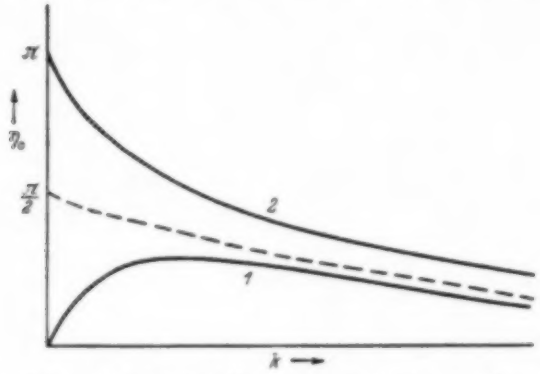

Figure 11. Phase η_0 as a function of k: 1 when no bound states exist; 2 when one bound state exists

values of q, it will then decrease again and tend to zero as $k \to 0$ (curve 1). If this occurs there are no bound states. For values of q smaller than a critical value, η_0 tends to π. When this occurs, a bound state of s-symmetry becomes possible. The quantities η_1, η_2, corresponding to p and d symmetry respectively, behave in a similar way.

For determining the heap-up of charge, we make use of the formula:

$$Q = \frac{2e}{\pi} \sum_l (2l + 1)\ \eta_l\ (k_M)$$

for the total charge in the shaded area of *Figure 10*a or b. This can easily be proved.[85] It will be seen that the charge depends only on the phases for the electrons with momentum k_M, and thus at the surface of the Fermi distribution.

For a screened Coulomb field, numerical integration shows that the first bound state appears when $(2/\pi)\eta_0(k_M) \sim 0{\cdot}5 - 0{\cdot}6$, and the phases for higher values of l do not contribute anything significant. It thus appears that a proton surrounded by a Fermi gas will, in its lowest state, certainly have a bound electron attached to it. This is, however, not necessarily the case when real metals are substituted for

the ideal Fermi gas, either for dissolved hydrogen or for zinc in copper for instance. The reason is that the energy at the bottom of the Fermi distribution is negative instead of zero. Calculations of the type outlined above are not in fact the most convenient in this case.

For actual metals, we shall begin by assuming that a bound state exists and determine the heats of solution, using a cycle. We shall then determine the position of the bound state relative to the bottom of the Fermi distribution, and shall assume its existence if the calculation shows that its energy is the lower. If a bound state exists, the heat of solution H of say, zinc, in copper should be made up of the following terms:

I The heat of vaporization of zinc, W_2; this is the energy required to remove a zinc atom from the metallic lattice.

II The ionization energy I_2 of zinc.

III The work done to take a copper ion out of the copper lattice and replace it by a zinc ion Zn^+. To a first approximation this is zero.

IV A negative contribution from the ionization energy I_1 of copper. This enables us to add the electron removed from a zinc atom to the copper ion.

V A negative term, *minus* the lattice energy of copper, W_1. This enables us to add the copper atom to the massive alloy.

VI A correcting term, to take account of the exchange interaction between the conduction electrons and the bound electron, and other terms of the same type. We call this δ.

Thus for the heat of solution we have:

$$H = (I_2 - I_1) + (W_2 - W_1) + \delta$$

At the time of writing, no calculations have been made of the correcting term δ, except for the corresponding x-ray problem discussed in the next section.

Some values of the heats of solution calculated from the first four terms are shown in *Table VIII.* Discrepancies must be attributed to the exchange term δ. The binding energies are taken from KUBASCHEWSKI and EVANS.[86]

Table VIII. Heats of Solution in ev

	W_1	I_1	W_2	I_2	H *calculated*	H *observed*
Cu–Zn	3·51	7·68	1·35	9·36	− 0·49	− 0·29
Cu–Al	—	—	3·3	5·96	− 1·9	− 1·3
Cu–Sn	—	—	3·38	7·3	− 0·5	− 0.5
Cu–As	—	—	1·31	10·0	0·1	− 2·7
Ag–Zn	2·95	7·54	1·19	9·36	0·05	− 0·18
Ag–Cd	—	—	1·16	8·96	− 0·36	− 0·19

We have now to ask whether the bound state, *i.e.* that of the second electron on zinc, is actually below the bottom of the Fermi distribution. We may take for the mean energy of the conduction electrons in copper $-(I_1 + W_1)$. The average energy of the electrons is higher by $\frac{3}{5}E_F$ than the bottom of the Fermi distribution. Thus the energy of the bottom of the Fermi distribution is:

$$-(I_1 + W_1 + \tfrac{3}{5}E_F)$$

For the energy of an electron in the bound state in zinc we have $-I_2'$ where I_2' is the second ionization potential of zinc. A bound state will exist if

$$I_2' < I_1 + W_1 + \tfrac{3}{5}E_F$$

Some values are given in *Tables IX* and *X*.

Table IX. Positions of the Bottom of the Conduction Band in Copper, Silver and Gold (ev)

Metal	*Lattice Energy* W_1	*Ionisation Energy* I_1	E_F	$I_1 + W_1 + \frac{3}{5}E_F$
Cu ..	3·51	7·68	7·1	15·44
Ag ..	2·95	7·54	5·52	13·80
Au ..	3·99	9·18	5·56	16·5

Table X. Second Ionization Potentials, I_2'*, of Certain Metals (volts)*

Zn 17·89	Cd 16·84	Hg 18·65	Al 18·74	Ga 20·43
In 18·79	Tl 20·32	Ge 15·86	Sn 14·5	As 20·1

It will be seen that the second electron of these elements is usually a few volts below the bottom of the conduction band, and so should go into a bound state.

We may summarize these results by saying that for Zn, Ga, Ge *etc* in Cu one electron certainly goes to the conduction band; the next may or may not be in bound states, while the additional electrons in Ga, Ge *etc* certainly are in a bound state. It would seem at first sight as through the hypothesis that electrons in zinc, gallium *etc* are not contributed to the conduction electrons would invalidate the Hume-Rothery rule. This, however, is certainly not the case. The bound states are subtracted from the conduction band, so that the total number of states in the first zone is twice the number of atoms, including the bound states.

A further point concerns paramagnetism. A dilute solution of Zn in Cu, for instance, if the outer electron on the Zn^+ ion is in a bound state, would seem at first sight to be an ideal paramagnetic with a susceptibility proportional to $1/T$. This, however, is almost certainly incorrect. For suppose that, as for zinc in copper, each zinc atom contributes one bound electron. Then the effective potential energy, including exchange forces, in which the conduction electrons move will not be the same for spins parallel or antiparallel to the bound electron. Suppose, for instance, that all the spins were parallel to each other. Then the conduction electrons with spins parallel and antiparallel to this direction would move in different fields; in their state of lowest energy the numbers with the two spin directions would not be the same. The conduction electrons thus introduce a coupling, which may cause ferromagnetism as in Zener's theory,[15] or may possibly have the opposite sign. In any case the spins in atoms dissolved in a conductor cannot be considered as free, even if there is no direct interaction. Nevertheless, some increase in paramagnetism is to be expected when atoms such as Zn, Mg or Pb are dissolved in copper, if the outermost valence electron is in a bound state. Such increases have in fact been observed for Cu–Mg and Ag–Pb.[87, 88] For Cu–Zn, on the other hand, the alloy is more diamagnetic than the pure metal.[89] This would perhaps suggest that in this alloy no bound state is formed. For further discussion see FRIEDEL.[85]

APPLICATIONS OF SOFT X-RAY SPECTROSCOPY

Several review articles[90–93] deal with the information about the electronic structure of solids which can be obtained from x-ray spectroscopy. In this section we shall discuss certain recent advances both on the theoretical and experimental side.

In observing the emission spectrum of a solid, we have to deal with transitions of the following type: initially—after bombardment of the anticathode—an x-ray level has a vacancy (*Figure 12*a). There is thus a positive charge located on an inner shell of one of the atoms. This, as explained in the last section, will normally give rise to an occupied bound state below the level of the conduction band. This level is shown in *Figure 12*a. But after the emission there will be a vacancy in the previously occupied levels, but no vacancy in the x-ray level. The width of the x-ray emission band is thus identical with the width of the occupied zone, *undistorted by any vacancy in the inner shells*. This holds true for metals or non-metals; in metals, however, and to a less extent in non-metals, there will be a broadening of the band due to the short life-time of the state shown in *Figure 12*b. We shall return to the calculations of LANDSBERG[36] and of

LEE-WHITING[37] on this subject when considering the life-time of excited states. The bound state of *Figure 12*a is not, then, directly observable in emission work; it has to be taken into account in calculating the frequency of the emission band, but not in calculating its breadth.

Turning now to absorption, the process depends on whether the absorbing material is an insulator* or a metal. In both we start with the solid in its normal state; after the absorption of an x-ray quantum there is a vacancy in an inner shell. In an insulator, the positive charge associated with this vacancy gives rise, as is well-known, to vacant

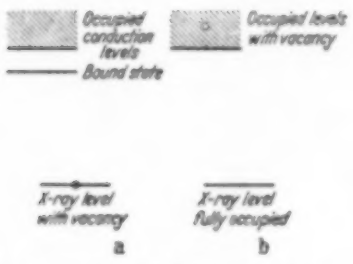

Figure 12. Level scheme for X-ray emission: a *before emission;* b *after emission*

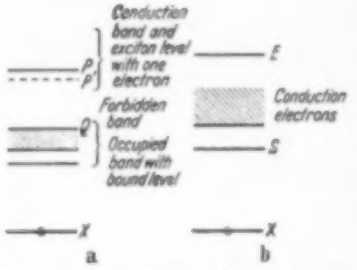

Figure 13. Level schemes for solids after absorbing an X-ray quantum: a *non-metals;* b *metals*

'exciton' levels lying below the empty conduction band. The electron may make transitions into these levels or into the conduction band. The spectrum to be expected thus consists of a series of lines leading up to a series limit. In this respect it is in no way different from the x-ray absorption spectrum for free atoms as observed for instance for argon by PARRATT,[94] or the ultraviolet absorption spectrum of alkali halide crystals, of which the theory is described fully by MOTT and GURNEY[93] (Chapter III).

In solids the spacing between the levels and the series limit will be less by a factor κ_0^2 than for free atoms, where κ_0 is the dielectric constant at high frequencies; it is doubtful whether these exciton lines have been observed as yet in x-ray spectra,[95] though they show up in ultraviolet absorption. It is clear that the absorption edge and the high frequency limit of the emission band should be separated by the interval $P'Q$ of *Figure 13*a—that is, by nearly the width of the forbidden band.† Finally, the existence of positive charge in an inner shell may give rise to a bound level below the full band. Such a level is shown

* In the category of insulators we include semi-conductors, both of the germanium and nickel-oxide types.

† It is, of course, true that emission may occur from the level P', if the excitation process leaves an electron in the level P'. A weak line on the high frequency side of the emission band might be expected in this case. So far as we know, it has not been observed.

in *Figure 13*a. Since such a level is full, transitions to it from the x-ray level are not possible.

Turning now to metals, the position after a transition is as shown in *Figure 13*b. As before, there will be a vacancy in the x-ray level, a (full) level below the conduction band (marked S), and an electron at E above the Fermi limit. It is immaterial whether we consider the electron as jumping from X to E, and an electron from the conduction band as moving down to S, or the electron from X moving to S, and an electron moving from the Fermi distribution to E.

The first point that is apparent is that in metals the absorption edge must coincide with the high frequency limit of the emission band. We shall begin by attempting a calculation of this frequency.

Calculation of the frequency of absorption edges in metals—To calculate this frequency, it is obviously appropriate to consider the electron as jumping from X to S (*Figure 13*b); the change in the energy of the Fermi electrons will then have to be calculated as a correction. This means that the x-ray K absorption limit of, for instance, metallic lithium should correspond closely to the energy of the transition for the free ion Li^+ from the state $(1s)^2$ to the state $(1s)^1\ (2s)^1$. The energy of this transition is given by BACER and GOUDSMIT,[96] and is 58·7 ev. The observed value of the limit is 54·5 ev. The difference is ascribed by Friedel to the exchange energy W_{ex} between the screening electron and the conduction band and to similar corrections, which can be calculated and give satisfactory agreement with experiment.

Similar calculations have been made for sodium. A further calculation of interest is the difference between the K absorption of Na or K in the metallic state and in the crystalline alkali halides. For the halides the computation has been given by MOTT and GURNEY[92] (Chapter III); the frequency ν of the absorption edge is given by*

$$h\nu = E + W_L - P - \chi$$

Here E is the energy required to remove a K electron out of the free ion Na^+; W_L is the lattice energy per ion pair; P is the energy of polarization of the lattice round a point charge; and $-\chi$ is the energy of the bottom of the conduction band. E, W_L, P are all positive quantities. For metals on the other hand we have seen that the frequency ν' of the series limit is given by:

$$h\nu' = E' - W_{ex}$$

where E' is the energy required to excite a metal ion, *e.g.* for sodium from the state $(1s)^2\ (2s)^2\ (2p)^6$ to $(1s)^1\ (2s)^2\ (2p)^6\ (3s)^1$, and W_{ex} is a calculable exchange interaction between the $3s$ or $4s$ electron and the conduction electrons.

* We have neglected any small correction due to exciton levels.

In the expression for the difference:

$$h(\nu - \nu') = E - E' - W_L - P - \chi + W_{ca}$$

everything is known or calculable except $(E - E')$, which is the energy required to remove an outer electron from a sodium ion in the state $(1s)^1\ (2s)^2\ (2p)^6\ (3s)^1$. We take this to be the same as the second ionization potential of Mg, or in the case of potassium of Ca. The values are given in *Table X*. The agreement seems reasonably satisfactory.

Table X. Energies in ev

	$E - E'$ *ionization potentials of* Mg^+, Ca^+	W_{ca} *computed*	W_L	P*	χ*	$h(\nu - \nu')$ *calc.*	$h(\nu - \nu')$ *obs.*
NaCl ..	14·96	2·41	10·33	1·52	0·53	5·0	4·0
KCl ..	11·8	1·32	8·78	1·44	0·07	2·85	3·1

Transition probabilities—No detailed theory of transition probabilities has been given since the introduction of the idea of bound states in metals; the following concepts are qualitative.

Let us consider the absorption process of *Figure 13b*. One can describe it physically in two ways. Either the electron jumps from X to S, and the conduction electrons throw up an electron to E, or the electron jumps to E, and a conduction electron drops from the conduction band to S. Since the final state is antisymmetrical in all the electrons concerned, the final states reached by the two processes are physically indistinguishable, and the transition probability will be the square of the difference of the related matrix elements.

Formally, the jump of the electron from the conduction band to E or S takes place because the field in which the conduction electron moves changes when the x-ray level loses an electron. The wave functions after the transition are therefore not quite orthogonal to those before, so that a jump from one state to another can occur.

The dependence of the transition probability from X to E on the crystal structure has been discussed by a number of authors. KRONIG[97] was the first to point out that fluctuations were to be expected due to the zone structure of the allowed energy states. Interpretations along these lines of the fine structure of the absorption coefficient have been given by SKINNER[90] and by JONES and MOTT.[52]

COSTER and KIESTRA[98] have recently examined the fine structure of various compounds of iron and have shown that at more than 70 ev from the absorption edge it is determined by the crystal structure of

* Values given by MOTT and GURNEY[91] (p 97).

the material, but nearer to the limit the nature of the atom is the determining factor. Now for the transition *XS* of *Figure 13b* the matrix element will depend only on the atom, and not on the crystal structure. Friedel[85] has shown how this may give a fine structure. The absorption spectrum will be similar to that of the lithium ion. We have supposed that after the transition there will be a bound electron, screening the residual positive charge, in the state $2s$, so that the whole ion is in the state $(1s)^1\ (2s)^1$. But alternatively the screening electron could be in the states $2p$ or $3p$, and in these cases the matrix elements corresponding

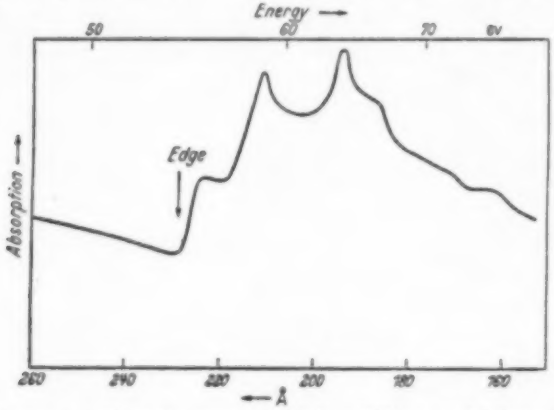

Figure 14. Absorption spectrum of lithium (Skinner and Johnston)

to the transitions *XS* will make a finite contribution to the transition probability, since the transitions will be allowed. One expects, then, sharp* maxima in the absorption spectrum for energies corresponding to these transitions. *Table XII* shows the energies concerned, and the calculated corrections W_{ex} for exchange.

Table XII. K Absorption of Lithium (energies in ev)

State of Screening electron	*Energy of Excitation of ion* $(1s)^2$	W_{ex} *calc.*	*Total*	*Distance from edge*
$2s$	58·7	3·25	55·4	—
$2p$	61·0	2·85	57·13	1·7
$3p$	69·0	5·15	63·8	8·2

It will be seen that we expect peaks at distances from the edge of 1·7 and 8·2 ev. Actually the observed spectrum (measured by SKINNER and JOHNSTON[99] does contain two sharp peaks (*Figure 14*) at distances of 3·5 and 8·5 ev from the edge. These may well be interpreted in this way. The alternative explanation, given by JONES and MOTT,[52] is

* The theory has not been developed to the point where it can be said how sharp these peaks should be.

in terms of the zone structure of the body-centred cubic lattice; peaks corresponding to the reflections from the (110) and (200) planes would give peaks at distances of about 2·8 and 12·3 ev from the edge. It would thus be of extreme interest to investigate the K absorption of an alloy of lithium.

X-ray emission from alloys—The x-ray emission spectrum of a metal such as Al, Sn or As dissolved in copper will give the most direct evidence as to whether bound states below the Fermi distribution exist.

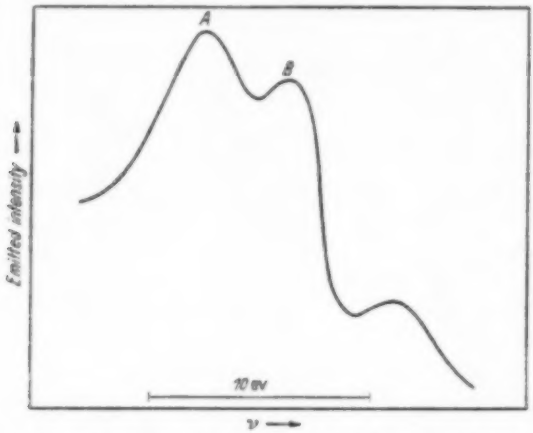

*Figure 15. K_β emission of aluminium dissolved in copper (Cauchois)**

If they do, one would expect the spectrum for transitions from the conduction to the x-ray level to show a line (broadened by Auger effect) to the low frequency side of the main band. At present experimental results exist only for the K-emission from aluminium.[100–102] CAUCHOIS[102] finds that the K_β emission band is divided between a rather sharp peak at the limit, about 2 ev wide, with a broader peak of width 4 ev about 4·5 to 5 volts from the edge (*Figure 15*).

We picture the Al atom dissolved in Cu as an Al^+ ion, the $3s$ electrons certainly being in bound states. Unfortunately the transition $3s$ to $1s$ is forbidden; a clear demonstration of these bound states will thus have to await the observation of L_{III} emission in say Sn dissolved in Cu, or K or L_{III} in As, for which bound electrons in s or p states must exist. The observed spectrum for Al is probably to be explained as follows: The peak A to the high frequency side must be thought of as due to transitions from the conduction band of the alloy to the x-ray level of aluminium. It is narrower than the band for pure copper for the following reason. The additional attractive field due to the replacement

* The author wishes to express his thanks to Miss CAUCHOIS for providing him with these curves prior to publication.

of Cu by Al, will attract the p components of the wave functions of the Fermi electrons and repel the s components, the bound $3s$ levels which are subtracted from the band being occupied. Thus the intensity of the top of the band is greatly strengthened at the expense of the bottom.

The peak **B** is, we suggest, due to a transition from the $3s$ to the $1s$ level of Al. Since this is a forbidden transition, we must picture it occurring via the conduction band. The $3s$ electron jumps into an empty state above the limit of the Fermi distribution, and one of the

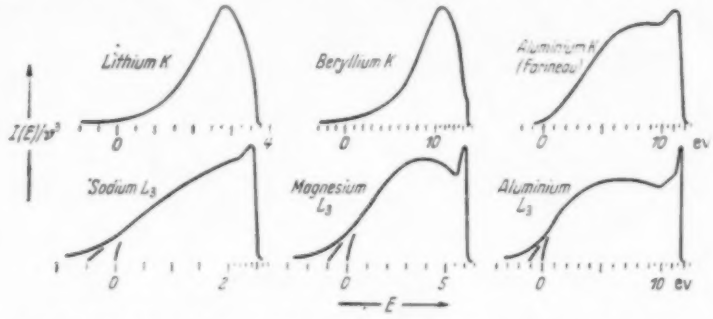

Figure 16. K and L_2 emission bands of certain metals. The curves are due to Skinner[103] *except that for aluminium K*

conduction electrons jumps down. Such a process would shift the band to lower frequencies than that for the direct transition, and broaden it.

The frequency of the upper limit of peak **B** does in fact correspond well with the expected frequency of the $3s$ to $1s$ transition. After the emission process, if there is a vacancy in the $3s$ level, the corresponding charge must be screened either by the conduction electron, or by a bound electron in a $3p$ level. Making the latter assumption, we should assume the energy interval **AB** of *Figure 15* to be the same as that between the states $3s^2$ and $3s^1 3p^1$ of the aluminium ion Al^+. This is 4·62 ev, in good agreement with experiment.

Lifetime of excited states—The intensity of an x-ray emission band for a given frequency is expected to be the product of $N(E)$, the density of states and $p(E)$, the transition probability. At the bottom of a band $N(E)$ behaves like $E^{\frac{1}{2}}$, and for the $L_{II,\ III}$ transitions $p(E)$ should tend to a finite value there. SKINNER,[103] however, observed that emission bands show a tail towards the low frequencies; some examples are shown in *Figure 16*. He suggests that this tail is due to the finite lifetime of the state illustrated in *Figure 17a*, where a vacancy is left in the Fermi distribution of electrons. A short lifetime will broaden the electronic states, and so lead to a tail of the observed type.

The lifetime will be limited by transitions of the type shown in *Figure 17b*; one of the conduction electrons (A) falls into the empty state, giving up its energy to another conduction electron (B) which is raised to a higher level (C). This is a type of Auger effect. The probability of such a transition is proportional to a quantity of the type $|M|^2$, where M is the matrix element of the electrostatic interaction between two electrons for the four states concerned.

Calculations of the broadening of this type have been carried out by LANDSBERG.[36] The matrix elements are easy to calculate; the difficulty is the summation over all allowed transitions, that is those in which the second electron jumps into an empty state. Landsberg finds that if for the interaction energy between the electrons one takes

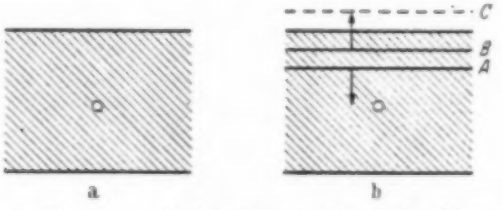

Figure 17. Showing conduction electrons of a metal with a vacancy

e^2/r, the pure Coulomb interaction, the transition probability and hence the line width tend to infinity. This is because of the very high probability of transitions in which each electron changes its momentum by only a small amount (small angle scattering). Landsberg, therefore, suggests that the interaction should be taken arbitrarily to be of the form

$$\frac{e^2}{r} \exp(-qr)$$

the second term representing the screening by all the other electrons of the electrons under consideration. In order to obtain agreement with experiment one must take $q \approx 10^8$ cm^{-1} (compare the considerations on pp. 85, 98).

An interesting result of Landsberg's calculations is that the lifetime is a minimum and the broadening is a maximum at the bottom of the full band, the latter tending to zero at the upper limit. This is because the only electrons which can fall into the vacant level are those in higher states. This theory does not therefore predict any loss of sharpness of the upper limit of the emission band. Any width of this limit must be due either to temperature,[90] or to the finite width of the x-ray level.

Landsberg's calculations have been extended by LEE-WHITING[37] to the absorption spectrum, and to the finite lifetime of electrons above the Fermi distribution. His results are shown in *Figure 18*. He also

uses a screening constant, and gives a method of calculating it, which gives the same result as that of BOHM.[38] The width Δ shown in *Figure 18* should tend to $6{\cdot}68\sqrt{E_F/E}$ for large E.

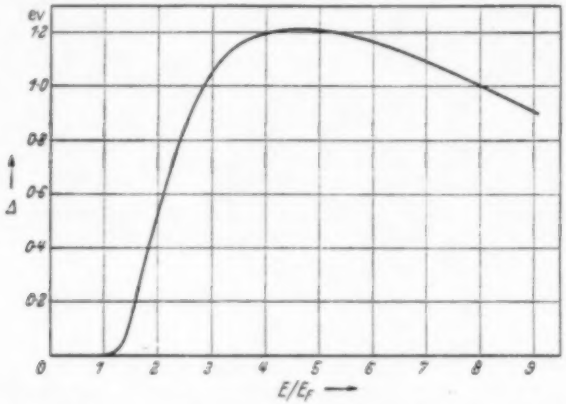

Figure 18. Width Δ (in ev) of the state where an electron is at any energy E above the maximum energy E_F of the Fermi distribution

DEFECTS IN SOLIDS

During the last few years much work has been done on various types of defect in solids, in particular dislocations, grain and twin boundaries and vacant lattice sites.

With regard to dislocations, a sufficiently accurate approximation can be achieved for most purposes by making use of the measured elastic constants of the material. To calculate the energy of a dislocation one proceeds as follows. One assumes that if one plane of atoms is sheared relative to the next through a distance x, and the distance between the planes is a, the energy per unit area is, for small strains

$$\tfrac{1}{2}Gx^2/a$$

where G is the appropriate shear modulus; and that for large strains it can be represented by

$$\frac{b^2G}{a\pi^2}\left(1-\cos\frac{\pi x}{b}\right)$$

where b is the Burgers vector. The validity of assumptions of this kind has been investigated by MACKENZIE[104] for solids in which the atoms are held together by van der Waal's forces, but no work has been done for metals.

Calculations have been made of the contribution to the electrical resistance due to dislocations in a cold-worked metal. MACKENZIE and SONDHEIMER[105] worked this out assuming that the strains round

the dislocation made the sole contribution to the resistance; the predicted effect seemed too small, and a correction by LANDAUER[106] took account of the scattering by the electric field likely to exist in the neighbourhood of a dislocation due to a flow of charge from the compressed to the expanded region. It may be added that the resistance in a cold-worked metal may not be entirely due to dislocations, but partly to vacancies.[2, 107]

Turning now to grain boundaries, much successful work has been done on calculating their energies in terms of dislocations. This then, does not involve electron theory directly. On the calculation of twin boundary energies and of the interfacial energies between two phases, which do involve electron theory, nothing has yet been done, though experimental material is being rapidly accumulated. The problems seem of considerable difficulty. In fact the simplest problem of this type, that of the surface energy of a metal, has not been solved satisfactorily. HUANG and WYLLIE[108] and HUNTINGTON[109] have recently attempted calculations of surface energy, and using rather different assumptions have obtained quite different results.

The energy of a vacant lattice site is of importance for self-diffusion and probably also for recovery, creep[2] and even melting.[110] Calculations for ionic crystals have been carried out by MOTT and LITTLETON[111] and refined by RITTNER, HUTTNER and DU PRÈS,[112] and by SEITZ and HUNTINGTON[113, 114] for one metal, copper. Here again the calculations are difficult, and there is clearly scope for further investigation in this field. It would be particularly interesting to make calculations of the energies of vacancies at grain boundaries, and their activation energies for movement. Measurements show very different energies for self-diffusion in the bulk material and along grain boundaries, *e.g.* those of HOFFMAN and TURNBULL[115] for silver give 49,500 and 20,200 kcal respectively.

REFERENCES

[1] COTTRELL, A. H. *Progress in Metal Physics* I p 77 London, 1949
[2] MOTT, N. F. *Proc. phys. Soc. B* 64 (1951) 729
[3] BURTON, K. V., CABRERA, N. and FRANK, F. C. *Phil. Trans.* 243 (1951) 299
[4] GRIFFIN, L. J. *Phil. Mag.* 42 (1951) 775
[5] DAWSON, I. M. and VAND, V. *Proc. roy. Soc. A* 206 (1951) 531
[6] MOTT, N. F. and JONES, H. *Theory of the Properties of Metals and Alloys* Oxford, 1936
[7] SEITZ, F. *Modern Theory of Solids* New York, 1942
[8] MOTT, N. F. *Proc. phys. Soc.* 62 (1949) 416
[9] LENNARD-JONES, J. E. and POPLE, J. A. *Proc. roy. Soc. A* 202 (1950) 166
[10] —— and HALL, G. G. *ibid.* 205 (1951) 357
[11] WILSON, A. H. *ibid.* 133 (1931) 458
[12] VERWEY, E. J. W., HAAYMAN, P. W. and ROMEYN, F. C. *Chem. Weekbl.* 44 (1948) 705
[13] ZENER, C. *Phys. Rev.* 82 (1951) 403

[14] SLATER, J. C. *ibid.* 49 (1936) 537
[15] ZENER, C. *ibid.* 81 (1950) 440
[16] HEISENBERG, W. *Z. Phys.* 49 (1928) 619
[17] SLATER, J. C. *Phys. Rev.* 82 (1951) 538
[18] KRAMERS, H. A. *Physica* 1 (1934) 182
[19] VAN VLECK, J. H. *J. Phys. Radium* 12 (1951) 262
[20] TROMBE, F. *ibid.* 12 (1951) 171
[21] BLOCH, F. *Z. Phys.* 61 (1930) 206
[22] WENT, J. J. *Physica* 17 (1951) 98
[23] STONER, E. C. *Proc. roy. Soc. A* 165 (1938) 372
[24] —— *Rep. Progr. Phys.* 11 (1946) 43
[25] —— *J. Phys. Radium* 12 (1951) 372
[26] WOHLFARTH, E. P. *Phil. Mag.* 40 (1949) 703
[27] HERRING, C. and KITTEL, C. *Phys. Rev.* 81 (1951) 869
[28] BARDEEN, J. *ibid.* 56 (1936) 1098
[29] WIGNER, E. *Trans. Faraday Soc.* 34 (1947) 678
[30] KOPPE, H. *Z. Naturforsch.* 2a (1947) 429
[31] WOHLFARTH, E. P. *Phil. Mag.* 41 (1950) 534
[32] HEISENBERG, W. *Z. Naturforsch.*, 2a (1947) 185; 3a (1948) 65
[33] FRÖHLICH, H. *Phys. Rev.* 79 (1950) 845
[34] —— *Proc. phys. Soc. A* 64 (1951) 129
[35] BARDEEN, J. *Phys. Rev.* 79 (1950) 1607
[36] LANDSBERG, P. T. *Proc. phys. Soc. A* 62 (1949) 806
[37] LEE-WHITING, G. E. *Proc. roy. Soc. A* In the press
[38] BOHM, D. *Phys. Rev.* 80 (1950) 903
[39] KEESOM, W. H. and KOK, J. *Physica* 3 (1936) 1035
[40] —— —— *ibid* 1 (1934) 175
[41] SILVIDI, A. A. and DAUNT, J. G. *Phys. Rev.* 77 (1950) 125
[42] KOK, J. and KEESOM, W. H. *Physica* 4 (1937) 835
[43] KEESOM, W. H. and VAN DER LAEN, P. H. *ibid* 5 (1938) 193
[44] ELSON, R. G., GRAYSON-SMITH, H. and WILHELM, J. O. *Canad. J. Res.* 18 (1940) 82
[45] DUYKAERTS, G. *Physica* 6 (1939) 401
[46] KEESOM, W. H. and KURRELMEYER, B. *ibid* 6 (1939) 364; 633
[47] —— and CLARK, C. W. *ibid* 2 (1935) 513
[48] PICKARD, G. L. and SIMON, F. E. *Proc. phys. Soc.* 61 (1948) 1
[49] KEESOM, W. H. and DESIRANT, M. C. *Physica* 8 (1941) 273
[50] DAUNT, J. G. *Phys. Rev.* 80 (1951) 911
[51] JONES, H. *Proc. phys. Soc.* 49 (1937) 50
[52] —— and MOTT, N. F. *Proc. roy. Soc. A* 162 (1937) 49
[53] MOTT, N. F. *Proc. phys. Soc.* 47 (1935) 571
[54] WOHLFARTH, E. P. *Phil. Mag.* 42 (1951) 106
[55] KEESOM, W. H. and KURRELMEYER, B. *Physica* 7 (1940) 1003
[56] WOHLFARTH, E. P. *Proc. roy. Soc. A* 195 (1949) 434
[57] MANNING, M. F. and CHODOROW, M. I. *Phys. Rev.* 56 (1939) 787
[58] JONES, H. *Proc. roy. Soc. A* 144 (1934) 225
[59] SILVERMAN, A. A. and KOHN, W. *Phys. Rev.* 80 (1950) 912
[60] HERRING, C. *ibid* 82 (1951) 282
[61] KUHN, T. S. and VAN VLECK, J. H. *ibid* 79 (1950) 382
[62] STERNHEIMER, R. *ibid* 78 (1950) 235
[63] PAULING, L. *ibid* 54 (1938) 899
[64] —— *J. Amer. chem. Soc.* 69 (1947) 542
[65] —— *Proc. roy. Soc. A* 196 (1949) 343
[66] —— and EWING, F. J. *Rev. mod. Phys.* 20 (1948) 112

[67] HUME-ROTHERY, W., IRVING, H. M. and WILLIAMS, R. J. P. *Proc. roy. Soc. A* 208 (1951) 431
[68] JONES, H. *Phil. Mag.* 41 (1950) 663
[69] ——, MOTT, N. F. and SKINNER, H. W. B. *Phys. Rev.* 45 (1934) 370
[70] HERRING, C. and HILL, A. G. *ibid* 58 (1940) 132
[71] RAIMES, S. *Phil. Mag.* 41 (1950) 568
[72] JONES, H. *Physica* 15 (1949) 13
[73] ZENER, C. *Elasticity and Anelasticity of Metals* Chicago, 1948
[74] FUCHS, K. *Proc. roy. Soc. A* 153 (1936) 622
[75] ZENER, C. *Phys. Rev.* 71 (1947) 846
[76] BOAS, W. and MACKENZIE, J. R. *Progress in Metal Physics* 2 p 90 London, 1951
[77] FUCHS, K. *Proc. roy. Soc. A* 151 (1935) 585
[78] JONES, H. *ibid* 147 (1934) 396
[79] HUME-ROTHERY, W. and RAYNOR, G. V. *ibid* 177 (1940) 27
[80] RAYNOR, G. V. *ibid* 180 (1942) 107
[81] LEIGH, R. S. *Phil. Mag.* 42 (1951) 139
[82] OWEN, E. A. and PICKUP, L. *Proc. roy. Soc. A* 140 (1937) 174
[83] RAYNOR, G. V. *Progress in Metal Physics I* p 1 London, 1949
[84] ISENBERG, I. *Phys. Rev.* 82 (1951) 339
[85] FRIEDEL, J. *Phil. Mag.* In the press
[86] KUBASCHEWSKI, O. and EVANS, E. Ll. *Metallurgical Thermochemistry* London, 1951
[87] DAVIS, W. G. and KEEPING, E. S. *Phil. Mag.* 7 (1929) 145
[88] SPENCER, J. E. and JOHN, M. E. *Proc. roy. Soc. A* 116 (1927) 61
[89] ENDO, H. *Sci. Rep. Tôhoku Univ.* 14 (1925) 479
[90] SKINNER, H. W. B. *Rep. Progr. Phys.* 5 (1939) 257
[91] CAUCHOIS, Y. *Les Spectres des Rayons X et la Structure de la Matière* Paris, 1948
[92] MOTT, N. F. and GURNEY, R. W. *Electronic Processes in Ionic Crystals* p 76 Oxford, 1940
[93] NIEHRS, H. *Ergebn. exakt. Naturw.* 23 (1950) 359
[94] PARRATT, L. J. *Phys. Rev.* 56 (1939) 295
[95] CAUCHOIS, Y. and MOTT, N. F. *Phil. Mag.* 40 (1949) 1260
[96] BACKER, R. F. and GOUDSMIT, S. *Atomic Energy States* New York, 1932
[97] KRONIG, R. DE L. *Z. Phys.* 70 (1931) 317
[98] COSTER, D. and KIESTRA, S. *Phil. Mag.* 41 (1950) 144
[99] SKINNER, H. W. B. and JOHNSTON, J. E. *Proc. roy. Soc. A* 161 (1937) 420
[100] YOSHIDU, S. *Sci. Pap. Inst. phys. chem. Res. Tokyo* 28 (1935) 243
[101] FARINEAU, J. *Phys. Radium* 10 (1939) 327
[102] CAUCHOIS, Y. *Compt. Rend.* 231 (1950) 574, and *Acta Crystallogr.* In the press
[103] SKINNER, H. W. B. *Phil. Trans.* 239 (1940) 95
[104] MACKENZIE, J. K. Thesis, Bristol, 1950
[105] SONDHEIMER, E. H. and MACKENZIE, J. K. *Phys. Rev.* 77 (1950) 204
[106] LANDAUER, R. *ibid* 82 (1951) 520
[107] SEITZ, F. Advances in Physics supt. to *Phil. Mag.* 1 (1952) 30
[108] HUANG, K. and WYLLIE, G. *Proc. phys. Soc.* 62 (1949) 180
[109] HUNTINGTON, H. B. *Phys. Rev.* 81 (1951) 1035
[110] LENNARD-JONES, J. E. and DEVONSHIRE, A. F. *Proc. roy. Soc. A* 169 (1939) 317; 170 (1939) 464
[111] MOTT, N. F. and LITTLETON, M. J. *Trans. Faraday Soc.* 34 (1938) 484
[112] RITTNER, E. S., HUTTNER, R. A. and DU PRÈS, F. K. *J. chem. Phys.* 17 (1949) 198, 18 (1950) 379
[113] HUNTINGTON, H. B. and SEITZ, F. *Phys. Rev.* 61 (1942) 315
[114] —— *ibid* 61 (1942) 325
[115] HOFFMAN, R. E. and TURNBULL. D., *J Appl. Phys.* 22 (1951) 634

4

TWINNING

R. Clark and G. B. Craig

THIS ARTICLE is a summary of the available literature on the twinning process in metals. It deals with the crystallography of the twin relationship, the conditions under which twins form, and with the atom movements involved in twin formation.

EVANS[1] has defined a twin crystal in the following manner: 'If in a compound crystal made up of two structures of the same form there is a co-linear common plane, but the structures are not co-directional, the common plane is termed a twin plane, and the common line which is its normal, a twin axis; and the two structures together constitute a twin crystal'. In most metals the lattice of the twin is a mirror image or reflection of the parent lattice in the twinning plane. The plane of junction between the twin components is known as the composition plane. This may be the twinning plane, another crystallographic plane, or a non-crystallographic surface.[2] The position of the twinning plane relative to the lattice has been the subject of much discussion. CARPENTER and TAMURA[3] considered that the twinning plane passes between equivalent parallel planes of atoms. MCKEEHAN[4, 5] concluded that no general rule could be formulated as to whether the twinning plane passed through atom centres since for face-centred cubic metals this caused the least lattice distortion but in silicon (diamond cubic) caused greater lattice distortion.

The physical conditions for twinning were summarized by PRESTON[6] as follows:

1. 'The twinning plane can only be one such that the operation of twinning does not bring atom centres closer than the closest approach of atoms in either component of the twin.
2. 'The components of the twin must have in common at least one plane of atoms. These conditions are justified for gold, silver, copper, lead, platinum, iridium, diamond, and silicon.'

In the common twinning plane there is a network of atoms belonging to both twin components. In general, there is distortion of this region caused by small changes in interatomic distances necessary for coherency of the lattice across the twin junction. The distortion is a minimum when the plane of junction corresponds to the twinning plane. Compared to ordinary crystal boundaries, the energy of twin interfaces (twin plane = composition plane) is relatively small.

The generally accepted theory of plasticity allows for two modes of

deformation: slip and twinning. The slip process does not change the relative orientation of the slipped portions; in twinning the twinned portion assumes a new and definite orientation relative to the matrix. These processes are illustrated in *Figures 1*a and *1*b.

Metallic twin crystals may be classified in two ways.

Congenital or Growth Twins—These twins form as the crystal grows (*i*) from the melt, from the vapour[7] and by electrolytic deposition[8] (*ii*) during and after recrystallization. Examples of growth twins in zinc[9] and silver crystals[10] deposited from the melt are shown in *Figure 2*.

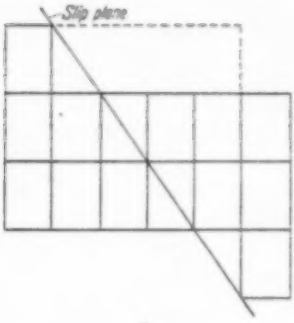

*Figure 1*a. *The slip process illustrated in a two dimensional grid*

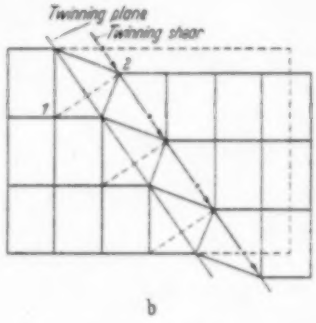

*Figure 1*b. *The twinning process in a two dimensional grid: points 1 and 2 are mirror images in the twinning plane*

The face-centred cubic metals exhibit twin bands after recrystallization. Their formation has been dealt with in the section on face-centred cubic metals. It should be pointed out that all metals can form annealing twins during recrystallization. It is purely a matter of chance, *i.e.* two crystals bearing twin relations form independently in the strained matrix and grow together. Because of the stability of the resulting twin interface, neither can absorb the other.

A theory for the formation of growth twins has been advanced by BUERGER.[11] He considers the energy of an atom as the sum of a series of energies relative to other atoms, the nearest neighbours having the larger effects. Thus, if an atom can satisfy its nearest and second nearest neighbour coordination requirements, little lattice distortion (or energy increase) will result. In general, atoms in twin interfaces satisfy or nearly satisfy their nearest neighbour requirements, and so, these are boundaries of low energy. Atoms or clusters of coordinated atoms could fall into twin positions on a growing surface and generate a twin if followed immediately by other groups. Individual atoms would probably be displaced from twin positions by local thermal

VOL.
3

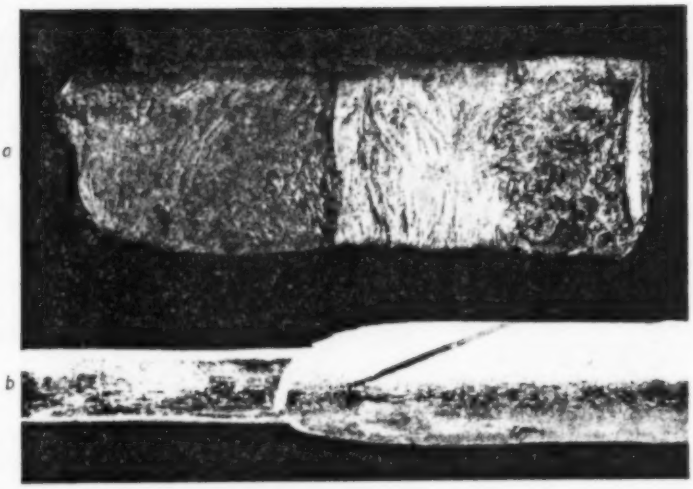

Figure 2a. Growth twin in zinc

Figure 2b. Growth twin in silver

VOL
3

fluctuations and energy conditions. Since the atoms are coming from a higher energy state (liquid or distorted solid) it makes little difference whether they assume correct or twin positions on the growing surface since both are lower, more ordered energy states. A high rate of addition of atoms to a surface would favour twin formation. GRENINGER[12] states that momentary fluctuations from the near equilibrium conditions under which crystals are growing favours twin formation.

Deformation Twins—These twins are observed in some plastically deformed metals. A study of energy conditions is helpful in understanding their formation. An atom must surmount energy barriers in order to move into a twinned position. The distribution of energy barriers is a function of the crystal structure of the metal, the type, number, and distribution of impurities and crystal imperfections, and the temperature. Since twin and parent lattices are of the same form, the potential energy of the twinned lattice is the same before and after twinning, but there is an increase in the total energy of the crystal. This energy is concentrated at the distorted boundary region, *e.g.* in face-centred cubes, third nearest neighbour coordination requirements are not satisfied.

Impact loading, that is, high rates of load application and release, favours twin formation. The process of twinning can form large twin bands in short time periods. The slip process seems to be resistant to shock loading, that is, the movement of dislocations for appreciable distances requires that the stress be applied for a considerable time period.

All possible parallel twinning planes do not operate, however large numbers of adjacent planes do, forming large twin bands. In the slip process, relatively small numbers of neighbouring slip planes are active.

Buerger attributes the irregular spacing of twin bands to lower local resistance to twinning in the vicinity of flaws or imperfections.[11] GOUGH and COX[13] consider that the process by which a metal deforms is a function of the energy to activate the change. Thus the low energy required for slip precludes the formation of deformation twins in face-centred cubic metals. In hexagonal metals slight variations in the direction of the applied stress can change the active deformation process from slip to twinning. These processes require only slightly different energies.

Often twin bands are observed within deformation twins, these are classed as second order twins. That is, the twin band is itself twinned and the resulting band bears a secondary relation to the matrix. Similarly, there are third, fourth *etc* orders of twins.

Identification of Twin Crystals—Microscopic examination of metals is often not sufficient to disclose the presence of twins, *e.g.* X-rays revealed heavily twinned magnesium crystals when visual examination failed.[14]

Further, Taylor has shown that twin-like structures observed in β-brass were due to duplex slip. The deformation bands reported by BARRETT[15] might be mistaken for twins during the early stages of deformation. However, further deformation increases the orientation differences across these bands and differentiates them from twins.

The angles between twin bands and slip lines, the angular relationships of second order twins, the traces of twins in two polished surfaces, and x-ray diffraction methods, have all been used to study twin relationships. Of these, the x-ray diffraction technique is the most conclusive. A rapid x-ray method for the determination of twinned orientations has been proposed by GRENINGER.[16] This method is applicable to any metal crystal in which deformation twins form. It is preferable that the twins be formed by impact since this leaves the matrix relatively free from distortion and thus facilitates interpretation of the x-ray (Laue) patterns. A Laue back reflection picture is taken of the original crystal. After deformation a second Laue pattern, including original and twinned portions, is taken. Comparison of the two pictures quickly identifies reflections from the matrix. The stereographic projection of the two orientations is then constructed and the twinning law revealed. This method has recently been used by CLARK, CRAIG, and CHALMERS[17] to redetermine the twinning plane in tin.

When fine grained material is plastically deformed it is often necessary to differentiate between slip lines and fine twin bands. Repeated polishing and etching will remove slip lines and accentuate twin bands. Electrolytic polishing is preferable when using this method since mechanical polishing can itself produce twins in some metals.

Table I. Twinning Planes for Face-centred Cubic Metals

Metal	*Twinning Plane*	*Reference*	*Metal*	*Twinning Plane*	*Reference*
Aluminium	{111} ..	15, 33	*Lead*	{111} ..	19
Copper	{111} ..	2, 15, 19, 102	*Iron*	{111} ..	19
Silver	{111} ..	15, 19	*Nickel*	{111} ..	19
Gold	{111} ..	15, 19	*Platinum*	{111} ..	19
Copper-Zinc	{111} ..	2, 15, 35, 40, 102	*Iridium*	{111} ..	19
Copper-Silicon	{111} ..	42			

FACE-CENTRED CUBIC TWINS

Twin crystals are noticeable features in the microstructure of most recrystallized face-centred cubic metals. The more common face-centred cubic metals in which twin crystals have been recognized are listed in *Table I.*

The formation of twinned crystals in these metals has been the subject of much research and conjecture. As early as 1912 it was known that undeformed crystals did not produce annealing twin bands.[3, 18, 19] There is little evidence that mechanical twins form in face-centred cubic metals.[3, 13, 20 to 25]

MATHEWSON and PHILLIPS[23] in 1916 suggested that annealing twins could grow from thin twinned lamellae (or faults) in the distorted

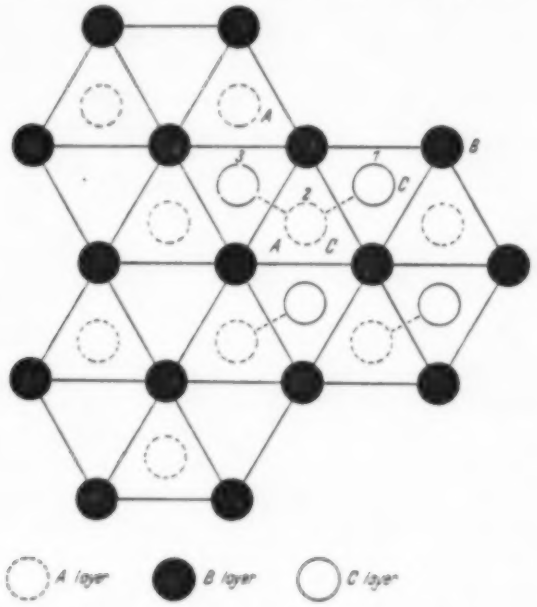

Figure 3. Slip and twinning movements on the close-packed planes of a face-centred cubic structure: movement 1 to 2 to 3 = slip; 1 to 2 = twinning

matrix. The formation of faults in face-centred cubic metals has been dealt with in detail by BARRETT.[26] A fault is a break in the sequence of stacking close-packed layers of spheres which build up a face-centred cubic lattice. The normal sequence is designated *ABCABC*. When the *B* layer of atoms is placed over the *A*, it can be fitted into either of two equivalent sets of hollows. If the *C* layer is placed on the *B* layer in such a manner as to repeat the *A* layer, the hexagonal close-packed structure results. If placed in the second set of hollows on the *B* layer, the face-centred cubic structure is formed. If the stacking order is changed to *ABCABABC* a fault or twin of minimum thickness is formed. The motion necessary to form a fault is the first half of the theoretical slip movement on the close-packed {111} planes of a face-centred lattice. This is illustrated in *Figure 3*, where the gliding of an atom in

the *C* layer from *1* to *2* to *3* represents the slip process and the movement of the *C* layer from position *1* to *2* the hypothetical twinning process. The resultant slip is in a ⟨110⟩ direction; twinning is in a ⟨121⟩ direction.

If an atom stops in a fault position there is no change in its number of nearest or even second nearest neighbours. Accordingly, moving atoms would find it difficult to distinguish between faulty and correct positions. However, each fault introduced converts four layers to the hexagonal close-packed structure and so the energy of the crystal is raised. Barrett states that shifting atoms face a lower energy barrier if they are about to stop in a faulty position than if they are in the correct hollow. Therefore, the probability of a layer stopping in a twin position is less than 50 per cent. This must be multiplied by the probability that a given layer would shift at all, when the layers to one side have shifted and somewhat relieved the stresses in this region. The probability of detectable deformation twins forming in face-centred cubic metals seems very small, and such structures could result only by accident. Possibly one such accident was found by SAMANS,[27] who obtained x-ray evidence indicating the presence of deformation twins in α-brass.

TAYLOR and ELAM,[28] and ELAM[29] had shown that the deformation of both copper and aluminium single crystals could be accounted for by slipping on {111} planes in ⟨110⟩ directions. MATHEWSON and VAN HORNE,[24] however, predicted that by directing the maximum resolved shear stress in a ⟨112⟩ direction on a {111} plane, deformation twins could be formed. From such controlled tests they concluded:

1 Apparently simple shear on {111} planes in ⟨112⟩ directions does not form visible twins in copper crystals.

2 It is probable that a complex deformation process forms twin nuclei which on subsequent annealing are either absorbed or grow into larger bands.

Cross-rolled copper samples, compared with straight-rolled samples, exhibit a lower hardness and a higher recrystallization temperature. BRICK and WILLIAMSON[30] attributed this to twin formation. The deformation texture of the cross-rolled specimens was primarily (110) [223] with considerable material twinned about central (111) poles.

Mechanical twins have never been observed in aluminium. ELAM[31] has reported banded structures that resembled twins but could not be identified as such by x-ray methods. MASON, MCSKIMIN, and SHOCKLEY[32] measured the voltages generated by a quartz crystal as an aluminium and tin test piece were pushed against it. With tin crystals the formation of twin bands was accompanied by fluctuations in the

voltage. With aluminium specimens no such fluctuations were observed. In recrystallized aluminium annealing twins of the spinel type, *i.e.* twinned on an octahedral plane, have been observed.[33, 34]

Twin Formation in Alloys—There is evidence that deformation twins do form in alloys of copper with zinc[30, 35] or tin.[19] PHILLIPS[35] found etch bands, similar to Neumann bands in α-iron, that lay parallel to traces of octahedral planes in the surface of rough ground 70–30 brass samples. Subsequent annealing produced twin bands, still parallel to {111} planes, that seemed to form directly from the deformation bands. Brick and Williamson[30] found deformation markings parallel to {111} planes in a brass crystal (70 per cent copper) that failed to work harden on being rolled from 50 to 70 per cent reduction. It was felt that the deformation markings could be mechanical twins, since twin formation could account for the failure of the sample to work harden.

The presence of zinc and tin atoms, metals which readily form mechanical twins, could conceivably alter the interatomic forces in face-centred cubic copper facilitating the formation of deformation twins. It is well known that impurities facilitate the formation of twin bands in magnesium, beryllium, cadmium, and α-iron. HIBBARD, LIU, and REITER[36] found that faults, or stacking disorders, which could account for the formation of annealing twins, form more readily in a 70–30 brass than in copper. On annealing, however, the brass exhibits fewer twinned crystals. This behaviour is analagous to that of zinc which readily forms deformation twins, that almost completely disappear on annealing.[37]

Annealing Twins—The formation of annealing twins has been ascribed to the presence and behaviour of faults.[19, 25, 26, 36, 38, 39, 40, 41] Up to the time of BARRETT's investigations[42] (1950), on copper-silicon alloys, there was no direct evidence that plastic deformation produced faults. He found that the number of faults and resultant twins increased progressively with silicon content.

Possible mechanisms of twin formation from faults are as follows:

i Nucleation by faulted areas lying in slip bands: MADDIN, MATHEWSON, and HIBBARD,[40] found that all recrystallized grains in a single crystal of brass deformed in tension, had an octahedral plane in common with the parent crystal. Barrett suggests[42] that such evidence indicates that conditions in slip bands are appropriate to nucleate twins.

ii A growing crystal encounters faults having a twin relation. This phenomenon has been observed in iron by BARRETT,[43] in copper by BURKE,[44] and in copper, gold, and iron-nickel (austenite) by HESS.[44] This type of twin formation is somewhat

restricted in that an octahedral plane of the crystal must be parallel to the growing face.

Other possible mechanisms which could account for the formation of annealing twins are as follows:

a Growth accidents: the energy of a twin interface in face-centred cubic metals is small; on a growing surface, therefore, atoms could conceivably fall into incorrect positions and generate a twin. As early as 1926 Carpenter and Tamura[3] suggested this possibility. Such twins have been reported by BROWN[8] in electrolytically deposited crystals, and by KIRCHNER and CRAMER[7] in thin layers of gold, nickel and copper, deposited in vacuum at high temperatures. According to BURKE[45] this type of twinning must be common since many annealing twins have orientations that could not be nucleated by mechanical faults.

b A growing crystal (after recrystallization is complete) encountering other crystals with twin or near twin orientations: BURGERS[46] has reported what appeared to be this type of formation in nickel-iron alloys.

Burke has studied the manner in which twin crystals grow.[45] Parallel-sided bands increase only in length. This is due to the inability of twin crystals to absorb one another. Twins defined by grain boundaries grow by simple boundary migration.

HEXAGONAL METALS

Table II. Twinning Planes for Hexagonal Metals

Metal	*c/a*	*Twinning Plane*	*References*
Beryllium ..	1·568	{10$\bar{1}$2}	19
Magnesium ..	1·623	{10$\bar{1}$2}	19, 48, 49, 50, 51
		{10$\bar{1}$1}	48
Zinc	1·856	{10$\bar{1}$2}	37
Cadmium ..	1·886	{10$\bar{1}$2}	19, 47

With the exception of zinc and magnesium very little work has been done on twinning in hexagonal metals. *Table II* gives the twinning planes as found by the investigations listed under 'references'.

In the case of cadmium and beryllium, the composition plane only has been determined, the twinning plane being deduced from the similarity of these metals to zinc. In zinc and magnesium the twinning law has been verified by x-ray and crystallographic measurements.

The {10$\bar{1}$1} twinning of magnesium has not been confirmed, in fact, no evidence of it could be found by BAKARIAN and MATHEWSON.[50]

They deformed single crystals at various temperatures from 20°C to 300°C, using both shock and static loading but succeeded only in producing $\{10\bar{1}2\}$ twins. BARRETT and HALLER[14] could find no evidence of $\{10\bar{1}1\}$ twins in polycrystalline magnesium subjected to rapid compression at low temperatures or slow compression at high temperatures.

Impurities have a marked effect on twin formation but no systematic investigation has been carried out. BENEDICKS[52] pointed out that 0·5 per cent cadmium in zinc favours twin formation but hinders slip. MATHEWSON[19, 37] states that the impurities increase the size and number of twin bands.

The temperature at which the metals are deformed or heat treated affects the form of the twin crystal. Here again few systematic investigations have been made. MATHEWSON and PHILLIPS[37] tested zinc in tension at 400°C and at a temperature of − 18°C. Fewer twins formed at 400°C than at room temperature while at − 18°C the twins were more sharply defined than at room temperature. Slip occurred very bodily on the basal planes of the twins (at 400°C), resulting in fracture before many twins had formed. An increase in individual size and total volume of twins was observed at elevated temperatures in the case of magnesium single crystals.[50] This is contrary to what is found with zinc and cadmuim.

Barrett and Haller[14] have investigated the effect of temperature on the formation of twins in polycrystalline magnesium. The magnesium used was in the form of rolled sheets and, therefore, exhibited preferred orientation, *i.e.* the basal plane tended to be parallel to the face of the sheet. At room temperature, − 77°C and 100°C, twinning was evident at 2 per cent compression and the specimen was fully twinned at 9 per cent compression. The compressive force was exerted parallel to the basal plane. In tests at 200°, 250° and 300°C, the reorientation of the material was gradual and not complete even at 50 per cent compression. It seems, therefore, that most of this deformation is caused by the slip process. This is directly opposed to the results of Bakarian and Mathewson[50] on magnesium single crystals where twin formation increased at the elevated temperature. It was found, however, that rate of strain is an important factor. At 300°C twinning was readily brought about by hammering and was complete at 13·5 per cent compression. Therefore, it is concluded that twinning is suppressed at elevated temperatures only if the deformation is at sufficiently slow rates. MILLER[53] found that zinc crystals which formed twin bands in ordinary short time tensile tests failed to do so in slow creep tests with comparable loads. In ductile zinc specimens (angle between basal plane and axis of stress $> 10°$) tested under creep conditions a second type of twinning was observed but not fully explained.

In general, it would appear that increasing the temperature decreases the amount of twinning by making it easier for the metal to deform by slip. Lowering the temperature has the opposite effect. It has been observed in zinc that prolonged annealing of deformed polycrystalline specimens produced polyhedral grains free from any signs of twin bands.[37] For large or single crystals the twin bands are absorbed at least in part and/or new crystals tend to form at the junction of the twin bands. The disappearance of the twins could be ascribed to the high energy of the twin interface which represents an unstable condition. Contrast this with the behaviour of strained face-centred cubic crystals in which deformation twins are not visible; here a high temperature anneal produces twins.

Boas and Honeycombe[54, 55] have recently subjected samples of polycrystalline zinc, cadmium, and magnesium to thermal cycles. This involved changing the temperature of the metal from 30°C to 250°C, or from 30°C to liquid air temperature. There was evidence of slight twinning as well as slip in zinc and cadmium. Evidence was presented to show that this effect was due to the anisotropy of thermal expansion in a non-cubic metal. No evidence of deformation could be found in magnesium but this was to be expected in view of the almost isotropic nature of its thermal expansion. In assessing this observation and that of Mathewson's[37] that twins disappeared on annealing it is well to remember the experience of Barrett and Haller. They found[14] that specimens which showed no visible evidence of twinning were actually heavily twinned when examined by x-rays.

Deformation—One important consequence of twinning is that the basal plane in the twinned position is more favourably situated for slip to occur. There are many references to this in the literature[37, 56, 57] and a calculation by Elam[2] demonstrates it very simply. A zinc crystal is considered and it is assumed that twins will form when the basal plane is between 8° and 16° from the axis of tension. This angle χ has an average value of 12°.

If s is the shear stress then :

$$s = \sin 12 \cos 12Z = 0{\cdot}20Z$$

where Z is the total load on the crystal. After twinning the basal plane is approximately 60° to the axis, therefore

$$s = \sin 60 \cos 60Z = 0{\cdot}43Z$$

Thus the shear stress on the new basal plane is twice that on the original one, and the new basal plane tends to glide. Since only the basal plane normally operates as a slip plane, the twinning operation plays a very important role in the plastic deformation of hexagonal crystals. The twinning operation by itself can only account for a total

extension of 7·39 per cent[2] but further slip on twinned basal planes allows a great deal more deformation. SCHMID and BOAS[58] state that subsequent glide in the twin (Zn or Cd) causes little or no shear hardening on the basal plane and may even cause a softening. This is due to the hardening of the slip planes by the original twinning action. This hardening is listed as 100 per cent for zinc and 200 per cent for cadmium.

A study of the stresses necessary to form twins is interesting since the directions of these stresses are vastly different even though the metals are all hexagonal.

HESS and DIETRICH[51] and BARRETT and HALLER[14] found that $\{10\bar{1}2\}$ twinning in magnesium was caused by tensile stresses parallel to the hexagonal axis or compressive stresses perpendicular to the hexagonal axis. This applied also to beryllium, but not to zinc and cadmium where the stresses are reversed.[26]

The amount and direction of the twinning shear governs whether or not an applied stress will cause twinning.[26, 58] Schmid and Boas give the formula for calculating this shear:

$$s = \left\{ \frac{(c/a)^2 - 3}{c/a\ \sqrt{3}} \right\}$$

where s is the amount of shear and c and a are the lengths of the axes. For beryllium and magnesium the shear is in the same direction but the shear passes through zero for a crystal having an axial ratio (c/a) of $\sqrt{3}$. The shear then increases in the opposite direction for zinc and cadmium. HESS and BARRETT[26] plan to investigate an alloy with this axial ratio. It should not form deformation twins.

GOUGH and COX[59] subjected zinc crystals to alternating torsional stresses. They observed that the most fully developed twins occurred at the positions of maximum basal slip. Only extremely small twins were found at positions where the resolved shear stress on the basal plane was a minimum. This made it appear as if twinning was a secondary result of slip. In further tests, GOUGH and COX[60] found that the six twinning planes operated as three pairs. Each pair, *e.g.* $(10\bar{1}2)$, $(\bar{1}012)$, at 86°, contains a primitive slip direction. Thus any stress condition which causes twins to form on one plane would also produce twins on the other. Twins do not form on those twinning planes which contain the operative slip direction.

Although a previous investigation[59] had indicated that the normal stresses acting on the twinning plane could influence the choice of operative twinning planes, Gough and Cox[60] decided that normal stresses were contributing, not controlling, factors. Thus the maximum resolved shear stress on the slip plane was thought to control the occurrence of twins as well as slip bands. DAVIDSON, KOLESNIKOV, and

FEDOROV[61] suggested for zinc, that as the normal force on the twinning plane increased, the resistance to twinning decreased.

The effect of continued deformation is to increase the size of twins already present and to create new twins. This is shown admirably by Barrett for zinc.[26] Since the macroscopic effect of twinning is the same as that for slip, the strain ellipsoid can be used to analyse changes in the shape of crystals due to twinning.

Figure 4 is a section through the undistorted reference sphere, the strain ellipsoid, and contains the twinning direction (n_1). K_1 is the twinning plane and n_1 the shearing direction. At any stage of deformation by slip there are two undistorted planes. This is also true for

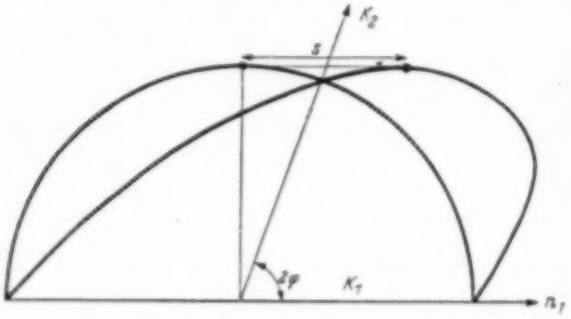

Figure 4. Undistorted reference sphere and strain ellipsoid showing twinning planes K_1 and K_2 and homogeneous shear stress s

twinning, but here the abrupt twinning movement causes the second undeformed plane, K_2 in *Figure 4*, to assume a unique position with respect to K_1. The amount by which a point at unit distance from the twinning plane (K_1) is displaced is defined as the shear strain s. The shear strain is related to the angle 2ϕ between the undistorted planes by the equation

$$\tan 2\phi = 2/s$$

The amount of shear is determined by the angle between the two undistorted planes. The two undistorted planes will divide a reference sphere into four regions. A specimen of which the longitudinal axis is contained in the obtuse angle between K_1 and the original position of K_2, will be lengthened by twinning. A specimen whose longitudinal axis is contained in the acute angle will be compressed or shortened. The increase in length is given by the formula:

$$\frac{l_1}{l_0} = \sqrt{1 + 2s \sin \chi \cos \lambda + s^2 \sin^2 \chi}$$

where l_1 = new length of crystal, l_0 = original length of crystal, s = shear strain, χ = angle between longitudinal direction and K_1

and λ = angle between projection of longitudinal direction on K_1 and n_1.

Critical Stress for Twinning—There is no conclusive evidence that there is a critical shear stress for twinning. Barrett[15] favours the idea that there is and cites the work of Davidson, Kolesnikov and Federov[61] who reported, for zinc, an increase in the resistance to twinning with decreasing temperature; Miller[53] who found the critical resolved shearing stress for twinning in zinc varied from 300 to 600 gm/mm^2, and Gough and Cox[59, 60] who observed with zinc, the greatest number of twins in areas of greatest slip. Barrett says this indicates that the necessary twinning stress decreased when the amount of preceding slip on the basal plane increased.

Schmid and Boas[58] on the other hand feel that there is not yet sufficient evidence to state that a critical twinning stress exists. In support of their view they cite: *a* the discontinuous nature of the twinning process itself; *b* the sensitivity of twinning to crystal imperfections which results in the formation of twins over a wide stress range; *c* the difficulty of studying the twinning process alone when it is nearly always preceded or accompanied by slip; and *d* that the work of Gough and Cox[59, 60] (cited also by Barrett) appears to indicate that a single initial law based on a limiting stress, such as governs glide, does not exist for mechanical twinning. More recently Yakovleva and Yakutovich[62] measured the critical shear stress for slipping and twinning of cadmium single crystals, varying in diameter from 0·09 to 0·7 mm. On reducing the diameter of the crystals to 0·1 mm it was found that the stress for twinning increased ninefold, but that of gliding only twofold. This could be taken as supporting the view of Schmid and Boas since there are probably fewer imperfections in the smaller crystals. Otherwise the change in the ratio of volume to surface area could be responsible.

General—The reversibility of the twinning process is well known.[14, 64] It occurs when the stresses which caused the twins to form are applied in the reverse direction. Dorn and Thomsen[65] and Carapella and Shaw[66] have suggested that untwinning due to residual microtensile stresses in the test piece takes place, but Hess and Dietrich could find no x-ray evidence to support this theory.[51] The discrepancies in the results were attributed, by Dorn and Thomsen, and Carapella and Shaw, to differences in test conditions.

Vogel[67] reports twin bands traversing patches of zinc-cadmium eutectic as if a single metal were present. This is ascribed to the uniform orientation of both hexagonal constituents. Mathewson and Phillips[37] made the following general observations on twin formation in zinc:

a basal cleavage, after considerable twin formation, resembled and could be mistaken for prismatic cleavage of the original crystal.

b even in ductile crystals (some crystals could be elongated 100 per cent) twin bands always formed prior to cleavage.

A study of the atom movements necessary to form twins in zinc shows that the process is not one of simple homogeneous shear.[19, 26] Barrett and Mathewson have discussed these movements in their articles and they will not be considered here.

TWINNING IN α-IRON

It was not until 1928 that Neumann bands were shown to be true {112} reflection twins.[68] Up to this time many divergent opinions had been expressed as to the nature of these bands. TSCHERMAK[69] (1874), SADEBECK[70] (1875) and LINK[71] (1892) all considered that these bands were twins but held differing views as to the laws of junction and twinning. Link's conclusion that Neumann lamellae form parallel to {112} planes was confirmed by OSMOND and CARTAUD[72] (1906) and is in agreement with the present day concepts. A diagram illustrating Link's proposed lattice movements is shown on p. 129. Some metallurgists[73, 74] doubted that twins did form in α-iron. ROSENHAIN and MCMINN,[74] felt that the bands were not twins since slip lines crossing them either continue undeflected or change direction in an apparently irregular manner. MATHEWSON and EDMUNDS[68] pointed out that slip in a ⟨111⟩ direction on any plane in the zone for which the twinning axis is the zone axis, can pass through the twin without change of direction. Slip on the other available systems could account for the irregular changes of direction that are observed.

O'NEIL[75] (1926) summarized the facts regarding Neumann lamellae as follows:

a they have often parallel sides like twins
b they deflect slip-bands as twins should do
c they etch to a different tint from their background, which suggests that they have a different orientation
d parallel ones have identical orientation
e the production of a twinned layer by simple deformation of ferrite along (112) planes appears to be easy.

Impurities, Temperature and Rate of Stressing—For a clear understanding of the conditions under which twins can form in α-iron, the effects of impurities, temperature, and rate of stressing, will be considered in turn assuming the other two as constants.

Silicon, tin, phosphorus and aluminum inhibit slip and favour twinning; that is, the relative stress requirements for slip and twinning are altered in such a manner that twin formation tends to become the

preferred process. The plane of twinning in alloyed ferrite is {112}.[68, 76, 77, 78]

In general, an increase in the deformation temperature causes a decrease in the tendency for twins to form; conversely, a decrease in the temperature of deformation favours the formation twin bands in α-ferrite. Regardless of deformation temperature, the twinning plane remains {112}.[72, 76, 79, 80]

McKeehan[81] observed that annealing iron crystals containing impact twin bands failed to cause either new crystals to grow, or the twins to grow. These observations suggest that twin boundaries in body-centred cubic iron are regions of low strain or interfacial energy.

Rapid loading (impact) favours twin formation, while slow rates of stressing facilitate slip. There is no evidence to suggest that changes

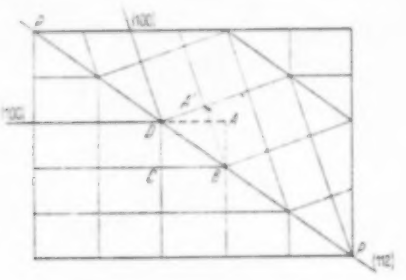

Figure 5. Lattice movements for {112} twinning (Link)

of stressing conditions cause a change of twinning plane. Barrett, Ansel, and Mehl[78] found that with slow torsional stresses, low temperatures were required to form twins in silicon ferrite. Their work suggests that the rate of stressing is the most important factor. With alloys containing 5 per cent silicon, only one slip system of the many possible ones could operate, and still lower temperatures were required to produce twin bands. On the other hand, McKeehan[81] observed large twin bands formed in ferrite deformed near the Ar_3 point.

Another factor of minor importance is grain size. Fine-grained pure ferrite does not form Neumann bands as readily as does coarse-grained ferrite.

Twinning Movement—Link proposed a simple shearing mechanism by which twin bands could be formed parallel to {112} planes in body-centred cubic iron.[71] This is illustrated in *Figure 5*, and corresponds to the movement of A to A^1. The shearing movement is parallel to the {112} plane in a ⟨111⟩ direction, P to P.

Mügge,[82] gave a more detailed description of the shearing mechanism shown in *Figure 5*, and developed formulae to express the relation

between indices of planes before and after twinning. If h_1, h_2, and h_3 represent the indices of a plane before twinning, the transformed indices (after twinning) are:

$$h_1^1 = -h_1 + h_2 + h_3$$
$$h_2^1 = h_1 - h_2 + h_3$$
$$h_3^1 = 2(h_1 + h_2)$$

The details of a simple shear mechanism which can account for the formation of twin bands on {112} planes in iron, are shown in *Figure 6*.

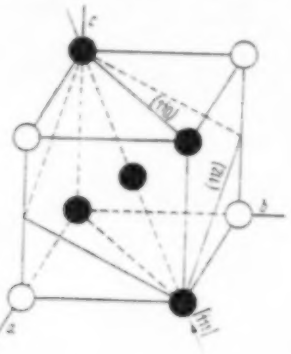

Figure 6a. Unit cube showing the (112) twinning plane, [$\bar{1}\bar{1}$1] twinning direction, and the (1$\bar{1}$0) plane of projection

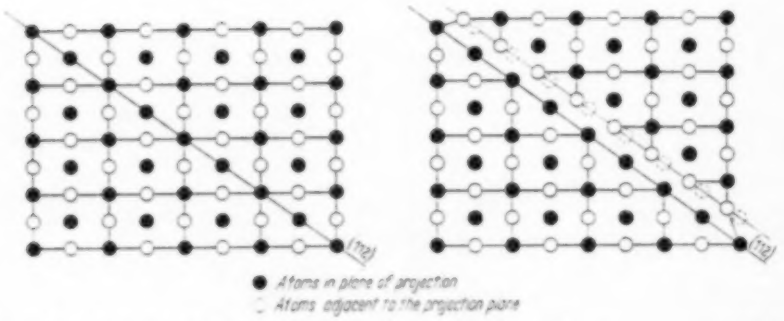

Figure 6b. Projection of body-centred cubic lattice on the (1$\bar{1}$0) plane

Figure 6c. Twinning movement applied to one layer

Figure 6a illustrates the position of the twinning plane (112), twinning direction [$\bar{1}\bar{1}$1] and the plane of projection (1$\bar{1}$0) in the unit cube. *Figure* 6b shows the projection of a body-centred lattice on the (1$\bar{1}$0) plane. The dots represent atoms in the plane of projection; the circles represent the atom layers adjacent to the plane of projection.

Figure 6c shows the shearing movement necessary to move the layer of atoms adjacent to the twinning plane into twinned positions with the corresponding shift of the block of material to the right of this layer. For simplicity the assumption is made that the twinning plane passes through atom centres.

Figure 6d shows this translatory movement applied to the second layer of atoms. The atoms in the region (*ABCD*) are now in a twin position with respect to the parent lattice.

The actual shearing distance required by this process is represented by the movement *E* to *C* (*Figure 6d*) and is equal to $\frac{\sqrt{3}}{6}a_0$. It can be seen from the drawing that a twinned position could have been reached

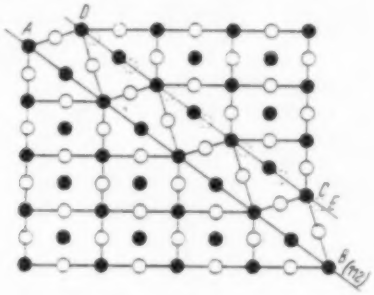

Figure 6d. Twinning movement applied to second layer. ABCD *is a twin band;* $E \rightarrow C$ *the twinning shear, equals* $\frac{\sqrt{3}}{6}a_0$

equally well by a shearing or translatory movement in the opposite direction [11$\bar{1}$]. This, however, would require that atoms move a distance equal to $\frac{\sqrt{3}}{3}a_0$, or twice as far as required by a shear in the [$\bar{1}\bar{1}$1] direction.

By plotting a plan view (*Figure 7*) of a (112) twinning plane, showing the immediately adjacent layers, it is somewhat easier to see what this directionality of the twinning movement means. Barrett has examined these atom movements with very interesting results.[26] In *Figure 7* atom *E* moves to a twin position with respect to atom *F*, by settling directly over *F* at *E'*. In arriving at this position, atom *E* is guided by the pair *AD* or *BC*. That is, atom *E* rolls in contact with either of these pairs. Atom *E* could also have moved to *E''*, directly over *G*, to form a twin. This would be a movement of atom *E* in contact with atoms *A* and *B*. This requires that atom *E* not only translate in the horizontal plane, but move upwards as well (or cause *A* and *B* to separate), thus requiring much greater local distortion than the movement *E* to *E'*.

It is quite likely that the stress required to cause the movement *E* to *E″* is greater than that to cause a movement from *E* to *E′*. The movement *H* to *E″* to *E* constitutes slip on {112} planes in body-centred cubic materials. It would appear that *H* to *E″* can occur at lower stress values than *E″* to *E* (or *E* to *E″*). Barrett suggests that a stress large enough to cause the movement of atom *E* to *E″* would also be able to continue the displacement of the atom to *H*. A stress capable of causing the twinning movement *H* to *E″*, however, would not necessarily be large enough to continue the movement from *E″* to *E*.

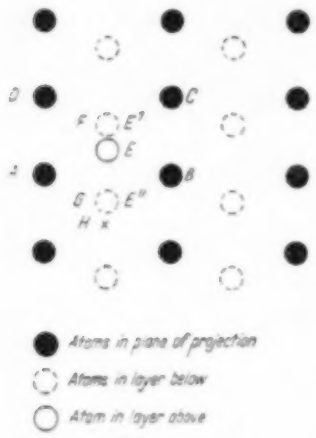

Figure 7. Plan view of a {112} plane illustrating the directionality of the twinning movement E to E′ or E to E″

If a stress is applied that can cause only the twinning movement *H* to *E″*, it is unlikely that the movement of one layer would relieve this stress, and therefore it seems probable that other layers would glide to twinned positions. Barrett believes the second layer to move would be adjacent to the first, since it would then contribute less to the total interfacial strain energy than if it is removed from the first.[26] Also as suggested in the opening paragraphs, the plane on which a twin starts is in a region of lowered resistance to twin formation.

It would appear that the above mechanism can account for the formation of visible twins in α-iron. If the twinning stress is relieved before an appreciable thickness of twin is built up, then a fault results. In body-centred cubic metals, faults form on {112} planes but not on the most densely packed {110} planes. According to Barrett, the many slip planes and slip systems in body-centred cubic metals complicate the picture of twinning.[26] The experimental evidence[78] indicates that twins form most readily under conditions of temperature and composition that restrict the operative slip systems as much as possible.

Little information is available about the formation of twins in body-centred cubic metals other than α-iron. ELAM[53] confirmed the presence of twin-like structures in body-centred cubic β-brass[54]. Barrett gives the twinning plane and direction for β-brass and wolfram as {112} ⟨111⟩.[15]

The foregoing discussion of atom movements, however, can be applied to these materials (β-brass, wolfram) as well as to any other body-centred cubic metal that forms deformation twins.

RHOMBOHEDRAL METALS

Table III. Twinning Planes for Rhombohedral Metals

Metal	*Twinning Plane*	*References*
Arsenic ..	{011}	85
Antimony ..	{011}	86, 87
Bismuth ..	{011} $(7\bar{5}1)$*	13, 88, 89*
Mercury ..	{011}	57, 90

The formation of twin bands in the metals arsenic, antimony, and bismuth, was investigated by MÜGGE.[85, 86, 88] Later investigators[13, 57, 87, 90] confirmed his work and extended the list to include mercury (*Table III*).

The formation of twin bands in antimony and bismuth crystals was found, by Gough and Cox, to be the only operative system of plastic deformation.[13, 87] ZAPFFE[91] concluded that in notch bar impact tests of bismuth specimens, plastic deformation begins with the formation of twin bands. However, slip can be produced in antimony and bismuth under suitable deformation conditions. Gough and Cox, observed that only two of the three possible {011} twinning planes operate for given stress conditions. The inoperative plane contains the direction of maximum atomic density in which the resolved shear stress is greatest.

The twinning law for antimony and bismuth was deduced by Gough and Cox from the position of secondary twin bands within primary bands.[13, 87] The lattices of the parent and twin were found to be mirror images in the observed {011} composition plane.

Twin bands appear along {011} planes, during the extension of mercury crystals, at 45° to the stress axes. When such a twin has formed, the glide plane in the twin, compared to the original glide plane, is equally or more favourably oriented for further slip. The formation of twin bands in mercury crystals facilitates the deformation process. The operative twinning planes make angles as near 90° as possible with the operative slip direction.

Very little can be deduced about the atom movements that occur when twin bands form in rhombohedral metals. The structures of these metals are complex and movement of atoms along the shortest geometrical paths into twin positions may not be along the paths of minimum energy. FOCKE[92] observed that the spacing of polonium groups in bismuth crystals was changed by twinning from $0{\cdot}55 \pm 0{\cdot}01\mu$ in the matrix to $0{\cdot}86 \pm 0{\cdot}03\mu$ in the twin. This change was reversible. It is thought that a simple homogeneous shearing movement could not change the effective distance between such groups of impurities.

The unit cells used to represent the atom configurations of the metals

antimony, bismuth, and mercury in the above investigations, do not correspond to those now listed by Barrett.[15] It is thought that this represents a change only of reference axes and, as in the case of tin, the indices of the twinning plane should be revised to agree with this new choice of axes.

β-TIN

Tin has a body-centred tetragonal lattice with $a = 5{\cdot}8194$Å and $c = 3{\cdot}1753$Å; the twinning plane is $\{301\}$[17, 94]. This has also been reported as $\{331\}$[95, 96] but the unit cell used to describe the metal was different: $a = 8{\cdot}22$Å and $c = 3{\cdot}1753$Å. These cells can be derived from the same lattice by rotation of the a and b axes by 45° about the same c axis.

β-tin readily forms deformation twins by impact and during ordinary tensile tests. CHALMERS,[94] found that twinning could occur when a compressive force, either impulsive or steady, was applied in a direction perpendicular to the 001 axis, or when tension was applied parallel to this axis. Reversion of the twinned portion to the original lattice could be brought about by impact parallel to the 001 axis, or by tension applied perpendicular to the 001 axis.

The formation of a twin band causes a change in the external shape of the crystal. The angle between the twin and matrix was measured by Chalmers and found to be 5°. This is what would be expected from lattice considerations and corresponds to a definite twinning movement occurring on each plane in the twin. Unfortunately the positions of the atoms in the unit cell used by Chalmers are incorrect and so his proposed atom movements are wrong.

ADDITIONAL EXPERIMENTAL EVIDENCE

Hardness of Twin Crystals—There is very little experimental evidence concerning the effect of twins on the hardness of metals. The previous evidence cited of the failure of brass to work harden due to twin formation and of the 100 to 200 per cent hardening of zinc and cadmium on twinning do not appear to be compatible.

CLARK and CRAIG[97] carried out a simple experiment on a single crystal of tin. A twin band was produced under impact conditions and a hardness survey carried out with a Tukon tester using a Vickers' diamond and a 25 gm load.

The results were:

a The hardness varied slightly between twin and matrix when measured on different crystallographic faces.

b On equivalent crystallographic faces ($\{100\}$), the hardness of twin and matrix was identical; however, a hardness traverse

across the twin interface indicated slightly higher hardness in the boundary region. This effect would be very difficult to detect in polycrystalline specimens because of lattice distortion and the unknown effects which grain boundaries exert on the mode of deformation.

X-ray Diffraction—Back reflection Laue patterns from tin and zinc twins formed by impact in single crystals are composed of clearly defined spots.[97] The twin patterns from aggregates of large zinc crystals deformed by static tensile loads have blurred spots, revealing signs of distortion. It has not been possible to obtain a picture of an undistorted twin in a polycrystalline matrix. The Laue patterns obtained from twin bands formed in a single crystal of tin after considerable elongation by slip, showed less distortion than patterns obtained from regions in which slip only had occurred. The deformation of the specimen was stopped immediately after the twin bands had formed. This suggests that the twinning process allows some reorganization of the distorted lattice.

DISCUSSION

Energy Associated with Twin Formation—Twinning requires a high concentration of strain energy and this is most readily available during impact loading. The energy absorbed by the lattice during the twinning movements is released as heat except for a small amount stored at locally distorted twin interfaces and that lost as sound waves. In the case of cadmium the heat liberated is of the order of 0·1 cal/gm of material twinned.[22] In β-tin the energy required is 8×10^5 erg/cc of twinned material.[94] This energy, released as heat, should correspond to a temperature rise of 0·05°C, which was observed within experimental limits.

It is possible to calculate the mean energy per atom involved in the twinning process. However, each atom does not play the same part, so little information of value can be derived. Chalmers found for tin that the mean energy per atom was not sufficient to cause local melting or bond rupture.[94]

Energy of Twin Boundaries—The relative energy of twin interfaces and other crystal boundaries has been estimated from measurements of equilibrium boundary angles,[98, 99] thermal etching characteristics,[100] rate of grain boundary migration[99] and attack by chemical etchants.[34] The low energy of twin boundaries is particularly noticeable in face-centred cubic lattices.[34, 100, 101] The energy of the twin boundary is a minimum when the composition plane coincides with the plane of twinning. A case of a composition plane becoming parallel to the {112} twinning plane on annealing silicon-iron has been reported.[99]

In cubic metals twinning on {111} or {112} planes leads to the same orientation. Barrett[15] shows calculations which illustrate that for a face-centred cube {111} twinning causes no change in the distance between neighbouring atoms, while {112} twinning would place certain neighbouring atoms at $\frac{a_0}{\sqrt{6}} = 0{\cdot}048a_0$ instead of the normal $\frac{a_0}{\sqrt{2}} = 0{\cdot}707a_0$.

The {111} twinning of body-centred cubic crystals would involve a decrease of 33 per cent in the spacing of certain neighbouring atoms whereas, {112} twinning would involve a decrease of only 5·8 per cent. The observed {111} twins in face-centred cubic and {112} twins in body-centred cubic metals thus obey the rules for twin formation outlined by Preston. Preston further concluded that the body-centred cubic twin boundary would have a higher energy than the face-centred cubic boundary.

Two problems which must be considered in the twinning process are the formation of a twin interface, and the propagation of this interface through the crystal.

In view of Barrett's work[26] which shows that twin 'faults' in face-centred cubic metals can be formed by means of half-dislocations, it seems reasonable that the formation of a twin interface can be described in terms of dislocations. No satisfactory mechanism for the propagation of the interface has so far been suggested.

The major difficulties are:

a To account for the movement of each plane relative to the next in the numbers necessary for the formation of observed twin bands.

b Even in the more complex metals (Mg, Zn, β-Sn, Bi, Sb) the overall external effect corresponds to simple shear,[15, 94] *i.e.* the movement of each layer during the twinning process is a fixed amount. This is not in agreement with the properties of dislocations postulated for the slip process.

c The twinning 'cry' is suggestive of a block movement. If dislocations are responsible for twinning as well as slip, this 'cry' should be detected when slip occurs.

d The conflicting evidence concerning a critical shear stress for twinning suggests that some process other than the movement of dislocations is responsible for twin formation.

e When a metal is plastically deformed there are two competitive processes, slip and twinning. The dislocations which are held responsible for slip move readily under the application of a steady load, whereas, the application of an impact load favours the formation of twins.

The slip process *i.e.* the movement of dislocations (or the production of the large numbers necessary) is inhibited by lowering the temperature, whereas, the twinning process is favoured.[78]

f Atomic movements necessary to form a twin in non-cubic lattices appear to be very irregular (*cf* BARRETT[26]). This makes it difficult to attribute twinned structures to the movement of dislocations.

It does not, therefore, seem reasonable to attribute deformation by slip and twinning to the movement of dislocations.

It is evident that our knowledge of the twinning process in metals is incomplete. A more detailed and systematic approach to this important mode of plastic deformation is needed.

VOL. 3

REFERENCES

[1] EVANS, J. W. *Proc. roy. Soc. Edinb.* 32 (1912) 416
[2] ELAM, C. F. *Distortion of Metal Crystals* Oxford
[3] CARPENTER, H. C. H. and TAMURA, S. *Proc. roy. Soc. A* 113 (1926) 161
[4] MCKEEHAN, L. W. *Nature, Lond.* 119 (1927) 392
[5] —— *ibid* 119 (1927) 120
[6] PRESTON, G. D. *ibid* 119 (1927) 600
[7] KIRCHNER, F. and CRAMER, H. *Ann. Phys., Lpz.* 33 (1938) 138
[8] BROWN, W. G. *Amer. J. Sci.* 32 (1886) 377
[9] CRAIG, G. B. Unpublished work
[10] THOMAS, R., STEWART, M. and WINEGARD, W. Private Communication
[11] BUERGER, M. J. *Amer. Min.* 30 (1945)
[12] GRENINGER, A. B. *Trans. Amer. Inst. min. (metall.) Engrs.* 122 (1936)
[13] GOUGH, H. J. and COX, H. L. *J. Inst. Met.* 48 (1932)
[14] BARRETT, C. S. and HALLER, C. T. *Trans. Amer. Inst. min. (metall.) Engrs.* 171 (1947) 246
[15] —— *Structure of Metals* New York, 1943
[16] GRENINGER, A. B. *Trans. Amer. Inst. min. (metall.) Engrs.* 117 (1935)
[17] CLARK, R., CRAIG, G. B. and CHALMERS, B. *Acta Crystallographica*, 1950
[18] ROSENHAIN, W. and EWEN, D. E. *J. Inst. Met.* (1912)
[19] MATHEWSON, C. H. *Amer. Inst. min. Engrs., Proc. Inst. Met. Div.* (1928) 7
[20] BARDWELL, E. S. *Bull. Amer. Inst. min. Engrs.* 1914, 2075
[21] ANDRADE, E. N. DA C. Discussion to 13
[22] CHALMERS, B. *Nature, Lond.* 129 (1932) 650
[23] MATHEWSON, C. H. and PHILLIPS, A. *Trans. Amer. Inst. min. (metall.) Engrs.* 54 (1916) 608
[24] —— and VAN HORNE, *Amer. Inst. min. (metall.) Engrs., Proc. Inst. Met. Div.* 1930, 59
[25] BURKE, J. E. and BARRETT, C. S. *Trans. Amer. Inst. min. (metall.) Engrs.* 175 (1948)
[26] BARRETT, C. S. *Symposium on Cold Working of Metals, Amer. Soc. Met.* 1948
[27] SAMANS, C. H. *J. Inst. Met.* 55 (1934) 209
[28] TAYLOR, G. I. and ELAM, C. F. *Proc. roy Soc. A* 108 (1925) 28
[29] ELAM, C. F. *ibid* 112 (1926) 289
[30] BRICK, R. M. and WILLIAMSON, M. A. *Trans. Amer. Inst. min. (metall.) Engrs.* 143 (1941) 84

[31] ELAM, C. F. *Nature, Lond.* 120 (1927) 259
[32] MASON, W. P., MCSKIMIN, H. J. and SHOCKLEY, W. *Phys. Rev.* 73 (1948) 1213
[33] ELAM, C. F. *Proc. roy Soc. A* 121 (1928) 237
[34] LACOMBE, P. *Report of Conference on Strength of Solids* 1947 Phys. Soc. (1948)
[35] PHILLIPS, A. J. Reported by Mathewson[19]
[36] HIBBARD, W. R., LIU, Y. C. and REITER, S. F. *J. Met.* 185 (1949) 635
[37] MATHEWSON, C. H. and PHILLIPS, A. J. *Trans. Amer. Inst. min. (metall.) Engrs* (1927) 143
[38] —— *Trans. Amer. Soc. Met.* 32 (1944) 38
[39] —— Discussion to 25
[40] MADDIN, R., MATHEWSON, C. H. and HIBBARD, W. R. *Trans. Amer. Inst. min. (metall.) Engrs* 185 (1949) 527
[41] KRONBERG, M. L. and WILSON, F. H. *ibid* 185 (1949) 501
[42] BARRETT, C. S. *J. Met.* 188 (1950)
[43] —— *Trans. Amer. Inst. min. (metall.) Engrs* 137 (1940) 190 (Discussion)
[44] BURKE, J. E. and HESS, J. B. Recorded by Barrett[42]
[45] —— *J. Met.* 188 (1950)
[46] BURGERS, W. G. and AMSTEL, J. J. A. PLOOS VAN *Metallwirtschaft* 17 (1938) 648
[47] ROMIG, O. E. *Trans. Amer. Inst. min (metall.) Engrs* (1927)
[48] SCHIEBOLD, E. and SIEBEL, G. *Z. Phys.* 69 (1931) 458
[49] SCHMID, E. and SIEBEL, G. *Metallwirtschaft* 13 (1934) 353
[50] BAKARIAN, P. W. and MATHEWSON, C. H. *Trans. Amer. Inst. min. (metall.) Engrs.* 152 (1943)
[51] HESS, J. B. and DIETRICH, R. L. *ibid* 175 (1948) 564
[52] BENEDICKS, C. Discussion to 37
[53] MILLER, R. F. *Trans. Amer. Inst. min. (metall.) Engrs* 122 (1936)
[54] BOAS, W. and HONEYCOMBE, R. W. K. *Proc. roy. Soc. A* 186 (1946)
[55] —— —— *ibid* 188 (1946–47)
[56] SCHMID, E. and WASSERMANN, G. *Z. Phys.* 48 (1928) 370–83
[57] ANDRADE, E. N. DA C. and HUTCHINGS, P. *Proc. roy. Soc. A* 148 (1937) 120
[58] SCHMID, E. and BOAS, W. *Plasticity of Crystals* London, 1950
[59] GOUGH, H. J. and COX, H. L. *Proc. roy. Soc. A* 123 (1929)
[60] —— —— *ibid* 127 (1930)
[61] DAVIDSON, N. N., KOLESNIKOV, A. F. and FEDOROV, K. V. *J. exp. theor. Phys.* U.S.S.R. 3 (1933) 350–60
[62] TAYLOR, G. I. and ELAM, C. F. *Proc. roy. Soc. A* 102 (1922–23)
[63] YAKOVLEVA, E. S. and YAKUTOVICH, M. V. *J. exp. theor. Phys.* U.S.S.R. 10 (1950) 1146–50
[64] CZOCHRALSKI, J. Untwinning of Zinc Twins, *Moderne Metallkunde*, 1924
[65] DORN, J. E. and THOMSEN, E. *Light Metal Age I* July (1943)
[66] CARAPELLA, L. A. and SHAW, W. E. *Trans. Amer. Soc. Met.* 38 (1947)
[67] VOGEL, R. *anorg. Chem.* 154 (1926) 399
[68] MATHEWSON, C. H. and EDMUNDS, G. H. *Trans. Amer. Inst. min. (metall.) Engrs. (Iron and Steel)* (1928)
[69] TSCHERMAK, S. B. *Akad. Wiss. Wien. Nat. Classe* 70 (1874) 443
[70] SADEBECK, M. *Ann. Phys., Lpz.* 156 (1875) 554
[71] LINK, Z. *Krystallogr.* 20 (1892) 209
[72] OSMOND, F. and CARTAUD, G. *J. Iron Steel Inst.* 3 (1906)
[73] EWING, J. A. *J. Inst. Met.* (1912)
[74] ROSENHAIN, W. and MCMINN, J. *Proc. roy. Soc. A* 108 (1925) 231
[75] O'NEIL, H. *J. Iron Steel Inst.* 113 (1926) 417
[76] HOWE, H. M. *Metallography of Steel and Cast Iron*, 1916

[77] Robin *Rev. Métall. a* 8 (1911) 436
[78] Barrett, C. S., Ansel, G. and Mehl, R. F. *Trans. Amer. Soc. Met.* 25 (1937) 702
[79] Hadfield, R. A. *J. Iron Steel Inst.* (1905) 248
[80] Pfeil, L. B. *Carnegie Schol. Mem.* 15 (1926) 319
[81] McKeehan, L. W. *Trans. Amer. Inst. min. (metall.) Engrs.* (1928)
[82] Mügge, O. *Jb. Mineral.* 2 (1899) 55
[83] Elam, C. F. *Nature, Lond.* 133 (1934) 723
[84] Johnson, F. *J. Inst. Met.* 5 (1920)
[85] Mügge, O. *Tech. Min. Petr. Mitt.* 19 (1900) 102
[86] —— *Neues. Jb. Mineral Geol.* (1884) 40
[87] Gough, H. J. and Cox, H. L. *Proc. roy. Soc. A* 127 (1930) 431
[88] Mügge, O. *Neues. Jb. Mineral. Geol.* (1886) 183
[89] Berg, W. F. *Nature, Lond.* 134 (1934) 143
[90] Fisher, A. *ibid* 156 (1943) 567
[91] Zapffe, C. A. *Metals Progress* 50 (20) (1946) 283
[92] Focke, A. B. *Thesis* Brown University
[93] Sproull, W. T. *X-Rays in Practice* New York
[94] Chalmers, B. *Proc. phys. Soc.* 47 (1935) 733
[95] Mügge, O. *Zbl. Min.* (1917) 233; *Z. Kristallogr.* 65 (1927) 603
[96] Tanaka, K. and Kamio, K. *Mem. Coll. Sci. Kyoto A* 14 (1931) 79
[97] Clark, R. and Craig, G. B. Unpublished work
[98] Aust, K. T. and Chalmers, B. *Proc. roy. Soc. A* 201 (1950)
[99] Dunn, G. D., Daniels, F. W. and Bolton, M. J. *J. Metals* 188, No. 2 (February, 1950)
[100] Chalmers, B., King, R. and Shuttleworth, R. *Proc. roy. Soc. A* 193 (1936)
[101] Smith, C. S. *Trans. Amer. Inst. min. (metall.) Engrs* 175 (1948) 15
[102] Phillips, A. J. *ibid* (1928) 429

5

FERROMAGNETISM

Ursula M. Martius

EVERY INTERPRETATION of ferromagnetic phenomena has to deal with two different sets of problems. It must first explain why certain crystals exhibit ferromagnetic behaviour at all and relate this to the structure of the particular substance. Secondly, the dependence of ferromagnetic phenomena on external factors must be explained and predicted.

Modern development in this field dates from the beginning of this century. At this time basic experimental information about the various ferromagnetic phenomena had been established. The existence of a ferromagnetic Curie temperature was known and it had also been noted that below the Curie point small external fields would produce magnetic saturation and that the magnetization of the specimen was sometimes several orders of magnitude larger than the magnetic energy of the field which caused the saturation.

In order to account for these observations WEISS[1] proposed two new concepts. In the first he postulated a strong and temperature dependent "molecular field" in the ferromagnetic substance and, following Langevin's interpretation of paramagnetism, he attributed the observed magnetization to the resultant magnetic moments of the individual atoms. The molecular field would keep these moments oriented, thus counteracting the thermal agitation. But since a ferromagnetic crystal can have zero magnetization in the absence of an external field there could be no complete orientation throughout the whole specimen. In order to overcome this difficulty Weiss, in his second concept, postulated the existence of discrete regions which he called 'ferromagnetic domains'. Within these domains the alignment of the magnetic moments was supposed to be uniform. But in the absence of an external field the domains were oriented at random, so that the specimen would establish no overall magnetization. The external field would then only orient the domain. These two concepts—the molecular field and the ferromagnetic domains—proved extremely fruitful and guided all future development in this field.

The condition under which ferromagnetism would occur was subsequently connected with the presence of the "molecular field." But it was only in 1928 that HEISENBERG[2] succeeded in showing the physical reality of the Weiss molecular field. He proved that the forces between the electron spins of a ferromagnetic substance provided molecular

fields of the required magnitude. These electrostatic forces, which quantum mechanics calls exchange forces, have their most prominent manifestation in the chemical bond, where the spins of the participating atoms are antiparallel in their relative orientations.

In a ferromagnetic crystal the alignment of the spins is parallel; this corresponds to the state of minimum energy. As a result of Heisenberg's explanation of the molecular field, a ferromagnetic substance is pictured as having the electron spins aligned parallel to each other over discrete regions, the regions being oriented at random. Immediately Heisenberg had developed his ideas BLOCH[3] determined the character of the transition layer, since then called the Bloch wall, that separates domains of different orientations. Further studies of the electronic structure of solids on the basis of the band model as well as the atomic model led to a qualitative understanding of the requirements for the occurrence of ferromagnetism.

In subsequent work, largely due to Becker and his co-workers, it was shown that the actual magnetization process could only take place in two different ways: by movement of a Bloch wall under the action of the external field, which corresponds to a change of volume of one domain at the expense of its neighbours, or alternatively by a rotation of a whole domain *i.e.* by changing the direction of magnetization of the domain with respect to the external field. By means of this concept it became possible to interpret the general picture of the magnetization curves.

In the ideal case the domains should change their volume or their direction under the influence of infinitesimal small external fields. The observed magnetization curves, however, showed that there is a certain 'resistance against the domain movement' which is strongly affected by structure. The wide variety of technical magnetization curves is a result of this marked structure sensitiveness of the ferromagnetic properties. In this development the domain concept furnished a very useful hypothesis for a fairly consistent explanation of the experimental results. The question of the origin of the domains still remained unanswered.

In 1935 LANDAU and LIFSCHITZ[4] pointed out for the first time that there is a thermodynamical reason for the existence of ferromagnetic domains, and that a domain configuration can be derived which constitutes a configuration of minimum energy. In 1944 NÉEL[5] stressed again the consequences of this paper and gave more detailed predictions; in the same year the domain structure of iron was calculated by LIFSCHITZ.[6]

It was also possible, however, to show the physical reality of the domains experimentally by the ferromagnetic powder technique. Williams and his co-workers found domain patterns that were in

complete accordance with the theory. They also succeeded in demonstrating by observations at a single boundary, that the magnetization process in lower fields is really achieved by wall movement and that the velocity of the wall is directly proportional to the rate of change of the magnetization. These recent developments are of extreme importance. Theoretically they mean a considerable clarification of the basic laws governing ferromagnetic phenomena and experimentally it is possible for the first time to check these laws under really unambiguous conditions.

It is the main purpose of this review to point out the general principles which led to these developments and the consequences arising from them.

One of the main difficulties arising in the study of ferromagnetic phenomena is the fact that the experimentally observed properties have their origin in various different sources. The "molecular field" is caused by quantum mechanical exchange forces between the electron spins and thus related to the electronic structure of the ferromagnetic substance. The magnitude of the magnetization so established depends on the number of spins participating. But the molecular field has strong directional properties. Its maxima and minima lie in certain prominent crystallographic directions. This makes spontaneous magnetization a powerful function of the interatomic distances in the lattice. This fundamental relationship between crystal structure and spontaneous magnetization also indicates that any deviation from the ideal crystal structure will strongly influence the ferromagnetic properties. Furthermore, the number and the size of the ferromagnetic domains in a given substance are largely determined by the shape and size of the specimen, so that even in the case of an ideal single crystal the complexity of the phenomenon is evident.

OCCURRENCE OF FERROMAGNETISM IN THE PERIODIC TABLE

A fair amount of theoretical work has been devoted to the problem of predicting the occurrence of ferromagnetism among the various elements of the periodic table, their chemical compounds and their alloys. Quantitative treatment of this problem is difficult even under extreme simplification of the model.[7] Thus we shall only indicate here the general trend of thought governing these investigations.

In a ferromagnetic substance the magnetized state is the state of lowest energy. That is why at low temperatures these substances are spontaneously magnetized over discrete regions. Spontaneous magnetization is brought about by parallel alignment of the electron spins. In order to predict the occurrence of ferromagnetism we must know what conditions produce such alignment. It can be shown theoretically[7, 8] that the spins responsible for spontaneous magnetization are

not the spins of the valence electrons but that ferromagnetic phenomena originate in the unfilled inner electron shells. Thus a ferromagnetic substance has to have incomplete inner shells. This condition is necessary but is not alone sufficient; in addition the exchange integral, being the expression proportional to the amount of spontaneous magnetization, must be positive, so that ferromagnetism can be exhibited. SLATER,[9] BETHE and SOMMERFELD[10] pointed out that this is most likely to occur when a substance with an incomplete inner electron shell of large radius forms a crystal lattice with small interatomic spacing. In *Figure 1* the ratio, v, of the lattice parameter to the radius of

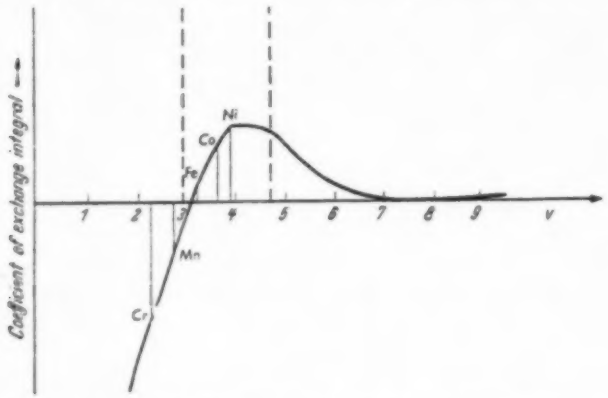

Figure 1. Estimate of the dependance of the exchange integral on v

incomplete shell is plotted as a function of the observed saturation magnetization for the elements of the transition group.

Although arguments in this vein only cover the complex situation approximately, they yield at least a qualitative understanding for some striking experimental facts. As early as 1898 Heusler had discovered ferromagnetic alloys which contained only nonferromagnetic constituents, for instance $AlMnCu_2$. Later a wide variety of metallic and non-metallic compounds and alloys with similar properties were found. The curve in *Figure 1* shows why these phenomena are possible. The exchange integrals of manganese, chromium and copper are only slightly negative. So it seems highly probable that for a manganese compound with a lattice constant smaller than that of pure manganese, the exchange integral could be positive since the diameter of the inner electron shell does not change appreciably when the compound is formed.

SATURATION MAGNETIZATION

The quantum mechanical treatment of atomic interaction showed that the magnetic moment of ferromagnetic substances arises from electron

spin motion.[7] The contribution of the orbital motion is far less prominent. KITTEL[11] concluded from results of microwave resonance experiments that approximately 90 per cent of the magnetic moment is due to the spin motion and 10 per cent to orbital motion. The observed saturation magnetization will thus depend on the number of electron spins per atom participating in the magnetization. If this number is calculated from the observed values of the saturation magnetization (extrapolated to 0°K), it usually proves to be non-integer which means that not every atom of the solid contributes the same number of electron spins to the total magnetization.

All calculations of electronic properties of solids are based on certain assumptions concerning the state of binding of the electrons. It is possible either to assume that all electrons are collectively shared by the atoms (band model) or to regard the electrons as more or less firmly associated with the individual atoms (atomic model). Which model is more suitable as a basis for the calculations will depend on the problem under investigation. On the basis of the band model it is easy to explain the non-integer value of the spin participating in ferromagnetic phenomena, while calculations of the exchange integral are often carried out by using the atomic model. (For calculations of the exchange integral with the band model see STONER.[12]) The general theoretical position of these problems has recently been reviewed by VAN VLECK.[8]

Table I gives the values for the saturation magnetization of iron, cobalt and nickel at room temperature. For data on ferromagnetic alloys STONER[12] and BECKER and DÖRING[13] should be consulted.

Table I. Values of the Saturation Magnetization at Room Temperature

Material	*Saturation Magnetization gauss*
Fe	1,707
Fe–Si (3·8% Si)	1,580
Ni	485
Fe–Ni (80% Ni)	908
(65% Ni)	1,129
Co	1,400
Co–Fe (56·3% Fe)	1,937

ENERGY RELATIONSHIP IN FERROMAGNETIC CRYSTALS

Although the problem of the occurrence of ferromagnetism can only be approached quantitatively in very simple cases and is only understood

in its general lines, our knowledge of the behaviour of ferromagnetic substances is much more satisfactory. Recent advances of the theory of ferromagnetic domains have led to a general and quantitative knowledge of the forces and laws determining the ferromagnetic behaviour. It is now possible to study and to predict the changes of these factors with changing experimental conditions. The whole theory of ferromagnetic domains has recently been reviewed comprehensively by KITTEL.[14] The subsequent section follows this survey.

We shall show why a ferromagnetic crystal establishes a domain structure and how this structure depends on the macroscopic and microscopic properties of the substance. We are interested in those contributions to the total free energy of the crystal which are related to the ferromagnetic properties. In the absence of external forces these contributions have three major sources:

A the exchange energy, which is the main contribution, furnishes the "molecular field" and has its origin in the exchange forces between the electron spins.

B the anisotropy energy, representing the dependence of the total free energy on the directional properties of the crystal.

C the magnetostatic energy, which is the contribution to the total free energy of the ferromagnetic substance arising from its resultant magnetic moment.

A *Exchange Energy*

The quantum mechanical treatment of the electronic interaction in solids leads to a mathematical expression for the forces between electron spins.[7] This expression is called the exchange integral and is usually denoted by J. The form of this integral depends on the model used for its calculation. In the atomic model J is by definition positive for parallel spin orientation, so that $J > 0$ is the necessary condition for the occurrence of ferromagnetism in the model. In the band model the corresponding integral is always positive. Here the condition for the occurrence of ferromagnetism must be related to the change in energy connected with any change in relative orientation of neighbouring spins. In this model the spontaneously magnetized state will be the stable modification if any change in electron configuration, resulting in a parallel alignment of the spins, leads to an energy gain.

The expression for J given here (notation following Kittel[14]) is derived from the atomic model. Let J_{ij} be the exchange integral referring to the atoms i and j, S the total spin quantum number of the atom and φ_{ij} the angle between the direction of the spins. The exchange energy density is then:

$$w_{ex} = -\sum_{i>j} 2J_{ij}S^2 \cos \varphi_{ij} \qquad \ldots \quad (1)$$

Assuming furthermore that the angle between neighbouring spins is small, the exchange energy per pair of spins (taking only nearest neighbour interaction into account) becomes:

$$\Delta w_{ex} \simeq JS^2\gamma^2$$

Since the atomic model regards every electron as being located at a specific atom, the exchange energy can also be expressed with respect to the crystal lattice. The direction cosines of the spin vectors with respect to the lattice are denoted by α_{ij}. It can then be shown[14] that:

$$w_{ex} = A[(\nabla\alpha_1)^2 + (\nabla\alpha_2)^2 + (\nabla\alpha_3)^2] \quad . \ . \ . \ . \ (2)$$

where $A = 2JS^2/a$ and a is the lattice parameter of a simple body-

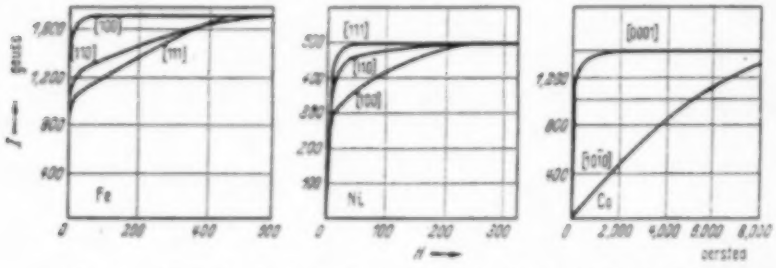

Figure 2. Magnetization curves for single crystals of iron, nickel and cobalt

centred cubic (b.c.c.) lattice. Here again only the nearest neighbours were taken into account.

The evaluation of J and its connection with experimentally available data is rather difficult; but recently some progress has been made.[15] The present results give $A = 2{\cdot}0 \times 10^{-6}$ ergs/cm for iron (b.c.c.; spin = 1).

B *Anisotropy Energy*

Figure 2 shows the magnetization curves for single crystals of iron, cobalt and nickel when the magnetic field is applied along different crystallographic directions. Whilst very small fields can produce saturation in certain directions, much larger fields are required to produce saturation in other directions. For iron [100] is a direction of 'easy' magnetization and [111] is a 'hard' direction. For nickel [111] is a direction of easy magnetization and [100] is hard. Whereas cobalt can be easily saturated along [0001].

The anisotropy energy of a crystal is defined as the additional energy necessary to produce saturation along a hard direction. This energy is about 10^3 times smaller than the exchange energy and varies considerably with substance, crystal structure and temperature. The formal representation of the anisotropy energy takes advantage of the

crystal symmetry. (For a more detailed discussion of this and related subjects see BECKER and DÖRING.[13])

Let the direction of the spontaneous magnetization with respect to the lattice be determined by the cosines α_i; then the anisotropy energy can be expressed as a power series in α_i, which must be invariant to any crystallographically identical transformation. This implies additional restrictions on the α_i. For cubic symmetry, for instance, odd powers of α_i are not consistent with the symmetry requirement, so that in this case

$$F_a = K_1(\alpha_1^2\alpha_2^2 + \alpha_2^2\alpha_3^2 + \alpha_3^2\alpha_1^2) + K_2\alpha_1^2\alpha_2^2\alpha_3^2 \quad . \; . \; . \quad (3)$$

where terms of α up to the sixth order are taken into account. The constants K_1 and K_2 can be determined from the experimental measurements of the anisotropy energy. The accuracy of these experiments does not justify the consideration of terms of still higher order.

Similar calculations lead to an expression for the anisotropy energy for hexagonal (hex.) crystals:

$$F_a = K_1^* \sin^2\theta + K_2^* \sin^4\theta \quad . \; . \; . \; . \quad (4)$$

where θ is the angle between the direction of magnetization and the hexagonal axis.

Table II gives some experimental values of the anisotropy constants. A detailed survey of recent results and experimental techniques has

Table II. Anisotropy Constants and Magnetostriction Constants at Room Temperature

Material	*Structure*	*Anisotropy Constants* $\times 10^5$ erg/cm^3 K_1	K_2	*Magnetostriction Constants* $\times 10^{-6}$ erg/cm^3 λ_{100}	λ_{111}
Fe	*b.c.c.*	4·2	1·5	19·5	− 18·8
Si–Fe (3·8% Si)	*b.c.c.*	2·8		—	—
Ni	*f.c.c.*	− 0·34	0·32	− 46	− 25
Fe–Ni (~ 35% Ni) ..	*f.c.c.*	0·32		− 8	25
(~ 70% Ni) ..		0		10	10
(~ 90% Ni) ..		− 0·10		− 18	− 8
Co–Ni (60% Ni)	*f.c.c.*	2		—	—
Fe–Co (~ 70% Co) ..	*b.c.c.*	− 4·2		—	—
(~ 45% Co) ..		0		—	—
(~ 10% Co) ..		3·2		—	—
Co	*hex.*	41	10	− 10	

been made by BOZORTH[16] and STONER.[12] The anisotropy constants are markedly temperature dependent. This phenomenon is one of the most difficult unsolved problems in the theory of magnetism. The

present state of our theoretical knowledge does not really allow an explanation of the origin of the anisotropy energy; the exchange energy which provides the major contribution to the total free energy of a ferromagnetic crystal depends only on the direction between the spins and is invariant to any change of lattice symmetry. Even the purely magnetic interaction of the electrons does not lead to an appreciable contribution.[10]

The present theory of the anisotropy energy[17, 18] explains the origin of this phenomenon as higher order effects of the spin–orbit interaction, as well as the change in resultant orbital angular momentum due to the influence of the molecular field of the crystal. It is not possible even along these lines to explain the amount and the sign of the temperature dependence of the anisotropy energy.

Due to the relation of the anisotropy energy to the crystallographic symmetry, it can be expected that crystals with high lattice symmetry will establish low anisotropy energy, while a low crystal symmetry should be associated with high anisotropy energy. Experimental results confirm this general trend.

In spite of the difficulty of explaining the origin of the anisotropy energy, the importance of this contribution to the total free energy has always been fully realized. The anisotropy energy expressed in equations 3 and 4 refers to an unstrained lattice of a given crystal symmetry. In this case it describes completely the dependence of the free energy on the crystal directions. But as soon as the crystal is subject to mechanical strains there will be an additional contribution to the total energy, arising from the interaction between the magnetization and the mechanical strain. This is the magneto-elastic energy which is by definition zero for an unstrained lattice.

The anisotropy energy is *not* independent of the state of strain of the crystal. Kittel stressed the significance of this relationship by pointing out[14] that this and only this is the reason for the occurrence of the phenomenon of "magnetostriction."

It has long been established experimentally[19] that a ferromagnetic substance changes its dimensions during the magnetization process. When a specimen of iron is magnetized, its length increases in the direction of the field while its dimensions perpendicular to the direction of the field decrease. The total volume is nearly conserved. [It is not possible to deal here with the complicated details of the process. They are treated extensively by BECKER and DÖRING.[13]] In nickel there is a decrease in length in the direction of the field and an increase in the dimensions perpendicular to the field. Since we know that the magnetization process is merely a reorientation of the domains, the occurrence of magnetostriction means that the lattice of the ferromagnetic crystal is deformed with respect to its ideal symmetry. This

VOL. 3

deformation occurs spontaneously during the formation of the crystal, when it is cooled down to its Curie point, because the deformed lattice has a lower anisotropy energy than the ideal lattice. The direction of the lattice distortion depends on the direction of spontaneous magnetization. Consequently, the change in dimensions can be observed in the course of the magnetization process. The constants of longitudinal saturation magnetization, usually denoted by λ_{100} or λ_{111}, are defined as the relative change in length of a specimen during magnetization from the demagnetized state up to saturation. The suffix denotes the direction of the field, the change in length being measured in this direction. For cubic crystals:

$$\frac{dl}{l} = \frac{3}{2}\lambda_{100}(\alpha_1^2\beta_1^2 + \alpha_2^2\beta_2^2 + \alpha_3^2\beta_3^2 - \tfrac{1}{3}) + 3\lambda_{111}(\alpha_1\alpha_2\beta_1\beta_2 + \alpha_1\alpha_3\beta_1\beta_3 + \alpha_2\alpha_3\beta_2\beta_3) \quad . \ . \ . \ . \ (5)$$

the α_1 are the direction cosines determining the direction of magnetization, the β_1 are the direction cosines determining the direction in which dl is measured. In the detailed treatment of these problems one has to keep in mind the fact that the ideal unstrained lattice cannot be realized experimentally and that any direct determination of magnetostrictive properties always yields relative values usually referred to the demagnetized state.[13] The spontaneous deformation also influences the experimentally determined values of the anisotropy energy. Measurements are usually carried out under constant stress and not under constant strain, which would correspond to constant lattice dimensions. Since the lattice can deform spontaneously, this furnishes an apparent contribution to the anisotropy energy, as BECKER[13] and KITTEL[14] have pointed out.

The contribution to the total energy arising from the interaction of the magnetization and the mechanical forces is of extreme importance when the crystal is subject to external or internal stresses. If T is a uniform tensile stress applied in the direction γ_1; γ_2; γ_3 and α_i, the direction cosines of the direction of magnetization, then:

$$F_T = -\frac{3}{2}T[\lambda_{100}(\alpha_1^2\gamma_1^2 + \alpha_2^2\gamma_2^2 + \alpha_3^2\gamma_3^2) + \lambda_{111}(2\alpha_1\alpha_2\gamma_1\gamma_2 + 2\alpha_2\alpha_3\gamma_2\gamma_3 + 2\alpha_3\alpha_1\gamma_3\gamma_1)] \quad . \ . \ . \ . \ (6)$$

In many cases it is permissible to assume isotropic magnetization: $\lambda = \lambda_{100} = \lambda_{111}$ so that:

$$F_T = -\frac{3}{2}T\cos^2\theta \quad . \ . \ . \ . \ (7)$$

where θ denotes the angle between the direction of tension and the magnetization, and $\cos\theta = \alpha_1\gamma_1 + \alpha_2\gamma_2 + \alpha_3\gamma_3$. The extent to which

this contribution enters into the whole picture of the energy relationship depends on the numerical values of λ and the ratio of λ to the constant K of the anisotropy energy. The larger the ratio is, the stronger will be the influence of the internal or external stresses on the ferromagnetic properties. Some of these values are compiled in *Table II*.

C *Magnetostatic Energy*

The next contribution to the total free energy is the magnetostatic energy. Since a ferromagnetic crystal is spontaneously magnetized over certain regions it has, even in the absence of an external field, a magnetic self energy in its own field. Furthermore we must consider the interaction energy with any external magnetic field. The self energy density F_S of a permanent magnet in its own field H_i is:

$$F_S = -\tfrac{1}{2}\vec{I}\,\vec{H}_i \qquad \ldots\ (8)$$

The interaction energy F_{int} per unit volume of the permanent magnet with an external field H_e is:

$$F_{\text{int}} = -\vec{I}\,\vec{H}_e \qquad \ldots\ (9)$$

For a ferromagnetic specimen of given shape, the internal field H_i can often be calculated. For an elipsoid magnetized along the principal axis the internal field H_i is given by:

$$H_i = -NI_S$$

where N is the demagnetization factor and I_S the saturation magnetization. Demagnetization factors for various specimen are tabulated by OSBORN.[20]

The magnetostatic energy can contribute, even in the absence of an external field, considerably to the total free energy, depending on the magnitude of the demagnetization factor. When an external field is present, the magnetic field energy will arise from both the internal and external field. The internal magnetic field can be calculated from Poisson's equations: the potential Ω is always,

$$\Omega = \int \frac{I_n}{r}\,\mathrm{d}S - \int \frac{div\ I}{r}\,\mathrm{d}v \qquad \ldots\ (10)$$

The internal field is caused by 'free magnetic poles' either superficial ($I_n \neq 0$) or internal ($div\ I \neq 0$).

Domains—Looking back on the expressions for the various contributions to the part of the total free energy which depend on the magnetization, a number of features have to be kept in mind.

The exchange energy as such only depends on the directions between spins; properties of the lattice do not enter into the expression.

The anisotropy energy indicates the dependence of the energy on the

crystallographic properties and thus yields the important connection between magnetization and mechanical properties.

The magnetoelastic energy provides the contribution of external or internal stresses to the energy relations; it is by definition zero for an unstrained lattice.

The magnetostatic energy brings the self-energy of the magnetic substance in its own field and the interaction energy with an external field into the picture. The amount of the magnetostatic energy depends, in the absence of external forces, on the internal field of the substance, which in turn is a strong function of the shape of the specimen.

Equation 10 shows how the internal field is related to the 'free poles' in the interior and on the surface. Consequently this and only this

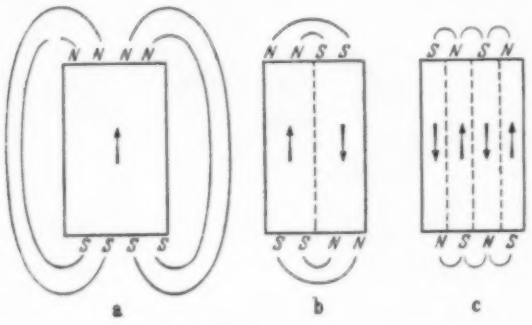

Figure 3. Magnetic substructure

energy contribution can be reduced in a given specimen by the formation of a 'magnetic substructure'. In the absence of external forces every other contribution for a given substance is fixed by the atomic and crystallographic properties of the specimen. But the same specimen will have a different magnetostatic energy if the crystal is either continuously magnetized over its whole volume or subdivided into domains.

Figure 3 illustrates the situation schematically: The specimen *a* is uniformly magnetized over its whole volume, the magnetic energy being $\frac{1}{8\pi}\int H_i \mathrm{d}V$. The formation of domains with an opposite direction of magnetization reduces this energy by a factor of approximately one half, *b*, or one quarter, *c*. This process of subdivision would go on indefinitely if it were not for the transition layers between the domains. Since they separate domains of different orientation, the changes in spin directions have to take place in these transition layers.

Bloch developed the theory of these "Bloch walls."[3] He showed that

the properties of the wall are characterized by two competing factors. Any change in spin direction involves first of all an increase in exchange energy. The smaller the angle between neighbouring spins, the smaller will be the total increase in exchange energy. This consideration should lead to a very gradual transition in a layer of considerable width. There is, however, also the influence of the anisotropy energy. Both the neighbouring domains are magnetized along easy directions; consequently the spins in the transition layer are directed away from these preferred orientations. This is energetically unfavourable and the anisotropy energy will always tend to reduce the thickness of the walls. The actual width of the transition layer will then be the thickness for which the sum of the exchange energy and anisotropy energy is a minimum. This makes it possible to derive an expression for the boundary energy, which is of extreme importance for the prediction of the domain structure.

We have seen that the process of subdivision of a ferromagnetic crystal into domains is connected with a decrease in the magnetostatic energy of the specimen. But setting up domains means also setting up transition layers. The process of subdivision will end when the formation of new Bloch walls requires more energy than is gained by further subdivision.

Table III compiled by BOZORTH[21] gives a survey of the various energy contributions and their approximate magnitude for iron.

Table III. Kinds of energy important in the domain structure of iron, and their approximate magnitudes under specified conditions

Kind of Energy and Expression	*Maximum Energy erg/cm³*	*Conditions Assumed*	*Equivalent Field Strength*
Crystal anisotropy $E_K = K(\alpha_1^2\alpha_2^2 + \alpha_2^2\alpha_3^2 + \alpha_3^2\alpha_1^2)$	10^5	$I_s \parallel [110]$	500
Strain energy $E\sigma = (3/2)\lambda_s\sigma \sin^2\theta$	a 10^5 b 10^2	*Breaking strain* *Magnetostrictive strain*	100 0·1
Surface charge $E_s = (1/2)N_d I_s^2$	a 10^7 b 10^4	*On sphere* *On ellipsoid, L/D = 100*	10,000 10
Bloch wall $\epsilon_w = 2\sqrt{kT_c/a}\sqrt{K + \lambda s\sigma}$	10^2 (1 erg/cm²)	*100 cm² of surface/cm³ in strain free crystal*	—
Interaction of H and I $E_H = -HI_s \cos\theta$	10^6 10^3	$H = 1{,}000$ $H = 1$	— —
Weiss molecular field $E = (1/2)NI_s^2$	10^{10}	$T \ll T_c$	10^7

ENERGY AND WIDTH OF THE BLOCH WALLS

Calculations of the energy per unit area of the transition layer were first carried out by BLOCH.[3] Later when the implications of these considerations on the general problem of ferromagnetic structure became apparent, theory and calculation were extended to more detailed models.[4, 22, 23]

The number of atoms N contained within the wall can be estimated by assuming that the energy of the wall σ_w is the sum of the contribution of the exchange energy and anisotropy energy. The estimate given here follows again Kittel's derivation[14] which must be consulted for the detailed calculations. The boundary energy per unit area $\sigma_w = \sigma_{\text{exchange}} + \sigma_{\text{anisotropy}}$. The boundary separates domains of opposite direction of magnetization. The exchange energy between the neighbouring spins with a difference in orientation ψ is: $\Delta w_{ex} = JS^2\psi^2$. If the total change in orientation occurs over the whole boundary containing N atoms, the exchange energy between neighbouring spins is:

$$\Delta w_{ex} = JS^2(\pi/N)^2 \qquad \ldots . \quad (11)$$

and the exchange energy for the line of N atoms going through the wall is:

$$w_{ex} = JS^2\pi^2/N$$

Since there are $1/a^2$ such lines per unit area, where a is the lattice constant, the contribution of the exchange energy to the wall energy becomes:

$$\sigma_{ex} = JS^2\pi^2/Na^2 \qquad \ldots . \quad (12)$$

The anisotropy energy will be approximately equivalent to the product of the anisotropy constant and the volume:

$$\sigma_{\text{anisotropy}} \approx KNa \qquad \ldots . \quad (13)$$

so that

$$\sigma_{\text{wall}} \approx JS^2\pi^2/Na^2 + KNa \qquad \ldots . \quad (14)$$

This is a minimum with respect to N when:

$$\frac{\partial \sigma_{\text{wall}}}{\partial N} = 0 = -(JS^2\pi^2/a^2N^2) + Ka$$

which means

$$N = (\pi^2JS^2/Ka^3)^{\frac{1}{2}} \qquad \ldots . \quad (15)$$

so that the wall thickness is equal to the square root of the ratio of the exchange energy and anisotropy constant per unit cell. For iron this is approximately equal to $N = 300 \times a$, or $\sim 1{,}000$Å. The total wall energy is for the same constants:

$$\sigma_{\text{wall}} \approx 1 \text{ erg/cm}^2$$

More exact calculations yield for a 180° wall in the (100) plane of iron the expression for the wall energy:

$$\sigma_{\text{wall}} = 2(A/K)^{\frac{1}{2}}$$

with K being the anisotropy constant and A the constant of the exchange energy density. σ_w is then equal to 1·8 erg/cm² which is in very good agreement with other calculations of the wall energy and with experimental estimates.

In the absence of an external field the domains are magnetized along the direction of easiest magnetization. Thus in a cobalt single crystal the direction of magnetization of adjacent domains will always be reversed, since cobalt has only one direction of spontaneous magnetization: The Bloch walls will always be 180° walls. In iron an orientation change of 180° or 90° can take place within the Bloch walls, because iron can be magnetized along any cube edge. In nickel the [111] direction is the direction of easiest magnetization. Thus the angle *vs* between the axes of magnetization of adjacent domains are 180°, 109° or 71°. LILLEY[24] recently calculated widths and energies for all these boundaries including the case of nickel which was not dealt with previously. The wall energy for a 180° wall in cobalt, iron or nickel is 8·20, 1·25 and 0·31 ergs/cm² respectively. For details of the calculations and the effect of the magnetostriction the original papers must be consulted. The energy of a Bloch wall is derived with the condition that the rotation of the spin direction within the wall takes place in such a way that no free magnetic poles are formed throughout the transition layer, which again corresponds to a minimum magnetostatic energy.

DOMAIN CONFIGURATIONS

With these data and formulae it is possible to derive theoretically the domain configurations which should exist in ideal single crystals. Let us first examine the domain structure which will spontaneously exist in a ferromagnetic single crystal in the absence of an external field. The guiding principle in these considerations is always the same. The stable configuration will be the arrangement that represents the minimum free energy for the whole system. In the previous sections the contributions to the overall energy which are connected with the magnetic properties have been compiled. The structure for which the sum of these contributions is a minimum will be stable and should be found experimentally.

The first calculation of this kind was carried out by LANDAU and LIFSCHITZ.[4] They derived the domain structure of cobalt and pointed out that the possibility of reducing the magnetoelastic energy is the

VOL 3

reason for the existence of a ferromagnetic substructure. Domain structures in cobalt were first shown by ELMORE.[25] The domain structure of iron was calculated by both NÉEL[22] and LIFSCHITZ.[6] *Figure 3* illustrates the effect of the subdivision on the magnetostatic energy. But the formation of slab-like domains still leaves free poles on the surface; it is possible to derive a structure in which the magnetic flux is completely closed through the specimen, thus corresponding to zero magnetostatic energy.

Figure 4 shows how this can be accomplished, starting from the subdivision *c* in *Figure 3*. Small triangular 'surface domains' are inserted between the slab-like domains of opposite directions of magnetization. The direction of magnetization of the surface

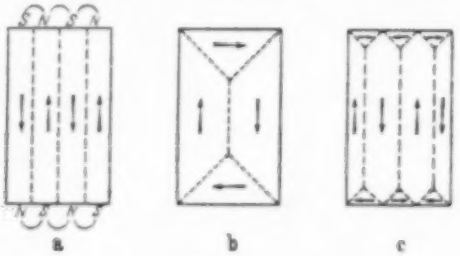

Figure 4. Closed flux configuration

domains is perpendicular with respect to the spontaneous magnetization of the 'interior domains'. An arrangement like this preserves the continuity of the normal component of the magnetization; this corresponds to the absence of free poles or to the closure of the magnetic flux within the specimen because the normal component of the magnetization is also continuous through the walls. In a cubic crystal like iron, both the surface domains and the domains in the interior can be magnetized along easy directions and domain structures of the predicted form were found experimentally by WILLIAMS, SHOCKLEY and BOZORTH.[26]

The structure of the surface domains is usually more complicated than *Figure 4* indicates. The number and size of these domains depends on the state of the surface of the particular sample, whereas the domains in the interior are much more characteristic for the fundamental properties of the substance. Thus the domains can usually be classified into two groups: the surface domains and the domains in the interior. Whilst the surface structure can be rather complicated, theory shows that the internal structure is fairly simple and regular.[14]

The derivation of the domain structure outlined above has one important consequence as far as the size of the domains is concerned; the domain size is *not* a fixed parameter characteristic of a given

substance. It varies with the shape of the sample and changes under the action of external magnetic fields and stresses. In cases where external forces are acting, the sizes and shapes of the domains vary in a particular crystal. The size of the domains as such, both surface and interior, is not a fundamental criterion. It is merely a consequence of the condition of minimum total energy which must be fulfilled for any stable configuration.

Figure 5 shows the subdivision of a uniaxial single crystal which has the shape of a rectangular cylinder. An estimate of the optimum wall thickness was obtained by KITTEL[14] in the following manner:

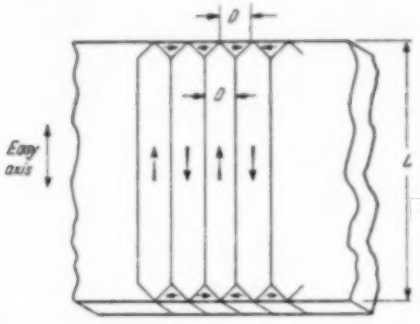

Figure 5. Domain configuration in a uniaxial crystal

The magnetostatic energy of this arrangement of charged layers normal to the paper is:

$$f_{\text{mag}} = 1{\cdot}7I_s^2D \text{ per unit surface area.} \quad . \ . \ . \ . \ (16)$$

The surface energy of the Bloch wall is σ_w per unit area surface and in the model (*Figure 5*) the area of the Bloch wall is L/D per unit area of the crystal so that:

$$f_{\text{wall}} = \sigma_w L/D \quad . \ . \ . \ . \ (17)$$

The total energy of the slab per unit surface area is:

$$f = f_{\text{mag}} + f_{\text{wall}} = 1{\cdot}7I_s^2D + \sigma_w L/D \quad . \ . \ . \ . \ (18)$$

which has a minimum with respect to D:

$$\frac{\partial f}{\partial D} = 1{\cdot}7I_s^2 - (\sigma_w L/D^2) = 0$$

$$D = (\sigma_w L/1{\cdot}7I_s^2)^{\frac{1}{2}} \quad . \ . \ . \ . \ (19)$$

which leads to a certain width of $D \simeq 10^{-3}$ cm for iron, where the constants are taken as $I_s = 1{,}700$, $L = 1$ cm, $\sigma_w = 2$ ergs/cm^2. These considerations do not take the surface domains into account, but this problem can be treated in a similar fashion. It is usually necessary to

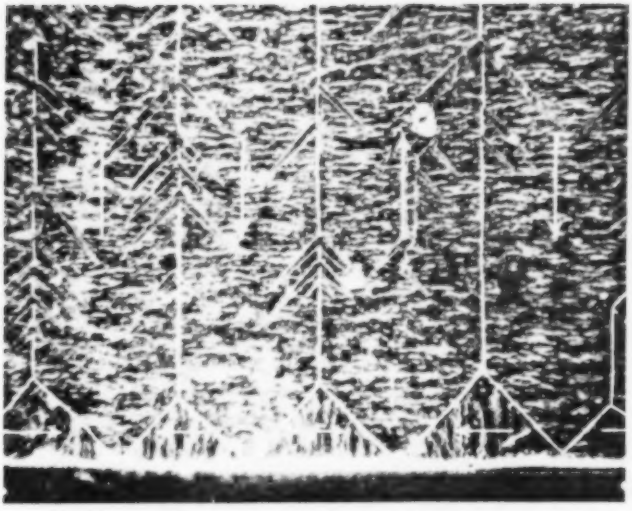

Figure 6. Domain configuration in a silicon–iron crystal

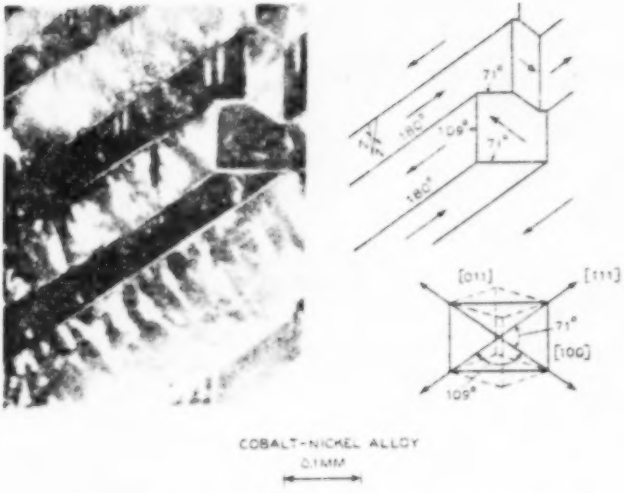

Figure 7. Domain configuration in a cobalt–nickel alloy

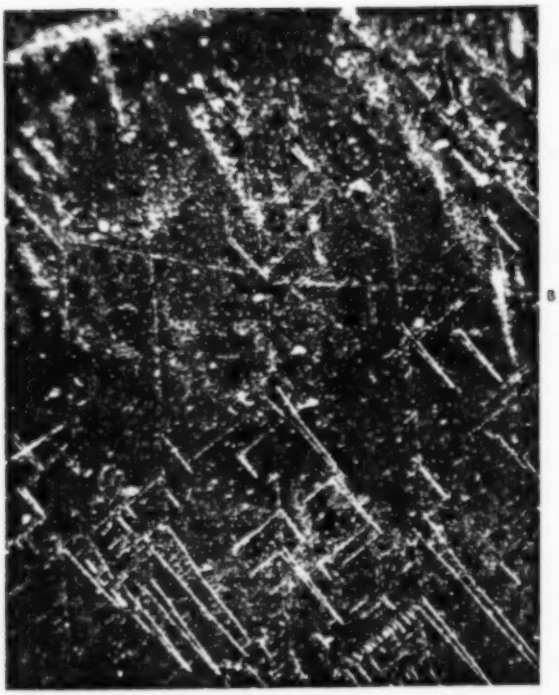

Figure 8. Domain structure on a bicrystal of nickel:
AB = *grain boundary*

consider possible increase in anisotropy energy of the system and the effect of the magnetostriction on the domains of closure.

The theory of ferromagnetic domains received its most brilliant support from the powder pattern. This technique which was first introduced by BITTER[27] was developed in subsequent work by ELMORE[25] and WILLIAMS[28] into one of the most powerful research tools in ferromagnetism. Ferromagnetic colloid is placed on the carefully prepared strain-free surface of the crystal. Wherever a Bloch wall intersects the surface there is a component of the magnetization normal to the surface. The field thus produced collects the ferromagnetic colloid in lines marking the position of the walls. According to this mechanism colloid concentrations will occur at any place on the surface which exposes free magnetic poles either when the surface cuts through a Bloch wall or when domains in an unclosed flux arrangement end at the surface, or when impurities or nonmagnetic inclusions produce discontinuities in the magnetization resulting in free poles.

Figure 6 shows a domain pattern in silicon iron obtained by WILLIAMS.[28] The photo is retouched and the directions of magnetization are added to emphasize the agreement with theory. BATES and NEALE[29] also studied domain pattern in silicon iron and especially the change in domain with increasing external field. Silicon iron ($\sim 4\%$Si) is often used instead of iron because it is very difficult to prepare pure single crystals of body-centred cubic iron. In *Figure 7* the pattern on a (011) surface of a face-centred cubic cobalt–nickel alloy, in which [111] is the direction of easiest magnetization is shown as obtained by BOZORTH and WALKER.[30] The anisotropy energy of this alloy is more than three times that of nickel. This high value was regarded as the reason why domain patterns were observed in this alloy but not in nickel. Only recently MARTIUS, GOW and CHALMERS[31] found a domain pattern on nickel.* The domain pictures were obtained on a (110) face of a nickel bicrystal in the course of investigations on the influence of the grain boundary on ferromagnetic properties. *Figure 8* shows the domain structure in the vicinity of the grain boundary in the absence of an external field.

The formation of surface domains in a crystal with only one axis of easy magnetization such as cobalt, requires work against the anisotropy forces. If the anisotropy energy of the crystal is high, surface domains may not form at all. Patterns obtained by ELMORE[32] on the hexagonal face of cobalt, show that the domains end abruptly on the surface without forming surface structures† Domain patterns

* *Note added in proof:* After this manuscript was submitted M. Yamamoto and T. Iwata, *Phys. Rev.* **81** (1951) 887, reported also domain pattern on single crystals of nickel.

† In this work on cobalt Elmore also discussed the energy relationship and the connection of the observed pattern to the predictions of LANDAU and LIFSHITZ.[4]

on cobalt have also been reported by MEE.[33] The free magnetic poles on the hexagonal face of cobalt can also be detected by electron diffraction. GERMER[34] observed electron scattering on these planes and could estimate the surface field to 10,000 Oersteds.

The results of the powder technique mentioned so far have been concerned only with the initial structure of ferromagnetic single crystals in the absence of external fields, stresses, or any deviations from the ideal crystal lattice. The work of Williams and his colleagues has resulted in a variety of powder patterns for various crystallographic orientations and different experimental conditions. Starting from patterns of single crystals the effects of an external field and of tension and compression were studied.[26] A similar energy consideration to that developed above can be applied to the more complex cases. Rigorous solutions are seldom possible owing to the additional mathematical difficulties, but the influence of the various factors entering into the energy relationship can usually be demonstrated in a semi-quantitative way at least.

SINGLE CRYSTALS IN AN APPLIED FIELD

Domain Structures—In order to determine the domain configuration of a single crystal in an external field, the same minimum energy problem which led to the initial domain structure has to be solved. But the presence of the applied field changes the expression of the magnetostatic energy. The internal field which entered into the equation in the case of the original domain structure has now to be replaced by the 'effective' field, being the vector sum of the applied field and the internal field.

NÉEL[22] and LAWTON and STEWART[35] treated this problem rigorously for the case of a single crystal of iron. In the absence of an external field the domains are magnetized along the six equivalent easy directions. The applied field destroys the equivalence. Depending on the direction and magnitude of the external field only certain distinct directions of domain magnetization (referred to the direction of the field) are stable. Néel calculated the resultant magnetization for these different configurations as a function of field and specimen shape. The magnetization curves obtained in these calculations agreed well with the experimental data. The magnetization of single crystals was studied thoroughly by Kaya, Honda and Webster. (Becker and Döring critically discuss these experiments.[13]) The domain configuration which Néel predicted for a single crystal of iron with and without an external field is shown in *Figure 9*.

Domain patterns obtained by Williams, Bozorth and Shockley on the surface of a silicon–iron crystal of the same shape were entirely consistent with Néel's prediction (though it could be that the real case

is still more complex) and thus gave strong support to the domain theory and the assumptions underlying Néel's calculations. The powder pattern of silicon iron obtained by BATES and NEALE[29] led to the same results.

Powder patterns also served to check another theoretical concept in one of the most important experiments utilizing this technique.

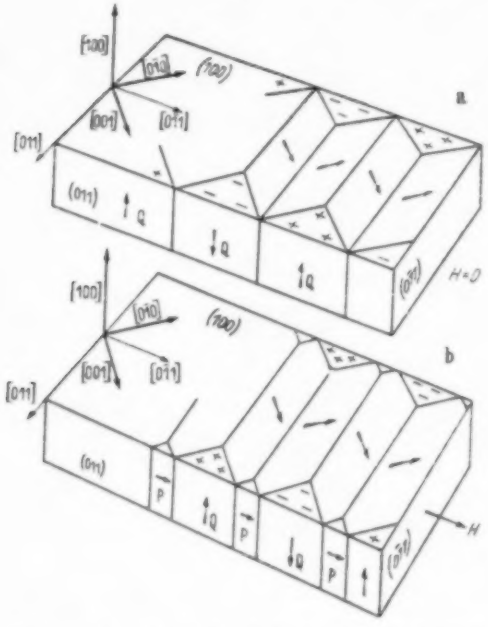

Figure 9. Domain structure in iron as predicted by Néel

It was carried out by Williams and Shockley in 1949.[36] They followed the motion of a Bloch wall in silicon iron in an external magnetic field, while recording the change in magnetization simultaneously with a flux meter. They found a linear relationship between the wall displacement and the change in magnetization. This was the first conclusive evidence that at low fields the magnetization process really takes place by domain wall displacement according to the views developed earlier. Long before this direct evidence was available the magnetization process was pictured as taking place either by wall displacement or rotation of the whole domain corresponding to change of domain volume and change of domain direction respectively. The detailed consideration of these processes by Becker and Döring and others have shown that the change in domain volume will appear at low fields while the domain rotations dominate near saturation. If an

external field is imposed upon a ferromagnetic crystal with domains magnetized along the easy axes, some of these domains will be energetically more favourable with respect to the field than their neighbours; so they will grow by wall displacement at the expense of the latter as long as the change in volume is connected with an energy gain.

Figure 10 taken from BECKER and DÖRING[13] illustrates this process. The domains *1* and *2*, magnetized to saturation J_s, form an angle θ_1 and θ_2 with the field H (which must be regarded as the 'effective' field, that is the vector sum of the applied field and the internal field). *Figure 10*a shows schematically the change in domain volume caused

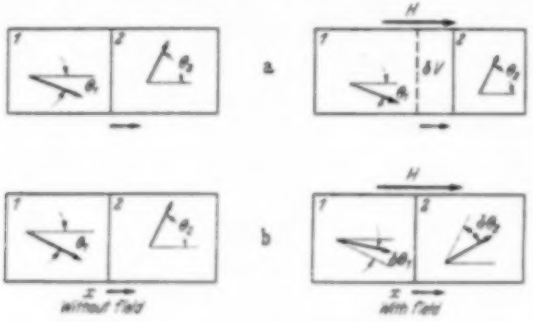

Figure 10. Schematical illustration of the processes of domain wall movement and domain rotation

by wall movement. With the field H in the given direction a change in volume ∂v occurs, corresponding to a change in magnetization $\partial J = J_s(\cos\theta_1 - \cos\theta_2)\partial v$. In the early derivation H was taken as the external field only. In the light of more recent developments this is not justified any more and the effective field must be taken instead. This can change locally in direction and magnitude (see later theories of coercive force) which makes a general treatment only possible, for very weak or very strong external fields—corresponding to the dominating influence of either the internal or the external field or other very restrictive assumptions. The general reasoning, however, is still applicable. *Figure 10*b illustrates the process of domain rotation with the change in magnetization. Here:

$$\partial J = V_1 J_s \partial(\cos\theta_1) + V_2 J_s\, \partial(\cos\theta_2)$$

This process is assumed to occur at a higher field strength after the possible changes in domain volume are completed.

Boundary Movements—Since major magnetization processes take place by movement of the Bloch walls, we shall outline the behaviour of a domain wall under external forces. Here again the general ideas about the underlying mechanism have been developed during the last

fifteen years. But quantitative calculations and experiments under completely controlled conditions have only been carried out recently. In an ideal strain-free single crystal a Bloch wall should, under the action of a very small external field, move immediately into its new equilibrium position. But the experimental facts show that there is a certain resistance to the wall displacement which has to be overcome by a finite field. This means that there are local variations of the internal

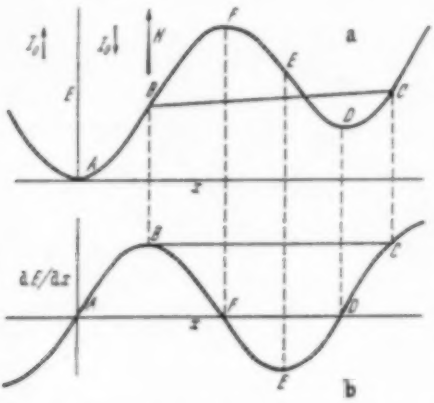

Figure 11. Schematical illustration of a domain wall in the local field of forces

energy of the specimen with the boundary position. They can arise through any deviation from the ideal lattice due to impurities, lattice imperfections, strains *etc.* The local variations will be different for every boundary; any theoretical treatment has to assume one cause of the lattice perturbations as being dominant. Otherwise the mathematical difficulties are too large (see page 153 *et seq*). Very recently experiments with single boundaries under completely controlled conditions have been reported[38, 41] and the quantitative theory of these basic arrangements has been developed. This basic approach is certainly the most promising way to attack the fundamental problems involved. But even with this information available very little is known about the structural properties of polycrystalline materials in general. This lack of knowledge will seriously handicap any generalization of such results.

Figure 11 shows schematically the dependence of the internal energy of a crystal on the position of a 180° boundary.[12] The equilibrium position in the absence of an external field will be at $x = 0$. In a field H the condition for equilibrium is:

$$\frac{\mathrm{d}}{\mathrm{d}x}(E - 2HJ_s x) = 0$$

In curve **b**, dE/dx is plotted against x. With increasing field the equilibrium position of the boundary moves in **a** to the right corresponding to an increase in dE/dx in **b**. With decreasing field the boundary will return to its initial position $x = 0$. The movement is reversible as long as the increase in dE/dx does not exceed the maximum value at B. If the external field is larger than the threshold H_0 corresponding to this maximum

$$H_0 = \frac{1}{2J_s}\left(\frac{dE}{dx}\right)_{max} \quad . \quad . \quad . \quad . \quad (20)$$

the equilibrium becomes unstable. Once the increase in energy—which is furnished by the reorientation of the local magnetization in the external field—is sufficient to overcome the local energy maximum at B, the boundary moves without further increase of H into the position C. If the field is now decreased the boundary cannot return to its initial position again. This second part of the wall movement is irreversible. For $H = 0$ the boundary will remain at D and a field of $-H_0$ is required to bring the boundary back to A.

This schematic diagram illustrates also how remanence, hysteresis and coercivity can arise from these local energy variations and can be pictured in terms of reversible and irreversible wall movements. The coercive force is given by the field necessary to move a Bloch wall from one position of low potential energy to a neighbouring position of similar character by overcoming an energy peak. The initial permeability can be pictured as the force resisting small displacements of the walls. Since the local variations of the internal energy will be different for any boundary and any position in the crystal, a general mathematical treatment is not possible. In order to treat these complex problems even semiquantitatively very restrictive assumptions about the local energy variation must be introduced. Before discussing these theories mention will be made of recent research on the movement of single boundaries.

Experimental evidence for the existence of single domains has been sought since the days of Weiss and when BARKHAUSEN[37] found marked discontinuities in the magnetization process these "Barkhausen jumps" were regarded as direct proof of a domain structure. They were investigated very thoroughly and it turned out that they were caused by discontinuities in the movements of the walls. The spontaneous displacement from B to C in *Figure 11* would correspond to such a jump. But the range over which these jumps take place depends entirely on the internal structure of the sample; usually the volume involved in a Barkhausen discontinuity is but a fraction of the domain volume. Only in special cases, for instance in material with strong preferred orientation or in single crystals containing few domains, can the observed

Barkhausen discontinuities correspond to the reversal of the magnetization over the whole domain. Although the size of the discontinuities cannot be directly related to the size of the domain[32, 36] the results of the investigations provide a large amount of information about the behaviour of domain walls under certain conditions. These problems, including the investigation of large discontinuities, were recently reviewed by STONER.[12]

The first fundamental experiment investigating the behaviour of a single wall was carried out by WILLIAMS and SHOCKLEY[36] when they correlated the change in magnetization directly with the displacement of a Bloch wall. A specimen was cut from a single crystal of silicon iron, all surfaces being parallel to (100) planes. *Figure 12* shows the domain structure, the broken lines indicating the positions of the Bloch walls.

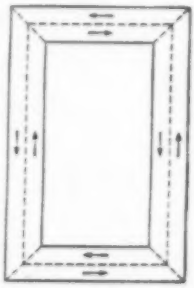

Figure 12. Domain structure in a single crystal of iron, used for measurements of the wall velocity

STEWART[38] recorded the magnetization curve of such a crystal and found that nearly half the magnetization took place in one single Barkhausen jump. This jump occurred quite slowly and it was even possible to stop it by switching off the field as soon as the galvanometer reading indicated the start of the wall motion. The speed of the wall movement could be measured as a function of the field strength, and the following relation between the velocity of the wall, v, and the fields was obtained.

$$V = A(H - H_0) \qquad \ldots . \quad (21)$$

where A is a constant (in this case $A = 6{\cdot}3$ cm/sec/oersted) and $H_0 = 0{\cdot}049$ oersted. Compared with the wall velocities reported in the earlier investigations of large Barkhausen discontinuities, the speed of the single wall is very low. SIXTUS and TONKS[39] report the value $A = 10{,}000$ cm/sec/oersted, DIJKSTRA and SNOEK[40] in similar experiments found $A = 50{,}000$ cm/sec/oersted. But in these experiments—as WILLIAMS, SHOCKLEY and KITTEL[41] have recently pointed out—the walls make a small glancing angle with the direction of propagation. This increases the effective wall thickness considerably and could cause an increase of A. Williams, Shockley and Kittel extended the experiments with single 180° boundaries[36] and evaluated the results quantitatively. In very weak external fields the velocity of propagation of the wall was found to follow the relation $V = \text{const.}\,(H - H_0)$, where the constant is approximately 4 cm/sec/oersted and $H_0 = 0{'}003$ oersted. A theoretical expression for this constant was developed. In the calculation the wall was assumed to be plane and to move uniformly. The external field was considered small compared with the internal field, and

the eddy current losses of the moving wall were regarded as the only factor determining the velocity. The calculations give the following expression:

$$V = (\pi^2 \eta c^2 / 32 B_s d) H \qquad \ldots . \quad (22)$$

where η denotes the electrical resistivity and d the specimen width. (Calculations were carried out for a square rod.) The theoretical values for V are in excellent agreement with the theory. They are shown in *Figure 13*.

The experiments were extended to higher fields; up to about 5

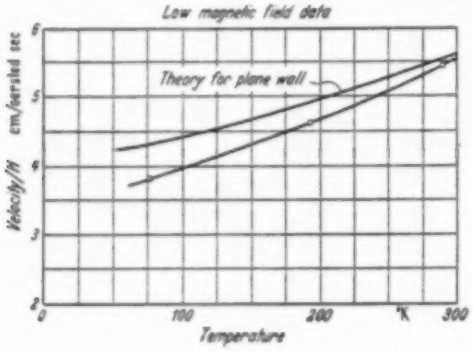

Figure 13. Theoretical and experimental value of the velocity of a Bloch wall in low fields

oersted the velocity of the boundary movement increased linearly with increasing field strength. At still higher fields the wall apparently did not move homogeneously over the whole crystal. The eddy currents seem to retard the motion of the wall more in the middle of the crystal than on the surface so that the boundary curves. It will eventually form a cylinder and collapse under its own surface tension as shown in *Figure 14*.

The quantitative theory developed for this model is confirmed by the experimental results from measurements up to fields of 80 oersted. The eddy current losses accompanying the motion of the wall were calculated for the different ranges of wall velocity. For details of these calculations the original paper must be consulted.

Since wall movements play such an important part in all ferromagnetic phenomena the laws governing the wall motion are of considerable theoretical interest. In 1948 DÖRING[42] pointed out that there is a difference in the energy of a Bloch wall whether at rest or in motion in an external field. The energy of the moving wall per unit area, σ, is larger than the corresponding energy, σ_0, of the wall at rest.

The increase in wall energy is proportional to the square of the wall velocity so that:

$$\sigma = \sigma_0 + \text{const. } v^2 \qquad \ldots\ldots (23)$$

The wall behaves as if it had an inert mass. In his calculations Döring finds that the wall energy for a 90° wall in iron at rest $\sigma = 0{\cdot}9$ erg/cm^2 and that the effective mass $m = 6{\cdot}0 \times 10^{-11}$ gm/cm^2 taking const. $= m/2$.

Further developments of this theory by BECKER[43] and KITTEL[44] can only be mentioned here. The inertia of a Bloch wall will have its

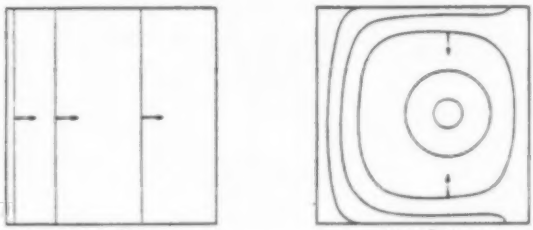

Figure 14. Behaviour of a Bloch wall in low and high fields

maximum effect when the walls are displaced by a high frequency field; under these conditions inertia and damping effects are observed experimentally.[45]

THEORIES OF COERCIVE FORCE

One of the ultimate aims in studying the behaviour of single domain walls is the desire to arrive eventually at a complete theory of the coercive force. *Figure 15* shows the familiar magnetization curve. It is obtained by the following process. A ferromagnetic specimen is magnetized to saturation; subsequently the field is decreased, then reversed and increased again. After saturation is reached in the negative field the cycle is repeated. *AO* represents the coercive force, *BO* the remanence and the area enclosed by the curve is a measure for the energy dissipated in the irreversible processes of the magnetization. It has already been shown (page 163) how these processes take place and how the coercive force can be pictured as the force necessary to overcome a local energy peak in the way of a moving Bloch wall. Any general theory of the coercive force requires a detailed knowledge of the local potential energy of the solid and its fluctuations; at present this knowledge is lacking. Only by making very limiting assumptions about the local energy variations is it possible to treat these problems.

The first assumption put forward to explain the nature of the local

obstacles in the way of the Bloch wall was put forward by BLOCH[3] and KONDORSKI.[46] They regarded the internal strains as the major source of the inhomogeneity which was qualitatively consistent with the experimental results. These ideas were extended by KERSTEN[47] and BECKER and DÖRING[13] but in a more quantitative treatment the stresses that are required to explain the observed values seem to be unreasonably high. (The consequences of the strain theory have been discussed by KERSTEN.[47]) These considerations led KERSTEN[48] later to the conclusion that probably other more important factors may influence the resistance against wall movement. He considered the effect of inclusions in the ferromagnetic matrix. If non-magnetic inclusions are incorporated in the wall they will decrease the surface tension and the wall will tend to remain in a position where inclusions cover as much wall area as possible. The effect of the inclusions on the surface tension will be a maximum when the diameter of the inclusions is about equal to the thickness of the Bloch wall. Kersten carried out his calculations for spherical inclusions in a regular super-lattice-like arrangement. If d is the diameter of the inclusions and S their distance and I_s is the intensity of magnetization then:

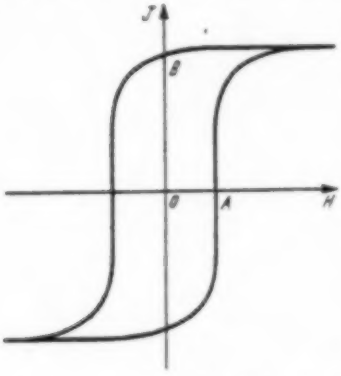

Figure 15. Magnetization curve

$$H_c = \pi\sigma_w d/2I_s S^2 \qquad \ldots\ (24)$$

These concepts have been revised in the light of the recent developments of the domain theory. NÉEL[49] pointed out the effect which inclusions have on the magnetostatic energy. If a non-magnetic inclusion exists in a ferromagnetic matrix, a discontinuity in the internal magnetization will occur, resulting in free magnetic poles around this inclusion. The additional magnetostatic energy thus introduced can be minimized by a secondary domain structure, as indicated in *Figure 16*. Williams succeeded in showing the physical reality of these configurations in a rather striking manner, as *Figure 16*b and c demonstrate.

Using this conception of the magnetostatic energy associated with the non-magnetic inclusion or cavities, Néel developed a new theory of coercive force. He seriously criticized the assumptions of a plane wall in the strain theory and the regular distribution of impurities in the inclusion theory. He attributed the apparent general agreement of the experimental results with the older theories to these assumptions only. The values of the coercive force which Néel calculated from the strain

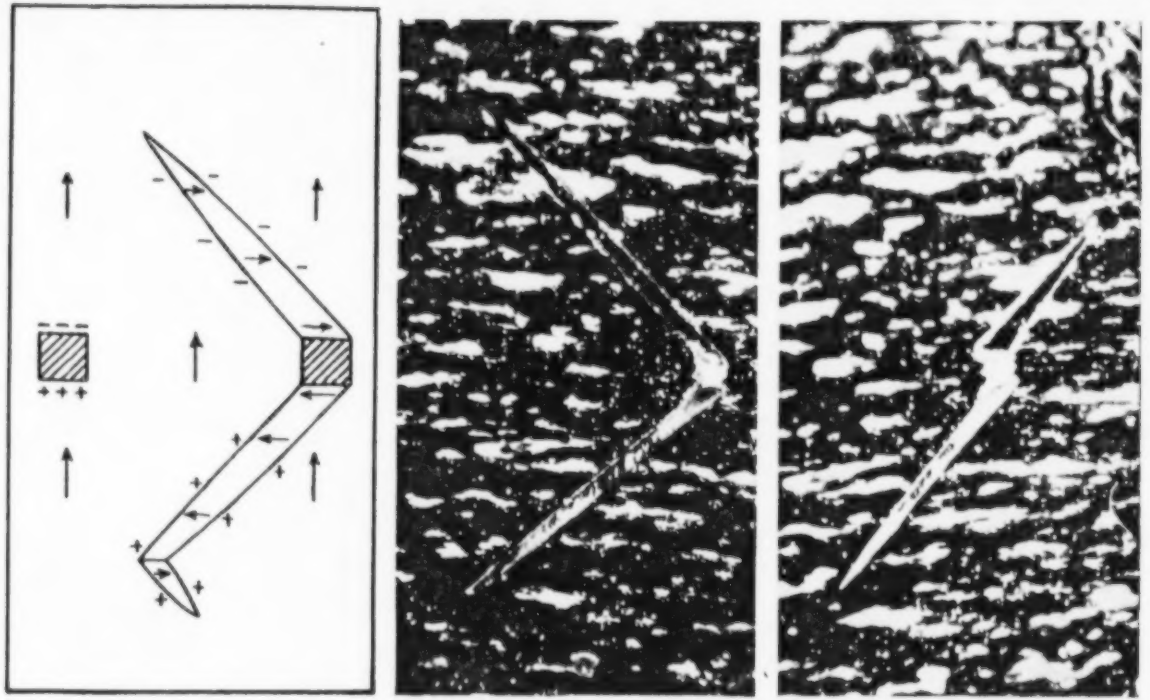

Figure 16. (a) *Predicted and* (b *and* c) *observed domain structure around inclusions. The structure* a *was predicted by Néel in 1944 on energy considerations; the predicted pattern was found experimentally by Williams in 1947*

VOL
3

theory and from the inclusion theory without assuming a plane wall or a regular distribution of the inclusions, are much smaller than the previous values. According to these calculations, internal strains and the surface tension effect of the inclusions would only influence the coercive force to a lesser extent. The main reason for the local change in energy is in Néel's theory the non-uniformity of the internal field caused by inclusions or cavities. The energy of these 'dispersion fields' depends on the position of the boundaries. *Figure 17* shows how a reduction of the magnetostatic energy of an inclusion can be achieved when this inclusion is incorporated in the wall. In a general treatment Néel evaluates the relative contributions of strains and inclusions. He arrives by means of a three dimensional Fourier analysis at the following expressions for the coercive force of iron and nickel:

For iron $\quad H_c = 2{\cdot}1v_s + 360v_i$

For nickel $\quad H_c = 330v_s + 97v_i \qquad \ldots\ldots (25)$

where v_s is the volume affected by the internal strains, which are assumed to be 30 kg/mm² and oriented at random; v_i is the volume of the inclusions.

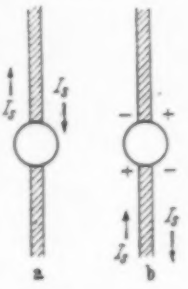

Figure 17. The effect of inclusions on the Bloch wall

It is quite obvious that in the real case strain and the various effects of inclusions would be superimposed in a rather complex manner and it would be difficult to estimate their relative importance. Much more experimental data obtained under very simple and clear conditions are needed before a general theory of coercive force can be established.

Dijkstra and Wert[50] have recently investigated the effect of inclusions on the coercive force of iron. They calculated the effect of inclusions on the surface tension of the wall and on the magnetostatic energy for a random distribution of spherical particles of equal diameter; the walls were assumed to be plane or only slightly curved. Lattice strains were not considered. The domains were regarded as cubes of equal size. (The cube edge L was taken to 10^{-3} cm for the numerical calculations.) *Figure 18* shows the contributions of the two effects for non-magnetic inclusions in iron as a function of the diameter of the inclusions, expressed in multiples of the boundary width δ. The volume fraction of the inclusions is 3×10^{-3}. For inclusions much smaller than the width of the Bloch wall the surface tension effect predominates; for larger particles the effect of the change in magnetostatic energy is much more important. The two effects are about equal for $d = \frac{1}{2}\delta$. The coercive force has a maximum for $d = \delta$ in this model related to the contribution of the magnetostatic energy. The same result was predicted by Kersten from his model.

Dijkstra and Wert carried out experiments on the coercive force of

iron with F_eC_3 particles of known size as inclusions. They found a distinct maximum at 1,200Å in good agreement with their calculations. The original paper[50] must be consulted for the limiting assumptions entering into the calculations and experiments.

Single Domain Particles—The influence of inclusions on the coercive force has long been known experimentally. Generally the coercive force increases with decreasing particle size; but it was particularly noted that substances with very high coercive forces usually consisted

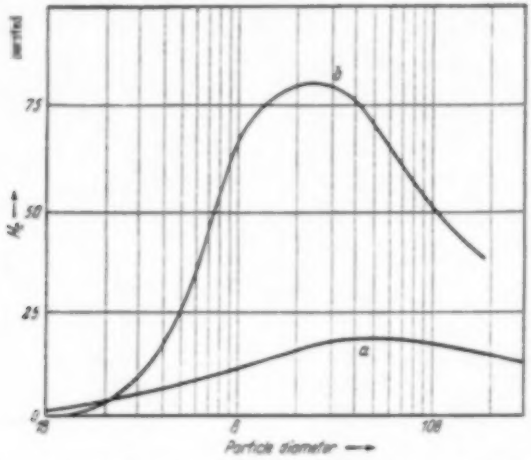

Figure 18. The coercive force, H_c, of iron as a function of the size of the non-magnetic inclusions: a *surface tension effect,* b *magnetostatic energy effect*

of very fine grain material, of fine powder or of precipitates of small particles in a matrix of different magnetic properties. A quantitative explanation for these phenomena was again furnished by the domain theory.

When discussing the theoretical domain structure we saw that the size and the arrangement of the domains is strongly influenced by the shape and size of the specimen. The process of subdivision into domains ends when the energy necessary to set up Bloch walls between the new domains cannot be furnished any more by the decrease in the magnetostatic energy obtained through the formation of new domains. The separate contributions to the total energy of a given domain configuration vary in a different manner with the actual particle size. The energy of the Bloch wall is a surface energy while the magnetostatic energy of the configuration is a volume energy. With decreasing particle size it is possible that it may be energetically more favourable not to set up domains at all, even though the particle has a finite magnetostatic self energy. The study of the behaviour of these 'single

particle domains' has contributed considerably to our general knowledge of ferromagnetic phenomena.

One of the most interesting factors is the critical size below which we can expect single domain behaviour. This size will depend on the anisotropy energy and on the shape of the particle. Calculations of this kind were carried out for the first time by KITTEL[51] in 1946. Considering the constants for iron, the critical length for the edge of a cubic particle is approximately 150Å while thin films of iron would establish domain behaviour below a critical thickness of about 3,000Å. Experiments by DRIGO and PIZZO[52] on the Barkhausen effect of thin films confirmed these results. They found an increase of coercive force with decreasing film thickness. Below a certain thickness the Barkhausen effect disappeared completely, indicating that the film did not contain Bloch walls any more. The limiting film thicknesses were for iron, cobalt and nickel, 1,300Å, 1,200Å and 80Å respectively. For spherical particles the critical radius depends also on the anisotropy energy. STONER and WOHLFARTH[53] in 1948 calculated the radius to 240Å, 320Å and 520Å for iron, cobalt and nickel respectively.

The only possible magnetization process for a single domain particle is rotation of the total magnetic moment of the particle. This process requires much more energy than a domain wall movement. In order to reverse the direction of magnetization in a small particle, the magnetic energy which the particle gains in the external field must exceed the internal energy tending to keep the domain in its original position and prevent rotation. This internal energy will be high if the anisotropy energy of the material that forms the single domain particles is high, if high anisotropic internal strains are present, or if the particle has a large demagnetization factor on account of its shape. *Table IV*[14] shows the magnitude of these effects. Here the maximum coercive

Table IV. Maximum Coercive Forces of Small Particles due to various Causes. (Complete orientation assumed; packing effects neglected.)

	Anisotropy	*Shape*	*Internal strain*
Expression	$2K/I_s$	$2\pi I_s$	$3\lambda T/I_s$
Fe	500	10,700	600
Co	6,000	8,800	600
Ni	135	3,150	4,000

$T = 2 \times 10^{10}$ dynes/cm²

force for small particles is calculated; in the case of the internal strains the applied stress was taken to 200 kg/mm².[53] For quantitative discussion of the various effects on the coercive force of small particles

including the influence of position and temperature, the reader is referred to the original papers. The experimental data of the coercive forces of fine powder or precipitated phases[54] are in good general agreement with this theory.

POLYCRYSTALLINE MATERIAL

Influence of the Grain Boundaries—In the preceding paragraphs the behaviour of the single domain particles was derived from results obtained from single crystals through considerations of the influence of the actual particle size on the domain structure. But in applying these results to the coercive forces of fine powders, or precipitation hardened materials, the particles are no longer well defined single crystals. In general, one should not overlook the ambiguity that lies in the generalization of results obtained under the assumption of single crystal structure to polycrystalline material. While some properties of the polycrystalline material can be calculated from the corresponding single crystal properties, there are nevertheless many instances in which the interaction of neighbouring crystals and the effects of the crystal boundary must be taken into account. For fine powder magnets the decrease in coercive force with increasing density of packing was established experimentally[55] and included in the calculations by means of a packing factor. In the case of small particles in a non-ferromagnetic matrix, the demagnetization field of the matrix can be taken into account—at least in principle. The increase in coercive force with decreasing grain size in a given substance is well known. The difficulty in explaining and predicting this in other than qualitative terms arises from the uncertainty in correlating the "grain size" in the crystallographic sense of the word to the "particle size" in its ferromagnetic meaning. We define a grain as a region of uniform crystallographic orientation, separated by grain boundaries from neighbouring similar regions with different orientations. In a given substance it will depend on the amount of this orientation difference whether two adjacent grains will belong to the same or to different magnetic configurations. For materials of high anisotropy energy small orientation differences will influence the domain structure, whereas powder patterns of substances of low anisotropy energy sometimes show domains going across grain boundaries without visible discontinuities.[36] In addition, the strains around a grain boundary which also increase with increasing angle of misfit have to be considered. The influence of the grain boundary on the domain structure of nickel was shown by MARTIUS, GOW and CHALMERS.[31]

In a polycrystalline material the domain structure will be set up according to the same fundamental principles that govern the domain

structures of single crystals. The subdivision of the polycrystalline substance will result similarly in an arrangement of domains which closes the magnetic flux as far as it is possible within the specimen. A configuration like this may contain one or more grains of the polycrystal, depending on the relative orientation of the grains. The polycrystalline ferromagnetic substance will thus consist of an assembly arrangement of such closed-flux shells as suggested by MARTIUS.[56] The mechanical properties of the material will determine the shell size, which has the single domain particle as its lower limit. The wall movements and domain rotations which constitute the magnetization process can only occur within each shell. The relative magnitude of the two processes is thus largely determined by the shell size.

Models such as this, will lead to a better understanding of the relation between magnetic and mechanical properties which is experimentally well established but has never been determined quantitatively. The model should facilitate the generalization of the single crystal results because the observed behaviour of the polycrystalline substance could be divided into processes occurring within the shells, where single crystal results would be completely applicable, and the interaction effects of the shells. This is especially appropriate if changes in ferromagnetic parameters are accompanied by changes in the mechanical state of the specimen, because then the shell size will change. Along these lines a qualitative explanation of the changes in coercive force caused by plastic deformation has been advanced. The internal demagnetization field of polycrystals and its variation with grain size was recently discussed by DÖRING.[57]

In spite of the wealth of information on ferromagnetic material of technical interest, much more data, especially from clear-cut simple experiments which can be treated quantitatively, are needed to clarify our knowledge of the detailed connections between magnetic and mechanical properties. However, the present line of approach seems to be established.

Approach to Saturation—Another section of the magnetization curve, where the influence of mechanical properties must be considered, is the region in which the magnetization approaches saturation. Although the amount of the saturation magnetization depends only on the number of spins per atom participating the approach to saturation is structure-sensitive. In these high field regions the change in magnetization is entirely achieved by rotational processes which can be treated theoretically with comparative ease. These phenomena have been investigated by several authors. The earlier work was again reviewed by BECKER and DÖRING[13] and more recently by STONER.[12]

If the changes in magnetization in this field range are attributed

entirely to domain rotation, the theoretical approach to saturation should follow a law:

$$I = I_0(1 - b/H^2) \quad \ldots . \quad (26)$$

where b can be related to the anisotropy constant K of the particular material since the ferromagnetic anisotropy provides the forces counteracting the external field. These calculations were carried out by AKULOV,[58] GANS[59] and BECKER and DÖRING,[13] and b was found to be given by:

$$b = 0{\cdot}076 \frac{K^2}{J_s^2} \quad \ldots . \quad (27)$$

The experimental results, however, indicated that the actual approach to saturation followed a law:

$$I = I_0(1 - a/H - b/H^2) + cH \quad \ldots . \quad (28)$$

the term c being related to the change in spontaneous magnetization; the coefficient a is structure sensitive and called *magnetic hardness* and b is related to the anisotropy energy in the way indicated above. The experimental data were obtained with polycrystalline material; the theoretical value of b for polycrystals was found by averaging over the single crystal results. Experiments show that, depending on the strength of the applied field, the law can be approximated for not too high fields by:

$$I = I_0(1 - a/H) \quad \ldots . \quad (29)$$

or for very high fields by

$$I = I_0(1 - b/H^2) \quad \ldots . \quad (30)$$

Several attempts have been made to relate the factor a to specific mechanical properties of the material[60] and recently the whole problem of the approach to saturation was reconsidered by NÉEL[61] and HOLSTEIN and PRIMAKOFF.[62] After a critical review of the previous treatments Néel includes the effect of the interaction between the grains of a polycrystalline substance (he treats the case of nickel) on the value of the factor b. In the range of field strength which is experimentally attainable, the new treatment leads to a value of b reduced by approximately a factor of two. This result is obtained by calculating the internal demagnetization field of the polycrystal. Holstein and Primakoff arrived independently at the same result.

In connection with the factor a Néel attributes the coefficient of magnetic hardness to irregular internal perturbations, giving rise to a demagnetization field. He regards cavities as the main cause of these perturbations and expresses a in terms of the volume, these cavities or non-magnetic inclusions occupy; he compared the formula thus obtained with experimental results for magnetic powders and obtained

fair agreement. The irregular internal perturbations can also originate from internal strains, and it seems to be difficult to distinguish between these contributions. There is, however, one characteristic distinction. Since the effect of cavities is directly due to the 'free magnetic poles' which they set up, their influence will vary with temperature just as the spontaneous magnetization does. But if magnetic hardness is caused by internal strains, the temperature variation should be given by the temperature dependence of the magnetostriction constants. Since the magnetic hardness of iron bears little relation to temperature, Néel concluded that it is mainly due to inclusions and cavities rather than internal strains.

This brings up the question of the relation between magnetic hardness as expressed by the coefficient a in the law of the approach to saturation, and the coercive force, which also depends on inclusions and internal strains. Although the connection between these phenomena is evident there are, however, some significant differences. The maximum effect of inclusions on the coercive force occurs when the foreign particles have a diameter comparable to the width of the Bloch wall, while larger irregularities have less influence. The approach to saturation, on the other hand, is not directly influenced by the size of the inclusions.

FERROMAGNETIC PERMEABILITY

If we regard the changes in magnetization in low fields as being caused by domain wall movements only, the permeability is determined by the restoring force tending to return the Bloch wall to its equilibrium position. The local energy variations, which are a function of the position of the boundary, were mentioned in connection with the coercive force. Recent studies of the frequency dependence of the permeability, which were a consequence of the rapidly increasing knowledge of ferromagnetic phenomena at high frequencies, have led to a new interpretation of the concept of the permeability, which now includes displacement and rotational processes. It is impossible to treat these developments here; they have been reviewed recently by RADO[63] and KITTEL.[44] The very promising results obtained during the last few years in the field of ferromagnetic resonance absorption will contribute considerably to our knowledge of the basic magnetization processes, their origin and their mutual relationship. Only with this fundamental information will it be possible to understand fully the experimental data accumulated in the practical development of magnetic materials and to predict exactly the factors influencing the technical properties of ferromagnetic substances. Reviews of the work done in developing magnetic material for special purposes have been made by SUCKSMITH,[64] STONER[13] and BECKER and DÖRING.[12]

REFERENCES

[1] Weiss, P. *J. de Phys. 6* (1907) 661
[2] Heisenberg, W. *Z. Phys.* 49 (1928) 619
[3] Bloch, F. *Z. Phys.* 74 (1932) 295
[4] Landau, L. and Lifschitz, E. *Phys. Z. Soujet.* 8 (1935) 153
[5] Néel, L. *Jour de Phys. et Rad.* 5 (1944) 241, 265
[6] Lifschitz, E. *J. Phys. U.S.S.R.* 8 (1944) 337
[7] van Vleck, J. H. *Rev. mod. Phys.* 17 (1945) 27
[8] —— *Physica* 15 (1949) 197
[9] Slater, J. C. *Phys. Rev.* 52 (1937) 198
[10] Sommerfeld, A. and Bethe, H. *Handb. Phys.* 242 (1933) 595
[11] Kittel, C. *Phys. Rev.* 76 (1949) 743
[12] Stoner, E. C. *Rep. Progr. Phys.* 11 p 43 London, 1948, *ibid* 13 p 83, 1950
[13] Becker, R. and Döring, W. *Ferromagnetismus* Berlin, 1939, Photolithoprint, Ann Arbor Michigan, U.S.A., 1943
[14] Kittel, C. *Rev. mod. Phys.* 21 (1949) 541
[15] Weiss, P. R. *Phys. Rev.* 74 (1948) 1493
[16] Bozorth, R. M. *J. appl. Phys.* 8 (1937) 575
[17] van Vleck, J. H. *Phys. Rev.* 52 (1937) 1178
[18] Brooks, H. *ibid* 58 (1940) 909
[19] Joule, P. *Phil. Mag. III* 30 (1847) 76
[20] Osborn, J. A. *Phys. Rev.* 67 (1945) 351
[21] Bozorth, R. M. *Physica* 15 (1949) 209
[22] Néel, L. *J. Phys. Radium* 5 (1944) 241
[23] Kittel, C. *Phys. Rev.* 70 (1946) 965
[24] Lilley, B. A. *Phil. Mag.* 41 (1950) 792
[25] Elmore, W. C. *Phys. Rev.* 53 (1938) 757
[26] Williams, H. J., Bozorth, R. M. and Shockley, W. *ibid* 75 (1949) 155
[27] Bitter, F. *Phys. Rev.* 38 (1931) 1903
[28] Williams, H. J. *Phys. Rev.* 70 (1946) 106
[29] Bates, L. F. and Neale, F. E. *Proc. phys. Soc. A* 63 (1950) 374
[30] Bozorth, R. M. and Walker, J. G. *Phys. Rev.* 79 (1950) 888
[31] Martius, U. M., Gow, K. V. and Chalmers, B. *ibid* 81 (1951)
[32] Elmore, W. C. *ibid* 54 (1938) 1092
[33] Mee, C. D. *Proc. phys. Soc. A* 63 (1950) 922
[34] Germer, L. H. *Phys. Rev.* 62 (1942) 295
[35] Lawton, H. and Stewart, K. H. *Proc. roy. Soc. A* 193 (1948) 72
[36] Williams, H. J. and Shockley, W. *Phys. Rev.* 75 (1949) 178
[37] Barkhausen, H. *Phys. Z.* 20 (1919) 401
[38] Stewart, K. H. *Proc. phys. Soc. A* 63 (1950) 761
[39] Sixtus, K. J. and Tonks, L. *Phys. Rev.* 43 (1933) 931
[40] Dijkstra, L. J. and Snoek, J. L. *Philipps Res. Rep.* 4 (1949) 334
[41] Williams, H. J., Shockley, W. and Kittel, C. *Phys. Rev.* 80 (1950) 1090
[42] Döring, W. *Z. Naturforsch* 3a (1948) 373
[43] Becker, R. *Jour de Phys. et Rad.* 12 (1951) 331
[44] Kittel, C. *ibid* p 291
[45] —— *Phys. Rev.* 80 (1950) 918
[46] Kondorsky, E. *Phys. Z. Sowjet.* 11 (1937) 597
[47] Kersten, M. *Phys. Z.* 39 (1938) 860
[48] —— *Grundlagen einer Theorie der ferromagnetischen Hysteresis und der Koerzitivkraft* Leipzig, 1943. Reprinted Ann Arbor, Michigan, U.S.A., 1943
[49] Néel, L. *Ann. Univ. Grenoble* 22 (1946) 299
[50] Dijkstra, L. J. and Wert, C. *Phys. Rev.* 79 (1950) 979

VOL 3

[51] KITTEL, C. *ibid* 70 (1946) 965
[52] DRIGO, A. and PIZZO, M. *Nuovo Cim.* 5 (1948) 196
[53] STONER, E. C. and WOHLFARTH, E. P. *Phil. Trans. A* 240 (1948) 599
[54] KITTEL, C., GALT, J. K. and CAMPBELL, W. E. *Phys. Rev.* 77 (1950) 725
[55] WEIL, L. *C.R. Acad. Sci. (Paris)* 225 (1947) 229
[56] MARTIUS, U. M. *Canad. J. Phys.* 1 (1951)
[57] DÖRING, W. *Z. Naturforsch* 4a (1949) 373
[58] AKULOV, N. S. *Z. Phys.* 69 (1931) 822
[59] GANS, R. *Ann. Phys., Lpz.* 15 (1932) 28
[60] BROWN, W. F. *Phys. Rev.* 60 (1941) 139
[61] NÉEL, L. *J. Phys. Radium* 9 (1948) 184, 193
[62] HOLSTEIN, T. and PRIMAKOFF, H. *Phys. Rev.* 59 (1941) 388
[63] RADO, G. T. *Advances in Electronics* II. Academic Press Inc., New York, 1950
[64] SUCKSMITH, W. *J. Iron Steel Inst.* 163 (1949) 9

VOL. 3

6

QUANTITATIVE X-RAY DIFFRACTION OBSERVATIONS ON STRAINED METAL AGGREGATES

G. B. Greenough

THE STUDY of the phenomena accompanying the deformation of metals has continued for centuries, but the tools available for use in such studies have become rapidly more numerous during the last decades. Initially, work was confined to the measurement of the external strains shown by aggregates of metal crystals during and after the application of stresses. While this allowed the laws of macroscopic behaviour of such aggregates to be deduced, which was of immediate and vital importance in the engineering field, it gave little information regarding the mechanism by which the deformation took place. The later introduction of the optical metallurgical microscope soon led to the discovery that deformation of the aggregates often caused markings on polished surfaces which appeared to differ in type according to the mode of deformation and the metal investigated. The later use of new methods of polishing and of etching, combined with the many powerful microscope techniques now available, has enabled very great progress to be made in the understanding of the mechanisms of deformation in metals following studies of these markings.

Although the optical metallurgical microscope, aided to a small extent by the electron microscope, is probably still the most powerful single tool available for the study of strained metals, x-ray and electron diffraction methods are rapidly attaining an importance almost as great. The fundamental difference is that, whereas microscopic evidence is confined to the effects of the bulk motion of the atoms on the external topography or on etching characteristics, the diffraction evidence is to be interpreted in terms of the atomic positions. It is not possible, however, to detect by diffraction methods whether one atom has taken the place of another *i.e.* the bulk displacement of a group of atoms over a second group by multiples of one atomic distance would be undetectable if it were not accompanied by other changes. The maximum amount of information can therefore only be obtained by utilizing both diffraction and microscopic methods in any particular problem.

It is often claimed loosely that x-ray diffraction methods provide more information than do optical methods because in the latter only

the surface is examined, whereas in the former a volume of metal contributes to the results. But the x-rays used in diffraction work in general penetrate the metal to a small depth only, and it can be shown that more than 50 per cent of the diffracted radiation comes from a surface layer of less than $0{\cdot}693/2\mu$ cm in thickness, where μ is the linear absorption coefficient of the radiation in the metal. In the case of Co$K\alpha$ radiation and iron specimens this gives a figure of $7{\cdot}6 \times 10^{-4}$ cm, which is less than the grain diameter in most iron specimens. It is clear that the metal contributing to the x-ray observations is so close to a free surface that the result is not necessarily representative of the behaviour of metal deep in the aggregate. This, while not detracting from the importance of x-ray diffraction methods, must be remembered when applying the results of such methods.

VOL. 3

X-ray diffraction methods can be divided broadly into two categories, those giving information which can be expressed in quantitative terms, and those giving 'pictures' which provide qualitative information only. Many of the methods falling into the latter category are based on the standard Laue* technique, which has been refined by BARRETT,[3] and made still more elegant by GUINIER,[4] so that it is now possible to see in which particular regions of the crystals there are variations in lattice spacing or in lattice orientation. Essentially, however, these refinements still give qualitative information only. This article is confined to x-ray diffraction work, the results of which have been expressed numerically.

The main material in this chapter is divided into two parts, the first dealing with observations made on aggregates when bulk macroscopic measurements indicate that they are elastically strained, and the second with observations made on plastically strained aggregates. The term 'elastic' is used in a very rough sense, and the type of mechanical strain measurements normally employed in experiments described in the appropriate literature have not been sufficiently exact to detect small departures from elasticity. Since most of the work described has been carried out on iron and mild steel at room temperature, anelastic phenomena can be generally neglected.

EXPERIMENTAL METHODS

If a beam of strictly monochromatic x-radiation, of wavelength λ, is allowed to fall on an aggregate of crystals as in the Debye–Scherrer method, diffraction effects occur. The most marked is the occurrence

* It is not proposed to give specific references to well known x-ray diffraction methods, but only to more recent developments. The standard methods are adequately described in text books.[1, 2]

of a series of cones of diffracted rays about the incident beam as axis. The positions of these cones are defined by Bragg's law:

$$\lambda = 2d \sin \theta \qquad \ldots . \quad (1)$$

where 2θ is the deviation of the diffracted beam from the path of the incident radiation, d the spacing of lattice planes giving rise to the particular cone and λ the x-ray wavelength. The normal to the planes of spacing d always bisects the angle between the incident and diffracted beams, which has given rise to the expression of '*hkl* reflection' to describe a diffracted beam from a lattice where the appropriate value of d is that between *hkl* planes. The region round the specimen is scanned by a recording device, usually a photographic film, and the intersections of the diffraction cones with the recording device give the Debye–Scherrer diffraction 'lines'.

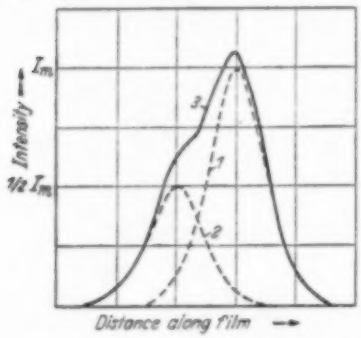

Figure 1. Relation between diffracted X-ray intensity and distance along recording film

These lines have, in fact, a definite breadth and a graph showing the intensity of x-rays plotted against angle θ, or distance along recording film, gives a bell-shaped curve as in *Figure 1* (curves 1 or 2). Three quantitative observations may be made on this diffraction line; the angle corresponding to the position of the peak intensity may be determined, the shape of the curve can be found, and the area under the curve (corresponding to a fixed quantity of incident x-radiation) may be measured. In point of fact, most research workers have not attempted to find the shape of the diffraction line, but have been contented with a measurement of its breadth, which is normally taken as the area under the diffraction line divided by the height of the peak, I_m, and hence is independent of the incident x-ray energy. The amount of experimental data available in each of these three fields of quantitative study is roughly proportional to the ease with which the measurements may be made; most work has been done on the determination of the angle θ, less on the determination of line widths and least of all on the determination of diffraction line intensities. A fourth measurement which can be made is that of the intensity of the x-radiation which is falling between the diffraction lines, again for a fixed value of incident x-ray energy. This intensity is very small and its measurement experimentally difficult, and very little research of this type has been reported.

While it is not intended to describe the standard methods of

eliminating experimental errors in the determination of these various quantities, there is one point arising generally in the work discussed which does not seem to be widely appreciated. x-ray diffraction work is usually carried out using doublets consisting of two wavelengths close together, in which the intensity of the α_1 component is very nearly twice that of the α_2. If the metal under investigation is annealed, it normally shows two well defined diffraction peaks, each of which may be measured. But after plastic deformation, two broad peaks arise corresponding to curves 1 and 2 in *Figure 1*, and the observed distribution of intensity is as in curve 3.

The difficulty of determining line breadths in such cases has received wide attention, but the systematic errors in determining the position of the diffraction line peaks in such cases have been neglected. NEERFELD[5] first pointed out that the actual photometer peak deviated from the true α_1 position and gave a method for determining the true position from the apparent value if an intensity distribution curve is plotted. He also made the very interesting observation that the peak position estimated by eye was between the true peak and that recorded by the photometer. FINCH[6] has also described a method of finding the position of the α_1 peak from the experimental intensity curve, while RACHINGER,[7] from whose paper *Figure 1* is taken, described a simple graphical method for separating the components.

In view of the widespread belief that recrystallization of a worked metal, evidenced by the appearance of sharp reflection spots in a Laue photograph, is an effective method of producing a strain free aggregate, it is worth calling attention here to the observation of CRUSSARD and AUBERTIN.[8] This is discussed further on page 198, but the important point is that recrystallization is not sufficient to remove all strains in the metal, and that considerably higher annealing temperatures are necessary to do this. In the work described in this chapter it is tacitly assumed that the initial material was always strain free, but authors seldom quote the evidence on which they base their assumption.

ELASTICALLY STRAINED AGGREGATES

Most x-ray diffraction work which has been performed on elastically strained aggregates has been concerned with the measurement of the movement of the x-ray diffraction line peak as the stress applied to the aggregate has been changed. The movement of the diffraction line has been evaluated as a change $\delta\theta$ in the Bragg angle of reflection, and the corresponding fractional change in the interplanar spacing calculated from the differential of the Bragg equation (equation 1). The strains thus obtained represent the average value of the strains in the directions of the normals to the lattice planes in those crystals so

orientated as to reflect the particular diffraction line examined. It is convenient to term these 'lattice strains'. The investigation of the lattice strains in elastically strained aggregates necessitates the examination of specimens under stress. Normally a case of simple uniaxial tension is investigated, the tensile stresses being applied either directly or by using a bent strip, but experiments using torsional stresses have also been reported. Considerable interest has been attached to these investigations, particularly because of their importance in the technological application of x-ray methods to the measurement of locked-up body stresses in fabricated metal components. Their theoretical interest lies in the light they shed on the elastic behaviour of an aggregate of crystals, each of which is anisotropic.

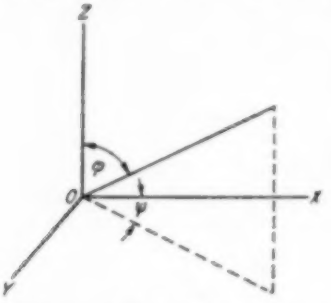

Figure 2. The definition of a direction in the aggregate, OZ is normal to the surface of the specimen

The elastic theory of isotropic bodies shows that the strain, ε, in any direction, defined by the angles ϕ and ψ shown in *Figure 2*, due to the two principle stresses σ_X and σ_Y is given by:

$$\varepsilon = [\cos^2\psi \sin^2\phi(\sigma_X - \nu\sigma_Y) + \sin^2\psi \sin^2\phi(\sigma_Y - \nu\sigma_X) - \nu\cos^2\phi(\sigma_X + \sigma_Y)]/E \quad . \quad (2)$$

where E and ν are Young's Modulus and Poisson's ratio.

It is generally accepted that if the strains are measured by mechanical means in fine grained metal aggregates in which the crystals are randomly orientated, this equation is obeyed for all angles ϕ and ψ for unique values of the constants E and ν. Since it is known that single crystals of most metals are elastically anisotropic *i.e.* they do not obey equation 2, it is clear that the 'quasi-isotropic' properties of the aggregate arise because an average is taken of the anisotropic properties in grains of a large number of random orientations. If the aggregate shows preferred orientation of the component crystals, then the mechanically measured strains do not generally satisfy equation 2.[1, 9]

In experiments employing applied uniaxial tensile stresses, the apparatus and directions of lattice strain measurement are usually such that $\sigma_Y = 0$ and $\psi = 0°$ *i.e.* equation 2 reduces to:

$$\varepsilon/\sigma = (\sin^2\phi - \nu\cos^2\phi)/E \quad . \quad . \quad . \quad . \quad (3)$$

where σ is written for σ_X. Observations have usually been carried out for two values of ϕ, in which case, if it is assumed that equation 3 is applicable, values of E and ν can be deduced and compared with the macroscopic values of the elastic constants. An alternative method is to compare the experimental values of the ratio of lattice strain to

applied stress with the calculated macroscopic ratio for the same direction; this is to be preferred because equation 3 is then assumed to be applicable to the bulk macroscopic strains only, which is justified.

MOLLER and BARBERS[10] first reported results for the values determined for ε/σ by x-ray methods. They examined the 310 reflection from steel for various values of the tensile stress σ and showed that the ratio of ε/σ at $\phi = 0°$ was significantly greater than the values calculated from equation 3 using the appropriate macroscopic values of E and ν. This experimental observation has been confirmed by more careful work by many authors,[11–15] who agree within the limits of experimental error that $(\varepsilon/\sigma)_{\text{x-ray}} = 1{\cdot}25(\varepsilon/\sigma)_{\text{mech}}$ for the 310 reflection from steel at $\phi = 0°$. Typical of the results in which the 'x-ray values' of E and ν are quoted are those which were deduced by MOLLER and MARTIN.[11] They showed that $E_{\text{x-ray}} = 22{\cdot}03 \times 10^3$ kg/mm^2 and $\nu_{\text{x-ray}} = 0{\cdot}374$, while $E_{\text{mech}} = 21.00 \times 10^3$ kg/mm^2 and $\nu_{\text{mech}} = 0{\cdot}28$. It does not appear that any work has been performed to measure the lattice strains for three values of ϕ in order to investigate whether single values of E and ν would satisfy equation 3 in all three cases. On the other hand, GLOCKER and SCHAABER[16] reported that the torsional modulus determined for mild steel using the 310 reflection was the same as the macroscopic value. The work using tensile stresses was repeated by NEERFELD[14] and HAUK[15] for the 211 reflection from steel. These workers agreed that the value of $(\varepsilon/\sigma)_{\text{x-ray}}$ at $\phi = 0°$ is significantly less than $(\varepsilon/\sigma)_{\text{mech}}$, but they obtained different values for $(\varepsilon/\sigma)_{\text{x-ray}}/(\varepsilon/\sigma)_{\text{mech}}$. Hauk found this ratio to be 0·77, while Neerfeld obtained the value of 0·90.

The lattice strains in directions normal to applied uniaxial tensile stresses have also been determined for copper[17] and for aluminium[18, 19]. For copper SMITH and WOOD reported that the ratio of $(\varepsilon/\sigma)_{\text{x-ray}}$ to $(\varepsilon/\sigma)_{\text{mech}}$ was 1·5 for the 400 reflection and 0·60 for the 331 reflection. In the case of the 420 reflection from aluminium, again at $\phi = 0°$, the same authors reported that the ratio determined by x-ray methods was the same as that calculated from the mechanical elastic constants. KOCHANOVSKA[19] has also investigated aluminium at $\phi = 0°$, and made measurements on the 222, 420 and the combined 511, 333 diffraction lines. She showed that the ratio of the lattice strain to the applied stress was the same in each case.

It was realized[10] from the beginning that the difference between the lattice strain/stress ratio and the value calculated using the elastic constants appropriate to the aggregate as a whole, arose because of the anisotropic elastic properties of the individual crystals composing the aggregate combined with the selective action of the x-rays. All the grains in the aggregate contribute to the mechanically measured strains

irrespective of the direction in which the strain is measured, consequently the values determined are the means of those in all the individual anisotropic crystals obtained by averaging over all orientations. On the other hand, if a crystal is contributing intensity to a particular x-ray line, the direction of the normal to the planes reflecting must be inclined to the incident beam at an angle $90° - \theta$, as shown in *Figure 3*. If the recording film is stationary, and measurements are made at a given point on the Debye–Scherrer ring, then the direction of the reflecting normal is fixed and its direction defines the direction of the lattice strains measured by the x-ray diffraction method. These strains are thus the means of the strains in those crystals whose reflecting normals are inclined at an angle ϕ to the perpendicular to the specimen surface. This mean, being an average over particular orientations, is not to be expected to be the same as the average for all orientations. It should be noted that the crystals contributing to a given diffraction line change as ϕ varies.

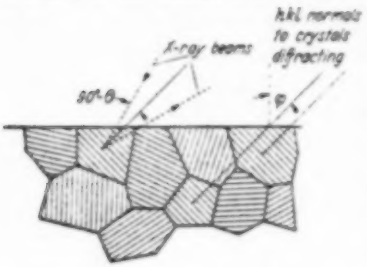

Figure 3. Directions of hkl planes in crystals of an aggregate; only those with [hkl] in appropriate directions contribute to the diffracted beam

Although the direction of the reflecting normal is fixed, the reflecting crystals may have any orientation about this normal. To represent the relation of the applied stress direction to the possible orientations of the crystals reflecting, it is easiest to use a stereographic projection in which the crystal is regarded as being fixed in space while the direction of the applied stress varies within the appropriate limits. *Figure 4* shows the locus of the applied tension for the case of the lattice strain measured at an angle ϕ using the *hkl* reflection.

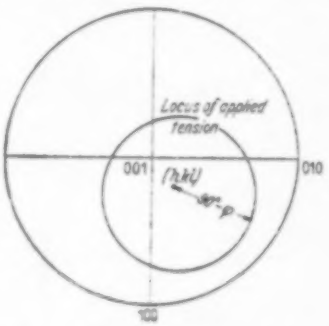

Figure 4. Possible directions of applied tension relative to crystal axes when hkl planes are reflecting

It is clear that it should be possible to correlate $(\varepsilon/\sigma)_{\text{x-ray}}$ with some value calculated from a knowledge of the single crystal elastic constants, but the fundamental mathematical difficulty in the calculation is to allow for the interaction of one crystal on its neighbours during the deformation. It is not possible for both stress and strain to be continuous across the boundary of contact between two anisotropic crystals

of different orientations, and some assumption must be made in the calculation as to which components do maintain continuity. Before the investigation of the lattice strain/stress relations was attempted, this type of calculation had been performed to relate the macroscopic elastic constants of a random aggregate to those of the component crystals and the calculations for the x-ray case are adaptions of the earlier work. So far, it appears that only the two simplest possible assumptions, first proposed by VOIGT[20] and by REUSS,[21] have been applied to the x-ray case, although more complicated assumptions were made by BRUGGEMAN[22] and by BOAS and SCHMID[23] for the case of macroscopic relations.

In the following short discussion of the theoretical treatments of random aggregates it must be remembered that three assumptions are implicitly made. The first is that the crystals in the aggregate are small compared with the volume examined, the second is that the crystals have a random orientation in the aggregate and the third is that the crystals in which the strains are examined are constrained by neighbours at all their surfaces. These assumptions should be made valid in any experimental investigation. In practice, it is easy to satisfy the first condition, and experimental checks would show whether there was the desired absence of preferred orientation in the aggregate. The third condition can never be completely satisfied, however, since the grain size of an annealed metal cannot be made small compared with the depth of penetration of the x-rays, for which a typical value is quoted in the introduction. The theoretical treatment can be applied to crystals of any symmetry, but the formulae quoted here are those applicable to cubic crystals. The notation used is that employed by Voigt, which differs from that employed by WOOSTER.[24]

VOIGT[20] (p 962) makes the assumption that the strains are the same in all the crystals and that the aggregate as a whole obeys the elasticity laws for isotropic bodies. The stress in each crystal is calculated and the average stress in the random aggregate determined by averaging over all possible orientations. The relations between the assumed strain and this calculated stress are used to obtain the following relations for Young's Modulus $E_{\varepsilon=\text{const}}$ and Poisson's ratio $\nu_{\varepsilon=\text{const}}$:

$$E_{\varepsilon=\text{const}} = \frac{(c_{11} + 2c_{12})\,(c_{11} - c_{12} + 3c_{44})}{2c_{11} + 3c_{12} + c_{44}} \quad \ldots\ (4)$$

$$\nu_{\varepsilon=\text{const}} = \frac{c_{11} + 4c_{12} - 2c_{44}}{2(2c_{11} + 3c_{12} + c_{44})} \quad \ldots\ (5)$$

Since the strain in a given direction in every crystal is assumed to be the same, this treatment leads to the result that the strain measured by x-ray methods should be independent of the reflection examined and

identical with the macroscopic strain. The lattice strain/stress ratio for all reflections is therefore:

$$(\varepsilon/\sigma)_{\sigma=\text{const}} = \frac{1}{E_{\sigma=\text{const}}} (\sin^2\phi - \nu_{\sigma=\text{const}} \cos^2\phi) \quad . \quad . \quad . \quad . \quad (6)$$

Reuss assumes[21] that the stress in each crystal in the aggregate is the same and is equal to that applied to the aggregate. The strains in a crystal of general orientation are then calculated and the average strains for the grains in the aggregate obtained by averaging over all orientations. This average value must, on this assumption, be equal to that of the aggregate which will obey the isotropic elasticity equations. This treatment gives for Young's Modulus, $E_{\sigma=\text{const}}$ and Poisson's ratio $\nu_{\sigma=\text{const}}$ the following relations:

$$E_{\sigma=\text{const}} = \frac{5}{3s_{11} + 2s_{12} + s_{44}} \quad . \quad . \quad . \quad . \quad (7)$$

$$\nu_{\sigma=\text{const}} = \frac{2s_{11} + 8s_{12} - s_{44}}{2(3s_{11} + 2s_{12} + s_{44})} \quad . \quad . \quad . \quad . \quad (8)$$

To apply this method to the case of strains measured by x-ray methods, as was done by MOLLER and BARBERS,[10] it is necessary to carry out the averaging of the strains in grains for which the stress σ lies on the locus shown in *Figure 4*. A recalculation of this value, using a notation dissimilar to that used by Moller and Barbers, shows that the relation between the strain measured by x-ray diffraction methods and the stress applied to the aggregate is :

$$(\varepsilon/\sigma)_{\sigma=\text{const}} = s_{11}\sin^2\phi + s_{12}\cos^2\phi - (s_{11} - s_{12} - \tfrac{1}{2}s_{44})(A_{13}^2A_{23}^2 + A_{23}^2A_{33}^2 + A_{33}^2A_{13}^2)(2\sin^2\phi - \cos^2\phi) \quad . \quad . \quad . \quad . \quad (9)$$

where A_{13} *etc* are the direction cosines of the reflecting normals of the particular planes diffracting with respect to the crystallographic axes. The value of this ratio depends on the diffraction line employed, and in general will be different from the macroscopic ratio. If the crystals composing the aggregate are isotropic, then it can be shown that the two formulae 6 and 9 become identical (since the condition for isotropy is $2s_{11} - 2s_{12} - s_{44} = c_{11} - c_{12} - 2c_{44} = 0$).

Experimental values for the macroscopic elastic constants of polycrystalline aggregates do not agree with the results calculated from either theory, but they do agree remarkably well with the mean of the two theoretical values. NEERFELD[14] and HAUK[15] both made observations on steel at two values of ϕ using the 310 and 211 diffraction lines. They calculated from their experimental observations the constants $-\nu/E$ and $2(1+\nu)/E$ appropriate to each diffraction line

assuming that equation 3 was applicable, and both authors concluded that there is no agreement between experiment and either of the individual theories. They agree that the experimental values for the 310 reflections are the same as the mean of the two theoretical values, but while Neerfeld found that the same conclusion applied for the 211 reflection, Hauk concluded that there was a significant difference (this disagreement arises because of the difference in experimental value determined by the two authors, already noted on page 181). The summary given by Neerfeld of his results for iron is shown in *Table I*. The experimental values found by SMITH and WOOD[17] for copper are also quoted in *Table I*, together with the appropriate quantities calculated from equations 6 and 9 using the single crystal elastic moduli determined by GOENS and WEERTS.[25] Results for $(\sigma/\varepsilon)_{\text{x-ray}}$ are available for the 420 planes of aluminium, but since single crystals of aluminium are almost isotropic, both the possible theoretical treatments give very similar results. Both agree with the experimental values within the limits of experimental error. NEERFELD[26] has also stated that the mean of the results from the two theoretical calculations agrees with values obtained experimentally from copper and brass as well as from iron, but the figures are not available.

Table I. Comparison of Experimental and Theoretical Values of Elastic Strain/Stress Ratios

Metal	*Method of Measurement*	*Factor Investigated*	*Theoretical Value* $mm^2/kg \times 10^5$			*Experimental Value* $mm^2/kg \times 10^5$
			Eqn. 6	*Eqn.* 9	*Mean*	
Iron ..	*Macroscopic*	$-\nu/E$	− 1·21	− 1·56	− 1·38	− 1·36
		$2(1+\nu)/E$	11·06	13·52	12·29	12·22
	310 *X-ray line*	$-\nu/E$	− 1·21	− 2·23	− 1·72	− 1·69
		$2(1+\nu)/E$	11·06	17·18	14·12	13·70
	211 *X-ray line*	$-\nu/E$	− 1·21	− 1·28	− 1·24	− 1·22
		$2(1+\nu)/E$	11·06	11·46	11·26	11·46
Copper ..	*Macroscopic*	ε/σ at $\phi = 0°$	− 2·29	− 3·39	− 2·84	− 2·85
	400 *X-ray line*	ε/σ at $\phi = 8·7°$	− 2·09	− 5·87	− 3·98	− 4·38
	331 *X-ray line*	ε/σ at $\phi = 12·4°$	− 1·87	− 1·87	− 1·87	− 1·71

It should be noted that if the agreement between the experimental value and the mean of the theoretical values is found to be general at all values of ϕ, then it follows from the form of the equations 6 and 9, which for a particular x-ray diffraction line contain only terms in $\sin\phi$, $\cos\phi$, and constants, that the simple equation 3 may be applied

to lattice strain measurements with x-ray values for E and ν. In this case some meaning may be attached to elastic constants determined by x-ray methods. It does not seem likely, however, that x-ray methods can be used to determine macroscopic values of elastic constants. HANSTOCK and LLOYD[27] have obtained agreement between values obtained mechanically and by measurements on the 420 reflection from duralumin, but this was probably a direct result of the almost isotropic properties of aluminium single crystals.

Since the crystals contributing to a given point on a Debye–Scherrer ring are not confined to a single orientation, but may have any orientation about the reflecting normal, it is evident that in a stressed aggregate these crystals will exhibit different amounts of strain. In addition, whereas the theoretical strain calculated for a crystal of a particular orientation applies to the average grain of that orientation surrounded by average neighbours, the strain in any individual crystal will be influenced by its particular neighbours and differ somewhat from the theoretical value. For both these reasons, of which the first is the more important, it is to be expected that the x-ray diffraction lines will broaden as the stress applied to an aggregate is increased. There may, of course, be additional causes of line broadening.

No experimental work has been carried out to correlate the possible line broadening with the theoretical treatment of elastically strained aggregates, and there are few references to any observations on the line broadening due to elastic strains. During the course of a quantitative investigation of the line broadening caused by stresses applied to aggregates, WEVER and PFARR[28] made some observations on elastically stressed specimens. They concluded that any line broadening which did occur was too small to be detected by their measurements. Smith and Wood, during their experiments on copper,[17] made qualitative observations on the line broadening and came to the conclusion that it was small when their specimens were elastically deformed. In general, the evidence available indicates that there probably is a certain amount of line broadening in elastically strained aggregates, but that it is small. It does not seem likely that present experimental methods of determining line broadening will be able to give results of sufficient accuracy to be compared with any theoretical values.

PLASTICALLY STRAINED AGGREGATES

x-ray diffraction methods have been widely employed to investigate plastically deformed aggregates, and quantitative observations have chiefly been made on the movement of the peaks of diffraction lines or on the change of their breadths. Occasional results have been given for the change of intensity of the diffraction lines after cold-working

metals, and very rarely for the x-ray intensity scattered into the background, although the development of more powerful x-ray tubes and the availability of curved crystal monochromators and of efficient Geiger counters should soon lead to more information in this last field of work. From the point of view of reaching a better understanding of the atomic movements accompanying plastic deformation, this is extremely desirable, since mathematical[29] treatments of certain postulated defects in crystal lattices have shown that intensity measurements should be susceptible to a more rigid interpretation than the other measurements.

Apart from a few notable exceptions, there has been a general tendency in published literature for experiments to be described in which only one of the three possible types of quantitative measurement has been made. In several instances the taking of more quantitative data would have removed a certain amount of ambiguity of interpretation of results. The advantages of making several types of observation during a single experiment are now becoming more generally realized, and the results of these experiments should be extremely valuable.

The outlook adopted in most of the research published up to the time of writing has been to report certain experimental observations and then to attempt an explanation. Experiments later carried out to verify any such explanation have usually employed the same type of technique as was used in the earlier work. It has thus been easiest to classify the available data in groups characterized by the nature of the experimental method used, rather than to attempt a classification based on the nature of the explanations put forward.

MOVEMENT OF DIFFRACTION LINE PEAKS

Experimental work in this field is usually an extension of research into the lattice strains in elastically strained aggregates, although additional results are also available. In addition to causing a movement of the diffraction line peaks, plastic deformation also causes a marked broadening of the x-ray diffraction lines and, as has been discussed on page 179, this may lead to a systematic error in the measurement of the position of the peak of the diffraction line; many authors do not make any correction for these possible errors. In general, results deduced from x-ray diffraction photographs in which the $K\alpha$ doublets are clearly distinguished and show displacements which agree with each other are probably free from systematic error, but care is necessary when interpreting results of experiments in which the amount of plastic deformation has been large enough to produce diffraction lines in which the α doublet is not distinguishable.

It has been pointed out already that if the peak of the diffraction line is displaced, it can only be interpreted in terms of a change of the average spacing of the *hkl* planes in all those crystals so orientated that they contribute diffracted intensity to the point of measurement of the Debye–Scherrer ring. This change in average spacing has been termed a lattice strain, although it seems unlikely that the term can be confined to those displacements of atoms from their equilibrium separations which result in movements of diffraction line peaks.

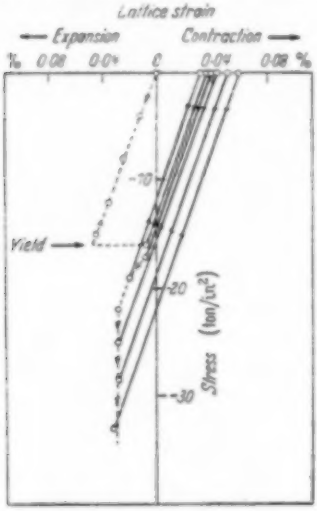

Figure 5. Lattice stress/strain curve for mild steel in compression where the strain refers to the percentage change in (310) spacing in the direction perpendicular to the stress

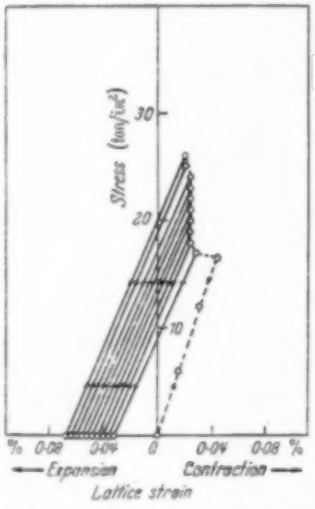

Figure 6. Lattice stress/strain curve for mild steel in tension where the strain refers to the percentage change in (310) spacing in the directions perpendicular to the stress

It is convenient to discuss first work in which the plastic deformation has been caused by simple uniaxial extension or compression. In its most complete form such work involves the construction of a curve showing applied stress as a function of lattice strain for stresses almost up to those causing fracture of the aggregate, incorporating cycles of unloading and loading for various intermediate stresses. *Figures 5* and *6* show two such curves for both tensile and compressive stresses determined by SMITH and WOOD[30] for steel using the 310 diffraction line in each case.

These curves show very clearly the two points of significance in the plastic range. While the lattice strain is proportional to the applied stress up to the yield stress* of the steel, as determined by mechanical

* No attempt appears to have been made in experiments on mild steel to differentiate between the limit of elasticity and the stress required to reach the yield point.

measurements, at higher stresses the increase in lattice strain per unit stress is less than that in the elastic range. In this region, of course, the increase in macroscopic strain per unit increase of applied stress is very much larger than in the elastic range. The second important point is that if the specimen is unloaded from a stress above the yield stress, there remains a lattice strain. This has been termed a residual lattice strain.[31] With angles of incidence of $\phi = 0°$, Smith and Wood have shown[12, 30] that the lines of unloading are parallel to the initial elastic line, so that the two observations appear to be connected. Similar curves have been described for the combined 651 and 732 diffraction line for steel by GREENOUGH[32] and for the 420 diffraction line for aluminium again by SMITH and WOOD.[18] Data of a similar type, although not given in the form of lattice strain/stress curves, has been obtained by HAUK[33] for the 420 reflection from aluminium and from an aluminium–copper–magnesium alloy.

Although these authors demonstrated the effects most clearly, they had been discovered some years earlier by WEVER and PFARR,[28] who investigated the 310 diffraction line from steel during tensile tests, and the observations had been confirmed by BOLLENRATH, HAUK and OSSWALD,[34] and others, under similar conditions. However, until Bollenrath *et al* directed attention to the matter, the earlier German work appears to have been more concerned with the behaviour of the lattice strain/stress curve in the elastic region.

All these authors agree that the region in which the lattice strain ceases to be proportional to the applied stress is confined to that above the macroscopic yield stress of the metal. But GLOCKER and HASENMAIER[35] have reported that for the 211 reflection for mild steel the lattice strain ceases to be proportional to applied stress for stresses above about three quarters of the macroscopic yield stress. This is directly contrary to the later experimental evidence by WOOD[36] who showed that for this particular diffraction line the limit of proportionality for the 211 reflection is the same as the macroscopic yield stress. Related observations have been made by GARROD[37] who, although not reporting the lattice strains determined on specimens under applied stresses, has observed that residual lattice strains appear on unloading from points below the yield stress. This was so for each of the 310, 211, 220 and combined 651 and 732 diffraction lines; *Figure 7* is taken from his paper. However, FINCH[38] has stated that if the loading of the test specimen was truly axial, the criterion for which he took as the development of well marked macroscopic upper and lower yield points, he observed that the lattice strain for the 310, 211 and 220 reflections was always proportional to applied stress up to the yield stress, and that residual lattice strains never developed until macroscopic plastic deformation had occurred. It is clear that the majority

of the experimental evidence is in favour of the view that the non-proportional region for lattice strains does commence at the macroscopic limit of proportionality.

The explanation of the lattice strain effects accompanying the plastic deformation of polycrystalline aggregates has been sought by several workers. They have all assumed that the residual lattice strain observed in unloaded specimens has been connected with the lack of proportionality between lattice strain and applied stress in the region above the yield stress, and have concentrated their attentions on

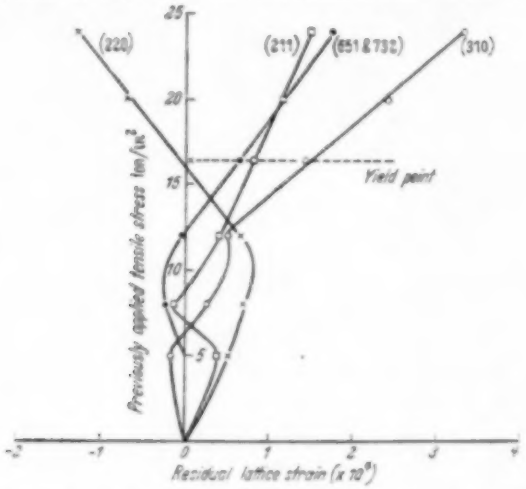

Figure 7. Residual lattice strains observed for various reflections from mild steel after removing applied tensile stresses of various magnitudes

explaining such residual lattice strains. The explanations which have been put forward fall into three main types which suggest that the effects are due to:

a some trivial experimental circumstance such as the bending of the test piece or a systematic error in the measurement of blurred diffraction lines

b a general expansion of the lattice

c some form of locked-up stress system. In this case there are several possible detailed interpretations of the stress system.

It is now clear that the effect cannot be due to bending of the test specimens caused by non-axial loading because, apart from experiments in which special precautions have been taken to ensure axial loading as in the work of Finch and that of Wood, measurements of residual lattice strains at opposite sides of specimens have been shown to agree.[32] NEERFELD[5] has examined the residual lattice strains determined for

the 310 reflection from mild steel after making corrections for the line broadening. He concluded that, although part of the strain could be attributed to systematic errors in measurement, a considerable fraction of the 'observed' strain was real. This was confirmed by Finch who also corrected his lines for broadening, and indirectly by Garrod and Greenough who observed residual lattice strains using molybdenum $K\alpha$ radiation, the doublet of which does not broaden sufficiently even after cold working to produce any appreciable error in the determination of the diffraction line peak. The residual lattice strain is thus a real phenomenon.

The suggestion that the residual lattice strain might be due to an all-round expansion of the lattice was first put forward by SMITH and WOOD[12] following an experiment in which they sectioned a plastically extended specimen, removed the cold-worked layer by etching, and observed an expansion of the 310 spacing in a direction parallel to the direction of elongation. Later they found[30] that this result might have been spurious. In the same paper these authors have shown that the residual lattice strain sometimes takes the form of a contraction, as in the case of the strain observed at $\phi = 0°$ for the 310 reflection from compressed steel, illustrated in *Figure 5*, and also in an extended specimen when ϕ is large. There is general agreement now that any overall expansion of the metal lattice cannot be the sole, or even the major, cause of the observed residual lattice strain. However, there is no evidence that the plastic deformation causes no increase in lattice volume whatever, and since many lines of approach *e.g.* by ZENER,[39] would indicate that cold working should produce some expansion of the lattice, it is quite possible that such an effect will make a small contribution to observed residual lattice strains.

The third possible explanation, that of a locked-up stress system in the aggregate, depends in all its modifications on the same mechanism for the development of the stress system. It is assumed that different parts of the aggregate have different tensile yield stresses *e.g.* that part *A* yields under a lower applied stress than part *B*. After the application of a tensile stress sufficiently great to deform the whole aggregate, the elastic strain in *A* will be less than in *B*. When the applied stress is removed, *B* will tend to contract further than *A* but will be prevented from so doing by the restraining influence of *A*. The final equilibrium state will be one in which *A* is in compression and *B* in tension such that the mean value of the residual loads across any plane section of the specimen vanishes. The argument, of course, can be applied generally when the specimen has a large number of different parts. All published work tacitly agrees this argument is correct, but controversy exists as to the exact nature of the parts *A*, *B etc.*

Bollenrath, Hauk and Osswald were the first to describe a precise

interpretation of this general explanation and gave evidence to support it. They pointed out that grains with a free surface probably had a lower yield stress than those which were completely surrounded by other grains. In terms of the above explanation, grains in the surface form part *A* of the specimen and grains in the interior form part *B*. This explanation is qualitatively reasonable and is generally in accord with many scattered experimental observations of various types other than x-ray diffraction work. Since x-rays penetrate the metal to a very small depth only, the measurements indicate the behaviour of the surface layer *A* only.

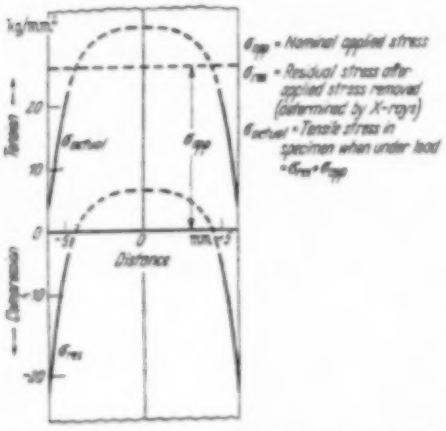

Figure 8. Distribution of tensile stress in a steel test piece of square cross section after a plastic extension of 3 per cent

Bollenrath and his co-workers plastically extended a mild steel specimen and observed the residual lattice strain at surfaces successively exposed by etching away layers of the metal. From the change of the lattice strain with depth, they constructed a curve showing the relation of the longitudinal stress remaining in the specimen to the position in the specimen. This curve is shown in *Figure 8*. It will be seen that the compressive stress at the surface is very high, almost as great as that applied to the aggregate to cause the plastic deformation, and that the depth of the stressed layer is about 1 mm. It seems to the present writer that the evidence presented in this paper is surprising for two reasons. First the 'strain-free' lattice spacing calculated from the measured strained values varies with the depth etched away from the surface of the specimen; the authors cannot account for this and it may indicate some large error in the stress measurement. Secondly, the residual compressive stress is very much higher than the maximum tensile stress presumably reached by the surface layer when the aggregate is under stress; it does not seem likely that the yield stress of the surface could be so different for tension and compression.

This result, however, is supported to some extent by the interpretation put on their own results by Glocker and Hasenmaier (see page 189). They interpreted the difference in apparent yield stress observed for the 310 and 211 diffraction lines as due to the difference in penetrative powers of the Co$K\alpha$ and Cr$K\alpha$ radiations used to record the reflections.

On the other hand, it is contradicted entirely by the results of SMITH and WOOD[40] who report that the residual lattice strain remains unchanged at surfaces exposed by successively etching away layers of the specimen. Moller and Neerfeld have reported,[26] very briefly, an experiment of the Sachs boring-out type in which mechanical strain measurements were used to examine the macroscopic residual stresses in plastically extended steel rods. They found no stress variation across the section of the specimen. A similar investigation by DAVIDENKOV and TIMOFEEVA[41] on stretched aluminium sheets also indicated that there was no residual compressive surface stress.

In connection with experiments involving the etching of steels, it is worth while drawing attention to a paper by LIHL[42] who has measured by x-ray diffraction methods the stresses caused by etching certain types of steel, either chemically or electrolytically, using acid solutions. These stresses are always compressional and Lihl states that they are brought about by the expansion of intercrystalline impurities and alloying material as a result of the absorption of hydrogen and preferential attack by the etchant. It is clear, therefore, that in any experiment designed to investigate the variation in lattice strain in steels as layers are removed by etching, care must be exercised in the choice of the steel and etching technique.

In a recent paper[43] the present writer describes results which indicate that a biaxial stress system exists in a very thin layer about 0·2 mm thick at the specimen surface. The stresses are much smaller than those reported by Bollenrath *et al*, being only about one fifth of the applied stresses, and are superimposed on an intergranular stress system described later in this article. The results are shown to be consistent with those of Moller and Neerfeld and of Davidenkov and Timofeeva (whose methods were not sensitive enough to detect the small stresses found), but not with those of Smith and Wood nor of Bollenrath *et al*.

In conclusion, it will be seen that the present position regarding the presence or absence of a surface macroscopic stress is by no means clear. But this evidence, together with that to be described, indicates that although surface macroscopic stresses might play some part in producing residual lattice strains, they are not the sole operative factor.

A second interpretation could be based on that put forward during an unpublished discussion in 1943 between Bragg, Orowan, Smith and Wood. It is possible that, during the process of plastic deformation, the accumulation of dislocations round obstacles to their propagation through the crystal would cause higher stresses there than in the remaining bulk of the crystal. These regions of accumulated dislocations form the parts *B* of the specimen, and after the removal of the applied stress they are left in a state of stress, these stresses being balanced by stresses in the bulk of the crystal remote from the

dislocations. The lattice strains in the regions of the dislocations would probably be insufficiently regular to contribute to the diffraction line, and the lattice strain observed would be that in the remaining bulk of the crystal. Later, Smith and Wood put forward a very similar hypothesis in which the grain boundaries were postulated as becoming amorphous and these amorphous regions were much harder than the crystalline remainder.[40]

It is not easy to make a simple experimental check of the hypothesis. It seems probable that the most direct evidence would be obtained by measuring x-ray diffraction line intensities and by studying the background due to the incoherent scattering of x-rays by the 'amorphous' parts of the specimen. Experimental evidence of this type is discussed later in this article, but conclusions drawn from it indicate that the amount of amorphous material formed by cold working is likely to be either zero or very small, particularly after plastic deformations of 1 or 2 per cent which are sufficient to develop residual lattice strains. This, although unfavourable to the hypothesis, cannot be said to disprove it completely since it is possible to argue that the amorphous material has a very high yield stress and a very small volume of it is sufficient to balance the stresses in the crystalline portions.

The last interpretation is based on that put forward[44*] by Heyn and by Masing to explain certain macroscopic phenomena as the Bauschinger effect associated with plastically deformed polycrystalline aggregates. Since the tensile yield stress of a crystal depends on its orientation, the individual crystals in the aggregate themselves act as the parts *A*, *B*, *C etc* in the specimen. Following the general argument given earlier, after the plastic elongation of the aggregate some crystals are left in tension and others in compression. GREENOUGH[45] pointed out that only those grains with the appropriate orientations would contribute to a particular diffraction line, and that, following Heyn's arguments, these grains were likely to be, on the average, in tension or in compression. Experimental evidence qualitatively in favour of this explanation has been given for iron and mild steel by GREENOUGH[45] (see also GREENOUGH[46]), by FINCH[38, 47] and by GARROD[37] (see *Figure 7* in the region for applied stresses above the yield point). Measurements on magnesium, aluminium, copper and nickel by GREENOUGH[31, 45] show that in these metals also different diffraction lines show different residual lattice strains, sometimes positive and sometimes negative (a positive sign is used to denote an increase in interplanar spacing, and a negative sign a decrease).

* It is customary to quote as a reference to this topic E. HEYN, *J. Inst. Met.* 12 (1914) 3. But while Professor Heyn discussed in this paper residual stresses arising from many causes, he did not mention the specific cause of importance in this case. SEITZ[44] gives other references to Heyn's work, and to that of Masing.

A summary of results for mild steel is given in *Table II*. Finch and Garrod were using specimens whose test dimensions were of the order of 0·5 cm × 0·3 cm, while Greenough was using wires of diameters

Table II. Residual Lattice Strains in Plastically Extended Mild Steel Specimens (No stress applied to the aggregate)

Plane Reflecting	*Residual Lattice Strains* $\times 10^5$		
	1	*2*	*3*
310	20	34	24
211	1	16	7
110	− 24	− 13	− 25
Stress previously applied kg/mm²	c 47	38	43
Plastic extension per cent ..	19	—	19

1 Finch[40] *2* Garrod[37] *3* Greenough[41]

0·5 mm. The experimental errors in the determinations were about $\pm 2 \times 10^{-5}$. It will be noted that while the *relative* values of the residual lattice strains are very similar in the three cases, the absolute values are significantly different. Finch has emphasized[38] that the x-rays are diffracted by the ferrite crystals in the steel, but that cementite is also present which will influence the residual stress distribution. A 'mild steel' may contain varying amounts of cementite, and its presence would tend to add a positive bias to all the measured residual lattice strains although it would have no appreciable effect on their relative values.

It should be possible to calculate the expected residual lattice strain theoretically from a knowledge of the mechanisms of plastic deformation of grains in an aggregate. Greenough has attempted this[31] using methods analagous to those described for the determination of elastic constants. Several approximations were made to simplify the calculations, but good agreement was obtained for face-centred cubic metals between the experimentally observed relative values of the residual lattice strains and the theoretical quantities, provided that it was assumed that each grain was undergoing the same change of shape as the aggregate as a whole by the combination of five glide motions discussed by TAYLOR.[48] The residual lattice strains should, theoretically, be proportional to the applied stress required to cause deformation of the aggregate, provided that this stress is big enough to cause plastic flow in all the grains. A similar calculation is impossible (in practice) for iron because of the large number of possible ways of selecting five glide motions out of those possible. However, it was concluded that,

although the Heyn intergranular stresses made a large contribution to the observed residual lattice strains, there must be some other effect since all the observed strains were more positive than anticipated. This second influence could be a surface macroscopic stress.

WOOD and DEWSNAP[49] do not think that Heyn intergranular stresses are likely to make a significant contribution to the observed residual lattice strains, because the Heyn stress in any grain is dependent on its neighbours. They state that 'since on the whole all arrangements of neighbours are possible, the various members of the group (of reflecting crystals) taken together will exhibit a whole range of stresses from tension to compression, *with a mean stress zero*' (my italics). They reported some results on large grained specimens which showed that the residual lattice strains of a grain of given orientation did, in fact, vary. GREENOUGH[50] agreed that the residual lattice strain in crystals of one orientation would vary as the orientations of the neighbouring crystals varied, but pointed out that the average strain taken over many grains of the particular orientation would not be zero 'but would depend on the difference of the yield tension of the grain with the given orientation and the average yield tension of the aggregate'. Such average values are obtained experimentally if fine grained aggregates are used. WOOD and DEWSNAP[51] have later again criticized the Heyn intergranular stress hypothesis in a paper in which they interpret experimentally measured residual lattice strains in iron and steel in terms of biaxial compressive stresses in the surface of the specimens; their interpretation, however, appears to be open to criticism (see discussion on the paper).

In concluding this discussion on residual lattice strains, it is emphasized that while the hypothesis of a surface macroscopic stress would lead one to expect that the residual lattice strains shown by all diffraction lines would be similar, and therefore cannot account for results such as shown in *Table II*, the idea discussed by BRAGG *et al* might, if pursued, lead to the prediction of residual lattice strains of magnitudes which vary with diffracting plane.

This section would not be complete without some reference to work in which changes in the diffraction line position have been observed after metals have been worked by stresses other than uniaxial ones.

Very interesting results were obtained by WOOD[52] following an examination of cold-rolled metals using x-ray beams incident normal to the surface and recording the high angle reflection lines. Much of this paper is taken up with a discussion of the line broadening which occurred, but mention is made of lattice strains which cause a movement of the diffraction line peaks. As the annealed metal was worked, the lines first broadened and the lattice spacing increased until some maximum value was reached. Then the diffraction lines suddenly

became sharper, and at the same time the lattice spacing decreased to a value even less than that of the original annealed value. These processes then alternated during further working. This appeared to be a general phenomenon occurring at least in copper, silver, nickel, molybdenum and iron, but not in pure aluminium, where recovery presumably took place at room temperature.

The line broadening results are discussed later. Here we are concerned with the changes in lattice spacing, which are not easy to explain. Wood himself thought that the increase in lattice spacing observed was, at least in part, due to an all-round expansion of the lattice. For instance, in the case of the copper where the reflection examined was 400 he states that 'the bodily shift of the (400) ring serves to demonstrate that the internal strain or distortion which can be imposed on the lattice is of the nature of an expansion, for the ring is made up of reflections from the three mutually perpendicular (400), (040) and (004) planes, and all these directions must have increased'. However, it is not true to say that all these directions in one given crystal have increased in length, since all cannot contribute to the diffraction line under the experimental conditions used. Thus although the (400), (040) and (004) directions in different crystals have separately increased, there may well have been a decrease in spacing along the other two mutually perpendicular directions in each case. It thus seems that the observed lattice spacing changes could be due to macroscopic stresses, microscopic Heyn stresses or stress systems associated with trapped dislocations, in addition to the lattice expansion hypothesis which, although not proven valid, is by no means improbable.

In work primarily concerned with textures formed during the rolling and recrystallization of commercially pure (99·5 per cent) aluminium, SPILLETT[53] has made some observations on the movement of the diffraction 'line 27' (combined 511 and 333 planes). He also observed that the corresponding spacing increased during rolling and that the diffraction lines became more blurred. He then annealed the rolled metal at successively higher temperatures, and observed that before recrystallization commenced there was a further increase in lattice spacing which was accompanied by a decrease of line broadening. This should be compared with the results of Wood, who found that in his rolled metal, when 'recovery' took place at room temperature, a decrease in lattice spacing accompanied a decrease in line breadth.

Spillett also observed that when the annealing was at a temperature high enough to cause recrystallization, the lattice spacing decreased almost, but not quite, to the normal unstrained value. Annealing at considerably higher temperatures caused a further decrease in the lattice spacing, the final value being accepted as the unstrained parameter. This observation is rather surprising in view of the widely held

opinion that a recrystallized metal is strain free, but it has been confirmed[8] by Crussard and Aubertin. These authors examined the recrystallization of rolled copper after annealing at successively higher temperatures, employing a camera in which very high θ values could be recorded. They showed that although stationary back reflection Laue photographs indicated that recrystallization was complete after annealing at 250°C, the average lattice spacing of the reflecting grains decreased after various further annealings at temperatures up to 700°C.

Very similar observations have been made by Owen, Liu and Morris.[54] They plastically compressed plates of high purity aluminium and after the removal of the stress measured the interplanar spacings in a direction normal to the plane of the sheet. They observed that immediately after compression the lattice parameter had increased from 4·0406 kX to about 4·0420 kX. This expanded 'parameter' then decreased with time, the more rapidly the more the initial cold work, until it reached a metastable value of 4·0412 kX. In this state many sharp Laue spots were visible on back-reflection photographs, but also some diffuse portions of Debye–Scherrer rings. This metastable parameter only reverted to the 'normal' parameter after annealing at a higher temperature. These authors performed most of their work using Co$K\alpha$ radiation giving 420 as the high angle line, but confirmed that identical results were obtained if lines 511 and 333, 331, 400 and 222 were also employed. Again it is not possible to say with certainty that an all-round increase in lattice parameter has taken place, since the normals to the several orientations of grains reflecting are all more or less parallel, but this last observation rules out the possibility that intergranular stresses are responsible for the effects.

Owen, Liu and Morris also showed that films made of compressed powder, although showing the initial increase in lattice spacing, showed no metastable value. Lastly they showed that a filed surface immediately after filing had a decreased lattice spacing which then increased with time to the high metastable value. Owen and Liu[55] have recently examined the effect of a single scratch on the surface of aluminium, and showed that the lattice spacings near it changed in the same way as after filing. In this recent experiment they showed that the lattice spacings in two different directions relative to the surface changed in the same way, thus showing it to be probable that this effect is due to a uniform change of volume of the lattice.

Measurements of a similar type have been made on specimens during fatigue *i.e.* undergoing rapid cycles of compression and tension. Most of this work by Wood and his collaborators has been qualitative in nature, but Wood and Thorpe[56] record some quantitative results on the movement of the peaks of the 331, 422 and 420 diffraction lines from brass during a fatigue experiment. The stress limits were

$\pm$ 8 tons/in^2, which is greater than the static yield stress. The increase in the interplanar spacings, which remained approximately the same during the major portion of the fatigue life, was 0·025 per cent of the annealed value. This observation is of particular interest, because this increase in interplanar spacing was not associated with much breakdown of the Laue spots as in the case of analagous residual lattice strains caused by slow plastic extensions or by rolling.

An interesting observation has been made by NICHOLSON[57] in connection with the dependence of lattice parameter on the size of the diffracting particles. He pointed out that the surface forces in particles must be balanced by elastic forces in the mass of the particles, and thus the lattice of the particle interior will have a parameter different from the normal unstressed value. The difference between the lattice parameter, a, in the middle of an infinite lattice and that in a cube of side l is given by the relation:

$$\frac{\delta a}{a} = -\frac{4T}{3lK} \qquad \ldots . \quad (10)$$

where T is the surface tension in the exposed faces of the particle, K is the bulk modulus of the material and l is the length of the cube edge. Nicholson showed that the change observed experimentally for cubic particles of magnesium oxide was roughly half that to be expected from the value of T calculated theoretically.

Some unpublished experimental work by the writer on the lattice parameters of isolated silver particles of diameters down to 200Å showed no observable change with particle size, but this could well have been due to the difficulty of preparing silver particles with really clean surfaces. On the other hand, RYMER and BUTLER[58] observed certain anomalies in the electron diffraction patterns from thin gold leaf which might well be explicable by surface forces. Owen, Liu and Morris have reported[54] that the parameter of annealed aluminium powder increases as the diameter of the powder grains decreases. If this were due to surface forces, their results would indicate that in the surface of aluminium crystals there is a *compressive* force of 2×10^5 dynes/cm. While it is possible for the forces in the surfaces of solid metals to be compressive, this value is about a hundred times that of the calculated[58] surface energy, which is not theoretically possible; it seems likely that there must be some other explanation of the results of Owen *et al.*

This type of argument might be applied to the grains in an aggregate. As has been discussed[9] by King and Chalmers, an intergranular boundary is associated with energy, and presumably with some form of surface forces. These could cause lattice parameter changes. A. P. GREENOUGH and KING[59] show that a reasonable figure for the maximum

intergranular surface energy of silver is 300 ergs/cm^2 when the orientation difference between the contiguous grains is large. Thus the surface force on a crystallite, which is unlikely to differ largely in orientation from its neighbour, will not be greater than 300 dynes/cm at the very most. For particles of size $0{\cdot}8 \times 10^{-5}$ cm, a value obtained by Wood for silver in his rolling experiments, this would give a lattice change of 5×10^{-3} per cent of the annealed value, which is only $\frac{1}{8}$ of the lattice parameter changes observed by Wood. It does not appear at the moment that this is a likely explanation of Wood's observations.

Broadening of Diffraction Lines

A cursory glance at an x-ray diffraction photograph taken from a metal that has been plastically deformed in any way is sufficient to show that such deformation has a marked effect on the breadths of the diffraction lines. In hard metals the broadening is sufficient to cause the $K\alpha_2$ peak to disappear, the photograph showing only one apparent peak, although such marked broadening is not commonly found for the softer metals. Since this was first noted by VAN ARKEL,[61] qualitative and quantitative studies of the effect have been pursued, and at one time there was great controversy regarding the explanation of the broadening. In the two extremes, the broadening could be caused either by the presence of very small particles or by variations of lattice spacing from crystal to crystal. As in the case of many other scientific controversies, it now appears probable that neither of the extreme views was entirely justified and the most probable explanation incorporates the ideas of both.

If the crystals are very small, albeit of constant spacing, there are so few planes in each crystal giving increments of diffracted radiation that the crystal is not effectively infinite, and a finite broadening occurs in the same way as in a light diffraction grating with a limited number of lines. JONES[62] has shown that, approximately, all theoretical treatments give the following relation for the broadening, β_p, of any *hkl* reflection:

$$\beta_p = \lambda/\eta \cos \theta \qquad \ldots\ (11)$$

where β_p is the breadth of the line, λ is x-ray wavelength and η is the effective particle size. If the particles are markedly acicular or platelike this formula must be modified so that different reflections are differently broadened.

If the broadening is due to variations in strain for which the Laue breadth of the distribution curve is ε then, using a very general treatment, STOKES and WILSON[63] have shown that the resultant broadening, β_s, is given by:

$$\beta_s = 2\varepsilon \tan \theta \qquad \ldots\ (12)$$

However, STOKES, PASCOE and LIPSON[64] thought it more reasonable to suppose that the stress rather than the strain distribution was isotropic (although this is not the assumption giving best correlation with experiment in the case of elastically strained aggregates). Equation 12 then becomes:

$$\beta_s = 2\sigma \tan\theta / E_{hkl} \qquad \ldots\ (13)$$

where E_{hkl} is the value of Young's Modulus in the direction $[hkl]$ for a free single crystal. More recently, WILSON[65] has shown that in the case of bent crystal plates the result obtained by Stokes and Wilson is likely to be applicable only when the quantity $D^2/\lambda R$ is large, where D is the thickness of the plates and R their radius of curvature, particularly at small Bragg angles. If this quantity is small, then the broadening at low angles will vary with θ in a manner more resembling equation 11 than equation 13.

LIPSON[66] has recently discussed the problem from the point of view of the effect of small particle size or varying lattice strains on the reciprocal lattice. He has shown in outline how the reciprocal lattice points become areas whose size and shape are related to the effect and this approach enables the ideas to be expressed simply.

The breadth of a diffraction line (due to a single x-ray wavelength) is normally defined as the integrated intensity of the line divided by its peak intensity. The experimental measurement of this value is, however, not easy. In the first place the experimentally measured quantities give the profile of the α doublet which has to be separated into the α_1 and α_2 components. Secondly, the estimation of the level of the background intensity, which is taken as the 'base' of the diffraction line peak, is difficult, particularly for broad lines. Even in favourable cases it is not likely that an experimental accuracy of line breadth measurements of greater than 5 per cent may be attained.

The experimental breadth always depends on two factors, the geometry of the experimental arrangement such as the divergence in the incident x-ray beam or the size of the specimen, and the inherent properties of the specimen. Ideally, experiments would be designed so that the latter could be determined in an absolute manner for any specimen, but because such a procedure is extremely difficult the normal technique has been to compare the breadths, b and B, of the diffraction lines from annealed and worked specimens respectively.

From experiments in which the geometrical broadening has been made small, or eliminated, it is clear that annealed specimens give some line broadening, and thus a comparison of the annealed and cold-worked metal gives only the increase in breadth, β, due to the cold working. The exact determination of β from the two experimentally determined quantities b and B is not easy. The matter has been discussed by many authors, and there is no generally acceptable

method (*e.g.* see reference 66, page 387). The formula applicable in a particular case depends on the form of the mathematical function which gives the best fit with the profile of the diffraction line. If I is the x-ray intensity at any point distance x from the peak position, then if $I = I_0/(1 + k^2x^2)$ the formula originally used by SCHERRER[67] has been shown[68] to apply *viz*:

$$\beta = B - b \qquad \ldots . \quad (14)$$

On the other hand if $I = I_0\exp(-k^2x^2)$, the relation proposed by WARREN[69] has been shown[70] to be applicable. This is :

$$\beta^2 = B^2 - b^2 \qquad \ldots . \quad (15)$$

The difference between the values of β derived from equations 14 and 15 is greatest when B and b are nearly equal *i.e.* the value of β caused by the cold working is small.

Much quantitative work designed to decide between the two possible causes of line broadening has investigated the variation of β with the diffraction angle θ, and with the x-ray wavelength λ. Unfortunately, the possible values of λ which can be used to give high angle lines from most metals, at which the determination of β is most accurate, are all very close to one another, the ratio of the maximum to minimum value being about 1·4. But for metals with small lattice parameters and high Debye characteristic temperatures, it is possible to record high angle lines of adequate intensity using Mo$K\alpha$ radiation and for these metals it is possible to vary λ by a factor of 2·5 or 3. The only drawback to the use of Mo$K\alpha$ radiation is that different diffraction lines occur very close together and it is difficult to determine the true background of intensity from which to make measurements since the 'tails' of neighbouring diffraction lines merge into one another, but potentially it is the most powerful method of distinguishing between small particles and varying lattice strains; it has only recently been employed. The method of investigating the variation of β with θ can be used for all metals and has been employed frequently. It is usual to plot β against λ sec θ and against tan θ/E_{hkl} to determine whether equations 11 or 13 fit the experimental results best. Unfortunately, the two trigonometrical functions differ most at low θ values, which is the range in which β is small and cannot be accurately determined, and consequently this is not an easy experiment to carry out to obtain a certain decision between the two possibilities.

Brindley and his co-workers, whose results were later summarized by BRINDLEY,[71] examined the line broadening shown by filings of rhodium, copper and nickel for a large range of θ values but only a limited range of wavelengths. He concluded that the factor β cot θ was much more nearly constant than β cos θ/λ and so deduced that the lattice strain broadening greatly predominated, but his curves of β plotted against

tan θ do show some deviation from a straight line at low θ values, partly due to lack of correction for apparatus broadening. Similar work using filings was carried out on copper by Stokes, Pascoe and Lipson, whose results[64] are shown in *Table III*, and by MEGAW and STOKES[72] on filings of aluminium, copper, silver, lead, nickel and iron. In all cases it was shown that $E_{hkl}\beta \cot \theta$ was much more nearly constant than $\beta \cos \theta/\lambda$ and that the factor $\frac{1}{4}E_{hkl}\beta \cot \theta$ was roughly the same as the known ultimate tensile strengths of the metals, as is to be anticipated from equation 13.

Table III. Breadths of Diffraction Lines in worked Copper Filings (all lines recorded using Cu$K\alpha$ *radiation)*

hkl	*Breadth, β*		θ	$\beta \cos \theta$	$\beta \cot \theta$	E_{hkl} 10^{12} *dynes/cm²*	$E\beta \cot \theta$
	Uncorrected mm	*Corrected mm*					
111	0·64	0·18	21·7°	0·17	0·45	1·59	0·72
200	0·77	0·42	25·2°	0·38	0·89	0·78	0·69
220	0·84	0·44	37·1°	0·35	0·58	1·26	0·73
311	1·21	0·76	45·0°	0·54	0·76	1·02	0·78
222	1·01	0·47	47·6°	0·32	0·43	1·59	0·68
400	1·65	1·04	58·5°	0·54	0·63	0·78	0·49
331	2·18	1·24	68·2°	0·46	0·50	1·34	0·67
420	2·98	1·89	72·3°	0·57	0·60	1·03	0·62

Work of similar type, but using solid specimens, was carried out by SMITH and STICKLEY[73] who examined tungsten after grinding and α-brass after rolling. They too reached the same conclusion.

At this time (1945) the main support for an explanation of line broadening as a particle size effect was due to Wood. His experimental work differed from that previously described in that he made no attempt to examine the variation of the breadth β with θ or λ to differentiate between the two possible explanations. He based his conclusions that the breadths of the lines in certain conditions of the metal were due to the presence of small particles on qualitative arguments. (The qualitative comparison by WOOD[74] of the breadths of high angle diffraction lines from iron using Mo$K\alpha$ and Co$K\alpha$ radiations was rightly criticized,[75] and no significance can be attached to the apparent difference between the photographs.)

In his work on rolled metals, Wood observed[52] that the individual reflection spots first broke up and spread round the diffraction rings. The spread was so great that it could only be explained in terms of a breakdown of the original crystals to sizes $\sim 10^{-3}$ or 10^{-4} cm diameter. Further working caused line broadening and there appeared to be no

reason why the breakdown should not continue far enough to contribute to the line broadening. Eventually the broadening fluctuated between maximum and minimum values as the working continued, as did the average lattice strain discussed on page 196. Wood pointed out that it was reasonable to assume that the strains increased and decreased to cause these fluctuations, while the crystallite size remained constant. He stated that 'since the lattice distortion is accompanied by expansion of the lattice, the recovered state with its contracted lattice must give the amount of the residual line broadening due only to the Scherrer (small particle size) effect and therefore the corresponding lower limit of the crystallite size'. This can hardly be accepted as logical proof, but there appears to be some reason for assuming that the particle sizes may be deduced from the minimum line breadths in the worked state. Wood found particle sizes ranging from $0{\cdot}7 \times 10^{-5}$ cm for copper to $3{\cdot}2 \times 10^{-5}$ cm for iron, apart from aluminium for which the limiting size was $\sim 10^{-4}$ cm.

This approach, however, was not very convincing and it is probably true to say that in 1945 the general opinion was that line broadening in all cases of cold working of metals was due mainly to the presence of internal varying strains and not to the presence of small crystallites. Before this time, DEHLINGER and KOCHENDÖRFER[76, 77] had undertaken experimental work on the line broadening of rolled copper sheet and attempted a mathematical analysis of the results to determine whether both varying strains and small particles were contributing to the broadening. They concluded that both were present, that the limiting crystallite size of 6×10^{-5} cm was reached at an early stage of the working, but that the magnitude of the random strains increased gradually, eventually reaching values corresponding to stresses ~ 50 kg/mm^2. Their analysis was based on the assumption of triangular line shapes, which is unlikely to be true, thus vitiating the numerical results, but their approach was essentially that applied in modern work.

BRAGG[78] showed that there were strong theoretical grounds for anticipating that both particle size and varying strain broadening should occur. He pointed out that, since a part of a crystal could only slide over another by increments of one atomic distance, for a given size of crystal particle there was a critical elastic strain which must be attained before it was energetically advantageous for the crystal to deform plastically. *Figure 9*, taken from his paper, illustrates the argument. This immediately led to a relation between the yield stress in shear, T, and the thickness of the particle, t, *viz*:

$$T = Gs/t \qquad \ldots . \quad (16)$$

where G is the elastic shear modulus and s the interatomic spacing. If Wood's values for the limiting particle sizes are used for t in equation 16,

values of T are obtained which are in remarkably close agreement with the experimental values for the ultimate strength. However, in a further analysis of the problem BRAGG[79] showed that the strain broadening arising using the same model was much greater than the particle size broadening. The general approach, however, shows that it is possible to connect strains with particle sizes and the two may not be separate possibilities.

HALL[80] recently re-examined published results for both filings and solid metals to see if it was possible to find evidence that both varying strains and small particles were present. He pointed out that if both

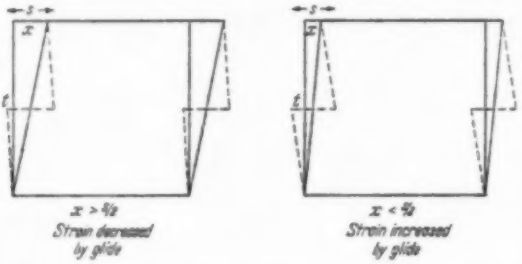

Figure 9. Illustrating relation between size of crystal and elastic strain limit

causes of broadening were operative, and the individual contributions to the breadths could be directly added as in equation 14, then:

$$\frac{\beta \cos \theta}{\lambda} = \frac{1}{\eta} + \frac{2\sigma}{E_{hkl}} \cdot \frac{\sin \theta}{\lambda} \qquad \ldots . \quad (17)$$

He plotted $\beta \cos \theta/\lambda$ against $\sin \theta/\lambda$ and *Figure 10* shows the graphs he obtained for the various results. If equation 15 should be used to add line breadths, then the graphs would not be straight lines but would have a gradually decreasing gradient at low θ values and give intercepts greater than shown. It is seen that the intercepts on the $\beta \cos \theta/\lambda$ axis give particle sizes which are of the same order as those originally put forward by Wood. One unsatisfactory feature is that the limiting crystallite size determined for copper is markedly dependent on whether results for rolled sheet or for filings are used.

Wood and Rachinger employed a rather different method of approach.[68] They pointed out that since both lattice strains and small particles may contribute to line broadening, it would be advantageous to eliminate one source experimentally. In filings the residual stresses due to working may have any orientation and magnitude, giving a large strain broadening. But in a uniaxially extended or compressed aggregate they state that the stress in the grains reflecting has a single value and direction. (This latter statement is not strictly true,[50]

although it is clear that the range of strain will be much less in the latter case.) They confined their work to the body-centred metals of high melting points, iron, molybdenum, tungsten and tantalum, and investigated them with a radiation of wavelength about 1·7Å and with Mo$K\alpha$, wavelength 0·708Å. This ratio of wavelengths is far larger

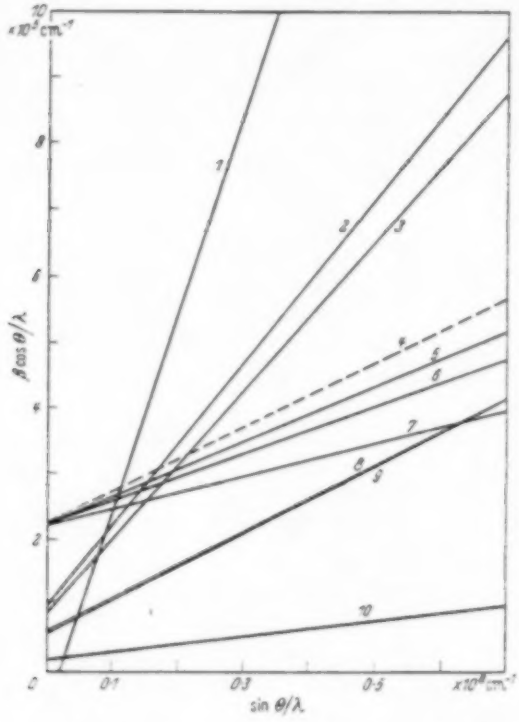

Figure 10. Various line breadth results plotted to show presence of both small particles and varying strains

Line	1	2	3	4	5	6	7	8	9	10
Material	*Martensite rod*	*Rhodium filings*	*Rhodium filings*	*Iron filings*	*Rolled Copper Sheet*			*Copper filings*	*Copper filings*	*Aluminium filings*
					rdn 99%	*rdn 60%*	*rdn 20%*			
Radiation	*Iron*	*Zinc*	*Copper*	*Cobalt*	*Copper*	*Copper*	*Copper*	*Copper*	*Zinc*	*Copper*

than any previously employed. They showed that the ratio of the broadenings in the two cases was the same as the ratio of the wavelengths employed *i.e.* the broadening was almost entirely due to the presence of small particles. The sizes were shown to be $\sim 3 \times 10^{-6}$ cm.

The authors do not show any of their experimental curves for

intensity as a function of θ for the Mo$K\alpha$ diffraction lines, and it is impossible to know how completely they overcame the difficulty of estimating the true background level. If this is taken too high, false evidence in favour of the particle size hypothesis is obtained. Apart from this possibility, it does not appear that any of the criticisms which have been made of the paper are such as to invalidate the authors' general conclusions.

To examine further the ideas originating from the investigation of line broadening, KELLAR, HIRSCH and THORP[81] have developed a back reflection Laue method employing very fine X-ray beams to examine worked metals. In the case of rolled aluminium they have shown that the working causes a breakdown of the crystals into small discrete crystallites of the order of 2×10^{-4} cm in diameter. Even such small crystals produce separate reflection spots using this technique, and their interpretation is free from the doubts which attend line broadening interpretations. It remains to be seen, however, whether this apparatus confirms the conclusions that much smaller crystallites are present in, say, rolled copper.

Later work[82–86] on the methods of using experimentally obtained diffraction line shapes have, in essence, developed Jones' analysis in more precise mathematical terms. The aim is to express the experimental curves as Fourier series, and if this is done for both annealed and cold-worked specimens, it is possible to obtain the intrinsic broadening due to cold working free from any instrumental broadening. Thus the Laue breadths, β, of the diffraction lines may be found if desired, but WARREN and AVERBACH,[85] and later HALL,[86] have emphasized the value of utilizing the additional information contained in the coefficients of the Fourier series. This type of treatment appears to be more reliable than the earlier techniques of using some arithmetical method of obtaining the intrinsic breadth β.

Hall has pointed out that if this form of Fourier analysis is used, it should be possible to interpret line broadening experiments in terms of the dislocation theories of the plasticity of metals. This approach is preferable to attempts to differentiate between possible small particles and varying lattice strains because, since dislocations in a metal may be arranged to produce either effect, the two 'possibilities' are intimately connected. Hall has developed this idea sufficiently far to be able to interpret[87] his experimental observations on aluminium and tungsten filings in terms of dislocations. He has shown that a cold-worked metal contains many dislocations randomly arranged, but that if it is allowed to recover the same number of dislocations are present in a regular array, probably of the polygonized type discussed by CAHN.[88] After recrystallization, the number of dislocations present decreases substantially.

The present position regarding the interpretation of line broadening observations can thus be summarized:

i in all worked metals, variations of strain from point to point of the irradiated area cause a broadening. In the case of a metal worked by heterogeneously directed stresses, as in filings or in ground surfaces, this strain broadening predominates,

ii in all cold-worked metals some fragmentation occurs giving crystallites of a size small enough to cause line broadening, probably of about 10^{-5} cm diameter in harder metals at room temperature,

iii it is likely that the most useful approach in future will be to examine the shapes of lines and to interpret these in terms of dislocations or some other fundamental theory of plastic deformation.

Apart from work in which the cause of line broadening has been the prime interest, there have been many attempts to relate the breadths of the lines to the degree of cold work, or to other experimentally observed quantities which also vary with the amount of cold working. In general, it is found that if a particular method of cold working is employed during the experiments, the line breadth is roughly proportional to the yield stress (*i.e.* stress required to cause further plastic deformation). In the early experiments of WOOD[89] on rolled α-brass, he found the breadths of both the 331 and 420 lines increased linearly with the Brinell hardness of the brass. A more recent investigation was carried out by PATERSON[90] of the relation between the line broadening shown by twisted copper wires, and the torque required to twist the wires. Although his results are complicated by the variation in plastic strain from the inside to the outside of the wire, he shows that the line breadth/plastic strain curve is very similar indeed to the curve showing torque as a function of plastic strain at various temperatures and for reversed twisting experiments. Most remarkable was the observation by PATERSON and OROWAN[91] that the greater broadening produced by a given plastic deformation at − 180°C was retained on 'annealing' for some days at room temperature. If further plastic deformation was then given to the specimen at room temperature, the line breadth first decreased rapidly and then tended towards the curve obtained for specimens deformed entirely at room temperature. *Figure 11* shows their results. This behaviour is exactly analagous to the behaviour of the yield stress after such treatments, as shown by Los.[92] One important deduction from this observation is that neither the line broadening nor the yield stress are limited by thermal recovery in the absence of an applied stress.

Such a relation between line breadth and yield stress is to be expected

following Bragg's work, but there is some evidence that the rate of variation of line breadth with hardness is dependent on the type of working. For instance, DEHLINGER[93] has shown that if a given metal is worked by different methods to produce the same increase in hardness, the line breadths are not the same. An even more marked dependence of the line breadth on the type of working used to increase the yield stress is demonstrated by the observations of Wood and Thorpe made during fatigue tests on an α-brass.[55] They found that cycles of stress of $\pm$ 9 tons/in^2, applied at 2,200 cycles/min, caused a

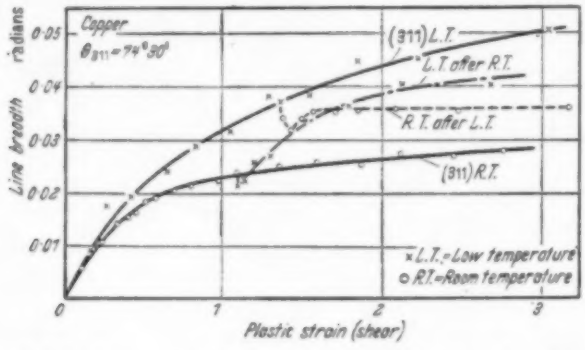

Figure 11. Relation between line broadening and plastic shear on surfaces of copper wires twisted at different temperatures

negligible change in the character of the original sharp reflection spots, and yet such treatment raised the limit of elasticity from 5 to 9 tons/in^2. A tensile stress of 9 tons/in^2 applied slowly caused considerable line broadening.

To some extent the variation of line broadening with type of working could be accounted for by the dependence of the degree of variation of lattice strain on the heterogeneity of working. This was clearly demonstrated by Wood and Rachinger, who showed[68] that filings gave a much greater line broadening than a tensile specimen pulled to fracture. An alternative type of explanation is that working by rolling or wire drawing, affects the extreme surface layers more than the interior and these contribute the major portion of the diffracted x-ray intensity, but make only a small contribution to the yield stress or hardness determination. Either explanation may be true of Dehlinger's results, but neither seems likely to explain Wood and Thorpe's observations.

Largely because of its technological importance, there have been several attempts to examine line breadths in relation to fatigue phenomena, with varying results. While GOUGH and WOOD,[94] working on steel, considered that the line breadth only increased markedly if the

applied stress was of such a magnitude as to cause eventual failure, BARRETT[1, 95] did not consider that there was any such correlation of line breadth with 'safe' and 'unsafe' stress values. This conclusion was also reached more recently by TERMINASSOV[96], who made many quantitative measurements of line breadth during the fatigue life of steel specimens tested at various stress levels. He found that the line breadths always increased during the first cycles and then remained approximately constant for all stress levels, and that there was no significant difference between the effects of 'safe' and 'unsafe' stress ranges.

It is difficult to reconcile the views of Gough and Wood and of Barrett although, as the latter has pointed out, it may be that the broadening of the diffraction lines is indicative of plastic straining which, by chance, only occurred in Wood's work above the fatigue limit. But since the theoretical view of fatigue[97] is that work hardening proceeds continuously during cycles of stress above the fatigue limit until fracture commences, it is surprising that the observations of Gough and Wood have not been more generally substantiated. It is possible that the effects only occur in very small volumes near the position of eventual failure which cannot be found until a crack has started, and that observations made elsewhere on the specimen do not provide useful information.

Lastly, an isolated observation, due to NIEMANN and STEPHENSON[98] has been made of line breadths in relation to the damping capacity shown by specimens after cold working. They used α-brass and concluded that there was no correlation between the two properties.

A general criticism of much of the work on line broadening in relation to the mechanical properties of metals, is that too frequently an attempt has been made to link the observations directly with the mechanical property. If some intermediate step were inserted, and both observations considered in the light of some basic theory, as of dislocations, it may be that some coherence could be given to observations that are, at the moment, rather disconnected and sometimes apparently contradictory.

Intensity of Diffracted X-rays

Unlike experimental x-ray intensity measurements made in connection with the determination of crystal structures, in which the relative intensities of various reflection spots on one photograph are required, the investigation of x-rays diffracted from metals after various deformations requires the comparison of intensities measured for two different specimens. Thus, in addition to possible errors due to extinction (originally discussed by Darwin and later by BRAGG and WEST[99]) there

may arise errors due to differences in the x-ray energy incident on the specimens in the two cases. Since the changes in intensity caused by severe plastic deformation are small, experimental work in this field must be carried out with very great care if the results are to be of value.

Before considering quantitative results, it is useful to consider an impression that is fairly generally held by persons who have not made quantitative studies of intensities, and that is exemplified by a statement made by Niemann and Stephenson. They state that, for α-brass, 'the measurement of the diffraction rings after cold working was difficult *because of the greatly increased amounts of background scattering* in addition to the very diffuse appearance of the rings'. This statement applies to the background in a photograph taken using an incident x-ray beam containing much 'white' continuous x-radiation in addition to the characteristic wavelengths. In such a photograph the background at high angles is due almost entirely to the Bragg reflection of this continuous waveband, and hence will change in intensity in exactly the same way as the diffraction 'lines'. The qualitative impression is that the intensities of the high angle lines decrease considerably (*e.g.* SMITH and WOOD[32] state that a decrease in intensity of 50 per cent occurs in the lines from steel after yielding has occurred), and it is clear that the two impressions are mutually incompatible. Experiments made under carefully controlled conditions show that neither visual impression gives any indication of the true changes, which are very small.

The theoretical relation of the intensities of the x-rays diffracted into both the lines and the background to the number and type of defects in the metal lattice have been examined by ZACHARIASEN,[29] by ECKSTEIN[100] and by EWALD.[101] The latter have emphasized the particular importance of the change in low angle background scattering which is easiest to interpret mathematically. GUINIER[102] has also pointed out that the investigation of the x-rays scattered near $\theta = 0°$ is important, since it is only in this region that the intensity of x-rays due to Compton scattering becomes zero. With this point in mind FOURNET and GUINIER[103] have paid particular attention to the mathematical problem of the low angle scattering. A somewhat different approach to the problem has been made by WILSON[104, 105] and by HALL[86] who examined mathematically the effect on diffracted intensities of line and screw dislocations. The treatments were not precise, but Hall in particular developed the theory so that the results could be applied to measured intensities.

At the moment, it is probably true to say that theoretical work is in advance of experimental research, and until more data are available, it is not possible to say in general whether the theoretical treatments are applicable to actual behaviour. Attention is thus more profitably directed towards an examination of published experimental results.

HENGSTENBERG and MARK[106] examined molybdenum, tantalum and tungsten after rolling, and duralumin during aging at room temperature. They used an ionization chamber in which the entrance was large enough to receive the whole of one diffraction line at once, and measured its intensity. They found that the intensity* of any particular line decreased after working, the change increasing with the diffraction angle θ. They showed that the decrease in intensity of the

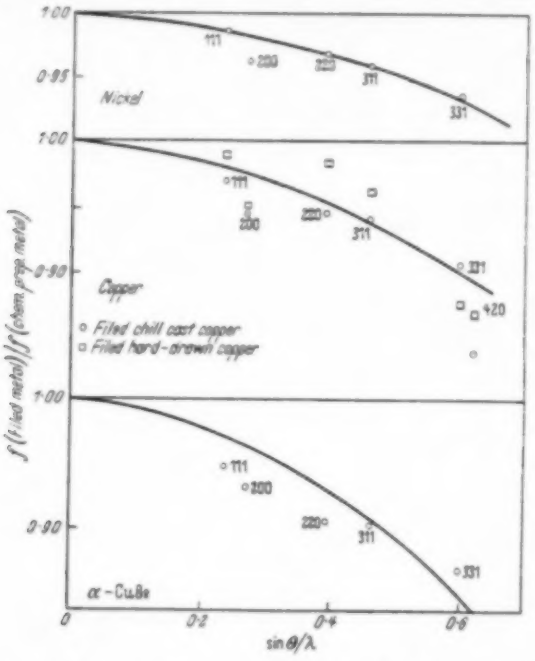

Figure 12. Ratio of scattering factors f from filed and chemically prepared metals; the full curves are calculated on the assumption that the atomic displacements resemble a 'frozen heat motion'

lines was very much of the same type as that caused by a rise in temperature *i.e.* the decrease in intensity followed the normal Debye–Waller temperature factor relation. It was as if the atoms had been left in a state of 'frozen heat motion' *i.e.* all had small random displacements from their mean positions.

In a series of careful experiments, Brindley and his co-workers, using film methods of recording, and arranging their apparatus so that photographs of the worked and chemically prepared metals were taken

* The intensity of a diffraction line is always taken as the total area between the extrapolated background curve and the profile of the diffraction line *i.e.* the integrated intensity. The peak intensity value is of little interest.

simultaneously on different films, confirmed that filings of nickel, copper and copper–beryllium alloy also showed similar effects. The decrease in intensity of the high angle lines was about 20 per cent, but this figure decreased as the θ value of the line diminished. *Figure 12*, taken from Brindley's paper,[71] summarizes the results in terms of the atomic scattering factor (which is proportional to $\sqrt{I}$). Boas[107] and Brill[108] have made measurements of the relative line intensities from gold and from iron respectively and these results also can be interpreted in terms of a 'frozen heat motion' of the atoms. *Table IV*, also taken from Brindley's paper, shows the values of the root mean square displacement of the atoms from their equilibrium positions.

Table IV. Data relating to Lattice Distortion in Filed Metals, assuming the Distortion to be of the Nature of a 'frozen heat motion'

Metal	$\sqrt{u^2}$ Å	*Energy as calc. by Boas cal/gm*
Copper	$0{\cdot}10_6$	7·4
Gold	$0{\cdot}11_9$	3·5
Nickel	$0{\cdot}08_3$	6·4
Rhodium	0·08	—
Iron	0·12	—

Boas[109] has developed a method by which the equivalent temperature of the metal may be calculated and hence its energy. These energies are shown in the last column and are roughly five times those that have been measured calorimetrically. Boas has suggested that if, instead of atoms being displaced purely at random, they were displaced in groups, the effect on the x-ray intensities would be the same but the energy associated with the displacements would be less.

In addition to their work on metals, Hengstenberg and Mark described in detail the examination of compressed single crystals of potassium chloride. They measured the intensities of the lines 200, 400, 600, 800 and 10,00 and also examined the crystals using a polarizing microscope. Potassium chloride deforms by glide, as do metals, and from their observations Hengstenberg and Mark concluded that the heaviest distortions were in or near the glide planes, while the bulk of the crystal was but little distorted. These authors endeavoured to treat the problem mathematically and to deduce the percentage of the atoms displaced as well as their average displacements. They were unable to use the results for the 200 and 400 reflections since these were greatly affected by extinction in the annealed crystal, and only the results for the 800 and 10,00 reflections were employed.

Since glide is known to occur only in certain planes in crystals, it is unlikely that all atoms will be equally displaced from their normal sites by cold working. A certain proportion near the operative glide planes probably suffer great displacements, while those of the remainder are small. Thus the type of treatment applied by Hengstenberg and Mark to the case of the potassium chloride, although more difficult to carry out, is likely to be preferable to one in which it is assumed that all atoms are equally affected.

In this earlier work, the incident x-radiation was either the direct filtered emission from the target or was monochromatized by reflection from a plane crystal. For the study of the x-ray intensity diffracted into the background, it is essential to use monochromatic radiation, and its use is advantageous when investigating the diffraction line intensities. Guinier has described[102] the use of a curved crystal monochromator which, if used in conjunction with an x-ray tube with a fine focal spot, gives high diffracted x-ray intensities which are focused at well defined points. Guinier himself used photographic methods of recording intensities, but later workers using similar apparatus have employed Geiger counters.

Using such a focusing monochromator, Hall has noted[86*] that the diffraction lines from cold worked metals have 'tails' which extend much further than the earlier workers had thought. These tails are not of a great intensity at any particular θ value, but since they extend over many degrees, the integrated intensity represented by them is quite large. AVERBACH and WARREN[110] have also noted such long tails, and *Figure 13*, taken from their paper, illustrates the feature. Hall considers it possible that the earlier workers may have failed to detect these tails and, consequently, their values for the integrated intensities of diffraction lines from cold-worked metals would be too low. The error would increase with increasing θ values.

The first careful observation of the x-ray intensity scattered into the background appears to have been made by GUINIER,[111] who confined his measurements to a range of θ values near 0°. In annealed polycrystalline copper he found that the background increased with increasing θ from $\theta = 0°$ to $\theta = 25°$, when its intensity became approximately constant. The intensity at $\theta \to 0°$ was negligible. After rolling, he found that this intensity had increased markedly. On the other hand, Guinier later showed[102] that if a single crystal of aluminium was examined after a plastic extension of 30 per cent, no change in the diffracted intensity was noted.

GREENOUGH[112] examined the intensity of the background scatter from steel wires after various amounts of plastic extension by direct

* Hall points out in his thesis that some of the experimental work was carried out in collaboration with G. K. WILLIAMSON.

stress, or drawn with extensions up to 98 per cent. For wires extended by direct stress there was no significant change, but in the very heavily drawn wires the background intensity had increased by 70 per cent $\pm$ 20 per cent. The experimental technique was very inaccurate compared with those to be described, and little reliance can be placed on the numerical results.

WAGNER and KOCHENDÖRFER[113, 114] employed a Geiger counter to measure the intensities of the diffracted x-rays. They made intensity measurements for the whole range of θ for single crystal specimens of zinc after various plastic extensions up to 32 per cent, and for poly-

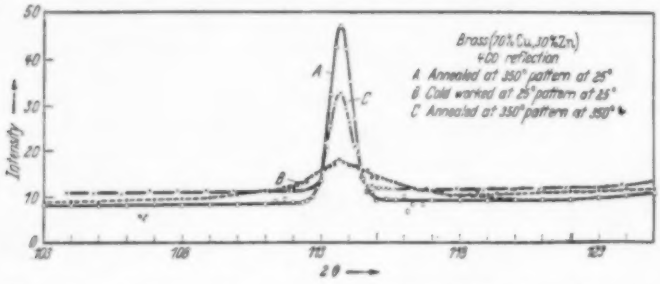
Brass(70% Cu, 30% Zn)
+CO reflection
A Annealed at 350° pattern at 25°
B Cold worked at 25° pattern at 25°
C Annealed at 350° pattern at 350°
Intensity
2θ

Figure 13. Intensity near (400) reflection for cold worked and annealed brass

crystalline specimens of aluminium and silver after reductions in thickness of up to 99 per cent by rolling. They found that there were no changes in the intensity scattered into the background exceeding the limits of the experimental accuracy of their measurements ($\pm$ 10 per cent). They did not measure many line integrated intensities, since the deformations were large enough to produce preferred orientations in the polycrystalline aggregates, which would obscure any changes due to internal disordering of the metal lattice.

This work was confirmed by Averbach and Warren who used filings of α-brass. These authors also employed a Geiger counter and measured the intensities of the diffraction lines as well as of the background scatter. They found that the intensity of the former increased on cold working due to the removal of extinction by the cold-working process, but found that the level of the background intensity remained the same. One difference between this work and that of Wagner and Kochendörfer was that while the latter found that the level of the background intensity rose slowly with increasing θ value, Averbach and Warren found it was approximately constant. By taking intensity measurements from a specimen at 350°C, they showed that the changes produced by cold work were quite different from those produced by increased thermal vibrations. The former caused the broad lines to have very long 'tails' and produced no detectable change in the background intensity

level, while the latter caused rather less line broadening, very much shorter tails but a marked increase in the background intensity. *Figure 13* illustrates some of these points and this, in conjunction with Hall's observation, throws some doubt on the validity of the older 'frozen heat motion' interpretation.

HALL,[86] too, employed a Geiger counter and confirmed Guinier's observation that the background intensity increased rapidly with θ at low values and thereafter very slowly, confirming the observations of Wagner and Kochendörfer rather than of Averbach and Warren. He found that the intensity of the background scatter from filings of both pure and commercial aluminium was increased at all θ values by about 10 per cent; this increase could not be estimated as accurately as the variation of intensity with θ because of the difficulty in deciding which was the true background intensity level. He also noted that the total integrated intensity of the pattern, that is the sum of the intensities in the lines and in the background, was the same both for specimens of filings and for the annealed material. Hall also obtained results which indicated that secondary extinction was of importance in his specimens of annealed aluminium, whereas it is normally assumed that primary extinction is the important factor.

In the course of this work, Hall measured the breadths of the diffraction lines and found that whereas the commercial aluminium showed marked broadening, the pure aluminium showed very little. He treated the intensity measurements and line shape observations together and proposed the following explanation. There were roughly the same number of dislocations left in each specimen of aluminium, so the amount of local disorder present in each was the same and hence there was the same increase in background scatter. But in the pure aluminium the dislocations were arranged in polygonized arrays,[88] while in the commercial aluminium they were trapped near impurity atoms; thus the long range order was greater in the pure aluminium and the line broadening less. Hall has recently described[87] similar work on tungsten.

With reference to the hypothesis of Smith and Wood that plastic deformation of the order of 1 or 2 per cent produces an amorphous layer round each crystallite (see page 194), it should be noted that there is no evidence of the development of such amorphous material which would lead to a very marked increase in background intensity at low θ values.

In his research on fatigue, Terminassov also measured[96] the variation of the ratios of the intensities of the 310 and 220 diffraction lines. He concluded that this ratio remained constant if the specimen was undergoing stress reversals in the safe range, but decreased with time after an induction period if the stress was great enough to cause eventual failure.

Terminassov does not seek an explanation of the observation, but it is of interest particularly because of the dubiety of the line breadth criterion of safe and unsafe stress ranges.

It is certain that the measurement of the intensities, both of background and of lines, is potentially the most powerful x-ray method of investigating the fundamental phenomena accompanying the plastic deformation of metals. But it seems probable that an accuracy of the order of ± 2 per cent in absolute intensity measurements will be essential before the experimental data can be of real use. This accuracy is now possible with the use of focusing monochromators and of efficient Geiger counters with adequate electronic circuits, as the work of Hall has indicated. Again it appears that the simultaneous measurement of line breadths and of lattice parameters would give additional data of assistance in the theoretical discussion of the observations.

The author wishes to thank those colleagues who made their manuscripts available prior to publication. This chapter is published with the permission of the Chief Scientist, Ministry of Supply.

REFERENCES

[1] BARRETT, C. S. *Structure of Metals* New York, 1943
[2] TAYLOR, A. *Introduction to X-ray Metallography* London, 1945
[3] BARRETT, C. S. *Trans. Amer. Inst. min. (metall.) Engrs* 161 (1945) 15
[4] GUINIER, A. and TENNEVIN, J. *Acta Crystallogr.* 2 (1949) 133
[5] NEERFELD, H. *Mitt. K.-Wilh.-Inst. Eisenforsch.* 27 (1944) 81
[6] FINCH, L. G. *Nature, Lond.* 163 (1949) 402
[7] RACHINGER, W. A. *J. Sci. Instrum.* 25 (1948) 254
[8] CRUSSARD, C. and AUBERTIN, F. *Rev. Métall.* 46 (1949) 354
[9] *Progress in Metal Physics I* London, 1949
[10] MOLLER, H. and BARBERS, J. *Mitt. K.-Wilh.-Inst. Eisenforsch* 17 (1935) 81
[11] —— and MARTIN, G. *ibid* 21 (1939) 261
[12] SMITH, S. L. and WOOD, W. A. *Proc. roy. Soc. A* 178 (1941) 93
[13] BOLLENRATH, F., OSSWALD, E., MOLLER, H. and NEERFELD, H. *Arch. Eisenhüttenw.* 15 (1941) 183
[14] NEERFELD, H. *Mitt. K.-Wilh.-Inst. Eisenforsch* 24 (1942) 61
[15] HAUK, V. *Z. Metallk.* 35 (1943) 156
[16] GLOCKER, R. and SCHAABER, O. *Ergebn. tech. Röntgenk.* 6 (1938) 34
[17] SMITH, S. L. and WOOD, W. A. *Proc. roy. Soc. A* 176 (1940) 398
[18] —— —— *J. Inst. Met.* 67 (1941) 315
[19] KOCHANOVSKA, A. *Rev. Métall.* 43 (1946) 192
[20] VOIGT, W. *Lehrbuch der Kristallphysik* Ed. B. G. Teubner, 1910 and 1928
[21] REUSS, A. *Z. angew. Math. Mech.* 9 (1929) 49
[22] BRUGGEMAN, D. A. G. *Z. Phys.* 92 (1934) 561
[23] BOAS, W. and SCHMID, E. *Helv. chim. Acta* 7 (1934) 628
[24] WOOSTER, W. A. *Crystal Physics* 237 Cambridge, 1938
[25] GOENS, E. and WEERTS, J. *Phys. Z.* 37 (1936) 321
[26] NEERFELD, H. Bd. Trade Tech. Inform. Docum. Unit Libr. *Ref F.D.1281/47* (1947)
[27] HANSTOCK, R. F. and LLOYD, E. H. *Proc. Instn. mech. Engrs, Lond.* 157 (1947) 52

[28] Wever, F. and Pfarr, B. *Mitt. K.-Wilh.-Inst. Eisenforsch* 15 (1933) 137
[29] Zachariasen, W. H. *X-ray Diffraction from Distorted Lattices* London, 1945
[30] Smith, S. L. and Wood, W. A. *ibid* 181 (1942) 72
[31] Greenough, G. B. *ibid* 197 (1949) 556
[32] —— *Metal Tr.* 16 (1949) 58
[33] Hauk, V. *Z. Metallk.* 39 (1948) 108
[34] Bollenrath, F., Hauk, V. and Osswald, E. *Z. Ver. dtsch. Ing.* 83 (1939) 129
[35] Glocker, R. and Hasenmaier, H. *ibid* 84 (1940) 825
[36] Wood, W. A. *Proc. roy. Soc. A* 192 (1948) 218
[37] Garrod, R. I. *Nature, Lond.* 165 (1950) 241
[38] Finch, L. G. *ibid* 166 (1950) 508
[39] Zener, C. *Trans. Amer. Inst. min. (metall.) Engrs.* (Met. Divis.) 147 (1942) 361
[40] Smith, S. L. and Wood, W. A. *Proc. roy. Soc. A* 182 (1944) 404
[41] Davidenkov, N. N. and Timofeeva, M. N. *J. tech. Phys. U.S.S.R.* 16 (1946) 283
[42] Lihl, F. *Arch. Metallk.* 1 (1946) 16
[43] Greenough, G. B. *J. Iron Steel Inst.* In press
[44] Seitz, F. *Physics of Metals* New York, 1943
[45] Greenough, G. B. *Nature, Lond.* 160 (1947) 258
[46] —— *ibid* 166 (1950) 509
[47] Finch, L. G. *Ph.D. Thesis* Sheffield, 1949
[48] Taylor, G. I. *J. Inst. Met.* 62 (1938) 307
[49] Wood, W. A. and Dewsnap, N. *Nature, Lond.* 161 (1948) 682
[50] Greenough, G. B. *ibid* 161 (1948) 683
[51] Wood, W. A. and Dewsnap, N. *J. Inst. Met.* 77 (1950) 65
[52] —— *Proc. roy. Soc. A* 172 (1939) 231
[53] Spillett, E. E. *J. Inst. Met.* 69 (1943) 149
[54] Owen, E. A., Liu, Y. H. and Morris, D. P. *Phil. Mag.* 39 (1948) 831
[55] Owen, E. A. and Liu, Y. H. *ibid* 78 (1950) 93
[56] Wood, W. A. and Thorpe, P. L. *Proc. roy. Soc. A* 174 (1940) 310
[57] Nicholson, M. M. *Ph.D. Thesis* Cambridge, 1947
[58] Fricke, R. *Z. phys. Chem.* 52 (1942) 284
[59] Rymer, T. B. and Butler, C. C. *Proc. phys. Soc.* 59 (1947) 541
[60] Greenough, A. P. and King, R. *J. Inst. Met.* 79 (1951) 415
[61] van Arkel, A. E. *Physica* 5 (1925) 208
[62] Jones, F. W. *Proc. roy. Soc. A* 166 (1938) 16
[63] Stokes, A. R. and Wilson, A. J. C. *Proc. phys. Soc.* 56 (1944) 174
[64] ——, Pascoe, K. J. and Lipson, H. *Nature, Lond.* 151 (1943) 137
[65] Wilson, A. J. C. *Acta Crystallogr.* 2 (1949) 220
[66] Lipson, H. *Internal Stresses in Metals and Alloys* Symposium. Inst. Met. (1948)
[67] Scherrer, P. *Kolloidchemie* p 287, 1920
[68] Wood, W. A. and Rachinger, W. A. *J. Inst. Met.* 75 (1949) 571
[69] Warren, B. E. *J. chem. Phys.* 2 (1934) 551
[70] Taylor, A. *Phil. Mag.* 31 (1941) 339
[71] Brindley, G. W. *Proc. phys. Soc.* 52 (1940) 117
[72] Megaw, H. D. and Stokes, A. R. *J. Inst. Met.* 71 (1945) 279
[73] Smith, C. S. and Stickley, E. E. *Phys. Rev.* 64 (1943) 191
[74] Wood, W. A. *Nature, Lond.* 151 (1943) 585
[75] Lipson, H. and Stokes, A. R. *ibid* 152 (1943) 20
[76] Dehlinger, U. and Kochendörfer, A. *Z. Metallk.* 31 (1939) 231
[77] —— —— *Z. Krystallogr. A* 101 (1939) 134
[78] Bragg, W. L. *Nature, Lond.* 149 (1942) 511
[79] —— *Proc. Camb. phil. Soc.* 45 (1949) 125
[80] Hall, W. H. *J. Inst. Met.* 75 (1950) 1127

[81] KELLAR, J. N., HIRSCH, P. B. and THORP, J. S. *Nature, Lond.* 165 (1950) 554
[82] SHULL, C. G. *Phys. Rev.* 70 (1946) 679
[83] STOKES, A. R. *Proc. phys. Soc.* 61 (1948) 382
[84] AVERBACH, B. L. and WARREN B. E. *J. appl. Phys.* 20 (1949) 885
[85] WARREN, B. E. and AVERBACH, B. L. *ibid* 21 (1950) 595
[86] HALL, W. H. *Ph.D. Thesis* Birmingham, 1950 (see also WILLIAMSON, G. K. *ibid* 1950)
[87] —— *J. Inst. Met.* 77 (1950) 601
[88] CAHN, R. W. *ibid* 76 (1949) 121
[89] WOOD, W. A. *Phil. Mag.* 19 (1935) 219
[90] PATERSON, M. S. *Ph.D. Thesis* Cambridge, 1948
[91] —— and OROWAN, E. *Nature, Lond.* 162 (1948) 991
[92] LOS, J. *M.Sc. Thesis* Cambridge, 1947
[93] DEHLINGER, U. *Z. Metallk.* 23 (1931) 147
[94] GOUGH, H. J. and WOOD, W. A. *Metal Progr.* 30 (1936) 91
[95] BARRETT, C. S. *ibid* 32 (1937) 677
[96] TERMINASSOV, J. C. *J. tech. Phys., U.S.S.R.* (1948)
[97] OROWAN, E. *Proc. roy. Soc. A* 171 (1939) 79
[98] NIEMANN, F. and STEPHENSON, S. T. *Phys. Rev.* 62 (1942) 330
[99] BRAGG, W. L. and WEST, J. *Z. Krystallogr.* 69 (1928) 118
[100] ECKSTEIN, H. *Phys. Rev.* 68 (1945) 120
[101] EWALD, P. P. *Proc. phys. Soc.* 52 (1940) 167
[102] GUINIER, A. *ibid* 57 (1945) 310
[103] FOURNET, G. and GUINIER, A. *C.R. Acad. Sci., Paris* 228 (1949) 66
[104] WILSON, A. J. C. *Research* 2 (1949) 541
[105] —— *ibid* 3 (1950) 387
[106] HENGSTENBERG, J. and MARK, H. *Z. Phys.* 61 (1930) 435
[107] BOAS, W. *Z. Krystallogr.* 96 (1937) 214
[108] BRILL, R. *Z. Phys.* 105 (1937) 378
[109] BOAS, W. *Z. Krystallogr.* 97 (1937) 354
[110] AVERBACH, B. L. and WARREN, B. E. *J. appl. Phys.* 20 (1949) 1066
[111] GUINIER, A. *C.R. Acad. Sci., Paris* 208 (1939) 894
[112] GREENOUGH, G. B. *Ph.D. Thesis* Cambridge, 1947
[113] WAGNER, G. and KOCHENDÖRFER, A. *Z. Naturforsch.* 3a (1948) 364
[114] —— —— *Ann. Phys., Lpz.* 6 (1949) 129

7

RECRYSTALLIZATION AND GRAIN GROWTH

J. E. Burke and D. Turnbull

METALS HAVE been worked and annealed since prehistoric times, but little attempt was made to explain the changes that occur during annealing until 1881, when KALISHER[1] observed that heating caused changes in the 'molecular structure' of cold-worked zinc. By then it was well known that metals are crystalline, and Kalisher assumed that the working destroyed the crystallinity of the metal, and that heating permitted it to recrystallize. From that time there has been a continuous series of papers describing, explaining and formulating the changes that occur during annealing. The results of the very early workers have been summarized by CZOCHRALSKI[2] and later reviews have been written by SCHMID and BOAS,[3] SACHS and VAN HORN,[4] BURGERS,[5] MEHL[6] and BURKE.[7]

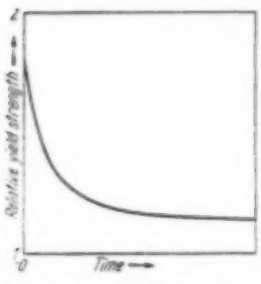

Figure 1. Isothermal recovery curve (schematic)

Terminology

The annealing process is complex and a deformed metal may pass through a number of stages while it is being restored to essentially perfect crystallinity. It has been customary to apply the terms recovery, recrystallization and grain growth to these stages. These terms, however, have carried different connotations of mechanism and driving force to different workers, so that it is often difficult to know which to apply to a given transformation. We shall use these terms with approximately their common meanings, but shall redefine them to permit their use with less ambiguity.

Recovery—This is the first change that occurs upon annealing a deformed metal. We shall apply the term to the essentially continuous changes in physical properties that occur in the unrecrystallized part of a deformed metal during annealing. Recovery has no incubation period and the rate decreases as the process proceeds, as shown in the typical recovery isotherm of *Figure 1*. It is intended that this definition should include the process of polygonization[8] but not the restoration of physical properties by the migration of grain boundaries which were

present prior to deformation. This latter process we consider to be grain growth.

Recrystallization—The recrystallization of a deformed metal resembles a phase transformation, in that it can be described in terms of a nucleation frequency $\dot{N}$ and a linear rate of growth G. After an incubation period, strain-free grains start to grow from a number of sites, the number of sites increases with time, and the strain-free grains grow until they have consumed the matrix. A graph of the fraction transformed as a function of time gives a sigmoidal reaction curve as shown in *Figure 2*. We shall consider recrystallization to be that transformation which occurs in a cold-worked metal with reaction kinetics of this type. It should be noted that this definition makes no assumption about the nature of recrystallization nuclei or about the mechanism of their formation. Part of the process may be identical to grain growth.

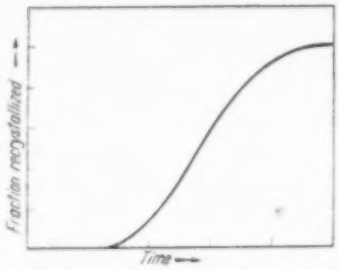

Figure 2. Isothermal recrystallization curve (schematic)

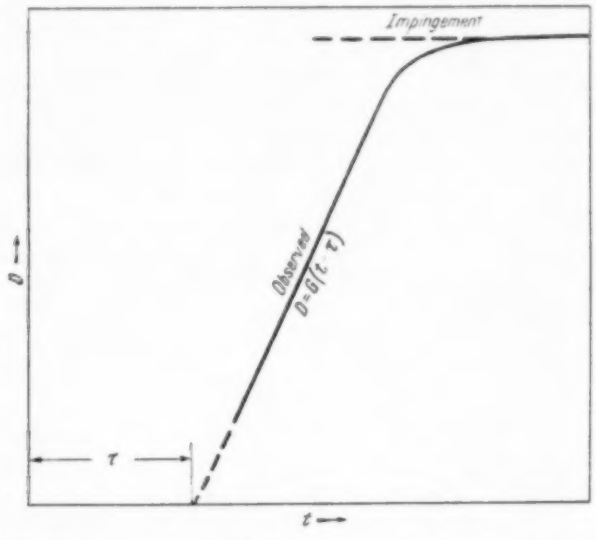

Figure 3. Size, D, *of recrystallized grain as a function of time (schematic)*

A process which is kinetically identical may occur under special conditions in a metal that has already undergone recrystallization. The term 'secondary recrystallization' has been applied to the process,

and because it can be described in terms of $\dot{N}$ and G we shall also use this term. Since prior deformation does not seem to be required for secondary recrystallization, it will be considered to be a special case of grain growth. Where it is necessary to avoid ambiguity, the term 'primary recrystallization' will be applied to recrystallization in a deformed metal.

Grain Growth—Grain growth occurs by the migration of grain boundaries that were present prior to annealing. It can occur in deformed specimens, but the term will be taken specifically to refer to the increase in grain size that results from annealing after recrystallization is complete. No reaction kinetics are specified for grain growth, and they may vary with the material. In an undeformed metal, if the grain size remains uniform, the rate of grain growth decreases as the grain size increases. During secondary recrystallization, the rate of growth is independent of time.

VOL 3

'*Laws of Recrystallization*'

By about 1920, the effects of a number of variables upon recrystallization and grain growth had been established qualitatively. These are usually presented as the laws of recrystallization. Briefly, these 'laws' are as follows:

1. a minimum deformation is necessary to cause recrystallization
2. the smaller the degree of deformation, the higher is the temperature required to cause recrystallization
3. increasing the annealing time decreases the temperature necessary for recrystallization
4. the final grain size depends chiefly upon the degree of deformation, and to a lesser extent on the annealing temperature, being smaller the greater the degree of deformation and the lower the annealing temperature
5. the larger the original grain size, the greater is the amount of cold deformation required to give equivalent recrystallization temperature and time
6. the amount of cold work required to give equivalent deformational hardening increases with increasing temperature of working
7. continued heating after recrystallization is complete causes the grain size to increase.

Where the quantities of interest are primarily a suitable temperature for annealing and the grain size that will result from annealing, the above laws give a satisfactory qualitative statement of the effect of variables on the process. A more quantitative description of the

process, however, requires a more detailed statement of the kinetics, and the atomic mechanisms by which the cold-worked metal is restored through annealing. We shall here consider the process from these standpoints.

Energies Involved

Since the transformations which occur during annealing will be considered largely from the point of view of energy, it is interesting to review the magnitude of the energies involved.

TAYLOR and QUINNEY[9] have measured calorimetrically the heat evolved on annealing cold-worked metals and find it to be of the order of 0·5 to 1·0 cal/gm, or for copper about 30 cal/gm atomic weight. Part of this energy will be evolved during recovery and part during recrystallization. During grain growth after recrystallization, the energies are an order of magnitude smaller. Assuming the grains are close-packed cubes the grain boundary area per cubic centimetre equals $3/D$ cm^2 where D is the grain diameter in centimetres. SEARS[10] finds the specific surface energy of grain boundaries to be about 500 ergs or approximately 10^{-5} cal/cm^2. Thus, for a grain size of 10^{-3} cm, the grain boundary energy is about 0·21 cal/gm atom for copper. If the grain diameter increases by a factor of ten, about 0·19 cal/gm atom will be evolved. These values may be compared with 3,100 cal/gm atom for fusion of copper.

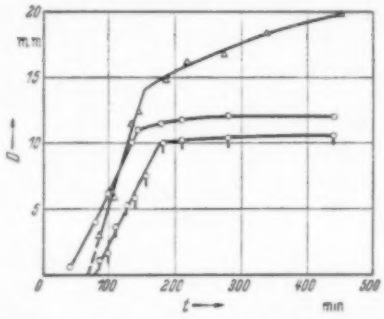

Figure 4. D *as a function of time for three grains in the recrystallization of fine-grained aluminium*

FORMAL THEORY OF RECRYSTALLIZATION KINETICS

Description of Nucleation and Growth—Microstructural observations have shown that the progress of isothermal recrystallization can be described, under certain conditions, in terms of the parameters $\dot{N}$, nucleation frequency and G, the linear rate of grain growth. Let a dimension of a grain growing isothermally into a strained matrix be D. Then it is frequently observed[11–13] that D varies with time, t, as shown schematically in *Figure 3*. From the time that the recrystallizing grain becomes distinguishable from the surrounding matrix until it impinges upon other recrystallizing grains or the specimen boundaries, D is generally described by the relation:

$$D = G(t - \tau) \quad . \quad . \quad . \quad . \quad (1)$$

where $\tau > 0$, G is the linear rate of growth, and τ is the nucleation period. The average τ is reciprocally related to the nucleation frequency,* $\dot{N}$. Description of the entire observable process of recrystallization requires the integration of the relations of the type shown in equation 1 in three dimensions for all the recrystallizing grains and the solution of the geometrical problem of impingement.

Let the total volume of substance be unity and X the volume (or fraction) recrystallized in time t. It is required to find $X = f(t)$. A derivation will be given that follows those of VON GÖLER and SACHS,[14] JOHNSON and MEHL[15] and AVRAMI (now MELVIN)[16] for general nucleation growth processes. Let G_x, G_y and G_z be linear growth vectors for the x, y and z directions. Then neglecting impingement the volume v of a particular recrystallized grain at time t is:

$$v = fG_xG_yG_z(t-\tau)^3 \qquad \ldots . \quad (2)$$

where the growth vectors are assumed to be independent of time and f is a shape factor. If $\dot{N}$ is the nucleation frequency per unit volume the number of grains dn originating in a time interval $d\tau$ is:

$$dn = \dot{N}(1-X)\underset{t=\tau}{d\tau} \qquad \ldots . \quad (3)$$

In the von-Göler–Sachs treatment an unimpinged volume X' is evaluated from the relation

$$X' = \int_0^t v\,dn = fG_xG_yG_z \int_0^t (t-\tau)^3\,\dot{N}(1-X)\underset{t=\tau}{d\tau} \qquad \ldots . \quad (4)$$

and X' is assumed equal to X. Because it does not take impingement into account, the von-Göler–Sachs equation can only be strictly applicable when $X \to 0$. In the Johnson–Mehl and Avrami derivations a number dn' is defined as follows:

$$dn' = dn + \dot{N}Xd\tau = \dot{N}d\tau \qquad \ldots . \quad (5)$$

where $\dot{N}Xd\tau$ is the number of 'phantom' grains that would have originated in the volume X had it not recrystallized. The extended volume X_{ex} calculated without regard for impingement and counting the phantoms is given by:

$$X_{ex} = \int_0^t v\,dn' = fG_xG_yG_z \int_0^t (t-\tau)^3 \dot{N}d\tau \qquad \ldots . \quad (6)$$

To complete the solution of the problem an equation relating X_{ex} and X is needed. Johnson and Mehl, and Avrami have written the necessary relation as follows:

$$dX/dX_{ex} = 1 - X \qquad \ldots . \quad (7)$$

* The word nucleation implies no particular mechanism but is applied to a process whose kinetics are partly described in terms of the parameter τ.

Any perimeter laid down at random on a cross section consisting of transformed and untransformed material will intersect untransformed material along $1 - X$ of its total length. Since the increment of the total length of the perimeter of all grains, intersecting a cross section including phantoms (to ensure complete randomness) is proportional to dX_{ex} equation 7 follows. A more rigorous derivation[16] has been given by Avrami.

Substituting equation 7 into equation 6 gives the basic relation common to the Johnson–Mehl and Avrami theories as follows:

$$\int_0^X dX/(1 - X) = -\ln(1 - X) = fG_xG_yG_z \int_0^t (t - \tau)^3 \dot{N} d\tau$$

or . . . . (8)

$$X = 1 - \exp\left(- \int_0^t v dn' \right) \quad . . . . (9)$$

In the recrystallization of thin sheets it may happen that the lateral dimensions of the recrystallized grains become much larger than the sheet thickness δ so that the value for v to be used in solving equation 9 is

$$v = fG_xG_y\delta(t - \tau)^2 \quad . . . . (10)$$

rather than equation 2 that holds for 'three dimensional' recrystallization. Similarly in the recrystallization of thin wires of diameter δ, where the length of the recrystallized grains is much larger than δ, the expression for v is

$$v = fG_y\delta^2(t - \tau) \quad . . . . (11)$$

Essentially the Johnson–Mehl and Avrami treatments diverge only in their assumptions on the form of the function $\dot{N} = f(\tau)$ to be used in the solution of equation 9. According to the Johnson–Mehl theory the function must, in general,* be evaluated by experiment while Avrami assumes an explicit form for it. According to Avrami's theory there are pre-existing in the untransformed matrix a limited number $\bar{N}$ of preferred nucleation sites each having a nucleation frequency ν. In ordinary phase transitions these sites may be occupied by inclusions that happen to catalyse the formation of nuclei of the new-forming phase. In recrystallization reactions positions where the strain is extraordinarily large may be the preferred nucleation sites. At any rate during recrystallization the sites are used up by becoming recrystallization nuclei and the number of potential nucleation sites $\mathcal{N}$ remaining after time τ is:

$$\mathcal{N} = \bar{N} \exp[-\nu\tau] \quad . . . . (12)$$

giving

$$\dot{\mathcal{N}} = \bar{N}\nu \exp[-\nu\tau] \quad . . . . (13)$$

* Johnson and Mehl did make some assumptions about the form of $\dot{N} = f(\tau)$ for the purpose of showing how equation 9 might be solved to give simple relations in specific instances.

Substituting in equation 9 and letting $G_x = G_y = G_z$ gives:

$$X = 1 - \exp\left\{-\bar{N}\,vfG^3 \int_0^t (t-\tau)^3 \exp[-v\tau]\mathrm{d}\tau\right\} \quad . \ . \ . \ (14)$$

and upon performing the integration:

$$X = 1 - \exp\{(\sigma fG^3\bar{N}/v^3)\,[\exp(-vt) - 1 + (vt) - (vt)^2/2! + (vt)^3/3!]\} \quad . \ . \ . \ . \ (15)$$

For vt very large this approximates to*:

$$X = 1 - \exp[-fG^3\bar{N}t^3] \quad . \ . \ . \ . \ (16)$$

while for $vt \to 0$

$$X = 1 - \exp[-fG^3\bar{N}vt^4/4] \quad . \ . \ . \ . \ (17)$$

Equation 17 is formally the same as obtained by Johnson and Mehl when $\dot{N}(=\bar{N}v)$ was assumed to be independent of time and $G_x = G_y = G_z$. Avrami proposes that for three dimensional recrystallization in general:

$$X = 1 - \exp[-Bt^k] \quad . \ . \ . \ . \ (18)$$

with

$$3 \leqslant k \leqslant 4$$

By substituting equations 10 or 11 in equation 9 and carrying out the indicated operations, it can be verified that equation 18 holds also for two dimensional recrystallization with

$$2 \leqslant k \leqslant 3$$

and for one dimensional recrystallization with

$$1 \leqslant k \leqslant 2$$

Table I summarizes some limiting equations obtained from the Johnson–Mehl and Avrami theories.

Table I. Limiting Equations obtained from the Johnson–Mehl and Avrami Theories

Type of Recrystallization	$X = f(t)$	
	Johnson–Mehl assuming $\dot{N}$ = *constant*	*Avrami k values in* $X = 1 - \exp(-Bt^k)$
Three dimensional	$X = 1 - \exp(-fG^3\dot{N}t^4/4)$	$3 \leqslant k \leqslant 4$
Two dimensional (e.g. sheet) . .	$X = 1 - \exp(-fG^2\delta\dot{N}t^3/3)$	$2 \leqslant k \leqslant 3$
One dimensional (e.g. wire) . .	$X = 1 - \exp(-fG\delta^2\dot{N}t^2/2)$	$1 \leqslant k \leqslant 2$

* When vt is very large N equation 12 $\to 0$ in a time that is very short relative to the time at which $X = 1/2$.

Although Avrami's theory is very flexible, as it stands it requires that $\dot{N}$ always decreases or remains essentially constant with time and makes no provision for the experimental facts (to be described in a following section) that $\dot{N}$ sometimes increases sharply with time. In describing this behaviour the Johnson–Mehl theory, that makes no assumption about $\dot{N} = f(\tau)$, is more flexible.

Some Alternative Descriptions of Recrystallization Kinetics—KRUPKOWSKI and BALICKI[17] have proposed that recrystallization is a first order reaction so that:

$$dX/dt = k(1 - X) \quad . \ . \ . \ . \ (19)$$

which when integrated with the condition $x = 0$ at $t = 0$ gives:

$$X = 1 - \exp[-kt] \quad . \ . \ . \ . \ (20)$$

The concept that recrystallization be described as a first order rate process is not compatible with the nucleation growth description unless the parameters $\dot{N}$, G decrease with time in an arbitrary manner. Apparently Krupkowski and Balicki envisage recrystallization as an essentially homogeneous process that can be treated in a manner analogous to the Bragg–Williams treatment[18] of the kinetics of order–disorder reactions. Since the form of most recrystallization isotherms is sigmoidal (*Figure 2*), contrary to the predictions of equation 20, the description of recrystallization as a first order rate process cannot be generally valid.

COOK and RICHARDS[19] also have proposed another description of recrystallization kinetics independent of the $\dot{N}$, G concept. They postulate that recovery is a first order rate process so that the fraction w of a specimen recovered in time t is:

$$w = 1 - \exp(-\beta t) \quad . \ . \ . \ . \ (21)$$

where β is a constant. They further postulate that the rate of recrystallization is a first order process confined entirely to the part of the specimen which has undergone recovery. It follows then that the rate of recrystallization is:

$$dX/dt = kw(1 - X) = k(1 - \exp[-\beta t])\,(1 - X) \quad . \ . \ . \ . \ (22)$$

where k is a constant.

Making the approximation

$$w = \beta t \quad . \ . \ . \ . \ (23)$$

valid only for $1 \gg w$, equation 22 was integrated to give

$$-\ln(1 - X) = (k\beta/2)t^2 = Ct^2 \quad . \ . \ . \ . \ (24)$$

Cook and Richards' equation 24 is identical in form with Avrami's equation 18 derived on the basis of the $\dot{N}$-G description for two dimensional growth. Should Cook and Richards' relation be found

applicable to a recrystallization process in which grains grew as polyhedra rather than as platelets the $\dot{N}$-G description could be satisfactory only if G decreased with time.

A basic assumption of the formal theory just presented, is that nucleation is equally probable in any volume element of the deformed specimen which is equal to or smaller than the minimum resolvable volume of the recrystallized grains. Data on recrystallization kinetics are probably not yet sufficiently extensive to require any more special assumptions for their description. However, a formal theory[15] that treats the problem of preferential nucleation at grain boundaries has been given by Johnson and Mehl.

Description of Experiments in Terms of Formal Recrystallization Theory—KARNOP and SACHS[11] first proved the applicability of the $\dot{N}$-G description to recrystallization by their experiments on lightly deformed (9 to 10 per cent) fine-grained aluminium. Their technique consisted in measuring the grain size D of particular recrystallizing grains after various periods of time at the annealing temperature. However, in order to reveal the grain boundaries, it was necessary, after each period of time at the annealing temperature, to cool the specimen to room temperature and etch. Their results demonstrated that D for each recrystallizing grain was satisfactorily described (before impingement) by equation 1. Some of their data are plotted in *Figure 4*.

Using a similar technique KORNFELD and PAVLOV[13] confirmed the validity of the $\dot{N}$-G description in the recrystallization of fine-grained aluminium wires deformed 3 to 8 per cent in tension and investigated the effect of temperature, strain and prior recovery treatments on $\dot{N}$ and G. KORNFELD and SAWIZKI[20] showed that the recrystallization of polycrystalline tin, cadmium, and iron strained 2·0, 0·6 and 3·5 per cent, respectively, is satisfactorily described in terms of $\dot{N}$ and G. Also, by using the cooling–etching technique, COLLINS and MATHEWSON[21] proved that the recrystallization of heavily deformed high purity aluminium single crystals takes place by an $\dot{N}$-G process.

The experimental technique of Karnop and Sachs and Kornfeld and co-workers has been criticized on the following grounds[22]:

i additional strains may be put into the specimen by heating and cooling the sample between room and the annealing temperature and by handling during etching

ii the etching treatment *per se* might modify the subsequent course of recrystallization.

A technique which circumvents these objections is that of viewing the progress of recrystallization through a window in the annealing furnace. This method is not often applicable to experiments on the recrystallization of metals because boundary migration progresses

more rapidly than boundary grooves can develop by thermal etching. However, MÜLLER[12] observed that during the recrystallization of deformed rock salt single crystals, crystal boundaries were clearly delineated at all stages of their progress by the different reflectivity of crystal faces and by thermal etch pits. From the standpoint of precision, reproducibility and completeness of data on the effect of variables on $\dot{N}$ and G, Müller's investigation stands as one of the most excellent in the field of recrystallization kinetics. His results prove that the recrystallization of rock salt crystals closely follows the $\dot{N}$-G description for strains (compression at 400°C) at least as large as 50 per cent.

The results that have been reviewed in the foregoing, show the validity of the $\dot{N}$-G description in recrystallization, but give no information on the applicability of the impingement theory. Some experiments of MEHL and co-workers[22–24] were designed to test the impingement theory and to measure $\dot{N}$ more quantitatively.

Mehl and his co-workers used a statistical procedure to measure $\dot{N}$ and G that consists in annealing various equivalent samples for different periods of time and then measuring the number of grains and total progress of recrystallization in each. The size of the aggregate sample is chosen so that a large number of recrystallized grains have formed during the chosen time intervals. Thus statistical fluctuations in $\dot{N}$ are small. G is determined by plotting the diameter of the largest unimpinged grain *versus* time and is assumed to be the same for all grains—an assumption making their description less than completely satisfactory for evidence will be cited which demonstrates that G varies widely for different recrystallizing grains. However, from their analysis G proved to be independent of time and $\dot{N}$ was found to be related to τ (equation 8) by the equation:

$$\dot{N} = a \exp[b\tau] \qquad \ldots . \quad (25)$$

where $\exp(b\tau) \gg a$ for all times of observation. According to equation 25 $\dot{N}$ increases sharply with time. This result is at variance with the prediction of the Avrami theory that $\dot{N}$ should decrease or remain constant with increasing time.

Substituting equation 25 into the general equation obtained by Johnson and Mehl for two dimensional transformations STANLEY and MEHL[22] obtain

$$X = 1 - \exp[-(2\pi G^2 \delta a/b^2)(\exp\{bt\}/b - bt^2/2 - 1/b - t)] \qquad \ldots . \quad (26)$$

Figure 5 compares the transformation curve calculated from equation 26 and the directly measured transformation curve for an isotherm obtained by Anderson and Mehl in the recrystallization of high purity

aluminium. The agreement is fair and deviations may possibly be explained by the orientation dependence of G in addition to the experimental uncertainties.

It has been demonstrated that the kinetics of secondary recrystallization of copper having a high degree of cube orientation[25] and of silver[26] are entirely analogous to the kinetics of primary recrystallization in lightly deformed specimens. D values for particular grains are satisfactorily described by equation 1. WARD[25] found that $\dot{N}$ in the secondary recrystallization of OFHC copper increases sharply with time according to the relation[22] (equation 25) found by Stanley and Mehl, $X = f(t)$ was found in both investigations to be satisfactorily described by equation 9.

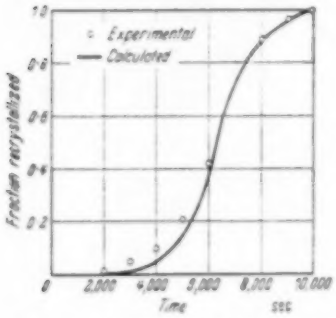

Figure 5. Comparison of experimental data with curve calculated from impingement theory for the recrystallization of aluminium: temperature = 350°C, ε = 0·051

In some studies of isothermal recrystallization $\dot{N}$ and G were not measured directly but certain observations were interpreted by making special assumptions about $\dot{N} = f(\tau)$, G as a function of orientation *etc.*

For example, Karnop and Sachs deformed a tapered (conical) specimen of electrolytic copper in tension to produce strains of 3 to 18 per cent along the length and annealed it for a definite period of time.[11] The strain at which the sample was estimated (by visual examination) to be approximately one half recrystallized and the size of the largest recrystallized grain in the region were recorded. The procedure was repeated for a sequence of times. G was calculated on the assumptions that it is independent of time and orientation and that $\tau = 0$ for the largest grain. $\dot{N}$ was calculated from the Johnson–Mehl equation* (*Table I*) for three dimensional recrystallization on the assumption that it is independent of time. In view of later experiments, the validity of all the Karnop–Sachs assumptions with the exception that G is independent of time are open to serious question. Certainly, the results can give no clue on how the impingement problem should be described.

There seems to be no direct microstructural proof that the nucleation and growth picture of recrystallization can be extended to heavily deformed fine-grained specimens. Detailed information on the progress of microstructural changes during recrystallization can be obtained readily only when a marked contrast in size between recrystallized and

* Karnop and Sachs actually derived this equation but by an erroneous procedure. Von Göler and Sachs recognized the error and derived equation 4.

deformed grains develop. Such a contrast is observed in the recrystallization of single crystals or when a lightly deformed polycrystalline matrix recrystallizes to several grains, but no marked grain size contrast is observed when a heavily deformed polycrystalline matrix recrystallizes to a fine grain size. For these reasons, microstructural evidence on the applicability of the nucleation growth picture to the recrystallization of heavily deformed fine-grained specimens is difficult to obtain. However, it has been found in a number of instances that the progress of recrystallization in such specimens can be described by kinetic relations derived from the nucleation and growth picture.

DECKER and HARKER[27] and SEYMOUR and HARKER[28] have measured the progress of recrystallization in heavily cold-rolled (98 to 99·7 per cent) strips of copper[27] and nickel–iron alloy[28] by measuring the change of intensity of an appropriate Bragg reflection* from the rolled surface of a strip as a function of time at the annealing temperature. The intensity measurements were made with a Geiger counter x-ray spectrometer. Decker and Harker found that the recrystallization isotherms of spectroscopically pure copper were described by equation 18 with $k \triangleq 3$. For OFHC copper $k \triangleq 3$ for high temperatures and $k \triangleq 2$ for lower temperatures. They interpret their results on the basis of the Avrami theory and suppose that $k \triangleq 3$ when grains grow as polyhedra and $\triangleq 2$ when grains grow as platelets (see k values for two and three dimensional recrystallization in *Table I*). This interpretation assumes that vt in equation 15 is very large or in different words that $\tau = 0$ for all grains. However, no microstructural evidence on how the grains actually grew was obtained. Alternative theories, also based on the $\dot{N}$-G picture, that explain their data as well are:

I when $k = 3$ recrystallization is two dimensional, $\dot{N} \triangleq$ constant and $G =$ constant

II when k = 2 or 3 $\dot{N} \triangleq$ constant but G decreases with time.

Cook and Richards have measured the isothermal rate of recrystallization of high purity copper rolled 80 to 98 per cent by following the change of hardness with time.[19] The hardness change was related to the fraction recrystallized in several experiments by microstructural observations. They assert that their isotherms are satisfactorily described by equation 24 derived from their concept of a sequence of two homogeneous reactions (recovery and recrystallization), but note that equation 24 is identical in form with equation 18 derived for two dimensional recrystallization on the basis of the $\dot{N}$-G theory with $k = 2$. Also, an analysis of their results shows that $k \triangleq 3 \pm 0{\cdot}5$ at

* For example, the rate of appearance of the (200) reflection from planes perpendicular to the rolling direction.

50° and 2 ± 0·3 at 27°C in fair agreement with Decker and Harker. Even in the event that the recrystallization observed by Cook and Richards was three dimensional at the lowest temperature, it is possible that G decreases with time in such a way that $k \simeq 2$. Thus, it appears probable that their results are consistent with the $\dot{N}$-G picture and that it is unnecessary to invoke a two-stage homogeneous recovery and recrystallization sequence in order to explain them.

Effect of Variables on G

It has been pointed out that the $\dot{N}$, G description is adequate for secondary recrystallization or discontinuous grain growth as well as

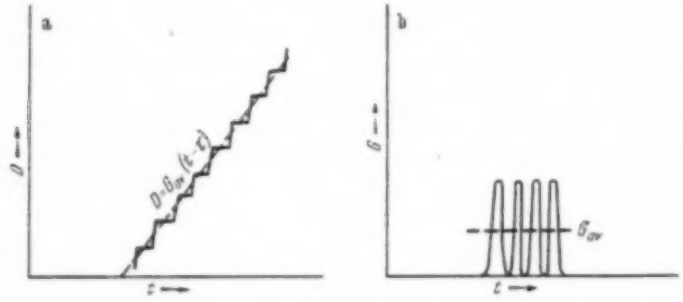

Figure 6. D *and* G *as a function of time in the recrystallization of rock salt single crystals (schematic.)*

for primary recrystallization processes. Also, there is good evidence that the kinetics of normal grain growth after completion of recrystallization are controlled in large part by a parameter G that is closely related to G values measured in primary and secondary recrystallization. For these reasons the effect of variables on G will be considered from a very general point of view and facts will be drawn from all types of processes in which G has been measured.

Time—It has been well established* that in the primary recrystallization of metals G is generally independent of time.[11, 13, 21–24] Recent data[25, 26, 29] have also confirmed the generalization for secondary recrystallization. However, interesting exceptions have been observed that merit serious consideration. Müller by his direct observation method found that G in the recrystallization of rock salt appeared to be independent of time in the low temperature range of his experiments.[12] However, in the high temperature range the boundary moved

* Mehl and co-workers[23, 28] have critically surveyed the evidence bearing on these questions for metals.

in 'spurts' so that the relation of D and G to t is as represented schematically in *Figure 6*. During each period of rapid motion the boundary moves a distance $\alpha \sim 20$ to 30 microns. It is evident that the observed relation between D and t can be closely approximated by equation 1 with $G = G_{av}$. Nevertheless, G is clearly a periodic function of time and its maximum value may be almost an order of magnitude larger than G_{av}. Also BURKE[30] has observed that the motion of boundaries during the primary recrystallization of zinc at room temperature is jerky.

Since even in the event of jerky boundary motion the relation between D and t can be approximated by equation 1, the question must be raised whether the periodicity of G with time is a general phenomenon. Certainly the resolution of most of the experiments on metals[11, 29] was not sufficient for any periodicity in G to be detected were δ the same order of magnitude as for rock salt. Further, a possible interpretation of Müller's failure to observe a periodicity of G in the low temperature recrystallization of rock salt is that $\delta < 1$ micron. Therefore, the significance and interpretation of G values measured in boundary migration experiments must be considered very carefully.

Occasionally it is observed that during recrystallization grains grow at a constant rate for a time and then practically stop growing before any impingement. Müller sometimes found this type of behaviour in the recrystallization of rock salt crystals containing 0·005 molecular per cent of strontium chloride as solute impurity. Similar phenomena have been observed in the secondary recrystallization of copper.[31]

Orientation—In general, G should be a function of relative grain orientations (specified by three parameters) and the boundary orientation (specified by two parameters). However, it appears that there are no completely quantitative data relating G to the orientation parameters though there is a large collection of qualitative data indicating that it is a sensitive function of them.

KORNFELD and RYBALKO[32] observed marked growth anisotropy in the recrystallization of aluminium single crystals (99·5 per cent pure) elongated 12 to 18 per cent in tension. At 570°C the anisotropy in G was about six to one, but at higher temperatures it was much less pronounced.

The orientation of the new grains produced in the secondary recrystallization of cube-textured copper is frequently related to the orientation of the matrix by a rotation about a common (111) pole. BURKE and TURKALO[33] found that G for the new grains was greatest for growth in the [110] direction in the matrix which lies in the common (111) plane. In the [110] matrix direction 90 degrees away, G was several times smaller. Here again, the anisotropy was more pronounced at low than at high temperatures.

After the recrystallization of lightly deformed polycrystalline aluminium, very small crystals are often found embedded in the large recrystallized grains. Presumably these are unabsorbed crystals of the original matrix. TIEDEMA, MAY and BURGERS[34] have shown that the orientation of these occluded crystals is either very nearly identical or twin related to the recrystallized grain surrounding them. The interpretation is that G is very much smaller for such close orientation relations than for those where the orientations of the recrystallized grain and matrix are very different and not twin related.

BECK, SPERRY and HU[35] observed that, of several crystals formed by recrystallization around a scratch or pin prick in a lightly deformed aluminium (single crystal) those related in orientation to the matrix grains by an approximately 30° rotation about a common [111] pole grow several times faster than the crystals of other orientation relations formed around the scratch. These experiments further confirm the orientation dependence of G and have been interpreted on the basis that the orientation relation for which G is a maximum always corresponds to the 30° rotation about the [111] pole in face-centred cubic metals. It is possible that the wide variation in G for individual recrystallized grains growing in a deformed aluminium matrix, as observed in the experiments of KARNOP and SACHS,[11] and KORNFELD and PAVLOV[13] for example, can be explained in terms of a relative grain and boundary orientation dependence.

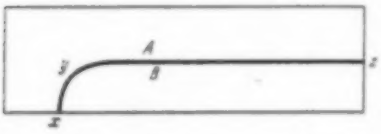

Figure 7. Schematic representation of technique proposed by Dunn[36] for measurement of grain boundary (xy) migration with a constant driving energy; crystal A grows at the expense of B

Recently DUNN[36] has suggested an experimental technique whereby it should be possible to measure G quantitatively as a function of the orientation parameters. *Figure 7* shows a specimen suitable for such measurements. Crystals A and B are prepared having a definite orientation relation by the technique worked out earlier by DUNN.[37] During the growth experiment boundary yz is consumed by the migration of boundary xy that retains a fixed curvature so that the driving force remains constant.

Temperature—For constant strain the dependence of G upon temperature has been described by the relation

$$G = G_0 \exp[-Q_G/RT] \qquad \ldots . \quad (27)$$

Equation 27 is valuable only when there are extended ranges of temperature for which G_0 and Q_G are single valued. Actually in most experiments, where G has been measured in primary or secondary

recrystallization, such extensive ranges of temperature have been revealed. Values of the constants G_0 and Q_G that satisfy equation 27 for various materials and strains are listed in *Table II*.

Also included in *Table II* are results of measurements on rates of normal grain growth. G in normal grain growth cannot have the same formal relation to atomic mobility as G in recrystallization. However, if it is supposed that the geometric sequence in normal grain growth is independent of temperature it follows that the difference in the relations is in the temperature independent factor. It may be assumed

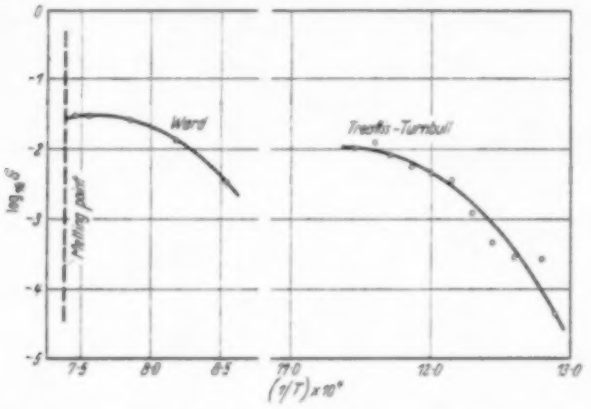

Figure 8. Log G as a function of 1/T in the secondary recrystallization of OFHC copper and spectroscopically pure copper

that the temperature independent factor aG_0 for normal grain growth contains a geometric factor a (in general $a < 1$) that is not present in G_0 for recrystallization.

It is sometimes found that G for a particular metal and with an apparent constant driving energy is not described by a single value of Q_G over the entire temperature range of the measurements. In a number of instances Q_G was found to decrease with increasing temperature. Karnop and Sachs calculated[11] that Q_G decreased continually with increasing temperature in the primary recrystallization of copper and at 10 per cent strain ranged from 50 kcal/gm atom at 310°C to 32 kcal/gm atom at 350°C. Because of their assumptions, the results of Karnop and Sachs may be questioned, however, WARD[25] and later TREAFTIS and TURNBULL[30] established by less questionable procedures that Q_G decreases sharply with increasing temperature in the secondary recrystallization of OFHC and spectroscopically pure copper, respectively. *Figure 8* shows the relationship between log G and $1/T$ found in these investigations.

Anderson and Mehl report values[23] of G_0 and Q_G for the primary

recrystallization of aluminium that diverge widely from the values[13] reported by Kornfeld and Pavlov for the recrystallization of aluminium wires at comparable strains (*Table II*). It is possible, of course, that this divergence may be attributed to factors such as purity, history, mode of deformation *etc*. However, a replot of the data of the two investigations on the same scale (*Figure 9*) reveals that the facts are also compatible with the interpretation that Q_G decreases with increasing temperature in the recrystallization of aluminium. For it is possible

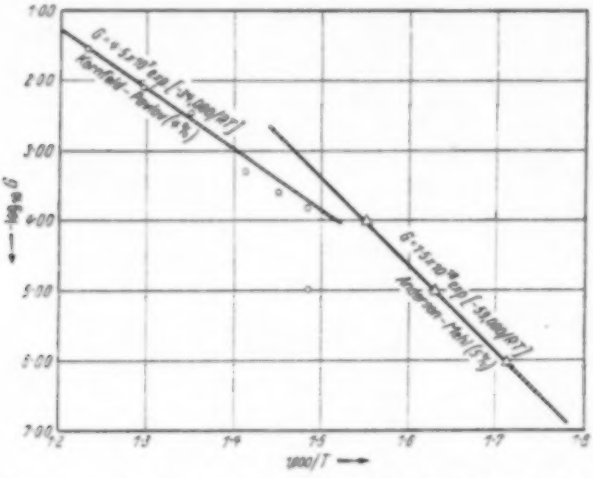

Figure 9. Log G as a function of 1/T in the recrystallization of fine-grained aluminium

to draw a continuous curve (*Figure 9*) through the experimental point of both investigations so that the maximum deviations are little more than the experimental error.

In the recrystallization of heavily deformed rock salt crystals[12] two values of Q_G are required to describe the data (*Table II*)—one valid in the range 400 to 800°C and the lesser value valid in the low temperature range 300° to 400°C. This variation of log G with $1/T$ is similar to the variation of log S with $1/T$ where S is the specific conductivity of rock salt crystals. It is found that two activation energies are required to describe the results with the lesser valid in the low temperature range.

Included in *Table II* are activation energies Q[19, 27, 28] evaluated from the slope of straight lines obtained by plotting log $(1/t_c)$ against $1/T$, where t_c is the time required for a constant fraction $X = c$ of the specimen to recrystallize. Q is not necessarily identical to Q_G because it is also partly determined by the activation energy for nucleation Q_N. However, for the cases considered Q proved to be independent of X within experimental error and the most reasonable interpretation of this fact is that $Q_N \approx Q_G \approx Q$.

Table II

Substance	Primary Recrystallization: Temperature Range °C	Primary Recrystallization: Strain % (reduction in area)	G_0 cm sec^{-1}	Q kcal/gm atom
Aluminium[15]	425–540	4	$4{\cdot}5 \times 10^7$	34·0
Aluminium[21]	310–370	5·1	$1{\cdot}5 \times 10^{16}$	59·0
Rock salt[12]	650–770	1,000* gm/mm^2	9×10^{11}	59·0
Rock salt[12]	400–520	4,000* gm/mm^2	$4{\cdot}2 \times 10^8$	32·0
Rock salt[12]	320–400	4,000* gm/mm^2	10^3	14·5
Copper[13]	300–360	10	10^{23} to 10^7	50·0 to 32·0
Copper (OFHC)[37]	200–250	99·7	†	29·9
Copper (spec. pure)[27]	40–140	98	†	22·4
Copper[19]	25–125	99	†	44·0
Silicon ferrite[24]	740–800	7	$1{\cdot}7 \times 10^{11}$	73·0
Nickel–iron[25]	500–600	98	†	56·5
	Secondary recrystallization			
Silver[26]	433–533		2×10^9	28·0
Copper (OFHC)[26]	900–1000‡		10^{11}	73·0
Copper (spec. pure)[29]	500–520		10^{22}	95·0
	580–600		$10^{5\cdot4}$	29·4
	Grain Growth		Q_G, kcal/gm atom	
	Temperature Range	aG_0 cm sec^{-1}		
Aluminium[28] (0·3 mm grain size)	400–500	10^{21}	87·0	
α-*Brass (comm. purity)*[39]	450–700	10^6 to 10^9	60·0	
α-*Brass (high purity)*[40]	450–850	$0{\cdot}83 \times 10^4$	40·0	

* Expressed as stress on specimen rather than strain.

† G_0 cannot be calculated from data.

‡ Both Q_G and G_0 decreased very sharply ($Q_G \to 0$) at temperatures approaching the melting point.

Strain (ε)—The available data on the relation between G and ε at constant temperature for metals [11, 13, 23, 24] show that G increases as ε^n, where n is substantially greater than unity, for small strains ($\varepsilon < 5$–10 per cent). For larger strains ($\varepsilon > 15$–20 per cent) the indications are[4] that G is practically independent of strain. Anderson and Mehl's measurements[23] on G as a function of ε in the recrystallization of high purity aluminium at 329°C are plotted in *Figure 10*. Their results clearly show a sigmoidal relation between G and ε consistent with the above generalizations with G approaching a constant value at $\varepsilon \simeq 15$ per cent.

The limited data available[12, 23] indicate that both Q_G and G_0 decrease with increasing strain. According to Anderson and Mehl Q_G for aluminium decreases from 62 kcal/gm atom at $\varepsilon \simeq 2$ per cent to about

52 kcal/gm atom at $\varepsilon \simeq 20$ per cent, while G_0 decreases by a factor of approximately 10 over the same range of strain. Müller correlated G for rock salt with stress rather than strain.[12] His measured Q_G values are plotted against stress in *Figure 11*. They fall sharply from a value of approximately 60 kcal/gm atom at a stress to 10^5 gm/cm² to a limiting value of approximately 30 kcal/gm atom at stresses ranging from 2×10^5 to 4×10^5 gm/cm². G_0 decreases by a factor of about 200 as the stress increases from 10^5 to 2×10^5 gm/cm².

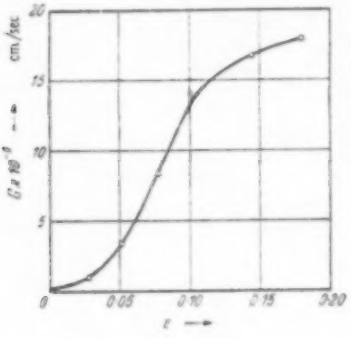

Figure 10. G *as a function of strain, ε, in the recrystallization of aluminium*

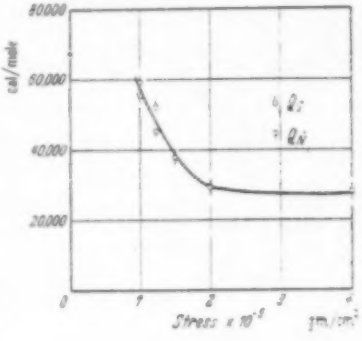

Figure 11. Activation energy for N *and* G *as a function of stress in the recrystallization of rock salt single crystals*

For both aluminium and rock salt the change in Q_G with increasing strain is of the order of 1,000 times the magnitude of the energy of cold deformation. However, G_0 tends to change with increasing ε in a way that partly compensates for the change in G due to the decrease in Q_G.

It has been proved by Beck and Polanyi[41] that G is very dependent upon the specific type of deformation as well as upon the overall strain.

Aluminium single crystals were bent and approximately one half of each crystal was re-straightened. The re-straightened part of the crystal P_1 proved to be harder than the portion that remained bent P_2 yet G was very much larger in P_2 than in P_1.

Recovery Anneal—The available data[12, 13] indicate that recovery anneals (extended heat treatments at temperatures too low to cause visible recrystallization, but sufficiently high to alter the mechanical and electrical properties of cold worked materials) have no perceptible effect on G measured in subsequent recrystallization treatments. It should be noted, however, that these results do not rule out possible recovery effects on G at the recrystallization temperature during the nucleation period.

Purity—It is well known to metallurgists that minute quantities (often $< 0{\cdot}01$ per cent) of impurities may decrease the rate of recrystallization by many orders of magnitude so that the temperature of perceptible recrystallization is increased several hundred degrees. For example, SMART and SMITH[42] have shown that the 'half softening' temperature, $T_{1/2}$ of spectroscopically pure (99.999 per cent) copper may be increased more than 200° by the addition of traces of certain solute impurities. No quantitative conclusions regarding the magnitude of $\dot{N}$ and G can be drawn from the data, but they probably indicate the temperature range (centring around $T_{1/2}$) in which recrystallization takes place at an easily measured rate. The results for several solute elements (0·01 per cent by weight) are shown in *Table III*.

Table III. Data of Smart and Smith[42] showing Effect of Impurity Traces on Softening Temperatures

Element in copper 0·01 per cent by weight	*Half softening temperature* $T_{1/2}$ (°C)
None	140
Silver	205
Antimony	320
Cadmium	305
Tin	315
Tellurium	370

It appears that Müller has obtained the only quantitative data[12] on the effect of a controlled amount of a specific impurity on G. For deformed rock salt crystals containing 0·005 molecular per cent strontium chloride, $G \sim 1/12$ the value for similarly deformed crystals containing no added strontium chloride. Within experimental error, Q_G is independent of the amount of strontium chloride up to 0·005 molecular per cent. However, the interpretation of Müller's results is rendered ambiguous by the fact that G values for different compositions were compared at constant stress and it is not known whether or not the strain was constant.

An interesting effect obtained by Müller is that the periodic fluctuations in growth rate are imperceptible in rock salt crystals containing as little as 0·0025 molecular per cent of strontium chloride. On the other hand, in crystals containing 0·005 molecular per cent strontium chloride, G sometimes falls abruptly to zero before impingement.

Effects of Variables on $\dot{N}$

Time—It has been established that in the recrystallization of lightly deformed fine-grained specimens of aluminium and silicon ferrite

$\dot{N} \simeq 0$ at $t = 0$ and increases sharply with increasing time. Kornfeld and Pavlov first observed[13] this effect in the recrystallization of aluminium wires of commercial purity and found that $\dot{N}$ was best described by the equation

$$\dot{N} = kt \qquad \ldots . \quad (28)$$

For high purity aluminium and silicon ferrite strip Mehl and co-workers found [22–24] $\dot{N}$ to be given by equation 25 (see graphical relation in *Figure 12*a).

In the recrystallization of lightly deformed coarse-grained aluminium strips Anderson and Mehl found[23] that $\dot{N}$ rises from zero to a maximum at τ_{max} and then falls to zero asymptotically as shown in *Figure 12*b.

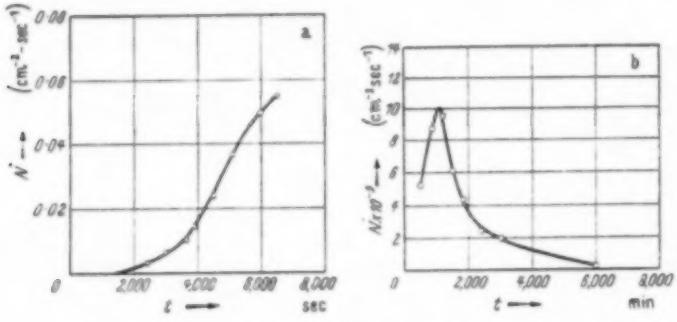

Figure 12. $\dot{N}$ *as a function of time in the recrystallization of* a *fine-grained and* b *coarse-grained (60 grains/mm²) aluminium; temperature = 350°C,* $\varepsilon = 0{\cdot}05$

Müller observed[12] that recrystallized grains always originate in the vicinity of the corners of deformed cubical rock salt single crystals. For a given load and temperature τ was, remarkably, reproducible to $\pm$ 3 per cent. This result can be interpreted on the basis that $\dot{N}(\propto 1/\tau)$ at the cube corner sites increases very sharply with time and much more so than in the recrystallization of polycrystalline aluminium. Only one nucleus forms per corner site because the amount of material available for nucleation is quickly consumed by crystal growth.

It has been observed also that $\dot{N}$ increases sharply with time in the secondary recrystallization of cube texture copper,[25] following equation 25.

Thus, for conditions such that only a relatively small number of crystals form in either primary or secondary recrystallization, $\dot{N}$ generally increases sharply with time and goes to zero at $\tau = 0$.

In the recrystallization of heavily deformed polycrystalline aggregates $\dot{N}$ can be deduced from isothermal recrystallization data only with the aid of special assumptions and no generalization on the relation of

$\dot{N}$ with τ for these conditions can be made. As already noted Decker and Harker interpret their data[27] on copper on the assumption that $\tau = 0$ for all grains but interpretations based on the concept that $\dot{N}$ is independent of time can also account for their data. The possibility that $\dot{N}$ increased with time in their experiments or those of Cook and Richards[19] is very remote.

Temperature—Since $\dot{N}$ is generally a sensitive function of time the problem arises on how to compare $\dot{N}$ at different temperatures. Several solutions have been proposed as follows:

a express the constants of the equation $\dot{N} = f(t)$ as functions of temperature (Kornfeld and Pavlov, and Anderson and Mehl)

b compare $\dot{N}$ at various temperatures for X = constant (Anderson and Mehl)

c compare $\dot{N}$ at various temperatures for a constant number of grains nucleated (*i.e.* compare τ of the *n*th grain at various temperatures; method of Müller).

From the standpoint of a complete description of the process of recrystallization it is most desirable to adopt method *a* for expressing $\dot{N}$ as a function of temperature. This procedure involves finding $k = f(T)$ for the Kornfeld–Pavlov equation, a and b as $f(T)$ for the Stanley–Mehl equation, and $\bar{N}$ and $\nu = f(T)$ for the Avrami equation. When the just recrystallized grain size D_0 is independent of temperature methods *b* and *c* give identical results and $\dot{N}$ for all times at a given strain and temperature is described by a single activation energy $Q_{\dot{N}}$ that is identical to the activation energy for grain growth Q_G. For this reason method *b* or *c* is the most useful way of expressing $\dot{N} = f(T)$ when D_0 is independent of T. However, when $D_0 = f(T)$ it appears that method *a* is the only meaningful way of describing $\dot{N} = f(T)$.

Generally it is found that $Q_{\dot{N}}$ evaluated by methods *b* and *c* is very nearly equal to Q_G in recrystallization. In *Figure 11* the Q_G and $Q_{\dot{N}}$ values measured by Müller on rock salt (high temperature range) are plotted against stress and it is evident that within the experimental uncertainty, they fall on identical curves. Eastwood *et al*,[43] and Walker[44] have demonstrated that D_0 for α-brass is independent of temperature thus indicating that $Q_{\dot{N}} = Q_G$ for all strains in the recrystallization of α-brass. Also in the recrystallization of silicon ferrite[24] $Q_G \simeq Q_{\dot{N}}$.

The results on aluminium[23] indicate that $Q_{\dot{N}} \simeq Q_G$ for tensile strains of the order of 10 per cent or greater. However, for very small elongations (of the order of 5 per cent or less) Anderson and Mehl found that $Q_{\dot{N}}$ measured by method *b* was significantly greater than Q_G. In general agreement with this result Kornfeld and Pavlov found that

d $\log_e k/\mathrm{d}T$ ($k = \dot{N}/t$) at 4 per cent elongation was very much greater at all temperatures than (d/n $G/\mathrm{d}T$). However, k could not be described by a single activation energy. Generalizing, $Q_{\dot{N}} \simeq Q_G$ excepting that for very small strains < 5 per cent $Q_{\dot{N}} > Q_G$.

Strain (ε)—In the recrystallization of rock salt crystals it was observed that $1/\tau$ varies by the same factor with a change in stress as does G. If $1/\tau$ for the nth grain in the recrystallization of metals changed with strain by the same factor as G then D_0 would be independent of strain as well as temperature.

However, for metals D_0 generally decreases with increasing ε as indicated by the typical results for α-brass[43] as plotted in *Figure 13*.

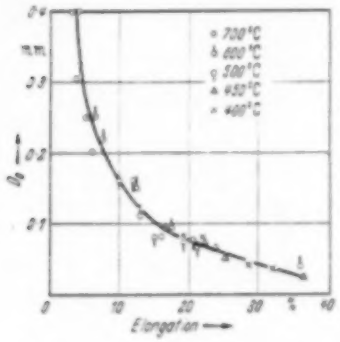

Figure 13. D_0 *at several temperatures as a function of prior strain for* α*-brass*

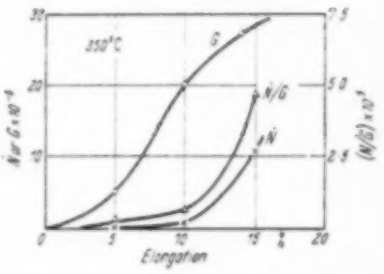

Figure 14. Ṅ, G *and* Ṅ/G *as a function of strain in the recrystallization of aluminium*

Since $Q_{\dot{N}} \simeq Q_G$ for all strains this result requires that $\dot{N}$ increase by a much larger factor with an increase in ε than does G (see equation 29).

In the recrystallization of lightly deformed aluminium the fact that $Q_{\dot{N}}$ is greater than Q_G at small strains is perhaps the most important factor in determining that D_0 becomes very large for small ε. In aluminium and silicon ferrite the approximate relation between $\dot{N}$ and ε at constant T is[23, 24]

$$\dot{N} = C \exp(k\varepsilon) \qquad \ldots\ (29)$$

In *Figure 14* $\dot{N}$ and G are plotted against ε for the three dimensional recrystallization of high purity aluminium. Apparently G becomes an insensitive function of ε where $\dot{N}$ is still changing rapidly. D_0 is a function[3] of the ratio $\dot{N}/G$ (*Figure 14*) and increases rapidly with ε.

Prior Recovery Treatments—Kornfeld and Pavlov have shown[13] that in polycrystalline aluminium of commercial purity $\dot{N}$ is greatly decreased by a 20 hr recovery anneal at 320°C, though G is unaffected. Without the recovery anneal the mean τ was 8 min compared with 36 min for samples subjected to a recovery anneal. On the other hand,

Anderson and Mehl found[23] no measurable effect of recovery anneals in the recrystallization of high purity aluminium strip.

Stanley found[24] that $\dot{N}$ was decreased in polycrystalline silicon ferrite (7 per cent elongation) as a result of a recovery anneal. However, the observed effect is quite small and of borderline significance.

In natural single crystals of rock salt Müller found[12] that a 1 hr recovery anneal at 500°C increased τ at 590°C by a factor of 2·2.

Collins and Mathewson observed[21] that $\dot{N}$ in high purity aluminium single crystals is decreased markedly by recovery anneals. On the other hand, quite a different implication has been drawn from the following results of KORNFELD and SCHAMARIN[45] on deformed aluminium single crystals of commercial purity:

1 the just recrystallized grain size is smaller in specimens subjected to a recovery anneal than in those not given this anneal
2 G is not changed by the recovery anneal.

These results prove that $\dot{N}$ is increased by the recovery anneal for the time interval $(t_1 - t_2 = \Delta t)$ at the recrystallization temperature during which grains appear. The usual interpretation assumes that t_1 has about the same magnitude whether or not the specimen has been subjected to a recovery anneal. However, an alternative interpretation that fits the facts as well and that has different theoretical implications is that t_1 for specimens given a prior recovery anneal is much larger than for specimens given no prior recovery treatment.* Since Kornfeld and Schamarin did measure G it seems likely that they noted t_1, and found it not essentially changed due to recovery treatments. In any event the general result is in disagreement with that of Collins and Mathewson.

Summarizing, it is apparent that the general effect of prior recovery treatments on $\dot{N}$ for either polycrystalline or single crystal specimens is far from clear at the present time.

Purity—Müller has observed that the addition of traces of (0·005 molecular per cent) strontium chloride to pure rock salt crystals decreases the reciprocal of the nucleation period $1/\tau$ and G by practically an identical factor (approximately 12). However, neither $Q_{\dot{N}}$ nor Q_G is changed by the impurity for a constant stress.

There seem to be no quantitative data available on the effect of impurities on $\dot{N}$ in metal systems.

Distribution of Nuclei in Recrystallization—It is significant that recrystallized grains do not originate at random in a strained matrix but preferentially at intersecting slip lines, strain markings, twin

* In different words Kornfeld and Schamarin's reported facts do not eliminate the possibility that the mean nucleation period $\bar{\tau}$ is larger for 'recovered' specimens than for 'unrecovered' specimens.

boundaries and often at a free surface, edges or grain boundaries. *Figure 15* shows a small recrystallized grain formed in a cluster of slip lines.[46] These preferential nucleation sites are generally supposed to be regions in which the stress is much higher than in the surrounding matrix.

Grain Size—In general the larger the grain size the smaller is $\dot{N}$. In fine-grained aluminium or copper specimens $\dot{N}$ is measurable for strains of 5 per cent or less. On the other hand for certain orientations of copper or aluminium crystals strained 20 to 30 per cent in tension $\dot{N}$ is virtually zero. Anderson and Mehl's more quantitative data[23] on aluminium also shows that $\dot{N}$ decreases markedly with increasing grain size.

Interpretation of the Effect of Variables on G

In the following sections we shall derive a general expression for G, compare the values computed from it with experimental ones, attempt to rationalize the apparent discrepancies between theory and experiment and finally offer some qualitative explanations of the effect of variables on grain boundary migration. So many variables can operate to influence the rate of boundary migration that the existing observations can be explained on the basis of many different hypotheses. There remains a need, however, for quantitative measurements that will permit decisions to be made on the validity of the various hypotheses.

Theory of Kinetics of Boundary Migration—With the aid of some simplifying assumptions we shall derive from rate theory a general expression for G that can serve as a 'handle' for the theoretical discussion of the problem. The formalism of the absolute reaction rate theory[47] will be followed. The method is entirely analogous to that used in deriving expressions for the rate of growth of crystals,[48, 49] into supercooled melts and the final result is similar in form. Recently MOTT[50] has, in effect, applied the theory to crystal growth in recrystallization.

Consider the energy of transfer of an atom across an interface from one grain to another where the driving energy is either strain or surface energy. Schematically the free energy of the atom in its various configurations may be represented as in *Figure 16*. In this figure, A and B are represented as crystal sites on opposite sides of a grain boundary. Either because of strain or boundary curvature (see sections on grain growth and effect of variables on G) the free energy of an atom in site B is greater than in site A by an amount ΔF per gm atom. ΔF_A is the free energy difference per gram atom between an atom in the activated state and state B. Let the jump frequency in the direction of A-B interchange be $\nu = kT/h$ in conformity with absolute rate

VOL.
3

Figure 15. A small grain growing in a highly strained region (magnification 2000 ×)

VOL
3

theory. Then the frequency of jumping of an atom from a B to an A site f_{BA} is given by:

$$f_{BA} = (kT/h) \exp [- (\Delta F_A)/RT)] \quad . \ . \ . \ . \ (30)$$

and the frequency of jumping from an A to a B site f_{AB} is:

$$f_{AB} = (kT/h) \exp [- (\Delta F_A + \Delta F)/RT)] \quad . \ . \ . \ . \ (31)$$

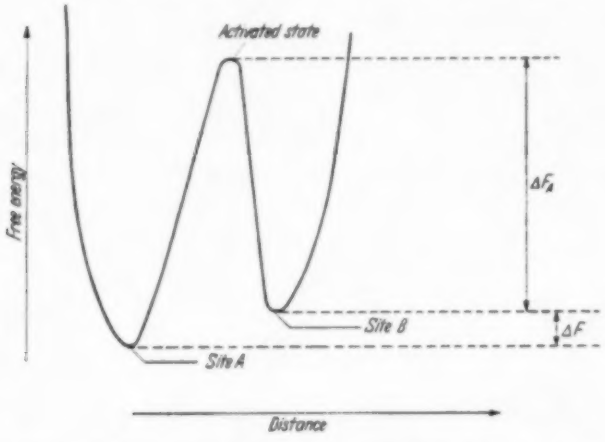

Figure 16. Schematic representation of free energy state of crystal sites on opposite sides of a grain boundary

The net rate of transfer per atom f is:

$$f = f_{BA} - f_{AB} = (kT/h) \exp [- \Delta F_A/RT] [1 - \exp (- \Delta F/RT)] \quad . \ . \ . \ . \ (32)$$

f is related to the linear rate of growth G by the equation:

$$f = G/\lambda \quad . \ . \ . \ . \ (33)$$

where λ is the interatomic spacing in the interface. Thus:

$$G = (kT/h)\lambda \exp [- \Delta F_A/RT] [1 - \exp (- \Delta F/RT)] \quad . \ . \ . \ . \ (34)$$

In recrystallization ΔF may be equated to $\mathcal{Z}$ the mean strain free energy* per gram atom in the recrystallized metal where it is assumed that $\mathcal{Z}$ is spread uniformly† throughout the strained matrix. When boundary migration is driven by surface energy

$$\Delta F = K\sigma V/r \quad . \ . \ . \ . \ (35)$$

* There are no data which relate $\mathcal{Z}$ to the energy of cold working ΔH measured[9] by Taylor and Quinney and in fact any such relation cannot be deduced with the methods of classical thermodynamics. In the following discussion it will be assumed without justification that $\mathcal{Z} = \Delta H$.

† For example it may be supposed that $\mathcal{Z}$ is contained entirely in the surface energy σ of sub-boundaries formed in cold working. Then $\mathcal{Z} = K\sigma V/r$ where r is the linear dimension of the sub-boundary.

where r is the boundary radius of curvature, V is the gram atomic volume of the metal and K is a constant of the order of 1 to 3. In any event ΔF is generally very small in relation to RT, for the maximum value of $\mathcal{Z}$ known to have been realized experimentally is of the order of 25 to 100 cal/gm atom[9], while free energies due to surface energy are much smaller for realizable grain sizes. Consequently

$$1 - \exp\left[-\Delta F/RT\right] \doteq \Delta F/RT \quad \ldots . \quad (36)$$

ΔF_A can be expressed as follows:

$$\Delta F_A = Q_G - T\Delta S_A - RT \quad \ldots . \quad (37)$$

where Q_G is the measured activation energy and ΔS_A is defined as the difference in entropy between the atom in its activated state and in site B. Substitution of equations 36 and 37 into equation 34 gives in general:

$$G = e(kT/h)\lambda(\mathcal{Z}/RT) \exp\left[\Delta S_A/R\right] \exp\left[-Q_G/RT\right] \ldots . \quad (38)$$

in boundary migration due to strain energy, and

$$G = e(kT/h)\lambda(K\sigma V/rRT) \exp\left[\Delta S_A/R\right] \exp\left[-Q_G/RT\right] \ldots . \quad (39)$$

in boundary migration due to surface energy. In equation 38 ΔS_A and Q_G can in general be orientation and strain dependent.* In equation 39 σ, ΔS_A and Q_G can be orientation dependent.

Comparison of Theoretical and Experimental Values of ΔF_A, Q_G and ΔS_A— It has been pointed out (p 234) that G could be represented by equation 27 where G_0 and Q are in general functions of strain and relative grain and boundary orientations. From equation 38:

$$G_0 = e(kT/h)\lambda(\mathcal{Z}/RT) \exp\left[\Delta S_A/R\right] \quad \ldots . \quad (40)$$

for boundary migration due to strain and

$$G_0 = (kT/h)\lambda(K\sigma V/rRT) \exp\left[\Delta S_A/R\right] \ldots . \quad (41)$$

for boundary migration due to surface energy.

Experimentally measured values of G_0 are shown in *Table III*. Reasonable estimates of all the quantities excepting ΔS_A entering into equations 40 and 41 can be made. For comparing theory with experiment there are the alternatives of either treating ΔS_A as a disposable parameter and drawing inferences about the activated state from its magnitude, or calculating G_0 absolutely on the assumption that ΔS_A is identical in value with ΔS_A in self-diffusion (preferably grain boundary self-diffusion).

* Note that although the difference in free energy of an atom in A and B sites is accounted for by $\mathcal{Z}$, the height of the activation hill and therefore, Q_G and ΔS_A can be strongly dependent upon strain.

ΔS_A and ΔF_A values calculated from measured G_0 values by assigning the following numbers to the quantities in equations 40 and 41: $e = 2{\cdot}72$, $(kT/h) = 10^{13}\ \text{sec}^{-1}$, $\lambda = 2 \times 10^{-8}$ cm, $(K\sigma V/rRT) = 10^{-4}$, $\mathcal{Z}/RT = 10^{-2}$, are listed in *Table IV*. For comparison the entropies and free energies of activation calculated from diffusion data are also given. In calculating ΔS_A and ΔF_A from grain growth data it was assumed arbitrarily that $a = 1$ (*Table III*).

From the results of these calculations the generalization can be made that $(\Delta F_A)_G < (\Delta F_A)_L$ where $(\Delta F_A)_L$ is the free energy of activation for lattice self-diffusion (as distinguished from grain boundary self-diffusion). Mobility B is defined as velocity per unit potential gradient and for ideal solutions has the following relation to the diffusion coefficient D:

$$\mathrm{B} = D/kT \qquad \ldots . \quad (42)$$

If B_G be the mobility of atoms in grain growth and B_L the mobility of atoms in self-diffusion, it follows that:

$$\mathrm{B}_G \propto \exp\left[-(\Delta F_A)_G/RT\right] \qquad \ldots . \quad (43)$$

and

$$\mathrm{B}_L \propto \exp\left[-(\Delta F_A)_L/RT\right] \qquad \ldots . \quad (44)$$

From the relative magnitudes of $(\Delta F_A)_G$ and $(\Delta F_A)_L$ it follows that $\mathrm{B}_G \gg \mathrm{B}_L$ for all the measurements reported in *Table III*. This result is expected because of the supposed large degree of disorder at crystal interfaces. However, it should be noted that wrong inferences about the magnitude of B_G and B_L would have been made in many cases by equating B to $\exp\left[-Q/RT\right]$ as is often done.

It may be significant that for silver $(\Delta F_A)_G$ ($\simeq 21{\cdot}5$ kcal/gm atom) is in much closer agreement with the free energy of activation for grain boundary diffusion $(\Delta F_A)_B$ ($\simeq 18{\cdot}6$ kcal/gm atom) than with $(\Delta F_A)_L$ ($\simeq 39{\cdot}0$ kcal/gm atom). Comparison of $(\Delta F_A)_B$ and $(\Delta F_A)_G$ for other substances would be very interesting, but cannot yet be made because of the lack of data on grain boundary self-diffusion. Certainly it is expected in general that $(\Delta F_A)_G$ should be closer in magnitude to $(\Delta F_A)_B$ than to $(\Delta F_A)_L$.

Although the relation between $(\Delta F_A)_G$ and $(\Delta F_A)_L$ is in qualitative accord with expectations based on theories of crystal interface structures the relations between the corresponding energies of activation (Q_G against Q_L) and entropies of activation [$(\Delta S_A)_G$ against $(\Delta S_A)_L$] are more difficult to explain. On the basis of the simple qualitative picture it might be expected that $Q_G < Q_L$ and that $(\Delta S_A)_G \ll (\Delta S_A)_L$. Actually, with few exceptions, $(\Delta S_A)_G$ is much larger than $(\Delta S_A)_L$ and Q_G is of the same order of magnitude or even somewhat larger than Q_L.

Rationalization of Discrepancies between Theory and Experiment—There are a number of ways in which the disagreement between the qualitative theoretical expectations on the correlation of $(\Delta S_A)_G$ to $(\Delta S_A)_L$ and of Q_G to Q_L and the experimental values can be explained. Mott has attempted[50] to rationalize the large value of $(\Delta S_A)_G$ by assuming that several atoms are activated in the unit process. Alternatively, it can be assumed that the measured values of Q_G are not representative of a single process, and are higher than the activation energy required for the transfer of a single atom across a boundary. As a consequence the computed value of $(\Delta S_A)_G$ is too high. Also large apparent values of Q_G might result from changes in the ΔF of equation 34 with temperature as a result of recovery or the solution of inclusions. Hypotheses that will explain these discrepancies are set forth in the following sections, but further quantitative experimental work is needed to show whether any of them can adequately explain the facts.

Mott Hypothesis—Mott has attempted[50] to resolve the problem of the apparently unreasonably large $(\Delta S_A)_G$ by postulating that n atoms are activated in the unit process. He proposes that the activation free energy is in effect the free energy of 'melting' the n atoms that after melting are free to recrystallize on one side of the boundary or the other. The disposable parameter n may be calculated from the experimental $(\Delta F_A)_G$ by the relation:

$$n(\Delta F) = (\Delta F_A)_G \qquad \ldots . \quad (45)$$

where ΔF is the free energy increase on melting at temperature T. Approximating ΔF by the relation:

$$\Delta F = Q_f(1 - T/T_0)$$

where Q_f is the gram-atomic heat of fusion and T_0 the absolute melting temperature he obtains:

$$G = e(kT/h)\ (\lambda n\mathcal{Z}/RT) \exp [nQ_f/RT_0] \exp [-nQ_f/RT]. \quad \ldots . \quad (46)^*$$

Mott's theory reduces the number of disposable parameters from two [Q_G and $(\Delta S_A)_G$] to one (n) and may be tested by comparing $(\Delta S_A)_G$ with $nQ_f/T_0 = n\Delta S_f$. Here ΔS_f = entropy of fusion per gram atom and n is calculated from the relation:

$$nQ_f = Q_G \qquad \ldots . \quad (47)$$

The comparison between $n\Delta S_f$ and $(\Delta S_A)_G$ is shown in *Table IV*.

Although the agreement is good in some instances (*e.g.* Anderson and Mehl's aluminium data,[23] Ward's data on copper[25]) in almost as many cases the agreement of $(\Delta S_A)_G$ with $(\Delta S_A)_L$ is equally good.

* We have modified Mott's equation slightly setting $\nu = kT/h$ and introducing the factor e in order to conform to the formalism of the absolute reaction rate theory.

Table IV

Substance	Strain % R.A.	Temp. range °C	ΔS_A cal/deg gm atom				Q kcal/gm atom			ΔF_A‖		
			$(\Delta S_A)_B$	$(\Delta S_A)_L$	$(\Delta S_A)_G$	$n\Delta S_f$	Q_B	Q_L	Q_G	$(\Delta F_A)_B$	$(\Delta F_A)_L$	$(\Delta F_A)_G$
			Primary Recrystallization									
Aluminium[13]	4	425–540		9·2*	18	36		37·5†	34·0		30·5	20·0
Aluminium[23] ..	5·1	310–370			58	63			59·0		32·0	24·5
Rock salt[12]	1,000 gm/mm²	650–770		18·4	39	55		51·4‡	59·0		33·0	20·0
	4,000 gm/mm²	400–520			23	30			32·0		38·0	15·0
Copper[11]	10	300–320		14·0	43	37		57·2[52]	50·0		49·0	24·0
	10	340–360			15	24			32·0		48·8	22·5
Silicon ferrite[24] ..	7	740–800		13·0	35	41		59·7§	73·0		46·2	36·5
			Secondary Recrystallization									
Copper[25]		900–1000		14·0	43·0	54·0		57·2	73·0		40·4	21·5
Silver[26]		433–533	2	9	7·4	23	20·2[119]	46·0[51]	28·0	18·6	39·0	21·5
			Grain Growth									
Aluminium[28] ..	0·03 cm grain size	400–500		9·2	88	93		37·5	87·0		31·0	23·3
α-Brass (com. purity)[39]		450–700			31·0				60·0			33·6
α-Brass (high purity)[40]		450–800			10·0				40·0			31·0

* Estimated from DUSHMAN–LANGMUIR equation. † Calculated from correlation of Q_L with heat of sublimation.[52] ‡ From anion conductivity data.[58]
§ From self-diffusion in α-iron[64] ‖ The average value of T was used to compute ΔF_A from eq. 37

There are several plausible alternative hypotheses for the abnormal magnitude of $(\Delta S_A)_G$ that merit consideration.

Recovery Hypothesis—In supposing that the rate of boundary migration is controlled by a single activation energy which is measurable from the slope of a log G *versus* $1/T$ straight line relation the tacit assumption is made that the driving free energy ΔF is essentially independent of time and temperature. The experimental evidence that G is independent of time supports the assumption that the strain energy $\mathcal{Z}$ driving boundary migration in primary recrystallization is time independent during the period of observable boundary migration. However, the possibility remains that $\mathcal{Z}$ is reduced by recovery processes which essentially go to completion prior to the detection of recrystallized grains. If the degree of recovery thus is a function of temperature then the problem can be described by setting $\mathcal{Z} = f(T)$ where $\mathcal{Z}$ is now the residual strain energy after the recovery process has run its course. G is independent of lower temperature recovery anneals because $\mathcal{Z}$ at a given temperature is determined before new grains appear.

If $\mathcal{Z}$ decreases with increasing temperature, as seems possible, the value of Q_G would apparently decrease for the same temperature variation. It was noted that Karnop and Sachs observed[11] that Q_G apparently decreased with increasing temperature and a similar conclusion for aluminium can be reached by combining KORNFELD and PAVLOV's[13] and ANDERSON and MEHL's[22] data. However, although the possibility of recovery must be taken into account in any theory of boundary migration, the recovery hypothesis alone provides no explanation for the fact that $(\Delta S_A)_G$ and Q_G are usually much larger than expected on the basis of rate theory and diffusion data.

In secondary recrystallization processes it is possible that $\sigma = f(t, T)$ and $r = f(t, T)$ (equation 39) due to concurrent grain growth in the matrix. However, since G values for these processes are also generally independent of time the equations must at least reduce to $\sigma = f(T)$ and $r = f(T)$. Thus $K\sigma V/r = f(T)$ and the description of the process becomes analogous to the description of primary recrystallization with $\mathcal{Z} = f(T)$.

Inclusion Hypothesis—It will be shown later that in the presence of inclusions the free energy decrease in boundary migration is given by

$$\Delta F' = K\sigma[1/r - \rho/r_0]V \qquad \ldots . \quad (48)$$

where r_0 is the radius of the inclusion and ρ its volume fraction in the matrix. Equation 48 may be written

$$\Delta F' = \Delta F - M \qquad \ldots . \quad (49)$$

where ΔF refers to strain or surface energy and M is an energy term due to inclusions and their dispersion. To take into account the

effect of inclusions on the rate of boundary motion $\Delta F'$ must be substituted for ΔF in equation 34. If the number and size of inclusions retarding grain growth is unaffected by temperature, the measured value of Q_G will be identical to that measured on a specimen for which $M = 0$. However, if M is wrongly assumed to be zero the calculated $(\Delta S_A)_G$ will be smaller than it actually is. In general the number and volume of growth retarding inclusions will decrease with increasing temperature so that M will decrease as T increases. This

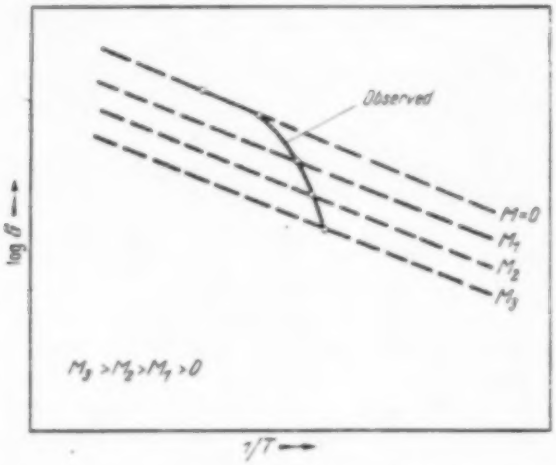

Figure 17. Schematic representation of log G *as a function of* 1/T *for various degrees of dispersion,* M, *of inclusions at grain boundaries*

variation of M with temperature will have the effect of making the apparent values of Q_G and $(\Delta S_A)_G$ larger than the values that would be measured with $M = 0$. In *Figure 17* log G is plotted against $1/T$ for several supposed values of M. The curves are all parallel (*i.e.* Q_G is independent of M) but have different intercepts on the log G axis giving different apparent values of $(\Delta S_A)_G$. Now if M were fixed with temperature, one of the family of parallel curves would be deduced from a set of experiments. However, since $M = f(T)$ values of G measured at different temperatures will lie on a different curve of the family and the perceived values of G will correspond to the hypothetical points shown in the diagram; thus apparent values of Q_G and $(\Delta S_A)_G$ will be calculated that are much greater than any set corresponding to a constant M.

In agreement with the theory just explained, Burke found[40] that Q_G for grain growth in high purity α-brass is 40 kcal/gm atom as compared with 60 kcal/gm atom for α-brass of commercial purity.

He also observed that the rate of grain growth in commercial purity brass could be increased many times by coalescing the inclusions and thus rendering them less effective. Also the inclusion hypothesis satisfactorily accounts for the variation of Q_G and $(\Delta S_A)_G$ with temperature observed by Ward, and Treaftis and Turnbull in the secondary recrystallization of copper.

Inclusions can be effective in retarding boundary migration in primary recrystallization as well as in grain growth processes. In primary recrystallization retarded by inclusions equation 49 becomes:

$$\Delta F' = \mathcal{Z} - M \qquad \ldots . \quad (50)$$

There is some evidence that inclusions do retard boundary migration in primary recrystallization. For example, the jerky motion of the boundary in the recrystallization of rock salt can be explained on the assumption that the slow motion occurs when inclusions lie in the moving boundary while the rapid motion occurs when the boundary moves. Whether or not the inclusion hypothesis applies to the rock salt results, it is clear that the average rate of motion of the boundary may not be the significant datum for comparison with the theory of boundary motion. Therefore, the values of Q_G and $(\Delta S_A)_G$ calculated by Müller to fit his data may be only apparent. Decker and Harker have found[27] that the activation energy for recrystallization of spectroscopically pure copper is about 7 kcal/gm atom less than that for recrystallization of OFHC copper. However, it is not certain whether this difference should be attributed to inclusions, soluble impurities or other factors.

If the driving energy for recrystallization $\mathcal{Z}$ is directly proportional to the strain (as might be supposed for small strains from the data[9] of Taylor and co-workers) then inclusions should be effective in retarding boundary migration only when the strain is the smallest necessary to produce recrystallization. As a consequence it is expected that in comparable temperature ranges Q_G should decrease sharply with increasing strains. In support of the inclusion hypothesis, Q_G is found to decrease sharply with increasing strain in the recrystallization of rock salt. However, in the recrystallization of aluminium Anderson and Mehl found[23] that Q_G is practically independent of strain between 2 and 8 per cent elongation in identical temperature ranges. Thus the inclusion hypothesis cannot be invoked to explain the very large value of $(\Delta S_A)_G$ calculated from Anderson and Mehl's results if it is supposed that $\mathcal{Z}$ is proportional to the strain. On the other hand if because of recovery processes, the value of $\mathcal{Z}$ effective in producing boundary migration is practically independent of strain ε the results of Anderson and Mehl for $\varepsilon > 2$ per cent can be interpreted satisfactorily on the basis of the inclusion hypothesis.

Dependence of G *on Strain*—The factors of equation 40 derived from rate theory that might be dependent upon strain ε, are $\mathcal{Z}$, $(\Delta S_A)_G$ and Q_G. The simple hypothesis that $\mathcal{Z} \propto \varepsilon$ and that Q_G and $(\Delta S_A)_G$ or more simply $(\Delta F_A)_G$ are independent of ε can be dismissed immediately on the basis of results for recrystallization after small strains. For example Anderson and Mehl observe that at 350°C G increases by a factor of about 20 for an increase in strain by a factor of 4. This change in rate with strain corresponds to a reduction in the free energy of activation for recrystallization of about 1·8 kcal/gm atom (compared to $\triangleq$ 21 kcal/gm atom total). Similar large decreases in $(\Delta F_A)_G$ at small strains with increasing strain have been observed by Müller, and Kornfeld and Pavlov, and are indicated by the result of Karnop and Sachs. On the other hand Anderson and Mehl found that G increases only slightly with ε for values of the latter ranging between 10 and 90 per cent reduction in area. This result is easily explained on the basis of the concept that recovery greatly reduces $\mathcal{Z}$ at large strains and that $(\Delta S_A)_G$ and Q_G are independent of ε when it exceeds a critical amount. A hypothesis which may account for the extraordinary sensitivity of G to ε for ε very small ($\varepsilon < 10$ per cent for aluminium) is that small strains increase by a large factor the number of lattice imperfections potentially capable of promoting boundary migration. Since the concentration of lattice imperfections Υ is very small for a lattice in thermal equilibrium*, increasing Υ by a factor of 10 for example would have no perceptible effect on the free energy of the lattice or on $\mathcal{Z}$. On the other hand such an increase in Υ would increase the rate of lattice diffusion by a factor of 10 according to current theories. However, it is not clear how an increase in the concentration of imperfections that promote lattice diffusion will affect mobility of atoms at migrating boundaries.

Dependence of G *on Orientations*—When boundaries migrate, atoms at the boundary must occasionally move past other atoms as in diffusion. Qualitatively as Beck has suggested[35], one would expect the energy barrier for movement to be high where the mismatch between the grains is slight because the structure will be nearly continuous across the boundary and there will be little space for the atoms to move past each other. When the mismatch is greater, the structure should be more open, Q_G should be lower, and the rate of boundary migration higher.

Evidence has already been presented to show that the boundaries between grains which are of nearly the same orientation, or are nearly twinned orientations, migrate very much more slowly than boundaries where the disregistry is greater. On the other hand, polygonization

* It has been estimated that the concentration of lattice vacancies in thermal equilibrium with copper at 700°C $\triangleq 10^{-7}$.

boundaries apparently migrate readily, and at least many deformation twin boundaries migrate with similar ease. The usual mechanisms proposed for the migration of twin boundaries and for the movements of dislocations will permit the atoms to move in a manner necessary for the grain boundaries to migrate without requiring a loose packing of the atoms. When the special conditions necessary for the operation of these mechanisms exist, the boundaries will migrate readily even though the disregistry at the boundary is slight.

If the boundaries between grains of similar orientation do migrate slowly because the activation energy for the atom movements involved is larger, the rate of migration of these boundaries should increase more rapidly with temperature than the rate of migration of boundaries with lower activation energies. There are no measurements available of the activation energy for grain boundary migration as a function of the relative orientation of the grains, but there are numerous examples of the fact that a grain embedded in uniform matrix will grow more readily in certain directions than in others. This, undoubtedly, results from the fact that the position of the boundary controls its structure and hence its ability to migrate. COOK and RICHARDS[55] have observed anisotropy in the growth of new grains about an indentation in cube texture copper, and BOWLES and BOAS[56] have suggested that the 'rate of migration of a boundary in any direction is influenced by the change in orientation which occurs on crossing the boundary in that direction'.

The observations of KORNFELD and RYBALKO[32] and BURKE and TURKALO[33] that growth anisotropy is decreased with increasing temperature indicates that Q_G is greater for directions of rapid growth than for direction of slow growth.

Theory of Recrystallization Nuclei

Some of the principal facts that theories of recrystallization nuclei should explain are:

1. nuclei form preferentially in parts of the specimen where it appears that the degree of deformation is the highest
2. for small deformation $\dot{N}$ increases with time
3. with few exceptions the activation energy for nucleation is not perceptibly different from the activation energy for boundary migration
4. $\dot{N}$ increases sharply with increasing strain
5. generally there is a fairly well defined orientation relationship between the deformed matrix and the recrystallized grains.

Two general types of theories for recrystallization nuclei will be considered. One theory, that will be called the 'conventional nucleation

theory', supposes nuclei to grow in a highly strained part of the matrix by a sequence of thermal fluctuations from original dimensions approaching those of the atom. A second type of theory supposes that the nuclei are small 'blocks' or crystallites of the cold-worked matrix and the nucleation period, τ, results from an initial slow growth rate of the blocks. The slow growth rate is ascribed to various causes that will be considered in the following discussion.

Conventional Nucleation Theory

Consider an ordinary phase transformation

$$\alpha \rightarrow \beta$$

where α and β are in equilibrium at T_0 and β is the more stable phase when $T < T_0$. When α is cooled to $T < T_0$ there may be a nucleation period τ before β apparently starts to form. According to nucleation theory the free energy of small masses of β (called 'embryos') relative to α may be expressed as the sum of a free energy term proportional to the surface area of the mass and a free energy term proportional to its volume. Thus:

$$\Delta F = Ai^{2/3} + Bi \qquad \ldots . \quad (51)$$

where i is the number of atoms in the β embryo, A is proportional to the interfacial free energy between α and β and B is proportional to the free energy released per unit volume when an infinite mass of α transforms to an infinite mass of β. At a given temperature when $B < 0$ ΔF goes through a maximum having coordinates:

$$\Delta F^* = (4/27)\,(A^3/B^2) \qquad \ldots . \quad (52)$$

$$i^* = -\,(2A/3B)^3 \qquad \ldots . \quad (53)$$

All embryos of β containing a number of atoms $i < i^*$ will tend to disappear while all aggregates containing a number $i > i^*$ will tend to grow and consume the α. According to the conventional theory the nucleation period τ is the mean time required at a given temperature for a sequence of fluctuations in the α matrix leading to the formation of a β 'nucleus' having the critical number of atoms i^*. The probability of such a sequence of fluctuations has been calculated for various kinds of phase transformations[48] and is proportional to $\exp\,[-\,\Delta F^*/kT]$. TURNBULL and FISHER[57] have shown that the rate of steady state (*i.e.* time independent) nucleation of crystals in a condensed system (mother phase liquid or solid) can be approximated by:

$$\dot{N} = n(kT/h)\,\exp\,[-\,(\Delta F_A)_G/RT]\,\exp\,[-\,\Delta F^*/kT] \qquad \ldots . \quad (54)$$

where n is the number of atoms of the mother phase per unit volume.

To apply the theory to recrystallization, it is assumed that the cold-worked matrix is analogous to a metastable phase α which transforms

to a strain-free phase β. The driving energy for the transformation is the strain energy $\mathcal{Z}$ per cubic centimetre and the surface energy is the boundary energy between the strained and unstrained grains σ.

Assuming that the nucleus is a sphere of radius r^* it follows from equations 52 and 53 that:

$$\Delta F^* = (16\pi/3)\sigma^3/\mathcal{Z}^2 = K\sigma^3/\mathcal{Z}^2 \quad . \quad . \quad . \quad . \quad (55)$$

$$r^* = 2\sigma/\mathcal{Z} \quad . \quad . \quad . \quad . \quad (56)$$

For recrystallization equation 54 may be rewritten as:

$$\dot{N}_\varepsilon = n(kT/h) \exp\left[-(\Delta F_A)_G/RT\right] \exp\left[-K(\sigma_\varepsilon)^3/(\mathcal{Z}_\varepsilon)^2 kT\right] \quad . \quad . \quad . \quad . \quad (57)$$

where $\dot{N}_\varepsilon$ is the nucleation frequency in a region of strain ε. The plausibility of conventional nucleation theory can be tested by calculating $\dot{N}_\varepsilon$ from equation 57 with reasonable assumed values of σ_ε and $\mathcal{Z}_\varepsilon$.

Consider the formation of 'unstrained' embryos in a homogeneously sheared portion of a cubical lattice shown in *Figure 18*. $\mathcal{Z}_\varepsilon$ is given by the equation:

$$\mathcal{Z}_\varepsilon = (1/2)\, E\varepsilon^2 \quad . \quad . \quad . \quad . \quad (58)$$

where ε is the shear strain and E is the shear modulus. It is clear from the figure that the embryo has a surface energy due to the elastic distortion at its boundary which exceeds the decrease in volume shear energy occasioned by its formation. A crude estimate of the surface energy can be obtained by assuming that the interface between large unstrained crystals and the strained lattice is made up of dislocations. The density of dislocations per unit length of boundary δ is approximately equal to the the density δ' at a grain boundary B between two unstrained grains having an angle of misfit $\theta = \arctan \varepsilon$. On this basis it is assumed that $\sigma_\varepsilon = \sigma$ where σ is the surface energy of B. DUNN and co-workers[37, 58] and CHALMERS and co-workers[59] have measured σ/σ_m where σ_m is the maximum grain boundary energy in the particular system, as a function of θ for a number of metals. From these data σ_ε can be calculated when σ_m is known.

The interfacial energy of high energy grain boundaries has been measured absolutely.[10, 60, 61] FISHER and DUNN[62] have surveyed the data critically and suggest 535 ± 50 erg/cm^2 as the best value of the Cu–Cu interfacial energy σ_{Cu}. By assuming further that $\sigma_{Cu} = \sigma_m$ and that the relation between σ/σ_m and θ for copper is identical with that found by Chalmers for lead grains rotated about a common [100] axis[59] numerical values can be assigned to σ_ε of copper embryos for given values of ε.*

* It is also supposed that σ_ε for nuclei is identical to σ_ε for large crystals. The validity of this supposition has been discussed elsewhere.[39]

Numerical values of r^* and $\dot{N}_\varepsilon$ as a function of ε have been calculated for copper and are tabulated in *Table V*.

The observed nucleation frequency $\dot{N}$ is related to $\dot{N}_\varepsilon$ by the equation:

$$\dot{N} = \Sigma \dot{N}_\varepsilon v_\varepsilon \qquad \ldots . \quad (59)$$

where v_ε is the volume fraction of material having strain ε. The results of the calculations indicate (*Table V*) that the only practically perceptible contribution to $\dot{N}$ is made by regions where $\varepsilon > 0{\cdot}20$. For example, if $v_\varepsilon = 10^{-6}$ for $\varepsilon = 0{\cdot}20$, $\dot{N} > 3{\cdot}6\ \mathrm{hr}^{-1}\ \mathrm{cm}^{-3}$. In regions where $\varepsilon \triangleq 0{\cdot}20$, $\mathcal{Z} \triangleq 350\ \mathrm{cal/cm}^3$ but the total strain energy contained in all such regions (approximately $0{\cdot}0004\ \mathrm{cal/cm}^3$ for $v_\varepsilon = 10^{-6}$) is

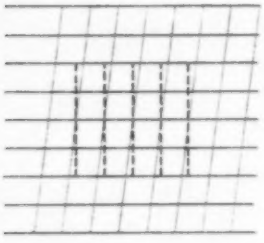

Figure 18. Unstrained embryo (- - - -) in homogeneously sheared (————) square lattice

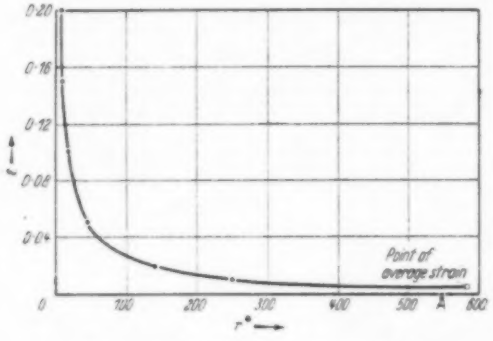

Figure 19. Critical radius for growth as a function of strain calculated on the basis of the model indicated in Figure 18

a negligible fraction of the average $\mathcal{Z}$ (approximately $0{\cdot}5\ \mathrm{cal/cm}^3$) of the cold-worked specimen. Suppose that the average strain energy $\mathcal{Z} \triangleq 1 \times 10^7\ \mathrm{erg/cm}^3$ corresponding to $\bar{\varepsilon} \triangleq 0{\cdot}005$. The theory of nucleation indicates that $\dot{N}_\varepsilon$ in regions where $\mathcal{Z}_\varepsilon = \mathcal{Z}$ is virtually zero. However, in order to grow at the expense of such regions, that constitute the major part of any specimen, a crystal must have attained the size $r > (r^*)_{\bar{\varepsilon}}$. Thus in the local region of very high strain where the nucleus forms, the distribution of strain must be such that $r > (r^*)$ for all values of the crystal size r after it has become a nucleus.

Figure 19 shows the relation between ε and r^*. The hypothesis that $\varepsilon \triangleq 0{\cdot}2$ in small regions of cold-worked metals does not seem to be inconsistent with any known experimental facts.

Some Predictions of Conventional Theory Compared with Experience—Conventional nucleation theory requires that the orientation relation between new crystals and the cold-worked matrix be such that σ_ε is a

minimum.* This condition leads in general to the fairly definite relation that the orientation of the nucleus be as nearly identical with the cold-worked matrix surrounding it as permitted by the elastic strains. The orientation relation for the example considered in the preceding section is clear from *Figure 18*. The prediction is consistent with the available experimental data since they do not eliminate the possibility that minor components of the recrystallization texture are always present in the cold-worked matrix.

The theory satisfactorily accounts for the existence of a nucleation period τ. The increase in $\dot{N}$ with time follows directly from the theory[62] for immediately after quenching from the cold-worked state to the annealing temperature, the concentration of embryos of all sizes will be virtually zero and a considerable time will be required for the steady state distribution of embryos and nuclei assumed in deriving equation 54 to be established.

In agreement with experience, the theory predicts that nuclei will form preferentially in the most highly deformed parts of a cold-worked specimen. Also $\dot{N}$ increases with decreasing grain size at a given strain because the volume v_s of regions that are highly stressed after deformation presumably increases with decreasing grain size.

If recovery anneals have the effect of decreasing ν_s, then $\dot{N}$ should, according to the theory, decrease due to such anneals. There is an alternative but less plausible possibility that nuclei form during the recovery period with the result that $\dot{N}$ observed at the recrystallization temperature is greater than in the absence of a recovery treatment.

If σ_s, $\mathcal{Z}_s$ and v_s are essentially independent of temperature it follows from equations 57 and 58 that

$$Q_S \simeq Q_G + NK(\sigma_s)^3/(\mathcal{Z}_s)^2 \qquad \ldots (60)$$

where N is Avogadro's number. From the results summarized in *Table V* it can be verified that $NK(\sigma_s)^3/(\mathcal{Z}_s)^2$ is of the same order of magnitude as Q for $\varepsilon \sim 0{\cdot}2$ to $0{\cdot}3$.

In the recrystallization of aluminium at small strains[13, 23] Q_S is considerably greater than Q_G in agreement with theory but at moderate and large strains $Q_S \simeq Q_G$ for most substances in disagreement with theory. The disagreement can be resolved within the framework of the theory if either of the following assumptions is valid.

1. Measured values of Q_G are complex and larger than the activation energy for the elementary growth process for reasons discussed in the preceding section.

* It has been asserted that conventional nucleation theory predicts no preferred orientation relation between recrystallized grains and the matrix. Such assertions appear to have been based on the erroneous concept that a completely amorphous region of the cold-worked matrix is required for the operation of the conventional mechanism.

2 σ_s and Z_s are essentially temperature independent but v' decreases sharply with increasing temperature due to a recovery process.

If $v_s \propto \exp[Q_R/RT]$ then as a gross approximation we have:

$$Q_N = Q_G + NK(\sigma_s)^3/(Z_s)^2 - Q_R \quad \ldots\ (61)$$

Evidently for a singular range of E values $Q_N \doteq Q_G$.

The data of Anderson and Mehl indicate[23] that the functional relations between $(Q_G - \varepsilon)$ and $(Q_N - \varepsilon)$ are quite different for pure aluminium so that either of the above assumptions provides a credible rationalization of the relation of Q_N and Q_G for aluminium in terms of conventional theory. However, Müller found[12] that the relation $Q_G \doteq Q_N$ holds quite closely for wide variations in applied stress (excepting at small stresses—*Figure 11*) and for significant changes in specimen purity in the recrystallization of rock salt single crystals. These results apparently are not compatible with the theory unless the implausible hypothesis is adopted that Q_R varies in the very singular way necessary to account for them.

Block Hypotheses

We shall now consider whether or not there are alternative mechanisms that permit nuclei to form more rapidly than they can form by the conventional nucleation mechanism. Several nucleation theories suppose[5] that nuclei form from blocks (small crystallites) already existing in the cold-worked matrix by mechanisms whereby the block functions more or less as a unit. These blocks are sometimes considered to be crystallites that have received much less than the average deformation of the specimen ('low energy block hypothesis'). Other theories assume that they are crystallites that have received a much greater deformation than the crystal as a whole ('high energy block hypothesis'). These high energy blocks then become recrystallization nuclei, not by the mechanism outlined in the previous section, but by a sequence of unit processes that progressively relieve the strain in the *block as a whole*. For example if the block is strained by virtue of a high concentration of dislocations in its immediate vicinity, nucleation occurs by the migration of these dislocations elsewhere or by their mutual cancellation.

According to the block hypotheses, the nucleation period is a period of relatively slow growth of the block to macroscopic dimensions or it can be a period associated with the relief of strain energy within the block.

The general kinetics of block growth can be treated as a problem of time dependent grain growth. Equation 38 can be rewritten as:

$$G = \mathrm{d}D/\mathrm{d}t = k(\Delta F) \quad \ldots\ (62)$$

Table V. $\dot{N}$ and r^* at Various Values of ε

ε	σ_a	Z_a(erg/cm^3)	r^*(Å)	$\dot{N}_a$ sec^{-1} cm^{-3}
0·01	48	0·38 × 10^3	250	—
0·02	107	1·52 × 10^3	140	—
0·05	210	9·5 × 10^3	44	10^{-300}
0·10	310	38·0 × 10^3	16	10^{-100}
0·15	385	86·0 × 10^3	9	10^{-31}
0·20	450	152·0 × 10^3	6	10^3
0·30	500	342·0 × 10^3	3	10^{21}

$E = 7{\cdot}5 \times 10^{11}$ erg/cm^3, $\sigma_m = 535$ erg/cm^2, $(\Delta F_A)_0 = 24$ kcal/gm atom (see *Table IV*), $T = 800°K$

where D is the block size and

$$k = (\varepsilon\lambda\nu/RT) \exp [\Delta S/R] \exp [-Q_D/RT]$$

For D very large experience indicates that dD/dt is constant and the interpretation is that:

$$dD/dt \simeq k(\Delta F_0) \quad \ldots . \quad (63)$$

where ΔF_0 is independent of t as assumed in deriving equation 38. However, when the block is very small ΔF is a function of time and dD/dt may be expressed as follows:

$$dD/dt = k[\Delta F_0 - \Delta F(t)] \quad \ldots . \quad (64)$$

where $\Delta F(t)$ is a function that decreases with increasing time so that at very long times $\Delta F_0 \gg \Delta F(t)$. Integration of equation 64 gives:

$$D = k\Delta F_0 t - \int_0^t k\Delta F(t)dt \quad \ldots . \quad (65)$$

Comparison of equations 1 and 65 gives in general for $t > \tau$

$$\tau = (1/\Delta F_0)\int_0^t \Delta F(t)dt \quad \ldots . \quad (66)$$

In the sections that follow various types of block hypotheses will be considered in greater detail and τ calculated when possible.

Low Energy Block Hypothesis—Most theories on the origin of nuclei from low energy blocks are not explicit on the form of $\Delta F(t)$ or why the blocks have escaped deformation. One concept that leads to a definite form of $\Delta F(t)$ is that growth of the blocks is retarded by their surface tension. This concept is no different from the basic concept in conventional nucleation theory excepting that it is now supposed that

the initial block size $D_0 > 2r^*$. Expressing equation 51 in terms of D and ΔF per gram atom, we have

$$\Delta F = (-a\sigma D^2 + \mathcal{Z}D^3)/D^3 = (\mathcal{Z} - a\sigma/D) \quad . \quad . \quad . \quad . \quad (67)^*$$

where a is a geometrical factor and $\mathcal{Z} > a\sigma/D$ for values of $D > D_0$. Substituting equation 67 into equation 62 and integrating, we have for D very large:

$$D = k\mathcal{Z}\{t - (a\sigma/k\mathcal{Z}^2) \ln [\mathcal{Z}D/(\mathcal{Z}D_0 - a\sigma)]\} \quad . \quad . \quad . \quad . \quad (68)$$

and by comparing equation 68 with equation 1, it follows:

$$\tau = (a\sigma/k\mathcal{Z}^2) \ln [\mathcal{Z}D/(\mathcal{Z}D_0 - a\sigma)] \quad . \quad . \quad . \quad . \quad (69)$$
$$\cong -(a\sigma/k\mathcal{Z}^2) \ln [(\mathcal{Z}D_0 - a\sigma)/\sigma]$$

One possible source of low energy blocks for recrystallization nuclei is metal supposedly contained in cavities of small plastically undeformed

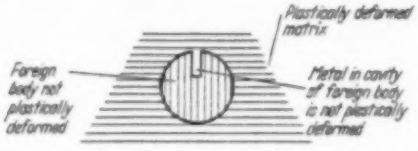
Plastically deformed matrix
Foreign body not plastically deformed
Metal in cavity of foreign body is not plastically deformed

Figure 20. Unstrained part of metal retained in the cavity of a hard inclusion

inclusions that may be present in the cold-worked specimen. For example, consider a hard spherical foreign body (*Figure 20*), embedded in the matrix that contains a cylindrical cavity, filled with the matrix metal. The stress that deforms the matrix plastically is supposed to be not high enough to cause plastic deformation of the foreign body. The metal in the cavity does not plastically deform to an appreciable extent and may then serve as the low energy block in recrystallization.

It has been objected that the low energy block theory does not account for the preference of new grains for the sites of highest matrix deformation and for the fact that $\dot{N}$ increases with ε. This objection is invalidated if the reasonable supposition is made that the low energy blocks are incapable of growth unless immediately surrounded by regions of very high strain energy. If this supposition is correct, the blocks must nucleate near sites of highest deformation and $\dot{N}$ must increase with ε in agreement with experience. In the example considered (*Figure 20*) the low energy block cannot grow out of the cavity unless the strain energy released by its growth is greater than the increase in surface energy occasioned by its growth.

* In the sense that we are using ΔF and $\mathcal{Z}$, the surface energy term of equation 51 should be negative and the strain energy term positive.

In general, it is expected that the low energy blocks will have orientations closely approximating the orientation of the parts of the cold-worked matrix immediately surrounding them. This orientation relation will also obtain for nuclei originating from blocks retained in hard spherical inclusions. If σ, Z, and v_a are independent of temperature, the theory requires that $Q_{\dot{N}} = Q_G$ in good agreement with most of the experimental data but in disagreement with the data on aluminium at small strains. The theory provides no clear explanation of the increase of $\dot{N}$ with time at small ε.

High Energy Block Theories—High energy block theories suppose that at $t = 0$ $\Delta F(t) > \Delta F_0$ and consequently $dD/dt < 0$. In contrast to the mechanism for the decrease of $\Delta F(t)$ with time outlined under the conventional nucleation theory, it is now supposed that some elementary process decreases the strain energy uniformly throughout the entire block.

The time required τ' for $\Delta F(t)$ to become reduced to the order of ΔF_0 may range from τ to a small fraction thereof. In the latter instance the formal theory for τ is essentially no different from the low energy block theory of τ. The nucleation theories recently proposed by DECKER and HARKER,[27] BECK[65] and CAHN[66] are essentially high energy block theories.

Decker and Harker suppose that the nucleation period is the time required for $\Delta F(t)$ to become substantially less than ΔF_0, but they propose no explicit form for $\Delta F(t)$. Beck and Cahn have suggested that high energy blocks undergo polygonization and that these polygonized blocks become recrystallization nuclei. Cahn's more detailed theory may be summarized as follows:

1. Highly stressed parts of the lattice 'local curvatures' polygonize in a time $\tau' \ll \tau$. On the basis of the evidence that 'weakly' bent single crystals polygonize at the same rate as 'sharply' bent ones it is assumed that τ' is independent of the local curvature ρ.
2. During the nucleation period the sub-structure formed by polygonization coarsens and at $t \sim \tau$ elements of the coarsened sub-structure start to grow at the expense of the surrounding matrix. It is assumed that $\tau \propto \rho$ since experimental evidence indicates that, though τ' is independent of ρ, the sub-structure coarsens more rapidly in sharply bent single crystals than in single crystals weakly bent.

In agreement with experience, Cahn's theory requires that nuclei form preferentially at points of highest strain and that the nucleation frequency increase with increasing strain.

The theory also predicts orientations of recrystallized grains whereby they are rotated about an axis in the slip plane and perpendicular to

the slip direction.[67] Cahn rationalizes exceptions to the Burgers–Louwerse orientation relation in aluminium on the basis of 'pencil glide' whereby slip occurs on any plane containing the [110] direction though the (111) plane is preferred.

In order to explain the acceleration of $\dot{N}$ with time, Cahn assumes that τ is fixed by ρ.* By choosing suitable values of τ (nucleation period for $\rho = 1$) and suitable number distribution curves for potential nucleation sites with respect to ρ, the experimental relations $\dot{N} = f(t)$ can be described satisfactorily.

The major weakness of the theory is the assumption that τ is fixed by ρ or the lack of a theory of substructure coarsening—although the constancy of τ observed by Müller in the recrystallization of rock salt crystals provides some empirical support for the validity of the assumption. Also, no clear explanation is offered for the general equality of $Q_{\dot{N}}$ with Q_G.

By making some plausible assumptions more explicit expressions can be obtained for $\Delta F(t)$ in high energy blocks. First suppose that $\Delta F(t)$ is directly proportioned to the concentration c of dislocations within the block and that c decreases with time according to a radioactive decay law and a suitable sink for the dislocations exists, then:

$$\Delta F(t) = a \exp [-bt] \quad . \quad . \quad . \quad . \quad (70)$$

Substituting equation 70 into equation 66 and integrating we have:

$$\tau = a/(\Delta F_0)b \quad . \quad . \quad . \quad . \quad (71)$$

In order to calculate τ on the basis of Cahn's theory, it will be assumed without justification that the kinetics of sub-structure coarsening are analogous to the kinetics of normal grain growth in the absence of inclusions and for isotropic σ. $\Delta F(t)$ may then be expressed as:

$$\Delta F(t) = 1/(a + bt^{1/2}) \quad . \quad . \quad . \quad . \quad (72)$$

and evaluating τ as before:

$$\tau = 2t^{1/2}/b \quad . \quad . \quad . \quad . \quad (73)$$

Though τ is proportional to $t^{1/2}$, the block size D will be virtually a linear function of t for $\tau > (t - \tau)$.

In general the high energy block theory qualitatively accounts for experience excepting that it provides no very plausible explanation for the general equivalence of $Q_{\dot{N}}$ and Q_G. In summary, it appears that a decision on which of the nucleation mechanisms considered is most

* According to conventional nucleation theory, for any homogeneously strained region there is only a probability $\dot{N}$ that a nucleation event occurs in any particular fixed time interval.

likely to operate generally in primary recrystallization cannot be made on the basis of the available experience.

Nucleation in Secondary Recrystallization—There is now fairly convincing evidence that the driving energy for secondary recrystallization is surface energy rather than strain energy. However, the mechanism of nucleation of the process is still no better understood than for primary recrystallization, and, in fact, there is little formal difference between the nucleation theories that have been proposed for the two processes.

According to conventional nucleation theory, nuclei of secondary crystals are formed in small stressed regions that are either retained after primary recrystallization or that are formed by straining deliberately or accidentally after primary recrystallization. However, it seems very unlikely that strains of the order of magnitude ($\varepsilon \sim 0{\cdot}10$ to $0{\cdot}20$) required for conventional nucleation could be retained in the specimen after primary recrystallization.

The block theories for the formation of nuclei in secondary recrystallization are formally the same as for primary recrystallization and the basic equations (64–66) may be used for calculating τ. However, the blocks for primary recrystallization are generally conceived to be sub-grains whereas in secondary recrystallization they are often thought to be entire grains.

Two block theories for secondary recrystallization nuclei that were not given specific consideration in the theory of primary recrystallization have recently attained considerable prominence. These are nucleation *i* due to solution of foreign bodies at grain boundaries and *ii* nucleation due to 'texture inhibition' of grain growth.

Nucleation Due to Solution of Inclusions at Grain Boundaries—Recently BECK, HOLZWORTH and SPERRY[68] have given a convincing demonstration that the nucleation period in some secondary recrystallization processes can be associated with partial solution of foreign bodies at grain boundaries. According to the qualitative picture, the inclusions hold up the motion of most of the boundaries, but a few grains are either sufficiently large to grow or the density of inclusions on their boundaries are insufficient to retard their growth.

The nucleation period may be associated with the time necessary for the density of inclusions at certain boundaries to decrease to a marked extent. However, an alternative possibility that is amenable to simple treatment is that the dispersion of inclusions is effectively a function of temperature only. In this event we may write (see equation 48)

$$\Delta F_0 = \sigma V(1/D_0 - M) \qquad \ldots\ (74)$$

where D_0 is the matrix grain size, M is determined by the dispersion of inclusions and σ is assumed to be isotropic. Assuming that the

'nucleus' is a grain having a diameter D at time t and D_1 somewhat larger than the matrix grain size at $t = 0$ we have:

$$\Delta F(t) = \sigma V/D \qquad \ldots . \quad (75)$$

It then follows that:

$$\tau = -[(D_0^2/(k\sigma v)\ (1 - MD_0)^2] \ln [D_1(1/D_0 - M) - 1] \qquad (76)$$

Grains capable of serving as nuclei must have an initial size

$$D_1 > D_0/(1 - MD_0)$$

Nucleation Due to Texture Inhibition of Grain Growth—Consider the growth of a crystal into a matrix having a high degree of preferred orientation, such that the interfacial energy σ_m between matrix grains (diameter $= D_0$) is very small. Under these conditions, the variation of D_0 with time can be neglected. Let $\sigma(\sigma > \sigma_m)$ be the interfacial energy between the secondary crystal or 'nucleus' and the matrix then:

$$\Delta F_0 = \sigma_m V/D_0 \qquad \ldots . \quad (77)$$

and the condition that $dD/dt > 0$ for the growth of the secondary crystal is:

$$D > D_0\sigma/\sigma_m \qquad \ldots . \quad (78)$$

Two theories or a combination thereof may be considered for the nucleation theory. In one it is supposed that secondary crystals of size $D_1 > D_0\sigma/\sigma_m$ are present in the matrix at $t = 0$. Then:

$$\Delta F(t) = \sigma V/D \qquad \ldots . \quad (79)$$

and

$$\tau = -(\sigma D_0^2/k\sigma_m^2 V) \ln [(\sigma_m D_1 - \sigma D_0)/D_0] \qquad \ldots . \quad (80)$$

We may also suppose that secondary crystals arise from isolated aggregates of grains having high energy boundaries and that the initial diameter of the aggregate is somewhat larger than D_1. Under these conditions $dD/dt < 0$ initially and the form of $\Delta F(t)$ may be assumed to be similar to equation 72. The total nucleation period will be the sum of equations 73 and 80.

In cube texture copper for a mean misalignment between grains of 4° it is estimated, assuming Chalmer's formal relation on lead to be applicable to copper, that $\sigma_m \doteq \sigma/2$. Therefore, in order to grow at the expense of the matrix by surface tension forces alone secondary crystals having $D_1 > 2D_0$ must be initially present or must form by some mechanism. For mean misalignment of 1° $D_1 > 5D_0$.

GRAIN GROWTH AFTER RECRYSTALLIZATION

General Observations on the Mechanism of Grain Growth

The growth of a single grain on a polished surface can be followed directly by measuring its diameter at intervals during growth, or by

heating on the microscope stage and following growth continuously. This method has the disadvantage that grain growth is inhibited by a free surface[38, 69] so that the phenomena observed may not be characteristic of those occurring inside the metal. Grain growth does occur on a free surface, however, and the advantages of direct observation are so great that the method has been used by several workers.

One of the earliest and most detailed series of observations of this type was carried out by CARPENTER and ELAM[70] in 1920. They used a tin alloy containing 1·5 per cent antimony. This is suitable for such observations, because upon heating to about 150° to 200°C and cooling again to room temperature, the position of the boundary at the elevated temperature remains visible as a thin line upon the surface. Upon reheating and cooling again, a second line is found, corresponding to the new position of the grain boundary. Using this technique, Carpenter and Elam arrived at the following conclusions concerning the mechanism of grain growth:

a Grain growth occurs by grain boundary migration, and not by coalescence of neighbouring grains, as two drops of water coalesce.

b Boundary migration is discontinuous: the rate of migration of a boundary is not constant in subsequent heating periods, even the direction of migration may change.

c A given grain may grow into a neighbour on one side and be simultaneously consumed by a neighbour on another side.

d The consumption of a grain by its neighbours is frequently more rapid just as the grain is about to disappear.

Using the same technique and alloy, SUTOKI[71] added the observation that:

e A curved grain boundary usually migrates toward its centre of curvature.

By using a statistical technique, HARKER and PARKER[72] confirmed observation *e* and further observed that:

f Where grain boundaries in a single phase metal meet at angles different from 120 degrees, the grain included by the more acute angle will be consumed, so that all angles approach 120 degrees.

Many of these points are illustrated by the series of photographs presented in *Figure 21*.[7] The metal is zinc, heated on the stage of the microscope and examined with polarized light, so the positions of the boundaries can be followed continuously. The white lines represent positions of the grain boundaries at an earlier stage of growth, and should be disregarded. The upper white grain marked X remained essentially unchanged for the first 30 minutes of heating except for

VOL.
3

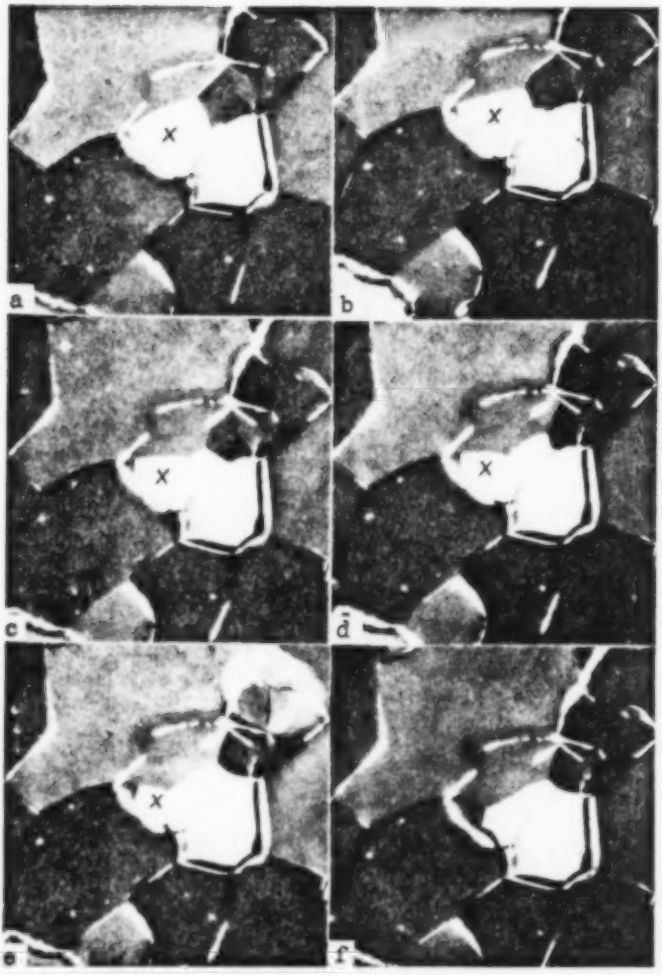

Figure 21. Grain growth in zinc observed with polarized light on a hot stage at about 200° C: the white grain marked X is gradually being consumed: **a** *0 min;* **b** *30 min;* **c** *37 min;* **d** *38 min;* **e** *40 min;* **f** *42 min*

VOL
3

slight migration of the curved boundary on the right as shown in *Figures 21*a and *21*b. Suddenly after 36 minutes the grains to the right and left grew in, changing X from a four sided to a three sided grain. The configuration was then more unstable, and the acute corner of the grain was slowly consumed and finally the whole grain disappeared (*Figure 21*f) after 41 minutes.

An additional observation on the mechanism of grain growth is pertinent. When a two component alloy is heated slightly above the solidus, melting starts at the grain edges and grain faces. Since the metal is now hotter than before one would expect grain growth to occur more rapidly, instead it stops completely.[40] In similar specimens heated to temperatures just below the solidus grain growth continues, and it will commence again in the partially melted specimens if they are cooled below the solidus temperature.

Driving Force for Grain Growth—Two different sources of decrease in free energy have been proposed as the driving force for grain growth after recrystallization. The first originally suggested by CZOCHRALSKI[73] postulates that the grains formed by recrystallization have residual strain energy, and that upon further heating the more perfect ones will grow at the expense of the less perfect ones. The second, suggested first by EWING and ROSENHAIN,[74] considers the interfacial energy of the grain boundaries to be the driving force for grain growth.

Many of the observations on the course of grain growth may be explained by the assumption that the driving force is a difference in residual strain energy between the grains, as it is in recrystallization. This assumption is refuted, however, by the fact that grain boundary melting stops grain growth. If the driving force were a difference in energy between adjacent grains, the mere interposition of a liquid layer would still permit grain growth to occur by the solution of the more strained grains in the liquid, and the redeposition of material from the liquid on the less strained grains.

The evidence supports the conclusion that the driving force is the surface tension of the boundaries. Numerous authors[75, 76] have pointed out that the shapes of metal grains are identical with the shapes of cells in foams: this would indicate that surface tension controls the shape of metal grains as well as the shape of foam cells. SMITH[77] has demonstrated that in a soap foam surface tension can lead to cell growth that simulates grain growth in metals. If the foam is prepared in a partially evacuated container, gas can diffuse across the cell walls from the convex to the concave side. Thus the boundaries migrate toward their centres of curvature exactly as in grain growth, foam cells disappear and the average cell size increases.

VOGEL[78] and more recently BRAGG[76] and HARKER and PARKER[72] have pointed out that the boundaries between undistorted grains should

behave as if they had a surface tension. Atoms on the concave side of a curved surface are more completely surrounded by atoms of their own crystal than atoms on the convex side. Thermal motion causes atoms at the curved interface to move continuously from one surface to the other, and since they are more stable on the concave side, there will be a net flow of atoms to this surface. Thus the boundary will migrate towards its centre of curvature. Similarly, if the surface tension of all boundaries is equal, where three boundaries meet at a point at an angle of other than 120 degrees, the atoms on the grain included by the most acute angle will be less surrounded and less stable than those on other grains. The net flow of atoms will lead to the consumption of the grain included by the more acute angle. DUNN and co-workers[37, 58] and CHALMERS and co-workers[59] have made use of these concepts to measure the relative surface energies of intersecting boundaries whose surface energies are different.

The effect of grain boundary melting on the rate of grain growth may be explained in terms of the surface tension theory as follows:[40] the driving force for grain growth due to surface tension will be:

$$\Delta F = \sigma V \left(\frac{1}{r_1} - \frac{1}{r_2}\right) \quad \ldots . (81)$$

where V is the atomic volume, σ is the surface tension, and r_1 and r_2 are the radii of curvature of the grains between which matter is transferred. In a solid metal, since there are no voids at the grain boundary:

$$r_1 = -r_2 \quad \ldots . (82)$$

Thus

$$\left(\frac{1}{r_1} - \frac{1}{r_2}\right) = 2\left(\frac{1}{r_1}\right) \quad \ldots . (83)$$

Now, if melting occurs at the grain boundaries, r_1 need not equal $-r_2$. Near grain edges, as shown in *Figure 22*, r_1 may have the same sign as r_2 if some melting has occurred, thus $\left(\frac{1}{r_1} - \frac{1}{r_2}\right) \ll \left(\frac{1}{r_1}\right)$ and the rate of growth will be markedly reduced.

It is interesting that even if melting is confined to the region near grain edges, grain growth will stop. This probably results from the fact that the curvatures near grain edges are more pronounced than in the centres of grain faces. When a new three grain junction is formed during grain growth, it will not in general have the equilibrium configuration. The adjustment of the interfacial angles to the correct value will introduce strong curvature into the grain faces, near the edges. These will gradually smooth out over the grain face, but since new junctions are continuously forming, the smoothing may not go to completion.

In view of the foregoing and much other evidence, there can be little doubt that the driving force for grain growth after recrystallization is the surface energy of the grain boundaries, and this driving force will be assumed in the arguments which follow.

Geometry of Grain Growth—A polycrystalline metal consists of an assemblage of polyhedra in contact along faces, edges and corners. To simplify this discussion, only a two-dimensional array of grains will be considered; these will be in contact along faces and edges, and it will be assumed that the surface tension of all boundaries is equal. In such an array of cells or grains, with only three grains meeting at one point, the average number of sides for a grain is six, but there is a distribution, with grains being found which have from three to nine, ten or even more sides. If all the cells had exactly six sides, it would be possible for each set of three grain boundaries to meet at a point at angles of exactly 120 degrees, even though the grain sizes were not uniform, and for all the grain sides to be straight. As Harker and Parker point out,[72] this would be a stable array, and there would be no tendency for the grain boundaries to migrate. However, if a grain is introduced with only five sides, it is geometrically necessary to introduce one with seven sides, so that the average number remains at six. Neither the five nor the seven-sided grain will have straight sides if the boundaries meet at angles of 120 degrees. Grains having less than five sides will have their faces concave inwards, while those having more than five sides will have their faces concave outwards. As a result of these curvatures, the grains with less than six sides will tend to grow smaller, and the grains with more than six sides will tend to grow larger.

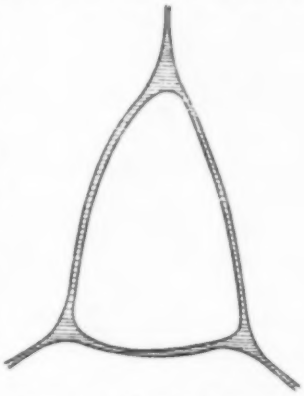

Figure 22. Change in shape at a grain boundary as a result of the grain boundary melting

For much of the time the boundary migration is continuous, but occasionally a grain gains or loses a side, then the rate of motion is discontinuous. There are only two fundamental mechanisms by which the number of sides change[79] in two dimensions. As shown in *Figure 23*, where four grains meet, two of them have a side in common, and the other two are separated by the common side of the first two. As a result of boundaries migrating toward their centres of curvature, the two separated grains approach each other until finally all four boundaries meet in a point. Further boundary migration brings the two separated grains into contact, causing each of them to gain a side, and separates the two grains which were originally in contact, causing

each of them to lose a side. As a result of changes like this, four-sided grains can change to three or less often to five, five sides go with about equal frequency to four or six, while six-sided grains can go to five or seven. If a three-sided grain appears, it usually disappears directly, with the loss of a side by each of the grains with which it was in contact. It is only when a three-sided grain disappears that grain growth can be detected by a counting technique.

Changes of this type would not occur in a perfect froth where all the grains had six sides, but in practice, one never finds such a froth or such a metal. The introduction of even one grain with a non-equilibrium shape upsets the balance of the whole system, and it cannot be restored in general, because as boundaries migrate in a direction to restore the equilibrium configuration, grains disappear so the non-equilibrium configuration is self-perpetuating. Thus occurs grain growth.

Formulation of Continuous Grain Growth—An expression for the rate of grain boundary migration where the surface energy of the boundary is the driving force has been presented as equation 39. For isothermal conditions, this may be simplified to

$$G = K'\sigma V/r \qquad \ldots\ldots (84)$$

where v is the gram atomic volume, G is the rate of grain boundary migration, σ is the surface energy of the boundary, r is the radius of boundary curvature, and the rate constant K' varies with temperature according to the relationship.

$$K' = K'_0 \exp(-Q_G/RT) \qquad \ldots\ldots (85)$$

To develop from this an expression for the rate of grain growth we shall make some simplifying assumptions about the nature and geometry of the process. Later, these will be tested with a model. It will be assumed that the boundary surface tension, σ, is independent of grain size or amount of grain growth, and that the efficacy of inclusions in retarding grain growth is independent of temperature and grain size. Secondly, it will be assumed that

$$r \propto D \qquad \ldots\ldots (86)$$

where D is the average diameter of the grains present. Thirdly it will be assumed that

$$\frac{dD}{dt} \propto G \qquad \ldots\ldots (87)$$

Thus, from equation 84 we may write

$$\frac{dD}{dt} = \frac{K\sigma V}{D} \qquad \ldots\ldots (88)$$

Integrating and evaluating the integration constant at $t = 0$

$$D^2 - D_0^2 = K\sigma Vt \qquad \ldots\ (89)$$

where D_0 is the grain size at $t = 0$. If D_0^2 is negligible compared to D^2, as it is when much grain growth has occurred, this simplifies to

$$D = (K\sigma Vt)^{1/2} \qquad \ldots\ (90)$$

Equation 89 predicts that if the logarithm of the average grain diameter, D, is plotted as a function of the logarithm of time a straight line with a slope of 0·5 should be given if D_0 is sufficiently small to be neglected.

FISHER[80] has reported that D is proportional to $t^{1/2}$ for the growth of soap foam cells in a partially evacuated container. In this case, the rate of boundary migration is controlled by diffusion of gas through the cell walls which like the rate of atom transfer across boundaries is proportional to the curvature of the cell walls. Similarly, the driving force for the diffusion is the surface tension of the cell walls, so the system makes a good model for grain growth in metals. The fact that $D \propto t^{1/2}$ indicates that the geometrical analysis is essentially correct.

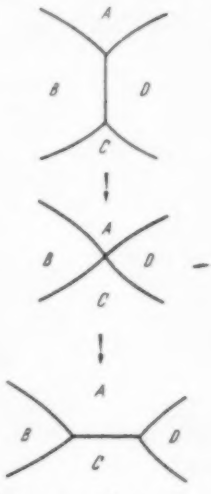

Figure 23. Changes in grain boundary configuration which occur during grain growth

Quantitative Observations of Grain Growth

Grain sizes are usually determined by counting the number of grains in a unit distance or area, on a polished surface, and are expressed as the average grain diameter. This measuring method reveals nothing about grain size distribution, and will reveal grain growth only when it has proceeded to the point where some grains have disappeared.

For engineering work it is customary to present isochronal growth curves, showing the increase in grain size with increasing annealing temperature for a constant heating time. Isothermal data, where the grain size is measured as a function of time, gives a better picture of the process, however. If the grain size is plotted directly against time, isothermal curves appear to indicate that growth stopped after relatively short annealing times, when grain sizes which appear to be characteristic of the temperature are attained. The time dependence of grain size is shown better by plotting the logarithm of the average grain diameter as a function of the logarithm of time (*Figure 24*), since this gives a nearly linear relationship, as indicated above. When grain growth curves are mentioned in the following discussion, the reference

will be to logarithmic plots of this type. First we shall present and discuss examples of continuous growth. Under many conditions the grain size does not remain uniform during growth; these cases of discontinuous growth will be presented later.

Isothermal data on the course of continuous grain growth have been obtained for relatively few metals. In most cases, the data may be represented by an equation suggested by BECK and his co-workers:[38, 82]

$$D = Kt^n \qquad \ldots . \quad (91)$$

This equation applies reasonably well if the grain size is large compared to the initial grain size and small compared with the limiting grain size imposed by inclusions. It is equivalent to equation 90 if $n = 1/2$, but as will be seen, the measured values of n usually are much less than 1/2. A wide range of values for the exponent have been found, assuming that equation 91 applies. Beck, Kremer, Demer and Holzworth, who first used this method of plotting,[38] found that the exponent increased from about 0·09 at 400°C to 0·32 at 600°C in high purity aluminium. In an aluminium alloy containing 2 per cent magnesium they found the exponent varied from 0·17 to 0·45 over the same temperature range. In 70 : 30 α-brass of commercial purity, both BECK[82] and BURKE[39] found the exponent to be independent of temperature, with a value of about 0·2. On the other hand, BURKE[40] found that in very high purity α-brass, the exponent increased from about 0·35 to a little over 0·5 over a temperature range of 500° to 850°C, with the value increasing with temperature. MILLER[83] has studied grain growth in a number of carbon steels between 815° and 1,250°C and reports values for n ranging between 0·08 and 0·22.

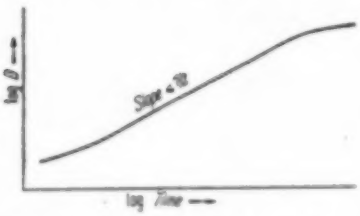

Figure 24. Typical isothermal growth curve for continuous grain growth (schematic)

Temperature—As indicated previously, the temperature dependence of the rate of grain growth should be given an equation of the type:

$$G = A \exp (Q_G/RT)$$

Values of Q_G the activation energy for grain growth, as determined by several workers are listed in *Table VII.*

No single activation energy can be computed from the growth curves obtained for aluminium, and the aluminium–magnesium alloy studied by BECK and his co-workers,[38] because the growth law changed with temperature. Nevertheless the rate of growth increased with increasing temperature approximately as rapidly as for the metals

Table VII. Values of the activation energy for grain growth Q_G

Metal	Q_G *kcal/gm atom*	*Observer*
*Brass** ..	60	*Burke*[39]
		Walker[39, 44]
*Brass** ..	62	*Beck*[42]
Brass† ..	40	*Burke*[40]
Tungsten ..	110	*Robinson*[64]
γ-Iron‡ ..	90–113	*Miller*[63]
α-Iron§ ..	110	*Burke and Chandler*[61]

* Commercial purity
† High purity
‡ Various commercial carbon steels
§ Westinghouse puron-deoxidized

where an activation energy can be computed. Actually, the activation energies reported for α-brass of commercial purity apply only over the temperature range of 500° to 750°C. Above that temperature the rate increased more rapidly than would be indicated by the activation energy reported. Other experiments indicated that at least part of the increase in rate resulted from the solution or coalescence of growth inhibiting inclusions, and it is of course possible that a similar solution or coalescence contributes to the increase in rate observed with all the other metals. This is discussed more fully in another section.

Composition—The effect of composition on grain growth is obscure and few specific experiments have been performed to elucidate the effect. It seems to be generally true that alloys have a greater tendency to display continuous grain growth than pure metals. Aluminium, iron, zinc and even spectroscopically pure copper, all show exaggerated growth with the development of mixed grain sizes. On the other hand, it is not possible to cause such exaggerated growth in brass even by slightly straining the specimen before annealing. In aluminium, this procedure produces such exaggerated growth that single crystals are manufactured this way. The addition of small amounts of silver to high purity zinc permits continuous growth to occur.[33] In this case the effect of silver is to retard grain growth at low temperatures. At higher temperatures growth occurs so slowly that the inclusions responsible for low temperature discontinuous growth dissolve before much growth has occurred.

Beck, Kremer, Demer and Holzworth investigated the relative rates of grain growth in high purity aluminium and in an aluminium magnesium alloy.[38] They found that the rate of growth was greater in the pure metal at small grain sizes, but as the grain size increased

the curves crossed, so that at coarser grain sizes, the rate of growth was greater in the alloy.

Limiting Grain Sizes—There has been much confusion concerning how large the grain size in a metal may become with prolonged heating. Grain sizes for engineering use are frequently reported as a function of heating temperature for a constant heating time. Since the grain sizes determined in this way are relatively insensitive to heating time when it is of the order of one hour, the impression has grown that these grain sizes are characteristic of the heating temperature. On the other hand, the formulation of grain growth just presented, and many of the growth curves indicate that grain growth should continue indefinitely until the specimen becomes a single crystal. Actually, there does seem to be a limiting grain size which is characteristic of the specimen material and the temperature, but in most cases it is larger than the grain size attained after relatively short heating times. This fact was well known to JEFFRIES,[66] who pointed out that the final sizes may be attained after a few minutes heating at high temperatures.

There are two important reasons why grain growth may stop before the piece becomes a single crystal. The first arises from the fact that grain growth is inhibited by a free surface.[38, 69] A striking example of this has been reported by Beck and his co-workers who found that in sheet specimens, continuous grain growth stops when the average grain size approximates to the thickness of the specimen. Similarly, in wires, it is not possible to grow grains having a dimension greater than the diameter of the wire by continuous growth. If the specimen is large, however, growth will stop before the grains approximate the dimensions of the piece. This results from the inhibition of grain boundary migration by inclusions.

Since the early work of Jeffries on the effect of thoria on grain growth in tungsten,[66] metallurgists have recognized that second phase inclusions inhibit grain growth. It is not necessary to have a continuous layer of a second phase at the grain boundaries, in fact, the more highly dispersed the second phase is, the more effective it will be in preventing growth. An example of how second phase inclusions can interfere with growth is shown in *Figure 25*. The points of the scallops on the boundary are points where the boundary is being held back by inclusions.

An excellent example of the effect of second phase inclusions on grain growth has been presented by BECK, HOLZWORTH and SPERRY.[68] The aluminium alloy they used contained 1·1 per cent manganese and a manganese–aluminium phase is present at 550°, 600° and 625°C but is completely dissolved at 650°C. Below 650°C a limiting grain size characteristic of the temperature is quickly reached, and no further grain growth occurs. Above that temperature, continuous grain

VOL.
3

Figure 23. Inclusions in α-brass retarding grain boundary migration

VOL.
3

growth occurs in the absence of inclusions, and proceeds until a large grain size is attained.

Burke found similar results in a 70 : 30 α-brass.[40] A limiting grain size of 0·55 mm at 800° and of 0·75 mm at 850°C was found in a brass of commercial purity, which contained a number of inclusions. In brass of exceedingly high purity, the limiting grain size was about 1·75 mm at only 800°C, and the specimen thickness was only a little larger than this. Had a larger specimen been available, even more grain growth might have occurred.

The increase in limiting grain size with increasing temperature may result from either the solution or coalescence of growth inhibiting inclusions. For this reason the course of grain growth in an inclusion bearing material may be influenced by prior heat treatments that control the dispersion of inclusions. In the brass of commercial purity just described, the grain growth rate could be increased by as much as fifty times by heating the specimen to 850°C and slowly cooling,[40] so that the inclusions were coalesced prior to the final working.

Rationalization of Grain Growth Observations

There are many factors which may contribute to decrease of the slope of isothermal logarithmic growth curves, so that the exponent n in equation 91 is less than 0·5. As equations 89 and 90 indicate, one would expect the slope to be 0·5 only in cases where D_0^2 is negligible compared to D^2. If it is not negligible, the slope of the log D/log t curve will be lowered, and in many of the published data, particularly those obtained at low temperatures after small amounts of grain growth, this explanation may apply.

Equation 89 indicates that grain growth will continue until the specimen becomes a single crystal. Grain growth may stop while the grain boundaries are still curved, however, either because the average grain size approximates the thickness of the specimen, or because inclusions prevent further growth. In the latter case, Smith[77] has reported a computation by Zener which indicates that the limiting grain size should be given approximately by the expression:

$$D_l = d/f \qquad \ldots . \quad (92)$$

where D_l is the limiting grain size, d is the average diameter of the inclusions and f is their volume fraction. Under these conditions, the rate of growth will be controlled not by the average grain size present, but by the difference between this grain size and the limiting one, so that assuming that D_l is independent of time and temperature:

$$\frac{dD}{dt} = K\left(\frac{1}{D} - \frac{1}{D_l}\right) e^{-\left(\frac{Q_g}{RT}\right)} \qquad \ldots . \quad (93)$$

where K is equivalent to $(K\sigma V)$ of equation 88. Integrating and evaluating the integration constant at zero time, one gets:

$$\left(\frac{D_0 - D}{D_i}\right) + \ln\left(\frac{D_i - D_0}{D_i - D}\right) = \frac{K}{D_i^2} t \exp\left(-Q_G/RT\right) \quad \ldots\ldots (94)$$

By experimentally determining Q_G, K and D_i, the isothermal growth curve can be computed for comparison with experimental results.

In *Figure 26* a series of curves computed in this way for very high purity brass[40] are shown. A value of 40 kcal/gm atom was used for

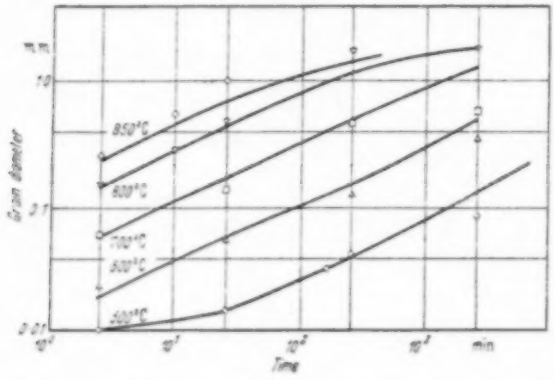

Figure 26. Comparison between grain growth data obtained with high purity brass and curves calculated using equation 93

Q_G, $5{\cdot}31 \times 10^5$ cm/min for K and the experimentally determined values of 0·005 mm for D_0 and 1·75 mm for D. The general agreement with the points plotted is excellent and would have been improved if the temperature dependence of D_i had been taken into account. Equation 94 does not fit grain growth curves in general. The shape of the curves is the same but the slope is usually found to be less than predicted. There are many possible interpretations of this discrepancy. They cannot be discussed quantitatively but it seems worth while to mention several of them and point out the direction in which they will operate.

If inclusions are present, the rate may be controlled solely by the rate of coalescense of the inclusions; in this case, the dependence on time is not yet clear. There is the further possibility that mobile inclusions may collect preferentially on grain boundaries by diffusion during grain growth. This will be more probable when the grain size is large and the boundaries are moving slowly. Thus, the inclusions will become increasingly effective as the grain size increases, and the slope of the growth curve will be decreased.

The surface tension of the boundaries may decrease with time. This may result from a change in texture or as Benedicks suggests[75] by diffusion of soluble impurities to the boundaries. This latter effect will become more pronounced as the rate of grain growth decreases, and will operate to decrease it further.

Changes in the distribution of grain sizes and interfacial angles can also change the rate of grain growth for a given average grain size, although they will not influence the rate of migration of a boundary of given curvature. Equations 89 and 90 were derived with the assumption that the grain size distribution and the grain boundary configuration is independent of the average grain size. Only under these conditions, does a constant proportionality exist between average grain size and average boundary curvature. If the grain size distribution becomes more uniform during grain growth, the smaller grains with more highly curved faces must be disappearing preferentially. The average radius of curvature of the grain faces present will thus increase more rapidly with increasing grain size than the average grain size, thus the rate of growth will decrease more rapidly than would otherwise be predicted. The rate of growth itself, of course, will be greater than would be predicted, because the migrating boundaries are more curved than they would be in a specimen having an equivalent uniform grain size.

Harker and Parker have shown that the interfacial angles may approach more closely to 120° as growth proceeds.[72] If this is so, the condition of geometrical similarity at all grain sizes is not met, and in effect the average radius of curvature of the grain boundaries will be decreasing more rapidly than the average grain size, so the slope of the log D/log t curve will be decreased.

Effect of a Free Surface—In a three dimensional array of grains, grain faces must extend from one three grain junction to another. The marked curvatures about two axes introduced by this requirement, will cause relatively rapid boundary movement. If on the other hand, the grains are two dimensional and extend completely through the piece, the face edges in contact with the surface can adjust their positions so the grain faces have simple cylindrical curvatures, thus the driving force for grain growth and the rate of grain growth will be much reduced. The increase in effective radius of curvature when the grains become two dimensional may be sufficient for the inclusions present to prevent any further grain growth.

This would indicate that in sufficiently thin sheets, even two dimensional grains should have sufficient boundary curvature to permit some growth. Burke studied this and found that in brass, the ratio of limiting grain size to sheet thickness increased with decreasing sheet thickness,[40] as predicted by the above explanation.

Secondary Recrystallization

Thus far, discussion has been confined to cases of continuous grain growth where the grain size increases uniformly after primary recrystallization. Under some conditions, primary recrystallization results in a fine grained structure which does not coarsen much upon further heating at a low temperature. As the temperature is raised, 'secondary recrystallization' may occur. Some grains start to grow after a nucleation period, and these rapidly growing grains consume their stable smaller neighbours. The kinetics of the process are apparently identical to those of primary recrystallization and have been treated in an earlier section. The driving force appears to be the surface tension of the boundaries as it is in ordinary grain growth, since the process will occur in the absence of deformation. Nevertheless, slight deformation may decrease the nucleation period, and promote the appearance of secondary recrystallization. Burgers has reviewed the results of a number of investigations of these phenomena, and more recent work has been reported by Beck, Holzworth and Sperry,[68] Kronberg and Wilson,[87] Ward,[25] Turkalo and Turnbull[88] and Rosi and Alexander.[26]

A necessary condition for the occurrence of secondary recrystallization is the inhibition of growth of the grains that results from primary recrystallization. Two mechanisms for this inhibition are well established: a proper dispersion of a second phase, or the presence of a marked preferred orientation.

Inclusion Inhibited Growth—Exaggerated grain growth in the presence of growth-inhibiting inclusions was first observed by Jeffries in thoria bearing tungsten wire.[86] He found that the coarsening temperature increased with increase in the thoria content until a thoria content was reached at which no growth at all occurred. Beck, Holzworth and Sperry studied aluminium alloys containing a dispersed manganese–aluminium phase.[68] They found that exaggerated growth occurred only at a temperature at which the manganese–aluminium phase was almost completely in solution. Below this temperature, little or no grain growth occurred. Above it, continuous growth took place. They also observed a nucleation period for the onset of the phenomenon which increased with temperature, and with decreasing amount of the second phase.

An important consequence of such exaggerated growth is that the limiting grain size is controlled only by the number of nucleation centres, and not at all by the number of inclusions or the dimensions of the specimen as in continuous growth. In fact, thin sheet specimens may be transformed to single crystals by secondary recrystallization. A common example of discontinuous growth, which is not so

pronounced as the cases cited, is the sudden coarsening of deoxidized steels, at a quite definite coarsening temperature.

Texture Inhibition—Similar discontinuous growth may occur in specimens with strongly preferred crystal orientations. An outstanding example is the secondary recrystallization of cube-texture copper. The growth of the as-recrystallized grains is slow, because, as Beck has suggested, grain boundaries between grains of nearly the same orientation migrate only with difficulty. The origin of the secondary grains is not clear, but there is a well defined nucleation period.

A striking fact is that the new grains have well-defined orientations with respect to the matrix—as Bowles and Boas[57], and Kronberg and Wilson[87] have reported, most secondary grains have an octahedral pole in common with the matrix, but are rotated about this pole by approximately $\pm$ 30°.

VOL. 3

RECRYSTALLIZATION TEXTURES

Two fundamentally different mechanisms for producing a preferred orientation by recrystallization will be considered. The first—the 'oriented nucleation' hypothesis—almost universally accepted until recently, postulated that the orientation of the recrystallized grains is controlled exclusively by the orientations of the recrystallization nuclei. The other, suggested most recently by Beck,[35] assumes that recrystallization nuclei may be randomly oriented, and that a selection is made among these by the orientation dependence of their growth rates. Thus the orientations found in the recrystallized metal will be those which were most favourably oriented for growth in the deformation texture. This will be termed the 'oriented growth' hypothesis. Since textures in non-ferrous metals have already been discussed in Volume I[89] of this series, we will concern ourselves here primarily with a discussion of the evidence favouring these two mechanisms of forming recrystallization textures in face-centred cubic metals.

From studies of the orientations of recrystallized grains in deformed aluminium single crystals, Barrett[90] and others have reported that the new grains definitely have orientations which differ from that of the grain from which they grew. He pointed out that the orientation relationship was reasonably consistent in many cases with a rotation about axes of the type [111] which the new and old grains held in common. Since that time a great deal of evidence has accumulated which indicates that this relationship frequently obtains. It has been observed in the secondary recrystallization of cube-texture copper,[56, 87] after the recrystallization of deformed brass,[91] and copper[92] and aluminium[35] single crystals.

In all cases, the magnitude of the rotations involved are reasonably

constant, they vary between 20 and 40 degrees. KRONBERG and WILSON[97] report that when two close-packed planes of atoms are rotated about a common normal, there are several specific rotations which place a number of atoms in each array in coincidence. Specifically, for rotations of 22 or 38 degrees, the coincidence sites lie on a hexagonal array with a parameter $\sqrt{7}$ times that of the primitive array. It might be pointed out that in these cases, rotations in opposite directions which total 60 degrees lead to two new orientations which are twins, thus a rotation of minus 22 degrees gives a twin of a plus 38 degree rotation. Kronberg and Wilson report that these rotations of 22 and 38 degrees most accurately describe the orientation relationship they observe in the secondary recrystallization of cube-texture copper.

BECK and HU[35] studied the relative rates of growth of grains having a number of different orientations by scratching the polished surface of a deformed single crystal and then heating it. They observed that grains having many orientations appeared along the scratch, but that those related to the parent by approximately a 30 degree rotation about a common octahedral pole grew most rapidly. They thus suggested that even if many orientations were nucleated, only those close to this most favoured orientation would appear in the recrystallized metal, and that the recrystallization textures can be accounted for solely on the basis of oriented growth.

While it is undoubtedly true that oriented growth must provide in this fashion a selection between favourably and unfavourably oriented nuclei, and must thus contribute to the formation of recrystallization textures, there are other observations that indicate that a nucleation is not completely random. If the orientations of recrystallization nuclei were completely random, then oriented growth would select all of those which had crystallographically similar orientations with respect to the matrix. Because of crystallographic symmetry, one would expect to find recrystallized grains appearing in face-centred cubic metals which were related by rotations about each of the four [111] directions and rotated in either direction about these axes. If the rotation is taken to be about 30 degrees, as Beck and Hu report, then this would give rise to eight new orientations—four sets of twins—corresponding to two possible rotations about each of four [111] axes. In the Kronberg–Wilson rotation, sixteen new orientations should be observed, corresponding to rotations in either sense by either of two possible amounts about four axes.

All of these possible new orientations are rarely if ever observed but certain of them seem to appear reproducibly following the same treatment. This could only result from the formation of nuclei having a limited number of orientations. For example, in the recrystallization of cube-texture copper, Kronberg and Wilson find that, with one

exception in 63 observations, the 22 degree rotations occur only in a clockwise fashion about the north west and south east [111] poles of the cube texture: the rolling direction corresponding to north. The 22 degree rotations are counter clockwise about the north east and south west poles. All 38 degree rotations are opposed to the 22 degree rotations.

There is also evidence to indicate that the new grains may be related to the parent by rotation about only a reproducible few of the possible four [111] poles. MADDIN, MATHEWSON and HIBBARD[91] found that upon recrystallizing deformed single crystals of brass, the new grains were related by rotations about the poles of the octahedral planes upon which slip occurred, and about no others. Similar observations have been made in copper by BECKER[92] and by one of us.[93] The deformation fibre texture of aluminium wire has a [111] axis parallel to the wire axis and that does not change upon recrystallization. BECK[94] has pointed out that even though the new grains had different orientations from their parents, if they were all related by rotations about an appropriate [111] direction, the new texture would be indistinguishable from the old. Here, however, only one of the four possible axes are chosen. Had the new grains been related by rotations about all of the [111] axes, a much more random texture would have been obtained.

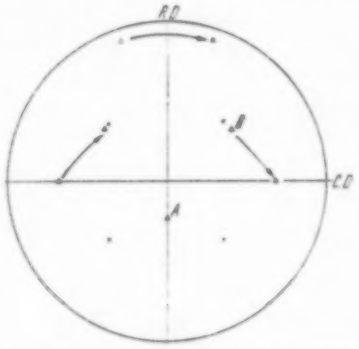

Figure 27. Derivation of recrystallization texture from deformation texture in aluminium by rotation about [111] *directions:* × *shows cube texture positions,* △ *and* ▲ *are different components of the deformation texture*

Similarly, the recrystallization texture of rolled aluminium differs only slightly from the deformation texture. BECK and HU[95] have explained this by a similar rotation. The deformation texture of aluminium consists of two pairs of orientations, only one of which is shown in *Figure 27*. The two halves of the pair are related by a rotation of approximately 40 degrees about an octahedral pole, *A*, which they have in common. If the new grains are related to the old by rotations in the correct direction about this pole, the halves of this component of the texture interchange, and the new texture will be indistinguishable from the old. If pole *B* is chosen for the rotation, a rotation of about 40 degrees will transpose the deformation texture into the well-known cube texture. Beck and Hu find traces of the cube texture in the recrystallized aluminium, and have microscopic evidence that the first

mentioned reorientation does in fact occur. While the new textures can be explained in terms of a rotation about a [111] pole, not all such poles are used, nor are rotations of both senses used. Again it seems necessary to assume that while some selection of orientations may have been made by oriented growth, only a limited number of orientations were produced at the time of nucleation.

There is little information to guide speculation on what controls the orientation of the nuclei. None of the theories of nucleation previously described predict the observed orientation relationships. The work of Maddin, Mathewson and Hibbard, and of Becker, indicates that the deformation process itself may control this orientation. In this connection it is interesting to note that HEIDENREICH and SHOCKLEY[96] have reported that deformation seems to produce some rotation about the normal to the (111) plane on which slip occurs. Similarly, Barrett reported[90] that the spread of orientations in a compressed aluminium single crystal could be explained by a rotation of about 10 degrees in either direction about the [111] poles which were perpendicular to the [011] compression axis.

Decker–Harker Theory—A completely different mechanism for the production of recrystallization textures has been proposed by DECKER and HARKER[64] and seems to be supported by experimental evidence in the case of silicon ferrite. The recrystallization texture of silicon ferrite is (110) [001]. Harker and Decker have demonstrated by direct x-ray studies of deformed coarse grained specimens that grains in the starting material which have this orientation are more distorted by a given reduction in thickness than grains having other orientations. Microscopic observation shows that deformed grains having these orientations also recrystallize first upon heating. However, they find that the orientations of the recrystallized grains are essentially the same as the orientation of the parent. Apparently this is a case of recrystallization *in situ*, a gross case of polygonization. Decker and Harker propose that in a fine-grained specimen, these recrystallized, strain-free grains will grow at the expense of the deformed matrix, and produce a recrystallized texture of this orientation. This does not happen in the very coarse grained material upon which the observations were made, because the distances involved in growth are too great, but it seems a reasonable process to occur in a fine grained material. It should be noted that the theory provides a mechanism for producing a recrystallization texture in a deformed material that does not have a well-defined deformation texture.

ANNEALING TWINS

One of the most prominent features of recrystallized face-centred cubic metals are the familiar annealing or recrystallization twins. These

usually appear as parallel-sided bands that run across grains; the parallel boundaries coinciding with (111) twinning planes. The structure is coherent across these boundaries, that is both parts of the twin hold a single (111) plane in common. Non-coherent boundaries also appear where a twin terminates within a grain, or where steps occur along a coherent boundary. At these composition surfaces a (111) plane is not held in common by both halves of the twin.

It is well known that the face-centred cubic structure may be formed by stacking close-packed layers of atoms (which are (111) planes) in the sequence *ABCABC*. A face-centred cubic twin may be formed by stacking in the sequence *AB*$\underline{C}$*BA*. This sequence also forms a close-packed structure in which the distance of closest approach of atoms is unchanged, but the right half is the mirror image of the left half. The $\underline{C}$ plane indicated by underlining is held in common by both parts of the twin.

Mechanism of Twin Formation—The mechanism proposed for the formation of annealing twins follows the concept that a change in stacking sequence is all that is necessary to form an annealing twin. This hypothesis was first presented by CARPENTER and TAMURA.[97] BURKE[98] obtained evidence that this mechanism must operate, and FULLMAN[99–103] has described auxiliary conditions necessary for its operation and has measured the surface tension of twin interfaces.

The change in stacking sequence necessary for the formation of an annealing twin may occur whenever a properly oriented grain boundary migrates. If the interface corresponds approximately to a (111) plane in the growing crystal, growth will proceed by the deposition of additional (111) planes in the stacking sequence *ABCABC*. Each newly added plane has of course the choice of two positions, but if the structure and orientation are to be maintained, this stacking sequence must be followed. If the newly deposited layer falls in the wrong set of positions so the sequence is *ABCABCB*, the first layer of a twin would be formed. This would not be difficult from an energy point of view, since coherent interfaces have very low surface energies and the number of nearest neighbours is unchanged by such a stacking error. Once a twin interface is formed, further growth may continue with the sequence in reverse order, *ABCAB*$\underline{C}$*BACBA*, forming a twin. A second accident of the same type at a later time on a parallel (111) plane will form a parallel twin interface and restore the original orientation. A twin band will now exist. If the accident occurs on a non-parallel (111) plane of the twin, the original orientation will of course not be restored, rather a second order twin of the original orientation will be produced. Such second-order twins are observed with reasonable frequency.

The growth accident may be expected to occur particularly when a

discontinuous change takes place in the nature of the matrix being consumed. One possible discontinuity is a twin fault* which provides a ready-made nucleus for an annealing twin. However, all of the annealing twins found even in freshly recrystallized metal cannot be nucleated in this way. Recrystallized grains almost always have a different orientation from the parent grain although frequently the parent and daughter grains have an octahedral plane in common. Although twin faults may exist on several (111) planes in the parent, only those on a common octahedral plane can nucleate annealing twins in the daughter grain. Thus by this mechanism, one can account for only one family of annealing twins in a given grain, although several are frequently observed.

A second type of discontinuity may be found when a grain gets a new neighbour either during recrystallization or grain growth, and it will permit the formation of an annealing twin on any possible plane in the growing grain. Grain growth occurs by the repetition of transformations like that shown in *Figure 23*. Grain *A* which was originally in contact with grains *B* and *D* at a single corner, gains a side so that it is now in contact with grains *B* and *C* at one corner and with grains *C* and *D* at another corner. When this transformation occurs, a twin may be formed in one of the four new corners, as shown in *Figure 28*b. This is in agreement with the observation that new twins appear to form frequently in grain corners.

Even though an accident of growth produces a new twin, the twinned orientation must present advantages if it is to grow to microscopically detectable dimensions. It is possible for the twin to have a more favourable orientation for growth into the grain being consumed, and evidence indicating that orientation may influence growth rates has been presented in an earlier section. Alternatively, the twin may permit a grain boundary configuration having a lower interfacial energy. Consider the three grain junction *ABC* shown in *Figure 28*a. The boundaries between grain *A* and grains *B* and *C* will have surface tensions σ_{AB} and σ_{AC} which depend upon the relative orientations of the grains *A*, *B* and *C*, and upon the positions of the boundaries *AB* and *AC*. Now consider the situation shown in *Figure 28*b. The boundaries between the twin *T* and the neighbouring grains will have surface tensions σ_{BT} and σ_{CT} and these values may differ from σ_{AB} and σ_{AC}

* A twin fault has the stacking sequence *ABCBCABC*, a single error in stacking producing a twin two atom layers thick (the underlined *CB*). MATHEWSON[104] suggested that a structure like this could be formed by slip since the slip in the observed [110] direction in face-centred cubic metals probably results from zig-zag movements in [112] directions. An odd number of [112] displacements would produce the required stacking sequence. Heidenreich and Shockley have pointed out[98] that dislocations in face-centred cubic metals probably dissociate into half dislocations that separate, but that are connected by a stacking fault of this type. BARRETT[105] has presented x-ray evidence that these twin faults can be produced by deformation in silicon bearing copper.

because the orientation of T differs from the orientation of A. In addition, there is a new boundary AT, with a surface tension σ_{AT} which numerous measurements show to be much less than the surface tension of grain boundaries. Let L_1, L_2, L_3 be the lengths of the boundaries between twin T and grains A, B and C respectively. Then if the following relationship holds:

$$L_1\sigma_{AT} + L_2\sigma_{BT} + L_3\sigma_{CT} < L_2\sigma_{AB} + L_3\sigma_{AC} \quad . \quad . \quad . \quad . \quad (95)$$

the total boundary energy will be decreased by introducing a twin at the grain corner. Fullman and Fisher[103] have measured the relative boundary energies in a number of cases where twins are found at boundary corners, by observing the depth of grain boundary grooves produced by thermal etching. They find that in the majority of cases the condition required by expression 95 is fulfilled. One would not

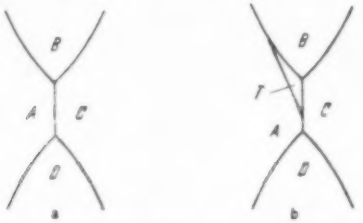

Figure 28. Twin forming in a grain corner

expect it to be fulfilled in all cases because not all twins found in grain corners will be newly formed ones. A number will be old twins which are being consumed, for these this condition need not obtain.

To summarize, annealing twins may be formed whenever a grain boundary migrates if the following conditions are fulfilled: the surface on which the twin forms must correspond to a (111) plane of the growing grain, so that a simple error in positioning of the next layer of atoms will produce a twinned orientation and the twinned orientation must be energetically or kinetically favoured. Discontinuities in the matrix being consumed favour the twinning act. Such discontinuities may be twin faults produced by deformation, or the appearance of new three grain junctions.

With this theory, most of the observations on the behaviour of annealing twins may be explained.

Absence of Twins in Cast Metals—Annealing twins are rarely if ever found in cast metals. However, grain boundary migration occurs only to a slight extent in cast metals, and in particular, the appearance of new three grain junctions is rare. Hence, there is little chance for a twinning accident to occur. Similarly, during solidification, the growing grains will encounter no discontinuities in the homogeneous melt which will be likely to induce the twinning act.

Growth of Twins during Grain Growth—The ratio of the width of twin bands to grain diameter appears to remain quite constant during grain growth. A very coarse grained metal will have grains in which the twins are many times wider than any grain that was present shortly after recrystallization. This appears to indicate that twin bands grow in width, by migration in a direction perpendicular to the (111) composition plane, during grain growth.

It has been demonstrated,[98] however, by measuring the same twin bands repeatedly during grain growth, that annealing twins do not grow in width. This is not surprising, because the low energy of the twin boundary results from the coincidence of the composition and twinning plane. An ordinary grain boundary is able to migrate past

Figure 29. Mechanism for the formation of wide twins during grain growth

an inclusion because it can bend, and eventually reform on the opposite side of the inclusion while continuously decreasing its area. A coherent twin boundary is unable to do this. Since the twins do not grow in width, a mechanism is necessary to account for the appearance of wide twins in coarse grains.

One possible mechanism is shown schematically in *Figure 29*. A twin which forms at the corner of a grain can grow in width because one of its sides forms part of the boundary of the growing grain. It will grow in width until a second twinning act terminates it to form a complete twin band. As was indicated above, twinning probably occurs when a grain changes its number of sides. The average distance of boundary migration before a grain loses or gains a side to produce new three grain junctions will be proportional to the grain diameter, hence the average distance of boundary movement between twinning acts, and the width of newly formed twins will be proportional to grain diameter.

Mechanism for the Disappearance of Twins—The number of twins present per grain decreases rapidly in the early stages of grain growth,[106] and then reaches a value which appears to be quite constant for the greater part of the growth processes. Since the mechanism above indicates that twins form continuously during grain growth, both these observations indicate that twins must disappear.

Although coherent twin boundaries, where the composition and twinning planes coincide, cannot migrate, there is evidence[98, 101] that if a twin terminates within a grain, the non-coherent boundary can migrate, to change the size of the twinned domain. In freshly recrystallized metal, many of the twins terminate within the grain. This is probably associated with growth in a deformed matrix,

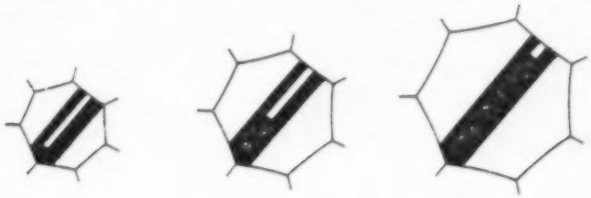

Figure 30. Migration of non-coherent twin boundary to cause disappearance of twins and increase in width of remaining ones

since both MADDIGAN and BLANK,[107] and BURKE and SHIAU[69] observed that grain growth in a specimen deformed too slightly to cause recrystallization, caused the appearance of many twin terminations. Apparently the residual strain energy permits the formation of the terminating interface, a phenomenon that would in most cases be impossible were surface tension the sole driving force for grain boundary migration. Once a termination is formed, the twin can decrease its length and eventually disappear, as shown in *Figure 30*. It should be

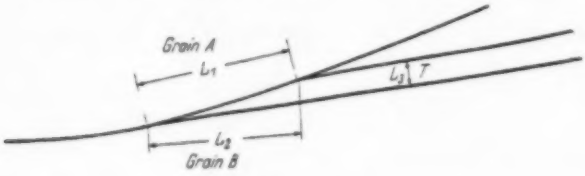

Figure 31. Conditions for the formation of non-coherent twin boundary

noted that this provides an alternate mechanism for the apparent growth in width of twins.

Fullman has further pointed out[103] that where surface energy is the sole driving force for grain growth, when a twin intersects a grain boundary with great obliquity, under certain conditions it may be energetically favourable to terminate the twin. In *Figure 31* if the twin T pulls away from the grain boundary between grains A and B, then the interface along L_1 changes from AT to AB and the coherent interface L_2BT is replaced by the incoherent interface L_3BT.

Now if

$$L_1\sigma_{AT} + L_2\sigma_{BT\text{coh}} > L_1\sigma_{AB} + L_3\sigma_{BT\text{incoh}} \quad . \quad . \quad . \quad . \quad (96)$$

it will be energetically favourable for the twin to pull away from the boundary. The terms $\sigma_{BT\text{coh}}$ and $\sigma_{BT\text{incoh}}$ refer to the surface energies of the coherent and incoherent boundaries respectively, between grain B and its twin T. If such a termination forms the twin may eventually disappear as mentioned above.

Measurement of Interfacial Energies of Twin Boundaries

Fullman measured the interfacial energies of twin boundaries in copper and aluminium.[100, 102] In copper the technique is interesting

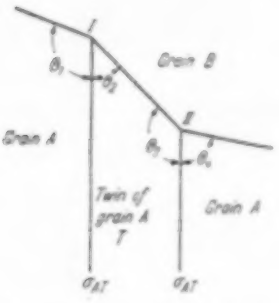

Figure 32. Angular relationships when twin intersects grain boundary

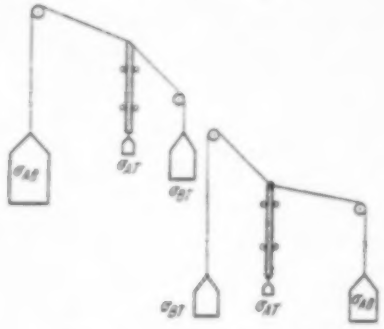

Figure 33. Mechanical analogy for Figure 32

and new. The angle opposite a twin boundary, where it intersects a grain boundary may be either greater or less than 180 degrees as shown in *Figure 32*.

The apparently negative surface tension of the AT boundary at the three grain junction I is a consequence of the inability of the coherent AT boundary to migrate. It can only lengthen or shorten. This is mechanically analogous to a rod, which cannot bend, and which is constrained by guides to move only longitudinally, see *Figure 33*. If σ_{AB} is slightly greater than σ_{BT}, then the configuration at the junctions I and II will obtain. Because of the surface tension of the twin boundaries, the left-hand part of the AB twin interface will not be quite parallel to the right-hand part of the AB interface. From the measurement of the angles θ_1, θ_2, θ_3 and θ_4 it is possible to determine σ_{AT} from the relationship:

$$\sigma_{AT} = \frac{\cos\theta_2 \cos\theta_4 - \cos\theta_1 \cos\theta_3}{\cos\theta_3 - \cos\theta_2} \cdot \sigma_{AB}$$

or

$$\sigma_{AT} = \frac{\cos\theta_2 \cos\theta_4 - \cos\theta_1 \cos\theta_3}{\cos\theta_1 - \cos\theta_4} \cdot \sigma_{BT}$$

A number of measurements made in this way indicate the surface tension of twin boundaries in copper is about 0·045 that of grain boundaries. Measurements of the same ratio, made by comparing the shape of grooves at grain boundaries and twin boundaries after annealing similar specimens in lead vapour lead to a value of 0·026, which is a reasonable check, considering the difficulty of the measurement. Thus, in copper, the twin boundary energy is from 0·03 to 0·05 that of an average grain boundary.

FULLMAN[102] also measured the surface tension of the rare twin boundaries in aluminium, by measuring the angle opposite the twin boundary where it intersected the grain boundary. Actually, the surface tension of many boundaries between grains which were not accurately in twinned relationship were also made. To interpret the data, the values of the surface tension were plotted as a function of the rotation away from the precise twinned relationship. By extrapolating these data to zero rotation, a value for σ_T/σ_{AB} of 0·21 was obtained.

Variation of Intensity of Twinning from Metal to Metal—Almost any hypothesis of twinning requires that the coherent twin interface should have low energy. If this interface has a large surface tension, it will be energetically difficult to form. If the interface is formed by an accident of growth, the accident will be more improbable if a high energy interface must be formed. In particular, in terms of the conditions presented in equation 95, if σ_{AT} is large, only rarely will the left-hand side of the inequality be less than the right-hand side. Thus, twinning occurs much more frequently in copper than in aluminium because the twin boundary energy in copper is much less than in aluminium. Presumably, the minor variations in twinning intensity observed in other metals with similar histories may be explained by less important variations in the surface tension of their twin boundaries.

Alternate Theories of Twin Formation—Two important alternate theories of twin formation have been suggested. These will be considered briefly here.

MATHEWSON[108] has proposed that annealing twins result from the growth of mechanical twins or twin faults produced by deformation. As has been stated above, twin faults apparently do have an important role in nucleating annealing twins. However, since coherent twin boundaries cannot migrate laterally, twin faults cannot grow directly into annealing twins, nor can one account, with this hypothesis alone, for the appearance of broad twins in coarse-grained metals. Many observations require that annealing twins be formed during grain growth, in the absence of twin faults.

BURGERS[109] has proposed that twins in aluminium may be formed during recrystallization by stimulation. If a growing recrystallized grain meets a dislocation-bearing fragment which lies accurately in a

twinned orientation to it, the fragment may discharge its dislocations to the large grain along the common (111) plane—dislocations migrate easily in this direction. Since the fragment has discharged its dislocations, it is now stress free and able to grow at the expense of the surrounding deformed matrix. Burgers has observed a number of such grains that are thus 'stimulated' to grow, and once stimulated, grow more rapidly than the stimulating grain. His theory does not account for the more rapid growth of the stimulated grain. It is possible that this occurs because the new grain is more favourably oriented for growth into the surrounding matrix than the stimulating grain.

While the mechanism of stimulation may operate, it appears equally possible that the stimulated grain arises merely through an accident of growth of the type that has been discussed above. In any case, this hypothesis, as Burgers also suggests, is unable to account for the origin of the majority of the annealing twins found in face-centred cubic metals.

VOL 3

REFERENCES

[1] KALISHER, R. *Ber. dtsch. chem. Ges.* 14/2 (1881) 2747
[2] CZOCHRALSKI, J. *Z. Metallk.* 19 (1927) 316
[3] SCHMID, E. and BOAS, W. *Kristallplaztizitat* Ann Arbor, Michigan, U.S.A.
[4] SACHS, G. and VAN HORN, K. R. *Practical Metallurgy* Cleveland, U.S.A., 1940
[5] BURGERS, W. G. *Handbuch der Metallphysik* 3, pt. 2 *Rekristallization Verformter Zustand und Erholung* Ann Arbor, Michigan, U.S.A., 1941
[6] MEHL, R. F. Ch. in *Metals Handbook* p 259 Cleveland, U.S.A., 1948
[7] BURKE, J. E. Ch. in *Grain Control in Industrial Metallurgy* Cleveland, U.S.A., 1949
[8] CAHN, R. W. *et al* Symposium on Polygonization in *Progress in Metal Physics* II, London, 1950
[9] TAYLOR, G. I. and QUINNEY, H. *Proc. roy. Soc. A* 143 (1934) 307; *ibid* 163 (1937) 157
[10] SEARS, G. W. *J. appl. Phys.* 21 (1950) 721
[11] KARNOP, R. and SACHS, G. *Z. Phys.* 60 (1930) 464
[12] MÜLLER, H. G. *ibid* 96 (1935) 279
[13] KORNFELD, M. and PAVLOV, W. *Phys. Z. Soujet.* 6 (1934) 537; *ibid* 12 (1937) 658
[14] GÖLER, F. VON and SACHS, G. *Z. Phys.* 77 (1932) 281
[15] JOHNSON, W. A. and MEHL, R. F. *Trans. Amer. Inst. min. (metall.) Engrs* 135 (1939) 416
[16] AVRAMI, M. (now MELVIN, M. A.) *J. chem. Phys.* 7 (1939) 1103; *ibid* 8 (1940) 212; *ibid* 9 (1941) 177
[17] KRUPKOWSKI, A. and BALICKI, M. *Ann. Akad. Sci. Tech. Varsovie* 4 (1937) 270
[18] BRAGG, W. L. and WILLIAMS, E. J. *Proc. roy. Soc.* 145 (1934) 699; *ibid* 151 (1935) 540
[19] COOK, M. and RICHARDS, T. L. *J. Inst. Met.* 73 (1947) 1
[20] KORNFELD, M. and SAWIZKI, F. *Phys. Z. Soujet.* 8 (1935) 528
[21] COLLINS, J. A. and MATHEWSON, C. H. *Trans. Amer. Inst. min. (metall.) Engrs* 137 (1940) 150
[22] STANLEY, J. K. and MEHL, R. F. *ibid* 150 (1942) 260
[23] ANDERSON, W. A. and MEHL, R. F. *ibid* 161 (1945) 140
[24] STANLEY, J. K. *ibid* 162 (1945) 116

[25] WARD, R. *General Electric Company Report*, Pittsfield, Mass. 1947
[26] ROSI, F. D. and ALEXANDER, B. H. *Trans. Amer. Inst. min. (metall.) Engrs* 188 (1950) 1217
[27] DECKER, B. F. and HARKER, D. *ibid* 188 (1950) 887
[28] SEYMOUR, W. E. and HARKER, D. *ibid* 188 (1950) 1001
[29] TREAFTIS, H. and TURNBULL, D. Unpublished work
[30] BURKE, J. E. Unpublished work
[31] TURKALO, A. M. and TURNBULL, D. Unpublished work
[32] KORNFELD, M. and RYBALKO, F. *Phys. Z. Soujet.* 12 (1937) 658
[33] BURKE, J. E. *Migration of Grain Boundaries*, Amer. Soc. Met. Symposium on *Atom Movements*, Cleveland, 1951
[34] TIEDEMA, T. S., MAY, W. and BURGERS, W. G. *Acta Crystallogr.* 2 (1949) 151
[35] BECK, P. A., SPERRY, P. R. and HSUN HU. *J. appl. Phys.* 21 (1950) 420
[36] DUNN, C. G. Private communication
[37] —— *Trans. Amer. Inst. min. (metall.) Engrs* 185 (1949) 72
[38] BECK, P. A., KREMER, J. C., DEMER, L. J. and HOLZWORTH, M. L. *ibid* 175 (1948) 372
[39] BURKE, J. E. *J. appl. Phys.* 18 (1947) 1028
[40] BURKE, J. E. *Trans. Amer. Inst. min. (metall.) Engrs* 180 (1949) 73
[41] BECK, P. A. and POLANYI, M. *Naturwissenschaften* 19 (1931) 505; *Trans. Amer. Inst. min. (metall.) Engrs* 124 (1937) 351
[42] SMART, J. S. and SMITH, A. A. *Trans. Amer. Inst. min. (metall.) Engrs* 152 (1943) 103
[43] EASTWOOD, L. W., BOUSU, A. E. and EDDY, C. T. *ibid* 117 (1935) 246
[44] WALKER, H. L. *Bulletin*, University of Ill. Eng. Expt. Sta. Bulletin Series 359, 1945
[45] KORNFELD, M. L. and SCHAMARIN, A. *Phys. Z. Soujet.* 11 (1937) 302
[46] BURKE, J. E. and BARRETT, C. S. *Trans. Amer. Inst. min. (metall.) Engrs* 175 (1948) 106
[47] GLASSTONE, S., LAIDLER, K. J. and EYRING, H. *The Theory of Rate Processes* New York, 1941
[48] *Volmer-Kinetiks der Phasenbildung* Dresden, 1939
[49] TURNBULL, D. *Thermodynamics in Physical Metallurgy* p 282 Cleveland, U.S.A., 1950
[50] MOTT, N. F. *Proc. phys. Soc.* 60 (1948) 391
[51] JOHNSON, W. A. *Trans. Amer. Soc. min. (metall.) Engrs* 143 (1941) 107
[52] STEIGMAN, J., SHOCKLEY, W. and NIX, F. C. *Phys. Rev.* 56 (1939) 13
[53] SMEKAL, A. *Handb. Phys.* 12 (1933) 883
[54] BAKALAR, I. D. and COHEN, M. *Sylvania Symposium on Powder Metallurgy*, Bayside, Long Island, 1949
[55] COOK, M. and RICHARDS, T. L. *J. Inst. Met.* 66 (1940) 1
[56] BOWLES, J. S. and BOAS, W. *ibid* 74 (1948) 501
[57] TURNBULL, D. and FISHER, J. C. *J. chem. Phys.* 17 (1949) 71
[58] DUNN, C. G., DANIELS, F. W. and BOLTON, M. S. *Trans. Amer. Inst. min. (metall.) Engrs* 188 (1950) 368
[59] AUST, K. T. and CHALMERS, B. *Proc. roy. Soc.* 201 (1950) 210
[60] BAILEY, G. L. J. and WATKINS, H. C. *Proc. phys. Soc. B* 63 (1950) 350
[61] VAN VLACK, L. H. *Thesis* Chicago, 1950
[62] FISHER, J. C. and DUNN, C. G. *Nat. Res. Coun. Conference on Imperfections*, Pocono, Penn. 1950
[63] TURNBULL, D. *Trans. Amer. Inst. min. (metall.) Engrs* 175 (1948) 774
[64] —— *J. appl. Phys.* 21 (1950) 1022
[65] BECK, P. A. *J. appl. Phys.* 20 (1949) 633
[66] CAHN, R. W. *Proc. phys. Soc. A* 364 (1950) 323
[67] BURGERS, W. G. and LOUERWERSE, P. C. *Z. Phys.* 167 (1931) 605
[68] BECK, P. A., HOLZWORTH, M. L. and SPERRY, P. *Trans. Amer. Inst. min. (metall.) Engrs* 180 (1949) 163

[69] BURKE, J. E. and SHIAU, Y. G. *Trans. Amer. Inst. min. (metall.) Engrs* 175 (1948) 141
[70] CARPENTER, H. C. H. and ELAM, C. F. *J. Inst. Met.* 24 (1920) 83
[71] SUTOKI, T. *Sci. Rep., Tôhoku Univ.* 17 (1928) 857
[72] HARKER, D. and PARKER, E. A. *Trans. Amer. Soc. Met.* 34 (1945) 156
[73] CZOCHRALSKI, J. *Int. Z. Metallogr.* 6 (1914) 289
[74] EWING, J. A. and ROSENHAIN, W. *Phil. Trans. roy. Soc. A* 193 (1900) 353
[75] BENEDICKS, C. *Kolloid Zeitschr.* 91 (1940) 217
[76] BRAGG, W. L. *Proc. phys. Soc.* 52 (1940) 105
[77] SMITH, C. S. *Trans. Amer. Inst. min. (metall.) Engrs* 175 (1948) 15
[78] VOGEL, R. *Z. anorg. Chem.* 126 (1923) 1
[79] SMITH, C. S. Private communication
[80] FISHER, J. C. and FULLMAN, R. Private communication
[81] BECK, P. A., HOLZWORTH, M. L. and HSUN HU *Phys. Rev.* 73 (1948) 526
[82] BECK, P. A., TOWERS, J. Jr., and MANLEY, W. O. *Trans. Amer. Inst. min. (metall.), Engrs* 175 (1951) 634.
[83] MILLER, O. O. *Trans. Amer. Soc. Met.* 43 (1951) 260.
[84] ROBINSON, C. S. Jr. *J. appl. Phys.* 13 (1942) 627
[85] BURKE, J. E. and CHANDLER, W. Unpublished work
[86] JEFFRIES, ZAY and ARCHER, R. S. *The Science of Metals* p 95 New York, 1924
[87] KRONBERG, M. L. and WILSON, F. H. *Trans. Amer. Inst. min. (metall.) Engrs* 185 (1949) 501
[88] TURKALO, A. M. and TURNBULL, D. *ibid* 185 (1949) 663
[89] RICHARDS, T. L. *Progress in Metal Physics* 1 London, 1949
[90] BARRETT, C. S. *Trans. Amer. Inst. min. (metall.)Engrs* 137 (1940) 128
[91] MADDIN, R. H., MATHEWSON, C. H. and HIBBARD, W. R. *ibid* 185 (1949) 655
[92] BECKER, J. Unpublished work
[93] TURKALO, A. M. and BURKE, J. E. Unpublished work
[94] BECK, P. A. and HSUN HU *Trans. Amer. Inst. min. (metall.) Engrs* 185 (1949) 627
[95] —— —— *ibid* 188 (1950) 1214, 1215
[96] HEIDENREICH, R. D. and SHOCKLEY, W. *Strength of Solids* p 57 Phys. Soc. London, 1948
[97] CARPENTER, H. C. H. and TAMURA, S. *Proc. roy. Soc. A* 113 (1926) 161
[98] BURKE, J. E. *Trans. Amer. Inst. min. (metall.) Engrs* 188 (1950) 1324
[99] FULLMAN, R. *J. appl. Phys.* 21 (1950) 1069
[100] —— *ibid* 22 (1951) 448
[101] —— *ibid* 22 (1951) 456
[102] —— Private communication
[103] —— and FISHER, J. C. *J. appl. Phys.* to be published
[104] MATHEWSON, C. H. *Trans. Amer. Soc. Met.* 32 (1944) 38
[105] BARRETT, C. S. *Trans. Amer. Inst. min. (metall.) Engrs* 188 (1950) 123
[106] HIBBARD, W., LIU, Y. C. and REITER, S. F. *ibid* 185 (1949) 635
[107] MADDIGAN, S. E. and BLANK, A. I. *ibid* 137 (1940) 170
[108] MATHEWSON, C. H. *Proc. Amer. Inst. min. (metall.) Engrs Met. Divis.* (1928) 7
[109] BURGERS, W. G. *Nature*, London, 157 (1946) 76
[110] HOFFMAN, R. E. and TURNBULL, D. *J. appl. Phys.* 22 (1951) 634

8

STRUCTURE OF CRYSTAL BOUNDARIES

B. Chalmers

IMPORTANT ADVANCES have been made in our understanding of the nature of crystal boundaries in the last two years; it is desirable, therefore, to bring the subject up to date by summarizing the work that has appeared since the topic was discussed in the first volume of this series.[1]

Since no method has been devised for the direct study of the structure of the region between the characteristic lattice of one crystal and that of its neighbour, it is still necessary to proceed by indirect methods. These consist, of necessity, of the observation or measurement of a property of a boundary and comparison of the results with the predictions resulting from hypotheses or theories of the structure of the region under consideration. This article comprises, therefore, an account of the experimental work that has been reported, and a discussion of the results and of the theoretical ideas that have been advanced.

COMPARISON OF BOUNDARY FREE ENERGIES

Since the atoms at the boundary between two crystals must be displaced from the positions which they would occupy in a crystal, their free energy is higher than it would be for atoms on an undisturbed crystal lattice. This follows from the concept of the crystal as the arrangement of atoms which has the lowest free energy. It is concluded that the boundary itself can be regarded as having associated with it a definite amount of free energy per unit area. It was shown by CHALMERS[2] directly and by SMITH[3] indirectly, and commented on by KING and CHALMERS[1], that it is possible to compare the free energies per unit area of different boundaries in the same specimen of a metal by observing the equilibrium angles between three boundaries which meet in a line. A technique for preparing suitable specimens, in which the orientations of the crystals are under control, was devised by CHALMERS.[4] He found in his preliminary experiments that the specific free energies of crystal boundaries in tin were independent of the differences of orientation over a wide range of angles. Since that time, however, at least three completely independent investigations have been made on this subject, and it is now apparent that the earlier experiments did not extend to small enough differences of orientation to detect the differences that are now known to exist.

Variation of Energy with Orientation—The three investigations on the variations of the energy with the difference of orientation are those of DUNN and his collaborators,[5] of AUST and CHALMERS[6, 7] and of GREENOUGH and KING.[8] Since the methods and techniques were quite different in the three researches each will be discussed in some detail. The one factor that is common to all three investigations is that they are based on the measurement of the dihedral angles between three surfaces which meet in a line. If the angles are A, B and C (*Figure 1*) and the

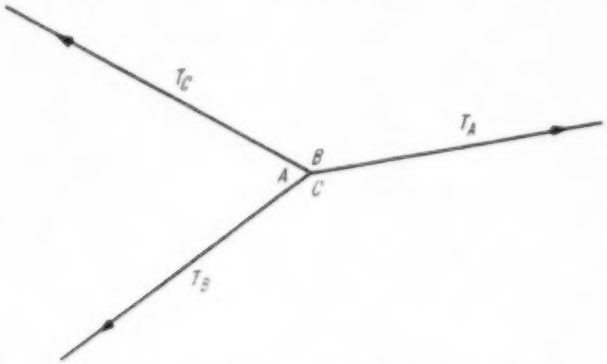

Figure 1. Relationship between surface tensions and angles

surface tensions are T_A, T_B and T_C, they are related by the following expression:

$$\frac{T_A}{\sin A} = \frac{T_B}{\sin B} = \frac{T_C}{\sin C}$$

on the assumption that the surface tension does not depend on the orientation of the surface with respect to the crystallographic axes of the neighbouring crystal or crystals. The reason that this assumption is necessary is that the expression is derived from the simple triangle of forces in which the lengths of the sides are taken to be proportional to the forces without reference to their directions. The general case in which this assumption is not made has been studied by HERRING,[9] who gives an expression that includes the variation of energy with orientation. There is considerable evidence of a circumstantial kind that the dependence of energy on angle is generally negligible except in the special case of coherent twin boundaries, which will be discussed in a later section. It is also necessary to assume that the boundaries have reached equilibrium positions before the angles are measured, and that the angles that are measured are in fact the true dihedral angles. The latter condition will only be satisfied when the boundaries are normal to the surface in which the traces of the boundaries are observed. Both of these conditions are satisfied if the specimen is annealed for a

VOL.
3

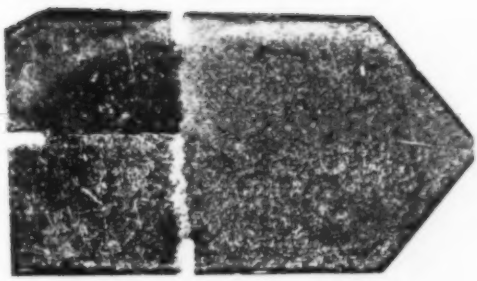

Figure 2. Three crystal specimen

VOL
3

sufficiently long time at a high enough temperature. The three investigations were, however, different in other respects and will be discussed, from the point of view of technique, in turn.

The Experiments of Dunn et al—Dunn and his co-workers prepared their specimens from an alloy of iron with 3½ per cent of silicon in the form of sheet.[5] A technique was developed for growing single crystals of any required orientation. A few large grains are first produced at one end of the specimen by critical straining followed by local annealing. One of these large grains is then selected and the material round it is cut so that the crystal is only joined to the rest of the specimen by a narrow 'neck'. Its orientation is then adjusted to the desired angle by bending or twisting the neck. The specimen is next passed through a furnace so that an extremely steep temperature gradient is produced in it. The selected crystal is in the region of high temperature and the specimen is moved so that the temperature gradient passes along the specimen away from the end containing the selected or 'seed' crystal. The result is that a very thin strip of metal reaches the temperature necessary for grain growth to occur, and growth takes place on to the already existing crystal. This occurs continuously as the specimen moves, and each part of the metal reaches the required temperature only when the growing crystal is so close to it as to form the most appropriate basis for rearrangement of the atoms in the form of new crystals. There is consequently a high probability that a single crystal will be formed. By using three seed crystals instead of one, Dunn was able to produce specimens consisting of three crystals, each with the required orientation. An example of a specimen of this type is shown in *Figure 2*. Prolonged annealing was shown to bring the boundaries to their positions of equilibrium, and the angles between them were measured by means of the microscope.

Aust and Chalmers' Method—The experiments of Aust and Chalmers, on the other hand, were made with specimens prepared by controlled freezing of molten metal.[6, 7] The metals used in these experiments were tin and lead, both of high purity. The procedure was as follows. The first stage is the preparation of a single crystal that is subsequently used as the seed crystal. This is achieved by melting the metal in a narrow trough or boat and allowing it to freeze slowly from one end. The boat is preferably so shaped that freezing starts at a point. There is then a high probability that the metal will freeze as a single crystal. If so, its orientation is determined by optical or x-ray methods. Further single crystals can be prepared from this seed by placing it at one end of the boat, filling the remainder of the boat with metal which is heated so that it melts and unites with the end of the seed, of which part must remain solid. Freezing is then allowed to take place slowly from the seed. In order to prepare a crystal of any required orientation, the

seed is inserted in the boat at the appropriate angle. When a suitable seed crystal has been produced, it is placed in a boat of the type represented in *Figure* 3a. The seed is placed in the position shown and the remainder of the unshaded space is filled with molten metal. It is heated by means of a heating coil or furnace so that the molten metal is kept hot enough to melt the end of the seed without melting the whole of it. The furnace is then moved slowly to the right so

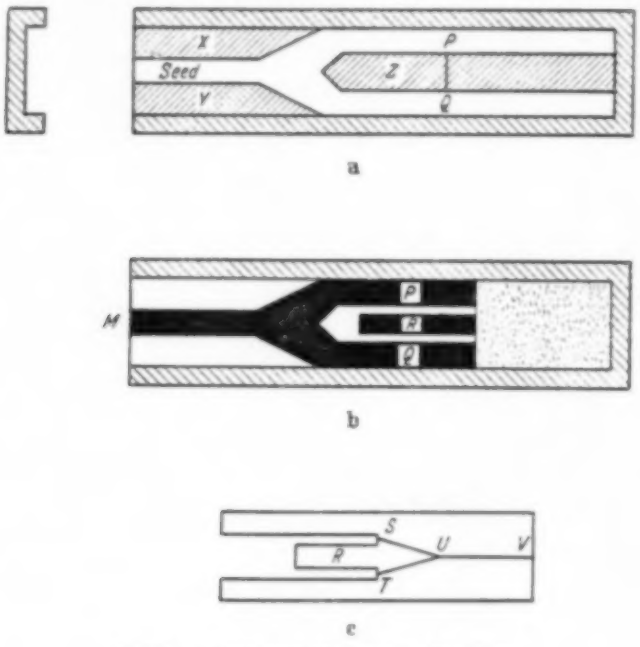

Figure 3. Preparation of three crystal specimen

that the metal freezes progressively from left to right. If conditions are correct, the whole of the metal freezes with the same orientation as the seed and forms a single crystal. This bifurcated single crystal is now removed from the boat and any desired difference of orientation is introduced by twisting or bending one or both of the legs *P* and *Q*. The composite seed crystal *PQ* is now placed in a boat like that shown in *Figure* 3b, that is, similar to the one used previously except that it has no inserts *X*, *Y*, Z. A seed *R* (*Figure* 3b) is now inserted between *P* and *Q* and liquid metal is poured in at *M* to fill the remaining space in the boat. As before, the liquid is allowed to freeze from left to right. Two crystal boundaries are formed, starting at the points *S* and *T* in *Figure* 3c. If the orientations have been chosen correctly, the two boundaries will converge towards the point *U* in

Figure 3c. From this point onwards to the right, the crystals P and Q will continue to grow and will form a third boundary UV. This technique is successful with both tin and lead. The reason for making P and Q from the same original seed is to facilitate the production of specimens in which the difference of orientation is accurately known. The differences are nevertheless measured by x-rays. The third seed R, is always of the same orientation and in most cases the seed P was of the same orientation as the original seed and the seed Q was twisted to produce the required difference of orientation between P and Q. Under these conditions, the difference of orientation between P and R is always the same, so that there is a standard for comparison. The

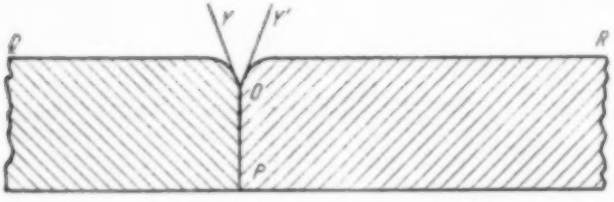

Figure 4. Boundary groove angle

specimens were annealed until the point U no longer moved with further annealing, and the three angles between the boundaries were measured after suitable etching. Measurements are made most easily on photomicrographs of the polished and etched surfaces.

In these experiments, therefore, a comparison is made between the surface tension of a boundary of fixed difference of orientation and other boundaries of various predetermined differences.

Greenough and King's Method—In the experiments of Greenough and King,[8] on the other hand, a comparison was made between the surface tension of the boundary, of known and predetermined difference of orientation, and the surface tension of the external surface of the crystal. The specimens were prepared by growing bicrystals of silver by controlled solidification of molten metal from two seed crystals of chosen orientations, so that the boundary between the crystals is perpendicular to the surface of the specimen, and then subjecting the sample to a prolonged thermal etching by maintaining it at a relatively high temperature for a long enough time for the surface to take up its equilibrium shape. The cross section of the specimen is then as shown in *Figure 4*, in which the two crystals A and B join at the boundary PO. The external surfaces of the crystals are represented by the lines OQ and OR. When equilibrium has been established, the three angles which are formed at the point O indicate the relative values of the surface tensions of the three surfaces that meet at O. The angle YOY'

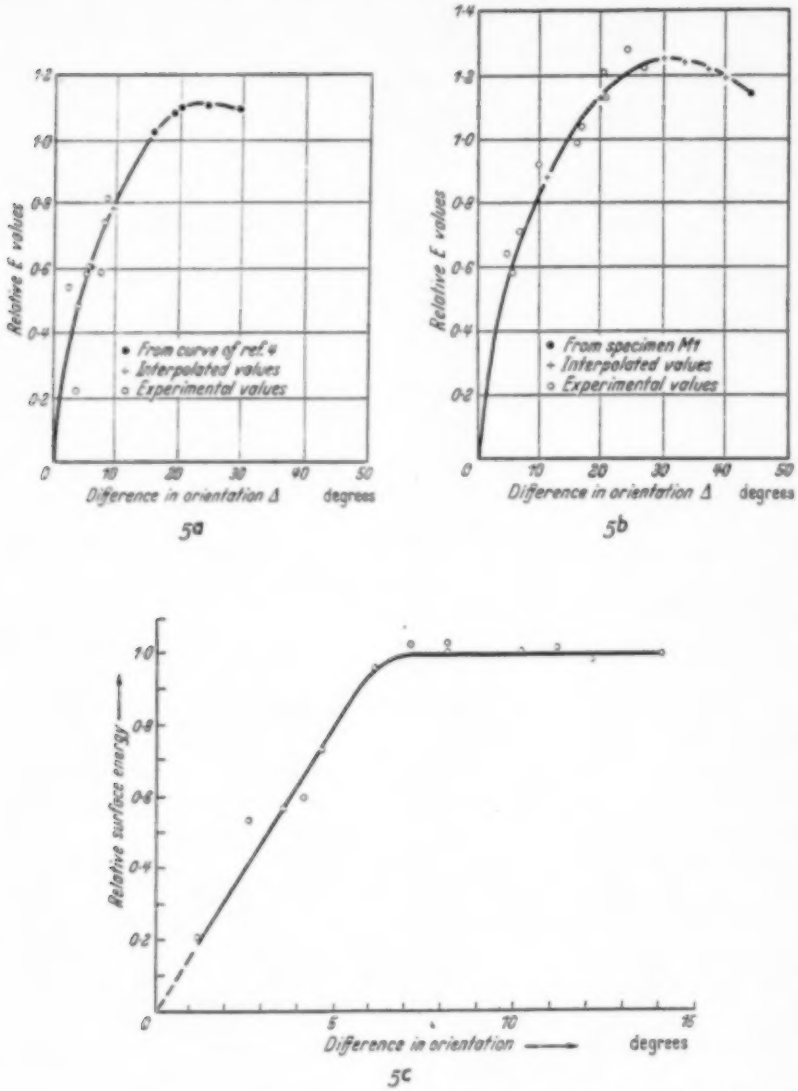

Figure 5. Curves relating boundary energies with difference of

between the tangents to the two external surfaces is measured by an optical method.

Decrease of Surface Tension at Low Angles—The object of each of the three investigations was to determine the variation of boundary energy with the difference of orientation θ between the corresponding axes of

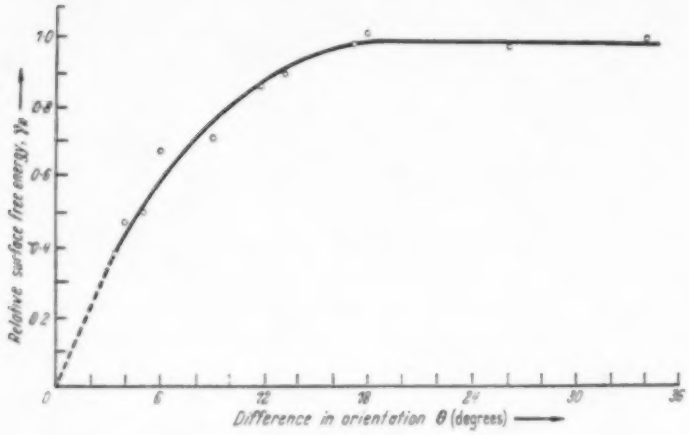

5d

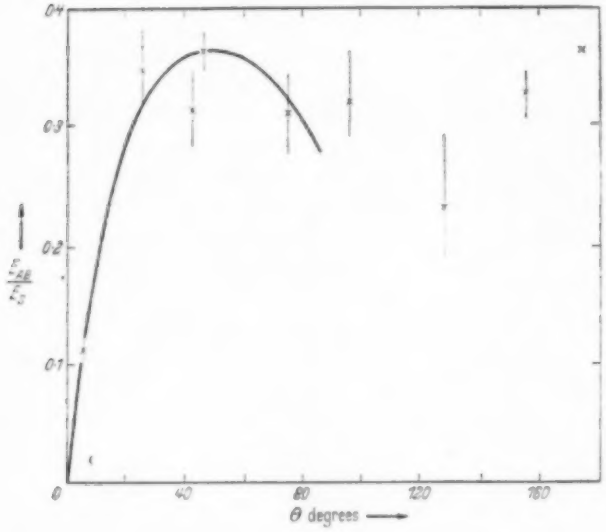

5e

orientation a *Silicon iron,* b *Silicon iron,* c *Tin,* d *Lead,* e *Silver*

the two crystals between which the boundary is formed. The result is therefore expressed in the form of a graph relating the relative energy E_R with the angle θ. There are at present five such curves; they are shown in *Figure 5*. The curves are for a silicon iron with a 110 axis perpendicular to the plane of the specimen for both crystals in each

specimen,[10] b similar to a but with a 100 axis perpendicular to the plane of the specimen,[10] c tin,[6] d lead,[7] e silver.[8] It will be apparent that all the curves are similar in that the value of the surface tension decreases rapidly at low angles and approaches zero as the value of θ approaches zero.

THEORETICAL INTERPRETATION

The results described become significant when they are considered in terms of the theoretical considerations of READ and SHOCKLEY,[11] the basis of which is as follows; it was suggested by BURGERS[12] and by BRAGG[13] that it is possible to represent the transition between any two crystals which have the same structure but different orientations by means of a suitable array of dislocations. Whether this correctly represents the actual structure at the boundary can only be settled either by proving that this particular arrangement of atoms has the lowest energy of any possible arrangement, or by experimental verification of the predictions that emerge from a detailed study of the proposed model. The former approach, that of determining theoretically the lowest energy arrangement of the atoms in the boundary region, has not so far been found to be possible, and we must therefore regard the second method as being the only available line of attack on the problem of the detailed structure of the boundary.

The first conclusion is that the observed variation of the boundary energy with θ is inconsistent with the idea of an amorphous layer, since the properties of such a layer would not vary with the orientations of the neighbouring crystals. The writer considers that the experiments discussed above constitute the first conclusive proof that the boundary between two crystals cannot be satisfactorily represented as an amorphous layer, although the conclusion has already been widely accepted.

Energy of an Array of Dislocations—Detailed consideration by Read and Shockley of the energy of an array of dislocations has been on the following lines; it has been pointed out by READ[14] that the general grain boundary has five degrees of freedom and the orientation of the boundary itself with respect to the grains has a further two. So far only the simpler special cases have been analysed, but there is no reason to doubt that the results will be found to be typical of the more general case. Read and Shockley have considered the case of a cubic crystal in which the two grains are so orientated that they have a common cube axis.[11] There is then only one degree of freedom for the relative orientations of the two crystals. The boundary itself also has one degree of freedom since it is allowed to rotate about the axis which is common to the two crystals. The result obtained by Shockley and Read for this case for the variation of the energy of the boundary

with the angle between their axes is the same as that found by Read for the simpler case which is defined as follows; the crystals are of cubic symmetry and have a common cube axis. Their difference of orientation is equivalent to a rotation of θ radians about the common axis. The boundary is situated in the symmetrical position *i.e.* at an angle of $\theta/2$ radians to a set of cube planes in each of the crystals. Since the treatment given by Read for the more restricted case is simpler, it will be outlined here. The reason for the choice of the particular type of boundary is that it can be represented as an array of similar edge dislocations, whereas the more general cases demand the consideration of combinations of more than one type. The case under consideration

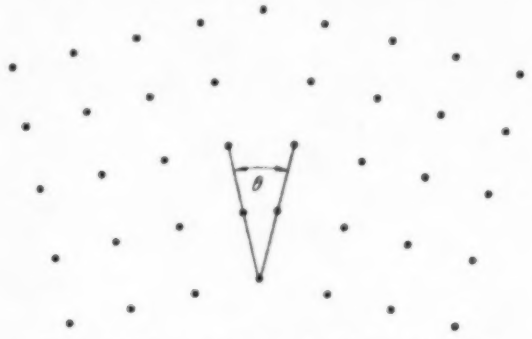

Figure 6. Schematic representation of crystal boundary

is represented in *Figure 6*. The angle θ between the axes of the crystals is equal to a/D where a is the lattice parameter and D is the distance between dislocations. The whole structure is considered to extend indefinitely in the direction perpendicular to the plane of the diagram.

Energy due to Elastic Strain—The total energy of the boundary is considered to be made up of two parts; one is the sum of the separate energies of the dislocations due to the very severe departure from the normal structure near the centres of the dislocations. The distortion is so severe both as regards spacing and coordination, that it is certainly non-Hookian and therefore the energy involved cannot be calculated from elastic theory. It is postulated that consideration is limited to values of θ which are small enough for there to be no interaction between these inelastic energies of neighbouring dislocations. The energy from this source is therefore directly proportional to the number of dislocations. The other part of the energy of the boundary is due to the elastic strain in the material surrounding the dislocations and this can be treated in terms of elastic theory. It was pointed out by Read and Shockley that there are three ways in which the elastic energy associated with the boundary can be calculated: *1* by taking the volume integral

of the strain energy density over the entire body, *2* by integrating the work done in producing the state of strain by the surface forces over the complete boundary, which includes any surfaces of discontinuity such as a slip plane, or *3* by determining the work done in creating the dislocations and bringing them together against their forces of mutual attraction and repulsion. They also conclude that the three methods must give the same amount of energy, and that the most convenient method is the second, which only requires integration of the shear stresses over the slip planes, since the external boundary is strain-free. It might be concluded that this method only takes the shear stresses in the material into account, but this is not the case since the method depends on the equivalence of the volume strain integrated over a volume with the surface strain integrated over the surface bounding the same volume. There are in fact both shear strains and volume strains, at least in the case of edge dislocations and if they could be computed separately and added, the corresponding energy would be the same as that arrived at by the much more elegant method of Read and Shockley. They start with KOEHLER's[15] result for the shear stresses associated with a single edge dislocation. The dislocation is at the origin of a coordinate system and the shear stress T_{xy} is given by the expression:

$$T_{xy} = \frac{x(x^2 - y^2)}{(x^2 + y^2)^2}$$

where the slip plane is in the x direction; lengths are expressed in terms of a and stresses in units of $G/[2\pi(1 - \sigma)]$

Calculation by Integrating Shear Stresses—The shearing stresses due to an infinite row of dislocations spaced at distances D_y along the y axis is:

$$\sum_{n=-\infty}^{\infty} \frac{x_n(x_n^2 - y_n^2)}{(x_n^2 + y_n^2)^2}$$

where $x_n = x + nD_y \cos\phi$ and $y_n = y + nD_y \sin\phi$; D_y can be shown to be given by $a/(\theta \sin\phi)$.

The infinite sum is shown to be equivalent to an energy E per unit area of boundary given by:

$$E = E_0\theta[A - \log_e\theta]$$

where E_0 depends only on the constants of the material and in the rather more general case considered by Read and Shockley, on the angle between the boundary and the y axis. The constant A depends on the energy associated with the material immediately surrounding the dislocation and has not so far been calculated.

The important feature of the Read–Shockley expression, given above, for the relationship between the boundary energy and the

angle between the axes of the two crystals is that it can be compared with the results of experiments of the kind described in the previous

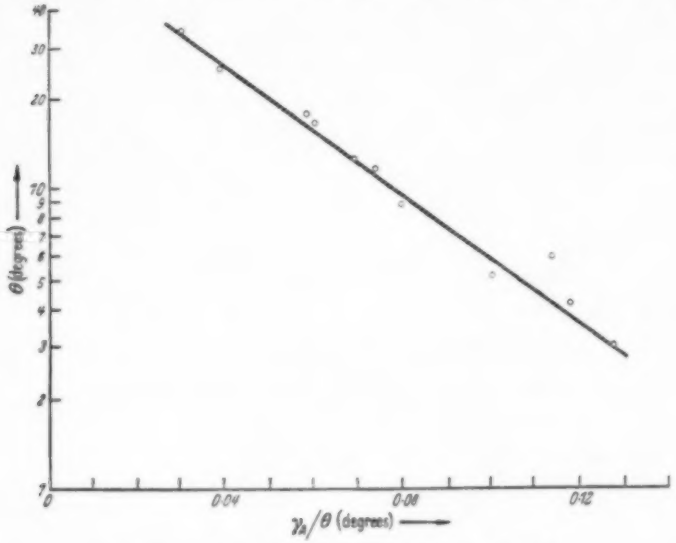

Figure 7. Data for lead plotted on logarithmic scale

section. The most direct method of making such a comparison is to plot the relationship between E/θ and $\log_e\theta$. This should give a straight

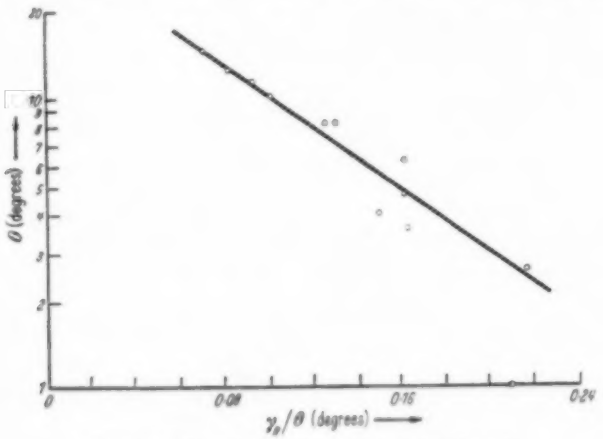

Figure 8. Data for tin plotted on logarithmic scale

line, of which the slope is given by E_0, which can be compared with the value calculated from the elastic constants and the slip vector. In the experiments so far reported, however, the value of E is not an absolute

value, but is given in terms of the energy of a boundary of standard difference of orientation. The value of E that should be used is therefore E_R, the relative energy, rather than E_A, the absolute value. The result of plotting E_R/θ against $\log_e\theta$ for the results of Aust and Chalmers for lead[7] is shown in *Figure 7*. It will be seen that the points fall on a very good straight line; the corresponding graph for tin[6] is shown in *Figure 8*. The points do not indicate such good agreement with the theoretical expression; this can perhaps be accounted for by the fact that tin is a rather poor approximation to the simple cubic lattice that is assumed by Read and Shockley. Examination of the curves in *Figure 5* shows that all the four metals studied so far give essentially the same result, the only difference being the value of the angle θ at which the curve reaches its maximum.

Calculation by Resolving into a Series of Dislocations—VAN DER MERWE[16] has carried out an analysis of the same problem in a rather more general form in the following way; in the first place he pointed out that there are three distinct types of boundary, namely one at which the lattice spacing changes, a twist boundary, that is one in which one crystal is rotated with respect to the other about an axis which is perpendicular to the boundary between them, and a tilt boundary, in which the rotation is about an axis in the plane of the boundary. In each of these cases the energy is calculated on the two assumptions that 'at the interface, the potential energy of an element of area of the one may be taken to be a sinusoidal function of its position relative to an element of area of the other', and 'the material elsewhere may be treated as an elastic continuum which obeys Hooke's law'. It is claimed that the use of this model results naturally in the resolution of the boundary into a series of dislocations; it could, perhaps, be said that the use of the sinusoidal assumption in fact introduces the series of dislocations into the model.

The result of the analysis, which involves approximations that make it invalid except at small angles, is broadly similar to that of Read and Shockley, and is therefore confirmed in a general sense by the experimental results which have been discussed.

Support for Theoretical Relationship—The most surprising feature of all these results is the fact that the theoretical relationship is found to hold up to quite large angles, to a remarkable degree of accuracy. In view of the approximations that are used in the derivation of the expression, it would not be expected that agreement should extend beyond a few degrees. The fact that agreement does extend to angles of twenty or more degrees suggests that a more rigorous derivation, avoiding small-angle approximations, would probably have to take into account other effects besides those discussed above.

If it can be assumed that the relationship $E = E_0\theta[A - \log_e\theta]$

really represents the variation of energy with angle up to the top of the curve relating E with θ, then the angle θ_m at which the maximum is reached is of some significance, and the maximum value of the energy E_m can be calculated from the relationship $E_m = E_0\theta_m$, where E_0 is calculated from known elastic data. This method of arriving at the absolute value of the surface tension is equivalent to that used by Aust and Chalmers, who found that the values for tin and lead were 100 and 200 ergs/cm^2 respectively.[6, 7] It should not be concluded that these figures represent absolute determinations of the energies of the grain boundaries in these two metals, because there are a number of assumptions in the rather roundabout method by which the results are obtained. The most important of these is the supposition that the experimental results agree with the theoretical expression up to the top of the curve because the approximations cancel out. It may be that the plateau value of the surface energy does not coincide with the maximum on the energy–angle curve. The fact that there is a plateau shows that the Read–Shockley expression does not hold after it would predict a drop of energy with further increase of angle. It remains to be explained why the agreement should cease to be valid just at the top of the curve. With these reservations, however, it would seem that the indirect method outlined above should give a fair approximation to the true value of the grain boundary energy. The main value of the "energy as a function of angle" type of measurement, however, does not lie in the possibility of obtaining absolute values, but rather in the support which is given to the dislocation model of the boundary structure. It should be emphasized that the dislocation model in its present form makes no predictions about boundaries with large angles. It depends on the concept of an array of dislocations that are sufficiently separated to maintain their identity as individual dislocations. It is not easy to visualize discrete dislocations if their centres are too close together. If their centres are separated by a distance of five atomic diameters, the angle between the axes of the two crystals would be about eleven degrees, and the angle would increase as the dislocations get closer together.

Limitations of the Dislocation Model—It would seem that the dislocation model, while apparently satisfactory at low angles, can hardly represent the true state of affairs at larger angles. The problem of the structure of large angle boundaries cannot be regarded as being settled on the basis of the small angle boundaries, but the following line of thought suggests that the structure might be a more elaborate form of the same kind of transition lattice. It may, for example, be found that a two dimensional array of dislocations, of the kind represented in *Figure 9*, would be stable and would provide a large angle boundary without the dislocations coming so close together that they lose their identity.

VOL. 3

IOA

In the first place, the energy of the boundary has been shown to vary continuously from a very small value at small angles through a range of increasing values with increasing angles to a fairly steady maximum that persists over a considerable range of angles. This suggests that there is no abrupt change of structure at any stage of the progress from zero to the maximum angle that is to be considered. The other consideration is the fact that the surface energy of the large angle boundary is found, by methods that will be discussed below, to be of the same order of magnitude as the values derived by the method outlined above.

Additional support for the transitional lattice structure for large angle boundaries lies in the fact that the boundaries formed at certain angles, in particular when the crystals have the twin relationship with

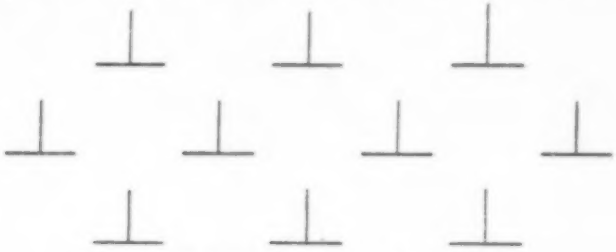

Figure 9. Two dimensional array of dislocations

each other, have lower energies than the ordinary large angle boundary. This applies particularly to coherent twin boundaries, but it also applies, although to a lesser extent, to non-coherent twin boundaries. The energies of twin boundaries will be discussed in detail below.

ABSOLUTE DETERMINATION OF BOUNDARY ENERGIES

Measurement of Surface Tension—The problem of the absolute determination of the surface tension of crystal boundaries has been discussed fully by FISHER and DUNN.[17] It has not so far been possible to make a direct measurement of the energy of a boundary, and all the determinations have been indirect in the sense that in each case the energy of a boundary has been compared with that of an external surface, of which the surface energy is measured by some other method. Let us first consider the measurement of the surface tension of solids. There are in general two methods which have been used; the first is to examine the effect of surface tension, in comparison with that of externally applied forces of known magnitude, on the shape of a piece of metal. The other consists in measuring the dihedral angles that are formed between the solid and a liquid of known surface tension when equilibrium has been established. In both methods it is necessary for the metal to be

exposed to a high enough temperature for changes of shape to take place at an appreciable rate under very low stresses.

Surface Tension of Foils and Wires—The former of the two methods has been applied both with foils and with wires, the essential feature in each case being the provision of a high ratio of surface to volume, since the surface tension force is proportional to the area of the surface, while the force opposing a change of shape depends on the volume. In either case the method of experiment is to measure the rate of extension or contraction when the foil or wire is suspended so that it supports a known weight. By using a series of weights it is then possible to find the weight that would just balance the shortening effect of the surface tension.

VOL. 3

The first reference to the effect of surface tension as the cause of shrinkage of metal foils when heated was made by CHAPMAN and PORTER[18], although the effect was recorded by FARADAY.[19] The first attempt at quantitative measurements was that of SHOTTKY[20] who, however, did not recognize the importance of establishing equilibrium conditions. Measurements of the surface tension of foils of gold and silver were made by SAWAI and NISHIDA[21] who used foils about 5×10^{-5} cm thick. The rate of extension (positive or negative) was plotted as a function of the load for a series of loads and the value required for zero creep rate was derived. This was repeated for a series of temperatures and the values obtained for the surface tensions are given in *Table I*, in which the values are those given by Fisher and

Table I. Values of the Surface Tension of Gold and Silver Foils at Various Temperatures

Temperature °C	*Gold*	*Silver*	
		$3{\cdot}1 \times 10^{-5}$ cm	$6{\cdot}3 \times 10^{-5}$ cm
650	108·6	95·7	87·4
700	124·5	107·8	105·3
750	133·5	119·3	118·5
800	144·6	128·0	123·2
850	155·6	137·0	136·6

Dunn on the basis of a more rigorous method of reduction of the experimental data.[17] It is suggested by these workers that the reported increase of surface tension with temperature is either not significant or else is due to a variation of adsorption effects with temperature. The surface tension of gold foil was also measured by TAMMAN and BOEHME[22] by an essentially similar method. Their results are given in *Table II*.

Table II. Values of the Surface Tension of Gold Foil at Various Temperatures

Temperature °C	*Number of Specimens*	*Surface Tension* mg/cm
700	5	1,845
750	7	1,830
800	5	1,800
850	5	1,770

The wire method was used by UDIN, SHALER and WULFF[23] and by ALEXANDER, BALUFFI, DAWSON, KLING and ROSSI[24]. Udin *et al* used copper wires of 0·004 and 0·006 cm diameter, and measured the changes in the distance between two knots about 2 cm apart. The load required to maintain the length constant was again found by interpolation on a graph relating creep rate and load, and the values obtained are given in *Table III*. The same method was used for gold

Table III. Values of the Surface Tension of Copper Wire at Various Temperatures

Temperature °C	*Radius*	*Surface Tension* dynes/cm
950	$6{\cdot}4 \times 10^{-3}$ cm	1,460
990		1,460
1,024		1,510
1,019		1,401
950	$3{\cdot}6 \times 10^{-3}$ cm	1,400
1,000		1,410
1,050		1,360

by Alexander *et al*, the main difference being the use of a considerably greater distance between the knots. Their results are given in *Table IV*.

Table IV. Values of the Surface Tension of Gold Wire at Various Temperatures

Temperature °C	*Number of Specimens*	*Surface Tension* dynes/cm
920	7	1,680
970	6	1,280
1,020	7	1,400

Liquid–Solid Systems—The alternative approach, that of equilibrating a liquid with the solid surface, has been adopted by SEARS[25] and by BAILEY and WATKINS,[26] who both worked with copper. In each case the liquid used was lead, which has the advantage that it is virtually insoluble in solid copper even when it is itself liquid. It does, however, dissolve some copper and this changes the surface tension which must be used for lead from the value for pure lead to the value for lead saturated with copper.

Sears allowed small drops of liquid lead saturated with copper to rest on a copper surface for a sufficiently long time for equilibrium to be reached, and then lowered the temperature as rapidly as possible so as to preserve as far as possible the geometry of the drop and the adjacent copper for subsequent measurement. The dihedral angles required for the surface tension comparison were determined from the horizontal and vertical dimensions of the drops. It was concluded that the ratio of the surface tensions of solid copper to liquid lead saturated with copper is 1·8. Sears takes the value of the liquid lead–air surface tension to be 400 dynes/cm and this gives a value for the copper surface of 720 dynes/cm.

Fisher and Dunn consider that a value of 435 dynes/cm is probably more accurate for the liquid lead–air surface in the temperature range 800° to 900°C.[15] If we accept this value, the surface tension of the solid copper becomes about 780 dynes/cm. It should be emphasized that this value is for copper in the presence of lead vapour.

Bailey and Watkins have also used the copper–lead system, and obtained a value of 780 dynes/cm for the surface tension of solid copper in the presence of lead vapour, and 1,800 dynes/cm for the surface tension of copper in its own vapour.

Comparison of Results—The following table, from Fisher and Dunn,

Table V. Summary of Equilibrium Surface Tensions of Solid Metals

Surface	*Investigator*	*Surface Tension*	*Temperature* °C	*Mean and Probable Error*
Copper	*Udin, Shaler, Wulff*	1,430 ± 15	950–1050	
	Bailey, Watkins	1,800	800–900	1,430 ± 15*
Gold	*Sawai, Nishida*	1,360 ± 55	650–850	
	Tammann, Boehme	1,850 ± 10	700–850	
	Alexander, et al	1,450 ± 80	920–1020	1,550 ± 100
Silver	*Sawai, Nishida*	1,180 ± 35	650–850	1,180 ± 100
Copper/Lead Vapour	*Sears*	720	800	
	Bailey, Watkins	800	800–900	760 ± 30

* Bailey and Watkins' value is not included

summarizes the values that are available for the surface tensions of solid metals;[17] the agreement between the results from quite different methods is remarkable and gives confidence in methods that might have been open to doubt on the grounds that it is difficult to be certain that equilibrium has been reached when relatively small forces are imposed on solids. These results become relevant to the study of crystal boundaries when comparisons are made between the energy of the surface and that of the crystal boundary. Such comparisons have been made by a number of investigators, in most cases by measuring the angles at the region where a boundary meets the surface, that is, in the 'boundary groove'.

Smith measured the groove angles that were formed where boundaries in copper reached a surface that was in contact with liquid lead.[3] The liquid lead was kept in contact with the copper surface at a high temperature for a long enough time for equilibrium to be established, then cooled rapidly and sectioned and measured. The crystal boundaries on which these measurements were made were those in polycrystalline copper, and so the directions of the boundaries in relation to the plane of the section on which the measurements were made were random, as were the differences of orientation across the boundaries themselves. A statistical method of assessing the results was therefore necessary, and little or no information was obtained regarding the variation of boundary energy with orientation difference. It was assumed, in fact, that very nearly all the boundaries in a random group would have the same energy, namely that corresponding to the 'plateau' of the curve relating energy and angle. The results already discussed show that this assumption is valid in the cases which have been examined so far. The result of Smith's investigation can best be expressed as the ratio of the surface tensions of the copper–copper interface *i.e.* the crystal boundary, and the copper–lead interface. Similar methods were used by SEARS,[27] by BAILEY and WATKINS[26] and by FULLMAN,[27] although the details differ to the extent that whereas Smith determined the ratio of the boundary energy to that of the solid-copper liquid-lead interface, Bailey and Watkins were able to express the ratio of the surface tension of the boundary to that of the copper–lead vapour surface, to that of the copper–copper vapour interface, and to that of the liquid lead–lead vapour interface. Sears gives the surface tension of the boundary in terms of the lead–lead vapour interface, while Fullman gives it in terms of the solid-copper copper–vapour interface. In each case it is possible to convert the comparative value into absolute terms by using the absolute values for the surface tensions of metal surfaces discussed above. There are therefore three different sets of data from which the absolute value of the crystal boundary energy for copper can be evaluated. Fisher and

Dunn, as a result of a careful analysis of the results, have come to the conclusion that the best value is 535 ± 20 dynes/cm.

Greenough finds that the plateau value of the boundary surface tension for silver is about 0·33 of the value of the surface tension of the free surface; he concludes that the absolute value of the surface tension of the boundary is 300 dynes/cm. Fisher and Dunn, however, give the value of 1,180 dynes/cm for the free surface and this gives 393 dynes/cm as the best value for the plateau boundary energy for silver. It is of interest that this value is the only one in which the boundaries, for which absolute values are available, were between crystals of known orientations; in all the other cases in which the orientations of the crystals were predetermined, it is not possible, with existing data, to obtain absolute values for the boundary energy except by assuming the validity of the Read–Shockley expression up to rather large angles.

TWIN BOUNDARIES

A special case of particular interest is the boundary between crystals which have a twin relationship. Such boundaries are of two types, described as *coherent* and *non-coherent*. A coherent twin boundary is one which coincides with the plane of symmetry of the twins, that is, the composition plane. This plane is one in which each atom is correctly placed with respect to the lattices of both the crystals. The non-coherent twin boundary, on the other hand, is any other boundary between crystals with the twin relationship. The atoms on such boundaries are not as favourably placed with respect to their neighbours as they would be in a coherent boundary, and we should expect that the energy of a non-coherent boundary would be higher than that of a coherent one. Qualitative observations of this effect were made on silver by Chalmers, King and Shuttleworth[29] who observed that coherent twin boundaries underwent far less thermal etching than the usual boundaries between crystallographically unrelated crystals, and that the non-coherent boundaries, which could sometimes be seen where twinned regions terminated within crystals, appeared to be similar to the ordinary boundary rather than to the coherent twin boundary in their behaviour under thermal etching conditions. The energy of twin boundaries has been studied quantitatively by Dunn, Daniels and Bolton[30] and by Fullman.[28] The problem is more difficult than the relative measurement of ordinary boundary energy, and this makes a comparison of the two more difficult, and secondly, the usual method of comparison by means of the dihedral angles cannot be applied because the energy of the coherent boundary only has its characteristic low value when it is strictly coherent. If its angle is changed, even by a small amount, the energy increases very rapidly. It is not

permissible, therefore, to interpret the results in terms of an analysis that assumes that the energy is independent of the orientation of the boundary. It is not satisfactory to use the triangle of forces relationship, which would in fact frequently lead to negative values of the surface tension of the coherent boundary, as in the case represented in *Figure 10*. Since the boundary cannot rotate out of its plane without the expenditure of a considerable amount of work, it follows that the correct procedure is to resolve the forces parallel to the plane of the coherent boundary, and then to equate the sum of these forces to zero. In their experiments, Dunn and his co-workers found that they could use the technique already described[5] and produce the twin relationship between two of the crystals and the ordinary boundary relationship with the

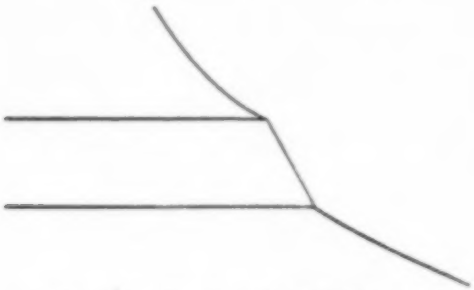

Figure 10. Boundaries of twinned crystals

third grain. The twin boundary automatically took up the coherent position. In their experiments on silicon iron, Dunn, Daniels and Bolton found that the free energy of the coherent twin boundary was about 0·22 of the plateau value for the grain boundary.

Fullman conducted his experiments on copper.[28] He used two methods of measurement. The first was to compare the energy of the coherent twin boundary with that of a grain boundary with which it is in equilibrium; this is done by measuring the dihedral angles and calculating the relative energies by equating the components in the direction parallel to the twin boundary. The value arrived at as a result of twenty-seven different experiments was that the coherent twin boundary energy is 0·045 $\pm$ 0·003 of the value for the plateau grain boundary. Fullman also used the dihedral angle at the base of the grooves formed by thermal etching where coherent twin boundaries meet the free surface. The thermal etching was carried out in the presence of lead vapour. Fullman found that this ratio is 0·0168 $\pm$ 0·0013. Using the values previously reported for the boundary and surface tension of copper, the absolute values for the twin boundary are found to be 24·0 dynes/cm by the first method and

12·8 dynes/cm by the second. Fisher and Dunn conclude that the best value is 18·4 ± 3·8 dynes/cm.

By the use of a method somewhat similar to the former of the two just described, Fullman has also measured the ratio of the coherent twin interface to the grain boundary in aluminium, and obtained a value for the ratio of 0·21, which is much higher than for copper, although both metals have the same structure, namely, face-centred cubic, and the same twinning system, (111) plane and [11$\bar{2}$] direction. The energy of a coherent twin boundary arises entirely from abnormal distances between third nearest neighbours, because the distances between nearest neighbours is the same at the twin boundary as it is within the crystal. It would appear to follow that the contribution of less immediate neighbours to the energy of the crystal is much greater in the case of aluminium than it is for copper.

Some observations have also been made on the energy of non-coherent twin boundaries by both Fullman and by Dunn, Daniels and Bolton who both found that it is about 0·8 of the crystal boundary energy; it is not surprising that it is much higher than the coherent boundary energy because there is considerable disturbance of the distances between nearest neighbours when the boundary is not coherent.

SLIP AT CRYSTAL BOUNDARIES

Two kinds of experiments on the relative motion of two crystals by slip in their mutual boundary were discussed in the article on crystal boundaries in the first volume of this series. They were those of Kê[31] in which the contribution of the crystal boundaries to anelastic behaviour was investigated, and those of King, Cahn and Chalmers in which it was demonstrated[3] that slip can take place in a macroscopically visible form on individual boundaries. Both these lines of investigation have been followed further since that time, and the progress in the last two years will be referred to here. The work of Kê has continued, but there is no new result of significance from the present point of view. Rotherham, Smith and Greenough[33] have also carried out tests on the same general lines on tin. Evidence was found for the existence of an effect similar to that of Kê, that is, for relaxation effects that can be attributed to slip on grain boundaries. As in Kê's work, Rotherham, Smith and Greenough were able to determine the activation energy for this relaxation, and this was found to be consistent with the activation energy for steady state creep. It was, however, very different from the value of the activation energy for self diffusion, which has recently been determined for various crystallographic orientations in single crystals of tin by Fensham.[34] This does not

support the conclusion of Kê, who claims to have demonstrated the equality of the three activation energies, and who regards this equality as an important theoretical result of his model of the structure of the boundary.[31] It is interesting to note, however, that if the viscosity of the boundary is calculated on the same basis and with the same assumptions as were used by Kê for aluminium, the value at the melting point is found to be close to the value for the liquid at the same temperature. The same agreement was found by Kê for aluminium. This should not be taken to imply that there is any evidence that the viscosity of the boundary is the same as that of the liquid or the supercooled liquid at any other temperature.

The value of the activation energy for boundary slip in tin derived from these measurements was found to be 19,000 $\pm$ 2,500 cal/mol, and this is in remarkable agreement with the value of 19,000 $\pm$ 2,000 cal/mol found by KING and PUTTICK[35] for the macroscopic slip of a single boundary. The experiments of King and Puttick were an extension of the preliminary work of King, Cahn and Chalmers, to which reference has been made previously. The work of King and Puttick was again on tin, and they made measurements of the rate of slip at various stresses and temperatures. They found that the rate of slip, when the stress is first applied, is reasonably consistent, and that, as indicated above, a reasonably well defined activation energy could be determined from the results.

Although the activation energies appear to be the same for the relaxation type of boundary slip, involving short times and quite small linear movements, and the macroscopically observable slow slip, there is not at present sufficient evidence to be able to say that the two processes of boundary slip have the same mechanism.

BOUNDARIES BETWEEN DIFFERENT PHASES

Measurement of Dihedral Angles—It has been amply demonstrated that the dihedral angles at the common line of three crystals approach equilibrium values when sufficient time is allowed at high enough temperatures. The most complete demonstrations are those of Dunn and his co-workers[5] and of AUST and CHALMERS[4] who not only showed that the same angles were obtained whether a given angle was approached from a higher or from a lower angle, but who were also able to give curves showing the changes of the angles with time. Unpublished work by AUST, LEAVER and SISCOE[36] on the rate of movement of the boundaries during the approach to the equilibrium position has yielded an estimate of the activation energy of this process. The value that was obtained was 7·0 $\pm$ 2 $\times$ 10^3 cal/gm atom, which is in good agreement with the values of FENSHAM[34] for the self diffusion of tin. The

extreme values (for the directions parallel and perpendicular to the c axis) given by Fensham are $5{\cdot}9 \pm 0{\cdot}4 \times 10^3$ and $10{\cdot}5 \pm 0{\cdot}5 \times 10^3$ cal/gm atom respectively. This suggests that movement of grain boundaries, when it takes place purely because of the resulting reduction of the surface area, and therefore the energy of the boundaries, is a process involving self diffusion, rather than plastic deformation.

It has been pointed out by C. S. Smith that a similar movement takes place when the boundary under consideration is that between crystals of different phases.[3] He has shown that the relative values of the energies of the boundaries between different phases and of the single phase crystal boundaries can be determined by measuring the various dihedral angles after suitable equilibrating treatment. Smith's experimental method was to equilibrate various alloys by annealing and then to section them and measure the angles that were visible on the polished surface at the common points of three grains. No attempt was made to measure the angles between the polished surface and the planes of the boundaries between which the angles are measured; but if a sufficiently large number of angles are measured it is possible to apply statistical methods for determining the average values of the true dihedral angles. By the use of this method, Smith found that the dihedral angles in a single phase metal did not differ much, statistically, from 120°. This is in agreement with the results that have been discussed above, in spite of the fact that some boundaries have been shown to have much lower energies than others, because the low angle boundary is a rather unlikely occurrence and will not be found often in a randomly oriented polycrystalline aggregate. It will therefore not greatly influence the mean value. The boundary between two crystals of the same phase therefore forms a satisfactory basis for the determination of the relative value of the surface energies of the boundaries between crystals of different phases in binary or polyphase alloys. Some typical results from Smith's paper are given in *Table VI.*

Value of Results—It is probably significant that the energy of the boundary between different phases is nearly always lower than that between the crystals of the same phase. The importance of these results at the present stage of our knowledge of crystal boundaries is not so much the possibility of determining absolute values of the energies of various sorts of boundaries, as in the fact that when they are interpreted correctly, as shown by Smith, they account for many of the previously unexplained structures that can be seen when alloys are examined under the microscope, and for some of the effects of small changes of composition on the behaviour of certain alloys. A second phase, which may be present in quite small amounts, may exist as a film at all the boundaries between crystals of the major phase, or, at the other extreme, it may occur as a series of small globules, quite

Table VI. Comparisons of Interfacial Tensions in three-phase CuSnPb *alloy*

Observed Dihedral Angles θ	*Ratio of Interfacial Tensions derived from* θ	*Computed Relative Interfacial Tensions*		
		Interface	*Relative I.F.T.*	*Based on Angle No*
1 α v β/β = 120°	$\gamma_{\alpha\beta} = 1{\cdot}00\gamma_{\beta\beta}$	$\alpha\alpha$	1·35	2
			1·31	3 and 5
			1·33	
2 β v α/α = 95°	$\gamma_{\alpha\beta} = 0{\cdot}740\gamma_{\alpha\alpha}$			
3 Pb v α/α = 90°	$\gamma_{\alpha Pb} = 0{\cdot}707\gamma_{\alpha\alpha}$	$\beta\beta$	1·00	1
			1·05	4 and 5
			1·03	
4 Pb v β/β = 110°	$\gamma_{\beta Pb} = 0{\cdot}872\gamma_{\beta\beta}$			
5 *3-Phase corner*				
a Pb v α/β = 110°	$\gamma_{\alpha\beta} = 0{\cdot}940$	$\alpha\beta$	1·00	*Standard*
b β v α/Pb = 120°	$\gamma_{\alpha Pb} = 0{\cdot}866$	αPb	0·96	3 *and* 2
			0·92	5
			0·94	
c α v β/Pb = 130°	$\gamma_{\beta Pb} = 0{\cdot}766$	βPb	0·87	4 *and* 1
			0·81	5
			0·84	

separate from each other. This difference is associated directly with the relative surface tensions of the crystal boundaries and of the interphase boundaries. The following example, given by Smith in his paper, illustrates the kind of conclusion that can be drawn from measurements of this kind. It is first necessary to consider the equilibrium shape of a liquid phase in a two-phase alloy in which the major phase is solid. This state of affairs would exist in an alloy containing two phases of widely differing melting points at a temperature between the two melting points. It will be assumed that the liquid phase is a rather small proportion, volumetrically, of the alloy. The distribution of the liquid phase depends on the relationship between the surface tension of the interface between solid and liquid, and that of the surface between the crystals of the solid phase. The ratio of these surface tensions determines the dihedral angle at the contact between the liquid phase and a crystal boundary in the solid. The dihedral angle can have any value from 0° to 180°; if the interfacial tension of the solid–liquid interface is less than one half that of the crystal boundary, the dihedral angle is zero, and the liquid can form a continuous film over the surfaces of the crystals. If the interfacial tension is less than one half of the boundary energy, then the dihedral angle is not zero, and complete spreading cannot occur.

Some possible shapes of a drop of the liquid phase at a grain corner of the solid[3] are shown, diagrammatically, in *Figure 11*. It is shown by Smith that a dihedral angle of less than 60° will correspond to spreading of the liquid along the grain edges, while spreading will occur over the intercrystalline surfaces if the angle is zero. It was also pointed out that there are a number of practical cases in which a liquid metal penetrates along the grain boundaries of the solid. The penetration of mercury into brass and the penetration of brazing solder into steel

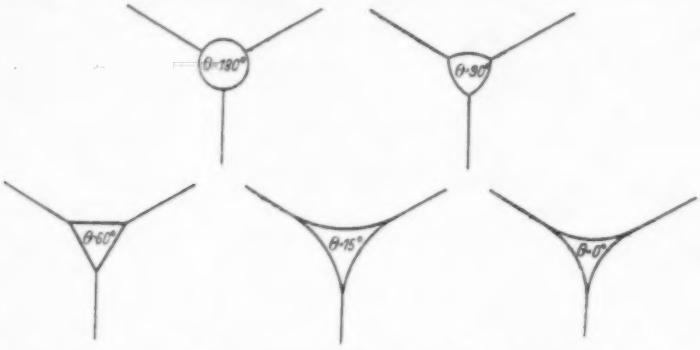

Figure 11. Shape of particle of a second phase as a function of the angle of contact

are examples of such effects. The condition for this to occur is that the dihedral angle is zero.

Effect of Composition on Structure—An interesting example, discussed in detail by Smith, is the distribution of lead and bismuth *etc* in copper and brass. Lead added to copper or α-brass does not spread over the surfaces of the crystals, but spreads along the crystal edges. This accounts for the hot weakness of leaded copper and α-brass, and corresponds to a small but finite value of the dihedral angle. When the zinc content is increased sufficiently for β-brass to be formed, the dihedral angle is increased to about 110°, and the lead is then present in the form of much more rounded drops. These do not cause nearly so much stress concentration as the more angular drops that are present in α-brass, and the hot weakness is suppressed.

The effect of bismuth on copper is to cause embrittlement, apparently because it spreads over the surface of the copper crystals. This is because the dihedral angle is zero. The effect of adding lead to the alloy is to increase the surface tension of the solid–liquid interface; that is, the interface between solid and copper and the liquid lead–bismuth phase. When this surface tension is raised sufficiently, the dihedral angle assumes a finite value, and the lead–bismuth mixture no longer spreads over the crystals of the copper. The copper is then no longer brittle. It is necessary to add about as much lead as there

is bismuth in order to eliminate the brittleness. Lead is not the only addition that works in this way; phosphorus, zinc, and oxygen have a very similar effect for an apparently similar reason.

CONCLUSION

In conclusion, it is fitting to summarize the present state of knowledge regarding the structure of the crystal boundary. The only evidence that is not completely indirect is that which has been obtained from the study of surface tension or surface energy. This is in remarkably good agreement with the predictions of Read and Shockley for the form of the energy–angle relationship for small angles. At large angles it may not be possible to treat the boundary as an array of dislocations either from the point of view of a mathematical treatment of the energy of the boundary as a function of the angle, or as a physical concept. Nevertheless, the energy of large angle boundaries is continuous with that of small angle ones, and seems to show abnormalities at angles at which some degree of coherence is to be expected. This suggests that the large angle boundary is not qualitatively different from the small angle case, and perhaps it can still be regarded as an array of atoms with abnormal coordination of which the array of edge dislocations is a simple case that is relatively susceptible to analysis. Some progress might be made along the following lines. A boundary can be regarded as an array of dislocations that must in the general case be a mixture of edge and screw types. By choosing suitable relative orientations, however, it should be possible to produce boundaries that consist entirely of either edge or of screw type dislocations. It will be necessary to take account of the fact that the dislocations that actually exist in, for example, the face-centred cubic crystals, may not be those that are usually considered in the simple cubic lattice.[37] It can be determined experimentally whether there is any difference in the energy–angle relationship in these two cases; if there is, it will provide extra support to the dislocation model of the boundary; and if differences persist up to large angles, it will be difficult to avoid the conclusion that some sort of array of dislocations represents the structure of the large angle boundary as well as that of the small angle boundary, which may be regarded as reasonably well established.

REFERENCES

[1] KING, R. and CHALMERS, B. *Progress in Metal Physics 1* 127 London, 1949
[2] CHALMERS, B. *Proc. roy. Soc. A* 196 (1949) 64
[3] SMITH, C. S. *Trans. Amer. Inst. min. (metall.) Engrs* 175 (1948) 15
[4] CHALMERS, B. *Proc. roy. Soc. A* 196 (1949) 64
[5] DUNN, C. G. *Trans. Amer. Inst. min. (metall.) Engrs* (1949) 72
[6] AUST, K. T. and CHALMERS, B. *Proc. roy. Soc. A* 201 (1950) 210

[7] —— —— *ibid A* 204 (1950) 359
[8] GREENOUGH, A. P. and KING, R. *J. Inst. Met.* 79 (1951) 415
[9] HERRING, C. Quoted by Read and Shockley in (11)
[10] DUNN, C. G. *J. Metals* (1950) 1245
[11] READ, W. T. and SHOCKLEY, W. *Phys. Rev.* 78 (1950) 275
[12] BURGERS, W. G. *Proc. phys. Soc.* 52 (1940) 23
[13] BRAGG, W. L. *ibid* 52 (1940) 54
[14] READ, W. T. *Pocono Conference on Crystal Imperfections and Grain Boundaries.* U.S. National Research Council
[15] KOEHLER, J. S. *Phys. Rev.* 60 (1941) 397
[16] MERWE, J. H. VAN DER *Proc. phys. Soc.* 63 (1950) [*A*] 616
[17] FISHER, J. C. and DUNN, C. G. *Pocono Conference on Crystal Imperfections and Grain Boundaries.* U.S. National Research Council
[18] CHAPMAN, J. C. and PORTER, H. L. *Proc. roy. Soc. A* 83 (1910) 65
[19] FARADAY, M. *Phil. Trans. roy. Soc.* 147 (1857) 145
[20] SHOTTKY, H. *Nachr. Ges. Wiss. Göttingen* 480 (1912)
[21] SAWAI, I. and NISHIDA, M. *Z. anorg. Chem.* 190 (1930) 375
[22] TAMMANN, G. and BOEHME, W. *Ann. Phys. Loz.* 12 (1932) 820
[23] UDIN, H., SHALER, A. J. and WULFF, J. *J. Metals* 1 (1949) 186
[24] ALEXANDER, BALUFFI, KLING and ROSSI Quoted in 14
[25] SEARS, G. W. *J. appl. Phys.* 21 (1950) 721
[26] BAILEY, G. L. J. and WATKINS, H. C. *Proc. phys. Soc.* 63 (1950) *B* 350
[27] SEARS, G. W. Unpublished, quoted in 14
[28] FULLMAN, R. L. *J. appl. Phys.* 22 (1951) 448 and 22 (1951) 456
[29] CHALMERS, B., KING, R. and SHUTTLEWORTH, R. *Proc. roy. Soc. A* 193 (1948) 465
[30] DUNN, C. G., DANIELS, F. W. and BOLTON, M. J. *Trans. Amer. Inst. min. (metall.) Engrs* 188 (1950) 1245
[31] KÊ, T. S. *J. appl. Phys.* 19 (1948) 285
[32] KING, R., CAHN, R. and CHALMERS, B. *Nature, Lond.* 161 (1948) 682
[33] ROTHERHAM, L., SMITH, A. D. N. and GREENOUGH, G. B. *J. Inst. Met.* 79 (1951) 439
[34] FENSHAM, R. *Aust. J. Sci. Res.* 3 (1950) 91
[35] KING, R. and PUTTICK *R.A.E. Report Met. 45*
[36] AUST, K. T., LEAVER, R. and SISCOE, R. Unpublished
[37] MARTIUS, U. and CHALMERS, B. *Nature, Lond.* 167 (1951) 681

Since the foregoing was written, a paper has appeared by L. H. Van Vlach[38] on the Inter-granular Energy of Iron and Some Iron Alloys. The energy of the γ iron grain boundary at 1105°C was found to be 850 ergs/cm^2, while the energies of the α/α and α/γ were found to be somewhat lower.

[38] VAN VLACH, L. H. *J. Metals* March (1951) 251